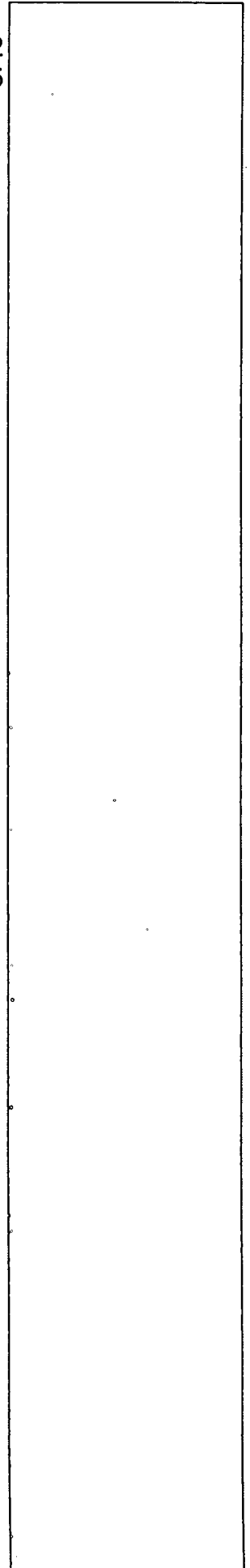


NUREG/CR-6972
ORNL/TM-2008/015

Validation of SCALE 5 Decay Heat Predictions for LWR Spent Nuclear Fuel



**AVAILABILITY OF REFERENCE MATERIALS
IN NRC PUBLICATIONS**

NRC Reference Material

As of November 1999, you may electronically access NUREG-series publications and other NRC records at NRC's Public Electronic Reading Room at <http://www.nrc.gov/reading-rm.html>. Publicly released records include, to name a few, NUREG-series publications; *Federal Register* notices; applicant, licensee, and vendor documents and correspondence; NRC correspondence and internal memoranda; bulletins and information notices; inspection and investigative reports; licensee event reports; and Commission papers and their attachments.

NRC publications in the NUREG series, NRC regulations, and *Title 10, Energy*, in the Code of *Federal Regulations* may also be purchased from one of these two sources.

1. The Superintendent of Documents
U.S. Government Printing Office
Mail Stop SSOP
Washington, DC 20402-0001
Internet: bookstore.gpo.gov
Telephone: 202-512-1800
Fax: 202-512-2250
2. The National Technical Information Service
Springfield, VA 22161-0002
www.ntis.gov
1-800-553-6847 or, locally, 703-605-6000

A single copy of each NRC draft report for comment is available free, to the extent of supply, upon written request as follows:

Address: Office of Administration
Reproduction and Mail Services Branch
U.S. Nuclear Regulatory Commission
Washington, DC 20555-0001

E-mail: DISTRIBUTION@nrc.gov
Facsimile: 301-415-2289

Some publications in the NUREG series that are posted at NRC's Web site address <http://www.nrc.gov/reading-rm/doc-collections/nuregs> are updated periodically and may differ from the last printed version. Although references to material found on a Web site bear the date the material was accessed, the material available on the date cited may subsequently be removed from the site.

Non-NRC Reference Material

Documents available from public and special technical libraries include all open literature items, such as books, journal articles, and transactions, *Federal Register* notices, Federal and State legislation, and congressional reports. Such documents as theses, dissertations, foreign reports and translations, and non-NRC conference proceedings may be purchased from their sponsoring organization.

Copies of industry codes and standards used in a substantive manner in the NRC regulatory process are maintained at—

The NRC Technical Library
Two White Flint North
11545 Rockville Pike
Rockville, MD 20852-2738

These standards are available in the library for reference use by the public. Codes and standards are usually copyrighted and may be purchased from the originating organization or, if they are American National Standards, from—

American National Standards Institute
11 West 42nd Street
New York, NY 10036-8002
www.ansi.org
212-642-4900

Legally binding regulatory requirements are stated only in laws; NRC regulations; licenses, including technical specifications; or orders, not in NUREG-series publications. The views expressed in contractor-prepared publications in this series are not necessarily those of the NRC.

The NUREG series comprises (1) technical and administrative reports and books prepared by the staff (NUREG-XXXX) or agency contractors (NUREG/CR-XXXX), (2) proceedings of conferences (NUREG/CP-XXXX), (3) reports resulting from international agreements (NUREG/IA-XXXX), (4) brochures (NUREG/BR-XXXX), and (5) compilations of legal decisions and orders of the Commission and Atomic and Safety Licensing Boards and of Directors' decisions under Section 2.206 of NRC's regulations (NUREG-0750).

DISCLAIMER: This report was prepared as an account of work sponsored by an agency of the U.S. Government. Neither the U.S. Government nor any agency thereof, nor any employee, makes any warranty, expressed or implied, or assumes any legal liability or responsibility for any third party's use, or the results of such use, of any information, apparatus, product, or process disclosed in this publication, or represents that its use by such third party would not infringe privately owned rights.



U.S.NRC

United States Nuclear Regulatory Commission

Protecting People and the Environment

NUREG/CR-6972
ORNL/TM-2008/015

Validation of SCALE 5 Decay Heat Predictions for LWR Spent Nuclear Fuel

Manuscript Completed: June 2009
Date Published: February 2010

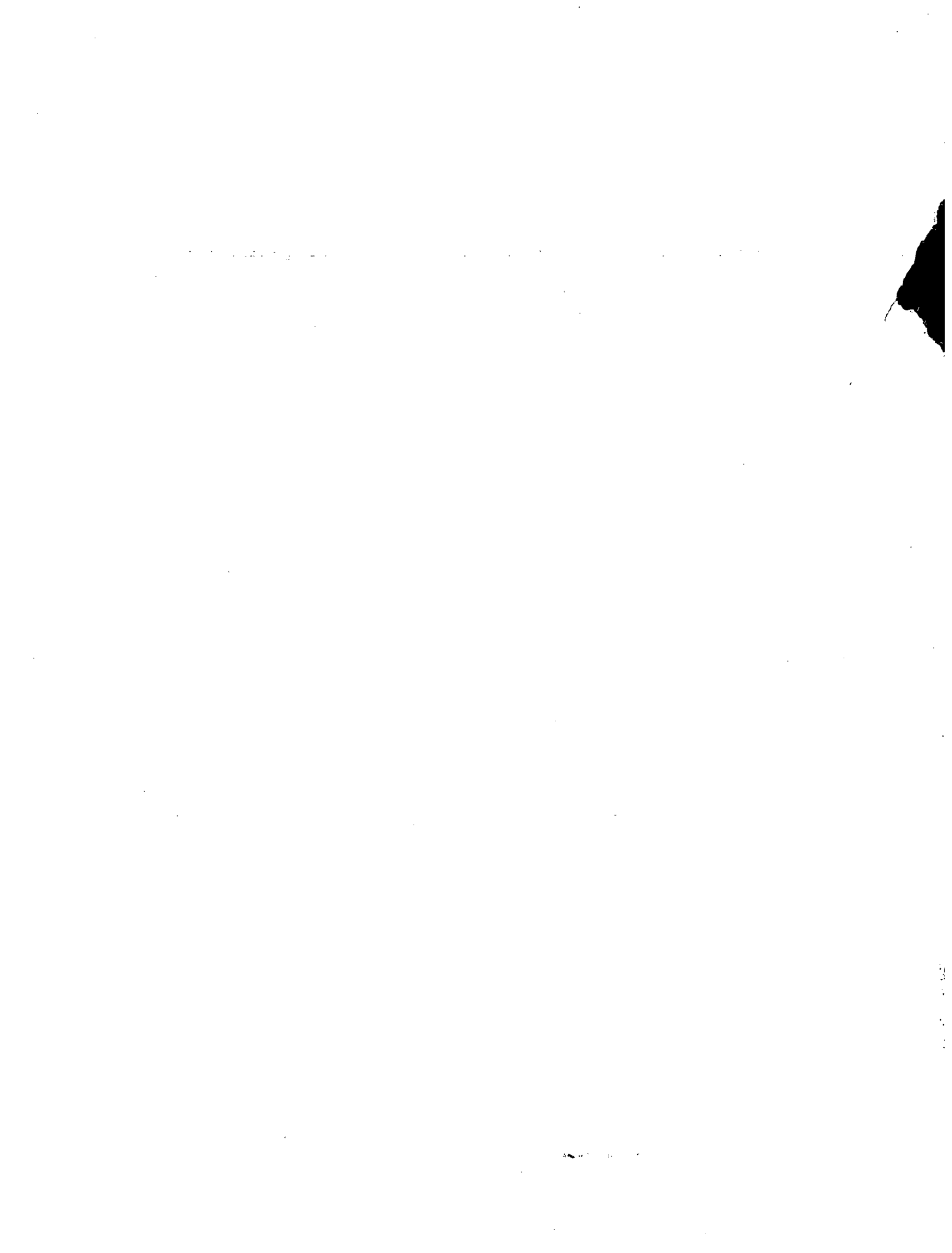
Prepared by
I.C. Gauld, G. Illas, B.D. Murphy, and C.F. Weber

Oak Ridge National Laboratory
Managed by UT-Battelle, LLC
Oak Ridge, TN 37831-6170

M. Aissa, NRC Project Manager

NRC Job Code Y6517

Office of Nuclear Regulatory Research



ABSTRACT

This report documents the validation of ORIGEN-S computer code predictions of decay heat using experimental benchmarks involving irradiated nuclear fuels. The experiments include the measurements of decay heat for (1) pulse fission irradiations for many fissionable materials in spent fuel for cooling times of interest to severe accident analyses ($< 10^5$ s), and for (2) full-length fuel assemblies over longer cooling times of importance to spent fuel storage and transportation. The fuel assembly measurements evaluated in this study include all previously reported measurements performed in the United States at the General Electric Morris Operations facility and at Hanford Engine Maintenance Assembly and Disassembly facility in Nevada. Recent fuel assembly decay heat measurements carried out at the Swedish Central Interim Storage Facility for Spent Fuel, CLAB, are also included. The purpose of this report is to evaluate the computational bias and uncertainty associated with decay heat predictions when using the ORIGEN-S code and cross-section libraries generated employing modules and nuclear data libraries of the SCALE 5 code system. This validation study includes a broader range of assembly designs, fuel enrichments, cooling times, and higher burnup values than has been reported previously. The results will be used to develop technical guidance and recommended margins for uncertainty in decay heat predicted with ORIGEN-S.

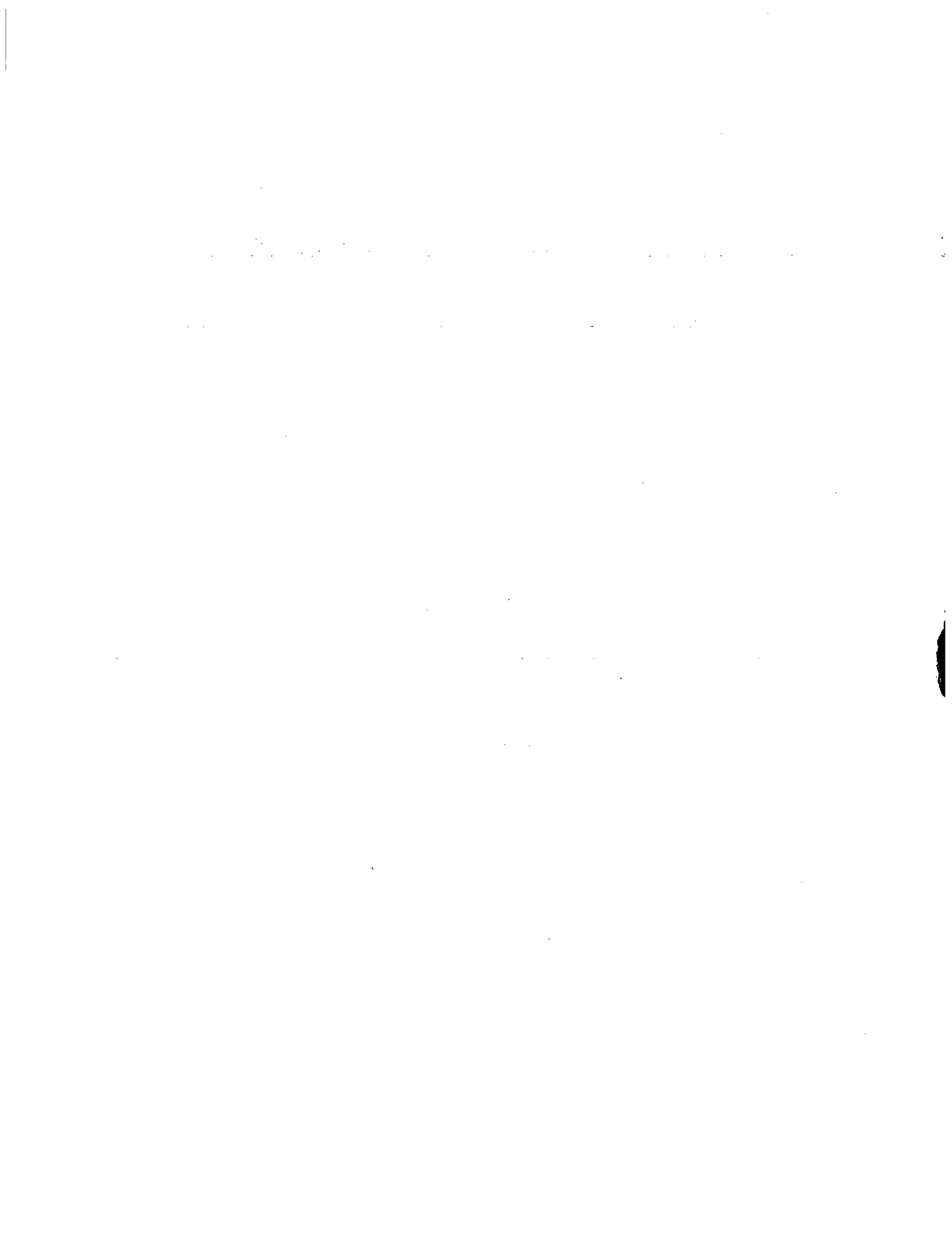


TABLE OF CONTENTS

	<u>Page</u>
ABSTRACT.....	iii
LIST OF FIGURES.....	vii
LIST OF TABLES.....	ix
ACKNOWLEDGMENTS.....	xi
1. INTRODUCTION.....	1
1.1 Background.....	1
1.2 Objective and Scope.....	1
2. FISSION EXPERIMENTS.....	3
2.1 Description of Measurements.....	3
2.1.1 Oak Ridge National Laboratory Measurements.....	4
2.1.2 Karlsruhe Measurements.....	4
2.1.3 Tokyo University Measurements.....	5
2.1.4 Uppsala University Measurements.....	5
2.1.5 University of Massachusetts, Lowell Measurements.....	5
2.2 Nuclear Decay Data.....	6
2.3 Fission Benchmark Results.....	9
2.3.1 ²³⁵ U Fission.....	9
2.3.2 ²³⁹ Pu Fission.....	12
2.3.3 ²⁴¹ Pu Fission.....	14
2.3.4 ²³⁸ U Fast Fission.....	14
2.3.5 ²³³ U and ²³² Th Fast Fission.....	15
2.4 Summary of Fission Experiment Results.....	17
3. ASSEMBLY MEASUREMENTS.....	19
3.1 Facility Descriptions.....	19
3.1.1 Hanford Engineering Development Laboratory.....	19
3.1.2 GE-Morris Operation.....	21
3.1.3 Swedish Central Interim Storage Facility for Spent Fuel.....	24
3.2 Summary of Measurements.....	25
4. FUEL ASSEMBLY DATA.....	27
4.1 Assembly Designs—U.S. Measurements.....	27
4.1.1 San Onofre 1 Assemblies.....	27
4.1.2 Turkey Point 3 Assemblies.....	33
4.1.3 Point Beach Assemblies.....	37
4.1.4 Cooper, Dresden, and Monticello Assemblies.....	41

TABLE OF CONTENTS (continued)

	<u>Page</u>
4.2 Assembly Designs—Sweden Measurements.....	49
4.2.1 BWR 8 × 8 Assemblies	49
4.2.2 BWR 9 × 9 Assemblies	57
4.2.3 BWR SVEA-64 Assemblies.....	60
4.2.4 BWR SVEA-100 Assemblies.....	63
4.2.5 PWR 15 × 15 Assemblies.....	66
4.2.6 PWR 17 × 17 Assemblies.....	70
5. COMPUTATIONAL METHODS AND MODELS	73
5.1 SCALE Depletion Methods and Data.....	73
5.1.1 ORIGEN-S Code	73
5.1.2 Depletion Analysis Methodology	74
5.1.3 SCALE Cross-Section Libraries.....	77
5.1.4 ORIGEN-S Data Libraries.....	77
5.1.5 ORIGEN-S Cross-Section Library Generation.....	77
5.2 SAS2H Assembly Models	81
5.2.1 Modeling Techniques	81
5.2.2 BWR Swedish Assemblies	83
5.3 TRITON Assembly Models.....	85
5.3.1 ORIGEN-S Cross-Section Libraries for U.S. Assemblies.....	85
5.3.2 ORIGEN-S Cross-Section Libraries for Swedish Assemblies	86
6. COMPARISON OF PREDICTIONS AND MEASUREMENTS.....	89
6.1 Assembly Decay Heat Results.....	89
6.2 Error and Uncertainty Analysis	92
6.2.1 Statistics for Uncertainty Analysis	92
6.2.2 Calorimeter Measurement Error.....	93
6.2.3 Differences Between Calculations and Experimental Data.....	97
6.2.4 Sensitivities and Uncertainties in Calculations.....	105
6.3 SAS2H Analysis Results	106
6.4 Effect of Using Assembly Average Burnup and Coolant Density	107
7. SUMMARY AND CONCLUSIONS.....	109
8. REFERENCES	111
APPENDIX A SPENT FUEL ASSEMBLY BENCHMARK DATA SUMMARY OF EXPERIMENTAL AND CALCULATED RESULTS.....	A-1
APPENDIX B ARPLIB INPUT FILE EXAMPLE TRITON INPUT FILES FOR SELECTED ASSEMBLIES	B-1
APPENDIX C SPENT FUEL ASSEMBLY BENCHMARK DATA COMPARISON OF TRITON AND SAS2H RESULTS.....	C-1

LIST OF FIGURES

	<u>Page</u>
Figure 2.1	Measurements of ^{235}U fission decay heat for a fission pulse from ORNL, Lowell, and YAYOI experiments compared with calculations..... 10
Figure 2.2	Measurements of ^{235}U fission decay heat for an equivalent fission pulse from Karlsruhe and Studsvik experiments compared with calculations..... 11
Figure 2.3	Decay heat for ^{235}U fission from Karlsruhe measurements compared with calculations for the experimental 200-s irradiation conditions 11
Figure 2.4	Comparison of ^{235}U fission decay heat for a fission pulse as predicted by the ANS-5.1-2005 standard with recommended uncertainties to the ORIGEN-S code result..... 12
Figure 2.5	Measurements of ^{239}Pu fission decay heat for a fission pulse ORNL, Lowell, and YAYOI experiments compared with calculations..... 13
Figure 2.6	Comparison of ^{241}Pu thermal fission decay heat for a fission pulse measured by ORNL with calculations 14
Figure 2.7	Measurements of ^{238}U decay heat for a fast fission pulse compared with calculations..... 15
Figure 2.8	Measurements of ^{233}U decay heat (YAYOI fast reactor) for a fast fission pulse compared with calculations..... 16
Figure 2.9	Measurements of ^{232}Th decay heat (YAYOI fast reactor) for a fast fission pulse compared with calculations..... 16
Figure 3.1	HEDL Spent Fuel Calorimeter 20
Figure 3.2	Schematic of GE-Morris calorimeter system components..... 22
Figure 3.3	Isomeric view of GE-Morris calorimeter 23
Figure 3.4	Spent fuel assembly calorimeter at the Swedish CLAB facility located at poolside and raised to show the assembly loading hatch above the water level 25
Figure 4.1	Layout of the San Onofre Westinghouse 14×14 assembly 31
Figure 4.2	Layout of the Turkey Point Reactor Westinghouse 15×15 assembly 34
Figure 4.3	Layout of the Point Beach Reactor Westinghouse 14×14 (LOPAR) assembly 39
Figure 4.4	Layout for the GE 7×7 fuel assembly 43
Figure 4.5	GE 7×7 fuel assembly dimensions 44
Figure 4.6	Layout of a BWR $8 \times 8-1$ assembly 56
Figure 4.7	Layout of a BWR $9 \times 9-5$ assembly 59
Figure 4.8	Layout of a BWR SVEA-64 assembly 62
Figure 4.9	Layout of a BWR SVEA-100 assembly 65
Figure 4.10	Layout of Ringhals PWR 15×15 assembly 69
Figure 4.11	Layout of Ringhals 3 PWR 17×17 assembly (with burnable absorbers) 72

LIST OF FIGURES (continued)

		<u>Page</u>
Figure 5.1	Calculational flow of SCALE depletion analysis (1-D and 2-D) for one time step.....	76
Figure 5.2	Pin-cell homogenization procedure used in SAS2H 1-D assembly models.....	82
Figure 5.3	Cutaway illustration of the ATRIUM-10 assembly layout with large internal square water channel.....	83
Figure 5.4	Layout for Type 2 assemblies with three and four BA rods.....	87
Figure 6.1	Measured vs predicted decay heat for all assemblies. The solid line represents the line of agreement between predictions and measurements.	90
Figure 6.2	Absolute error between calculated and measured decay heat	91
Figure 6.3	Relative error between calculated and measured decay heat	91
Figure 6.4	Regression analysis of repeat measurements	96
Figure 6.5	Repeat measurement results at the GE-Morris facility	96
Figure 6.6	Repeat measurements made at the Swedish CLAB facility	97
Figure 6.7	Approximate probability density function for error residuals.....	99
Figure 6.8	Comparison of standardized sample and normal cumulative distributions.....	99
Figure 6.9	Residual error for each measurement facility.....	100
Figure 6.10	Residual error for CLAB measurements by reactor type	100
Figure 6.11	Error for GE-Morris measurements by reactor type	102
Figure 6.12	Residual error in specific decay heat for GE-Morris measurements.....	102
Figure 6.13	Residual error in specific decay heat for CLAB measurements.....	103
Figure 6.14	Residual error correlation with assembly burnup.....	103
Figure 6.15	Residual error correlation with assembly cooling time.....	104
Figure 6.16	Residual error correlation with assembly enrichment.....	104
Figure 6.17	Ratio of decay heat calculated using assembly average parameters to that obtained using explicit axial calculations for selected Swedish BWR and PWR assemblies.....	108

LIST OF TABLES

		<u>Page</u>
Table 2.1	Summary of fission experiments used in present decay heat analysis	4
Table 2.2	Summary of fission product decay data sources	7
Table 2.3	ORIGEN-S fissionable isotopes with explicit fission product yields	8
Table 3.1	Summary of evaluated fuel assembly decay heat measurements	26
Table 4.1	Summary of fuel data for U.S. assembly measurements	28
Table 4.2	San Onofre Unit 1 reactor and fuel assembly design information	30
Table 4.3	Stainless steel composition data for San Onofre fuel assemblies	32
Table 4.4	San Onofre Unit 1 reactor and assembly irradiation data	32
Table 4.5	Turkey Point 3 reactor and fuel assembly design information	35
Table 4.6	Turkey Point reactor and assembly irradiation data	36
Table 4.7	Activated structural components in Turkey Point and Point Beach assemblies	36
Table 4.8	Point Beach reactor and fuel assembly design information	38
Table 4.9	Point Beach reactor operating history data	40
Table 4.10	Cooper, Dresden, and Monticello and fuel assembly design information	42
Table 4.11	Cooper Station reactor and assembly irradiation data	45
Table 4.12	Dresden 2 reactor and assembly irradiation data	46
Table 4.13	Monticello reactor and assembly irradiation data	46
Table 4.14	Activated structural elements in Cooper, Dresden, and Monticello assemblies	47
Table 4.15	Fuel assembly design data for BWR 8 × 8 assemblies	51
Table 4.16	Ringhals-1 reactor and 8 × 8 assembly irradiation history data	52
Table 4.17	Oskarshamn-2 reactor and 8 × 8 assembly irradiation data	52
Table 4.18	Forsmark-1 reactor and 8 × 8 assembly irradiation data	53
Table 4.19	Forsmark-2 reactor and 8 × 8 assembly irradiation data	53
Table 4.20	Barsebäck-1 reactor and 8 × 8 assembly irradiation data	53
Table 4.21	Barsebäck-2 reactor and 8 × 8 assembly irradiation data	54
Table 4.22	Oskarshamn-3 reactor and 8 × 8 assembly irradiation history	54
Table 4.23	Other data for BWR 8 × 8 assemblies	55
Table 4.24	Fuel assembly design data for BWR 9 × 9 assemblies	57
Table 4.25	Forsmark 1 reactor and 9 × 9 assembly irradiation data	58
Table 4.26	Fuel assembly design data for SVEA-64 assemblies	60
Table 4.27	Forsmark-2 reactor and SVEA-64 assembly irradiation data	61
Table 4.28	Oskarshamn-2 reactor and SVEA-64 assembly irradiation data	61

LIST OF TABLES (continued)

		<u>Page</u>
Table 4.29	Fuel assembly design data for SVEA-100 assemblies	63
Table 4.30	Oskarshamn-3 reactor and SVEA-100 assembly irradiation data	64
Table 4.31	Forsmark-3 reactor and SVEA-100 assembly irradiation data	64
Table 4.32	Fuel assembly design data for PWR 15 × 15 assemblies	66
Table 4.33	Ringhals-2 reactor and PWR 15 × 15 assembly irradiation data	67
Table 4.34	Fuel enrichment and initial uranium load for PWR 15 × 15 assemblies	68
Table 4.35	Fuel assembly design data for PWR 17 × 17 assemblies	70
Table 4.36	Ringhals-3 reactor and PWR 17 × 17 assembly irradiation data	71
Table 5.1	Cross-section positions and burnup values created in the SCALE libraries	80
Table 6.1	Measurement uncertainty estimates for each calorimeter facility	95
Table 6.2	Assemblies considered for axial decay heat studies	107
Table A.1	Summary of measured and predicted PWR fuel assembly decay heat (U.S. measurements only)	A-3
Table A.2	Summary of measured and predicted BWR fuel assembly decay heat (U.S. measurements only)	A-4
Table A.3	Summary of measured and predicted PWR fuel assembly decay heat (SKB measurements only)	A-8
Table A.4	Summary of measured and predicted BWR fuel assembly decay heat (SKB measurements only)	A-10
Table C.1	Comparison of TRITON and SAS2H decay heat results for selected Swedish PWR fuel assemblies	C-3
Table C.2	Comparison of TRITON and SAS2H decay heat results for selected Swedish BWR fuel assemblies	C-5

ACKNOWLEDGMENTS

This work was performed under contract with the U.S. Nuclear Regulatory Commission Office of Nuclear Regulatory Research. Many people made valuable contributions to this work. Measurement data for the fission experiments performed at University of Lowell, Massachusetts, were provided by G. Couchel and W. Schier; data measured at the University of Tokyo YAYOI fast reactor were provided by J. Katakura and Y. Ohkawachi; and J. K. Dickens provided valuable information on the measurements performed at Oak Ridge National Laboratory. The results of recent spent fuel assembly calorimeter measurements performed at the Central Interim Storage Facility for Spent Fuel in Sweden were made available through a technical cooperation agreement between Oak Ridge National Laboratory and the Swedish Nuclear Fuel and Waste Management Co., SKB. L. Agrenius, Agrenius Engineering Co., facilitated the exchange of data and information required for the computational analysis of the Swedish fuel measurements and provided many helpful discussions and guidance. M. McKinnon at Pacific Northwest Laboratory was instrumental in making the General Electric Morris operation calorimeter design information available; this helped guide the design of the calorimeter constructed by SKB for the Swedish measurements. Finally, the authors would like to thank S. M. Bowman, SCALE Project Leader, G. Radulescu and B. L. Broadhead for their peer review of this document, C. C. Southmayd for editorial comments, A. C. Alford for clerical support, and W. C. Carter for her preparation and formatting of the final report.



1. INTRODUCTION

This report documents the validation of decay heat calculations performed using the ORIGEN-S isotope generation and depletion code,¹ a module of the SCALE 5 code system,² against experimental decay heat measurements. The measurements include (1) total energy release (decay heat) following fission of ^{235}U , ^{239}Pu , ^{241}Pu , ^{238}U , ^{232}Th and ^{233}U over very short cooling times of interest to severe accident analysis, and (2) calorimetric measurements for more than 160 full-length commercial spent fuel assemblies that cover cooling times from several years to about 30 years after discharge from the reactor.

1.1 Background

An increase in the need for dry storage casks and other independent spent nuclear fuel storage installations (ISFSIs) is expected in the next decade as spent fuel storage pools reach their design capacities. Onsite dry storage at nuclear power plants is recognized by the utilities as an effective interim approach to spent fuel management while a program for long-term disposition of the fuel is implemented. One of the new challenges faced by facility designers and regulators is that spent fuel now being discharged from nuclear plants has significantly higher burnup and higher initial enrichments than previously seen. Advances in fuel design over the past several decades, including use of higher enrichment fuels and increased use of burnable poisons, and improvements in core optimization have led to discharge assembly burnups of 60 GWd/MTU or more.

Experimental programs designed to measure spent fuel assembly decay, an important design and safety criterion for dry spent fuel storage facilities, were performed in the United States (U.S.) in the 1980s using calorimeters operated at General Electric Morris Operation and at the Hanford Engineering Development Laboratory. These programs measured approximately 80 assemblies, with assembly designs available at the time and fuel with a maximum burnup of 39 GWd/MTU and 27 GWd/MTU for pressurized-water reactor (PWR) and boiling-water reactor (BWR) fuels, respectively. The measurements have been used to validate computer code predictions³ that form the technical basis of the decay heat values in the U.S. Nuclear Regulatory Commission Regulatory Guide 3.54 on decay heat for ISFSIs, revised in 1999.⁴ The characteristics of modern fuel however have moved well beyond the regime where the computer code predictions of decay heat have been validated and beyond the range of the current regulatory guide RG 3.54.

Recently, an experimental program to measure decay heat for spent fuel assemblies at the Central Interim Storage Facility for Spent Fuel (CLAB) located in Sweden was initiated under a project managed by the Swedish Nuclear Fuel and Waste Management Company Svensk Kärnbränslehantering AB (SKB). Under this program decay heat measurements have been performed for more than 86 fuel assemblies⁵ having relatively modern designs, and higher enrichments, burnups, and cooling times than previously reported. Oak Ridge National Laboratory (ORNL) has collaborated with SKB to assist in the computational analysis of the measurements performed at CLAB using ORIGEN-S and the SCALE code system. The new measurements made at the CLAB facility greatly increase the amount of data available for code validation and allow the range of code application to be accurately quantified over a wide range that includes most modern design fuels.

1.2 Objective and Scope

The objective of this report is to document the validation of ORIGEN-S over a wide range of spent fuel characteristics that includes modern fuel designs, enrichments, discharge burnup, and cooling times. The validation includes all earlier calorimeter measurements made at the GE-Morris Operation and Hanford facilities, and the newer measurements made at the CLAB facility in Sweden. The measurements provide

an expanded database of benchmarks necessary to extend the validation range of current regulatory guide RG 3.54 to include modern high-burnup fuels. The computational bias and uncertainty associated with predictions of assembly decay heat using the ORIGEN-S code of the SCALE 5 code system are presented. Fuel design information, plant operating data, and the results of the measurements are summarized in this report in sufficient detail to allow independent evaluations of the experiments to be performed using other methods and data. Additional and more detailed information is available from the primary references cited in this report.

In addition to the spent fuel assembly benchmarks described, this report includes validation at short decay times following fission for many of the major actinides in commercial spent fuel. Although a detailed quantitative uncertainty analysis of the fission benchmarks is beyond the scope of this report, the results demonstrate the accuracy of the computation methods for a wide range of potential applications at time values typically addressed by decay heat standards.

A summary of the validation studies for the fission experiments (short cooling times) involving individual fissionable isotopes is given in Sect. 2. The remainder of the report describes the validation using spent fuel assembly measurements. Section 3 provides an overview of the fuel assembly decay heat measurements and a brief description of the experimental facilities. Details of the fuel assembly data (assembly design, reactor operating conditions, and irradiation history) are presented in Sect. 4. The computational methods, nuclear data libraries in the SCALE system, and the models used to generate fuel assembly cross sections for the burnup analysis are described in Sect. 5. Finally, a comparison of predicted and measured values of decay heat for all evaluated assemblies is presented in Sect. 6 along with a statistical analysis of the results and recommended values of bias and uncertainty derived from the computational analysis. The appendixes to this report include a summary of all reported decay heat measurements and the results of code predictions, and provide examples of the fuel assembly models used to generate the cross-section libraries for the ORIGEN-S depletion calculations.

2. FISSION EXPERIMENTS

Energy release (decay heat) from the decay of fission products in irradiated fuel is important in the safety analysis of nuclear reactors after shutdown. Nearly 7% of the total energy from fission is released by the decay of radioactive fission products after the fission process ends. Approximately 25% of the residual decay energy from fission is released in the form of beta and gamma rays in the first 10 s after fission, and about 50% is released within 100 s of fission. The accumulated fission products continue to release energy long after fission ends; this energy source plays an important role in the evaluation of postulated loss-of-coolant accidents and emergency core cooling system performance that considers a time range of less than about 10^5 s after fission.

The rate of energy dissipation over short times after fission has been measured extensively. Because the measurement of full-length fuel assemblies at such short cooling times is impractical, these experiments generally involve a small sample of fissionable isotope irradiated in a neutron flux for relatively short periods of time. These experiments are often referred to as "pulse" fission experiments and have been widely used in fission product decay heat standards development.

These decay heat measurement methods generally fall into two categories: spectroscopic and calorimeter. The spectroscopic method involves measuring the gamma and beta radiation spectra using detectors, unfolding the spectra to obtain the emitted energy distribution, and deriving the decay heat from the individual gamma and beta energy components. Evaluations of the measurements^{6,7} have found a consistent and systematic bias between the spectroscopic and calorimeter results at some decay times that has not been resolved. The calorimeter measurements are observed to yield systematically larger results than the spectroscopic measurements by upward of 2%, or about one standard deviation assignment to the calorimetric results, in the timeframe of $t < 100$ s after fission; the differences though are in general statistically insignificant at the 95% confidence level.⁶ Any evaluation of the decay heat after fission and the assigned uncertainty based on experimental data will therefore be influenced by the selection of the experiments used in the analysis.

2.1 Description of Measurements

The benchmark measurements selected for this work are listed in Table 2.1. They include measurements performed after 1980 of energy release from fission of ^{233}U , ^{235}U , ^{238}U , ^{239}Pu , ^{241}Pu , and ^{232}Th . Only those experiments reporting measurements of total decay heat or reporting both the beta and gamma components were considered, because calculations were performed only for the total decay heat. These experiments used mostly spectroscopic measurement methods and involved relatively short irradiation times with respect to the decay times at which the decay heat was measured. The latter feature makes these experiments highly relevant to the direct evaluation of decay heat from a pulse fission event at short cooling times. The results using spectroscopic techniques yield very consistent agreement with one another. However, it must be emphasized that for some time regimes the spectroscopic results are lower than corresponding calorimeter results and tend to be in better overall agreement with the calculations presented here. A comprehensive review of other experiments performed predominantly before 1980 can be found in publications by Tobias,⁸ Schrock,^{9,10} and Dickens.⁷ The experimental results evaluated in this study also tend to be lower than the values obtained from the American National Standard ANSI/ANS-5.1 on decay heat.¹¹ The values in the Standard are intentionally developed to be conservative and are not based on any single set of measurements or even a least-squares best estimate evaluation of more than one experiment. Consequently, the ANS-5.1 values are more likely to overpredict than underpredict values for the decay heat. The most recent measurements, performed circa 1997, were made at the University of Massachusetts at Lowell. The Lowell data have not been included in the development of the

ANS-5.1 Standard. These measurements are notable because they include decay times < 1 s after fission, well below most other measurements.

Table 2.1 Summary of fission experiments used in present decay heat analysis

Data set	Isotopes	Method ^a	Author(s)	Institute	Pub. year (circa)
1	²³⁵ U, ²³⁹ Pu, ²⁴¹ Pu	γ, β spec.	Dickens et al.	Oak Ridge National Laboratory	1980, 1981
2	²³⁵ U	calorimeter	Baumung	Karlsruhe	1981
3	²³³ U, ²³⁵ U, ²³⁸ U, ²³⁹ Pu, ²³² Th	γ, β spec.	Akiyama et al.	Tokyo University	1982
4	²³⁵ U	γ, β spec.	Johansson	Uppsala University/ Studsvik	1987
5	²³⁵ U, ²³⁸ U, ²³⁹ Pu	γ, β spec.	Schier and Couchell et al.	University of Massachusetts, Lowell	1997

^a spec = spectroscopic method.

2.1.1 Oak Ridge National Laboratory Measurements

Oak Ridge National Laboratory (ORNL) performed measurements of gamma-ray and beta decay energy release following thermal fission of ²³⁵U, ²³⁹Pu, and ²⁴¹Pu at the Oak Ridge Research Reactor.^{12,13} The gamma measurements were made with a NaI(Tl) scintillation detector. Beta measurements were made using a NE-110 plastic beta ray scintillator with gamma coincidence. The results were computationally unfolded using the detector response functions to obtain spectral distributions of moderate resolution. The resulting energy spectra were then integrated to obtain the total energy released. Decay heat values (gamma and beta components) were measured at time intervals from 2 to 14,000 s after fission. The decay heat was determined from the integrated detector counts over each counting time interval. The irradiation time of the samples was varied to obtain an adequate number of integral counts at each of the decay times considered.

The absolute number of fission events was determined experimentally by separately counting the samples after irradiation in a low-background counting room using a high-resolution Ge(Li) detector. Characteristic gamma emissions for the fission products ⁹⁹Mo, ¹³²Te, ¹⁴³Ce, and ⁹⁷Nb-⁹⁷Zr were selected to determine the integral fissions that occurred in each sample. All results were reported on a per fission event basis. The decay heat values were corrected for loss of noble gases from the samples after fission by experimentally measuring the rate of ⁸⁸Kr diffusion from irradiated samples.

2.1.2 Karlsruhe Measurements

Calorimetric measurements for ²³⁵U fission by thermal neutrons were performed at Karlsruhe and reported by Baumung in 1981.¹⁴ Small sample pellets were irradiated for 200 s in the thermal column of the Karlsruhe research reactor. The decay heat was measured by the temperature rise on an adiabatic calorimeter and corrected for the fraction of gamma ray energy that escaped the calorimeter as determined

by detector measurement. The fraction of gamma energy escaping the pellet was reported as about 30 to 40%, depending on the sample size. The escaping gamma energy was measured separately and added to the energy measured by the calorimeter to obtain the total decay heat. The decay heat was reported for decay times from 15 to 4000 s after fission.

Many of the reported calorimetric measurements of decay heat involve sample irradiation times that are large relative to the decay times. Consequently, the measurements are not representative of a pulse fission event. The calculations for the Karlsruhe experiment were performed for the experimental conditions of 200-s irradiation. The measured decay heat values were subsequently adjusted to an equivalent fission pulse using conversion factors calculated from the ratio of the decay heat for pulse fission and experimental conditions, for the purpose of comparing the Karlsruhe results with the other experimental data.

2.1.3 Tokyo University Measurements

Experiments to measure gamma and beta decay following fission were performed at the University of Tokyo fast research reactor, YAYOI.¹⁵⁻¹⁷ These experiments, referred to here as the YAYOI experiments, were very similar to the ORNL measurements in terms of the methodology. However, they included measurement of several additional fissionable materials for fast neutron induced fission. The measurements reported here include fission of ^{233}U , ^{235}U , ^{238}U , ^{239}Pu , and ^{232}Th . The difference between the decay heat from fast neutron induced fission of ^{235}U and ^{239}Pu is estimated to be less than 1% as compared with that of thermal neutron induced fission.⁷ This difference is considerably smaller than the experimental uncertainties, and the fast fission data are therefore generally considered applicable for thermal fission benchmarking purposes.

2.1.4 Uppsala University Measurements

Additional independent measurements of ^{235}U decay heat following fission carried out using the spectroscopy method have been reported by the University of Uppsala at the Studsvik research center in Sweden.¹⁸ The measurements were similar to the spectroscopic methods described previously. The beta ray measurements were made with a Si(Li) detector system, and the spectra were computationally unfolded using the measured energy response of the detector. The gamma ray detection system consisted of a 12.5 cm \times 12.5 cm NaI(Tl) scintillator. Absolute number of fissions in each sample were determined experimentally using fission chambers and a Ge(Li) gamma detector system.

The measurements were performed for ^{235}U and ^{239}Pu thermal fission and ^{238}U fast fission (2.3 MeV). Fast neutrons were produced by a Van de Graff accelerator, and in the case of thermal irradiations, thermal neutrons were produced with a paraffin moderator. After the samples were irradiated they were transferred to the beta and gamma detectors where the spectra were measured over 16 consecutive time intervals from 10 s to 10,000 s after fission. At this time, results for both gamma and beta decay heat measurements have only been reported for ^{235}U fission.

2.1.5 University of Massachusetts, Lowell Measurements

The University of Massachusetts at Lowell has measured the gamma and beta energy release for the fission of ^{235}U , ^{239}Pu , and ^{238}U at decay times from about 0.2 s to 40,000 s after fission (referred to here as the Lowell measurements).¹⁹ The thermal neutron irradiations were conducted at the University of Massachusetts Lowell 5.5-MV Van de Graff accelerator using thermal neutrons from the $^7\text{Li}(p,n)^7\text{Be}$ reaction to induce fission in ^{235}U and ^{239}Pu . Fast neutrons from the 1-MW pool-type research reactor were used to induce fissions in ^{238}U . The gamma spectrometer consisted of a 5 \times 5 in. NaI(Tl) scintillation detector in coincidence with a thin beta detector. The beta spectrometer was a 3 \times 3 in.

plastic scintillation detector gated by a thin surface scintillator. The detectors covered an energy range of 0.1 to 8 MeV. The measured gamma and beta spectra were unfolded using the detector energy response functions to obtain the actual energy spectra from which average energies and total energy release were deduced.

One of the key features of the Lowell measurements is the very short decay times; in many cases less than 1 s after fission. The number of gamma rays and the gamma energy per beta particle were used to normalize the measurements using calculated values of gamma decay heat. This normalization was necessary because the absolute number of fissions in the samples was not measured. The measurements were also subject to loss of noble gases from the irradiated samples during counting. The loss of noble gases and their decay progeny from the samples was corrected using factors calculated from the total decay heat both with and without the noble gas contribution. At the longer cooling times of the experiment, this correction can become substantial, and the results are therefore influenced by the accuracy of the calculation. Consequently, the measurements are not considered as reliable at longer decay times as at the shorter decay times where the correction factor is smaller. Although the normalization of the measurements and the noble gas correction using code calculations limits the value of the Lowell measurements as an absolute benchmark to some extent, the very short decay times of the measurements (where the largest fraction of energy is released) make these measurements attractive for code validation.

Gamma and beta decay heat results were provided in tabular format by G. Couchell and W. Shier at Lowell.²⁰ The counting intervals for the gamma measurements were different than those for the beta measurements. The results of the beta measurements were therefore interpolated to the times of the gamma measurements, and the total decay heat was then obtained by combining the gamma and beta results. The additional uncertainty introduced by interpolation was estimated to be less than 2% in the total decay heat values.

2.2 Nuclear Decay Data

Decay heat calculations were performed for each of the fission benchmark problems described in Table 2.1 using the ORIGEN-S code and associated nuclear data libraries. The accuracy of the decay heat predictions for the fission experiments is dependent primarily on the fission yields, the decay schemes (metastable levels, decay modes, branching fractions, and half lives) and the recoverable energy per decay (Q values) for each fission product. The fission yields implemented in the ORIGEN-S data library are derived from ENDF/B-VI. Independent yields for the nuclides ^{74m}As, ^{85m}Se, ^{86m}Br and ^{162m}Tb were combined with the yields to their ground states. A review of the 1999 Table of Isotopes²¹ indicated that these metastable states have been eliminated in the current decay scheme evaluations. Furthermore, yields to the second metastable states of ¹¹⁶ⁿIn, ¹¹⁸ⁿIn, ¹²⁰ⁿIn, ¹²²ⁿIn, ¹²⁴ⁿSb, ¹²⁶ⁿSb, ¹³⁰ⁿIn, ¹⁵²ⁿPm and ¹⁵²ⁿEu were combined with their decay progeny because ORIGEN-S currently does not support nuclide identifiers for excited levels beyond the first metastable state. The decay energy was assigned to the daughter in such a way as to mitigate the effects of this approximate representation on the decay heat predictions.

The nuclear decay data and decay schemes are also primarily from ENDF/B-VI. Decay data were compiled for 1093 individual fission products having direct fission yields from ENDF/B-VI. Approximately 230 fission products with direct yields were not included for lack of evaluated decay schemes. Most of these were low yield isotopes located far from stability. The sources of nuclear decay data in the ORIGEN-S library are listed in Table 2.2.

Table 2.2 Summary of fission product decay data sources

Number of nuclides	Stability, status, and data source
146	Stable nuclides
764	Radioactive, ENDF/B-VI decay data
172	Radioactive, ENSDF decay data
11	Radioactive, JEF-2.2 decay data
26	Ternary fission products and decay progeny (JEF-2.2)
1119	Total fission product library size

Fission product yields for thermal-neutron induced fission were implemented for all materials evaluated in this study except ^{238}U and ^{232}Th , for which fast fission yields were applied (represented in ENDF/B-VI as neutrons having an incident energy $E_n=500$ keV). The actinides in the ORIGEN-S library with explicit fission product yields and the corresponding energy of neutron-induced fission are listed in Table 2.3.

Table 2.3 ORIGEN-S fissionable isotopes with explicit fission product yields.

Number	Fissionable isotope	ENDF/B-VI MAT number	ORIGEN-S ID	Fission energy ^a
1	²²⁷ Th	9025	902270	thermal
2	²²⁹ Th	9031	902290	thermal
3	²³² Th	9040	902320	fast
4	²³¹ Pa	9131	912310	thermal
5	²³² U	9219	922320	thermal
6	²³³ U	9222	922330	thermal
7	²³⁴ U	9225	922340	fast
8	²³⁵ U	9228	922350	thermal
9	²³⁶ U	9231	922360	fast
10	²³⁷ U	9234	922370	fast
11	²³⁸ U	9237	922380	fast
12	²³⁷ Np	9346	932370	thermal
13	²³⁸ Np	9349	932380	fast
14	²³⁸ Pu	9434	942380	fast
15	²³⁹ Pu	9437	942390	thermal
16	²⁴⁰ Pu	9440	942400	thermal
17	²⁴¹ Pu	9443	942410	thermal
18	²⁴² Pu	9446	942420	thermal
19	²⁴¹ Am	9543	952410	thermal
20	^{242m} Am	9547	952421	thermal
21	²⁴³ Am	9549	952430	fast
22	²⁴² Cm	9631	962420	fast
23	²⁴³ Cm	9634	962430	thermal
24	²⁴⁴ Cm	9637	962440	fast
25	²⁴⁵ Cm	9640	962450	thermal
26	²⁴⁶ Cm	9643	962460	fast
27	²⁴⁸ Cm	9649	962480	fast
28	²⁴⁹ Cf	9852	982490	thermal
29	²⁵¹ Cf	9858	982510	thermal
30	²⁵⁴ Es	9914	992540	thermal

^aNeutron energy causing fission: thermal = 0.0253 eV; fast = 500 keV.

2.3 Fission Benchmark Results

The measured and calculated decay heat results are presented as a function of time after fission, in units of MeV/fission. Decay energy decreases after fission approximately as $1/t$, where t is time after a fission event. A common convention used to present these data is to multiply the energy release rate per fission (MeV/s per fission) by the decay time (s) to obtain the units of MeV/fission reported in the studies. The calculated energy release rates after fission for ^{233}U , ^{235}U , ^{238}U , ^{239}Pu , ^{241}Pu , and ^{232}Th are compared with measurements in the following sections.

2.3.1 ^{235}U Fission

Decay heat from thermal fission of ^{235}U was measured in all of the selected experiments listed in Table 2.1. All but one of the measurements (Karlsruhe) were made by gamma and beta ray spectroscopy of the particles emitted from the irradiated samples. The calculated results are compared separately to the ORNL, Lowell, and YAYOI measurements in Figure 2.1, and to the Karlsruhe and Studsvik measurements in Figure 2.2. The measurements are presented separately because the time range of the data in Figure 2.2 is much less than the data in Figure 2.1.

The Karlsruhe and Studsvik results are observed to have somewhat larger uncertainties in the decay time range of 10 s to 100 s after fission compared with the other results and in general are seen to yield slightly larger estimates of decay heat than the other measurements. The Lowell results for the longer cooling times are observed to be significantly lower than all other measurements; this is an effect due likely to errors introduced by the calculations to correct the measurements for noble gas loss; this effect becomes more important at longer decay times.

The Karlsruhe results shown in Figure 2.2 are presented for a basis of one fission pulse. However, the experiments actually involved an irradiation time of 200 s. Therefore, the results, particularly at short decay times, are clearly not representative of a fission pulse. For the purposes of comparison with other experimental data, the Karlsruhe results in Figure 2.2 were obtained by adjusting the measured data to an equivalent fission pulse using the conversion factor

$$\eta(t) = f(t) / F(t), \quad (2.1)$$

where

$f(t)$ = calculated decay heat for a fission pulse event,

$F(t)$ = calculated decay heat per fission for the experimental irradiation times.

No additional uncertainty was assigned to the Karlsruhe data to cover the calculational uncertainty. The conversion factors (η) ranged from about $\eta = 0.2$ at 15 s after fission, to about $\eta = 0.97$ at 4000 s (indicating that at 4000 s the experiment very nearly simulates a pulse fission). The Karlsruhe data are separately compared with the calculations for the actual experimental conditions in Figure 2.3, i.e., without correction factors. The results are consistent with those of Figure 2.2 in that the calculations exhibit a small negative bias, but are within the stated uncertainty of the measurements over all decay times. The agreement suggests that the error associated with η is relatively small.

Overall, the agreement between calculation and experiment is seen to be within the level of the measurement uncertainties. It is important to emphasize here again that many of the calorimeter measurements not included in this study (pre-1980) yield decay heat estimates that are larger than the data

sets selected in this work and that inclusion of these earlier data would likely indicate a larger deviation between prediction and measurements than is indicated by the current results.

A comparison of the decay heat calculated using ORIGEN-S and the ANS-5.1-2005 Standard values for a ^{235}U fission pulse¹¹ is illustrated in Figure 2.4. The decay heat predicted by ORIGEN-S is observed to be less than the Standard and outside the one standard deviation of the uncertainty assigned to the Standard over the time range $< 10^3$ s. The differences are seen to be largest in the time range of about 5 to 100 s. The differences largely reflect the different experiments used in the development of the standard. Because the standard conservatively reflects differences between experimental data sets used in the development, it will understandably yield decay heat predictions that are larger than those obtained using the best estimate values that have not applied any margin for uncertainty. The Standard is developed to be conservative and is thus weighted toward those experiments with the larger values of decay heat. For longer cooling times corresponding to spent fuel storage, actinides can contribute a significant fraction of the total decay heat. Because the Standard currently does not include a comprehensive actinide treatment, it can not be used for spent fuel storage applications without supplementary actinide methods or data provided by the user.

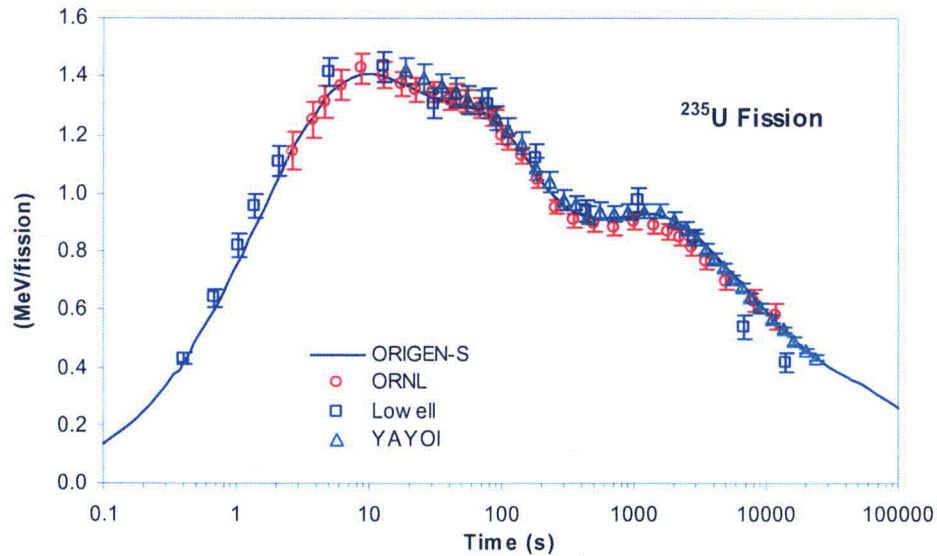


Figure 2.1 Measurements of ^{235}U fission decay heat for a fission pulse from ORNL, Lowell, and YAYOI experiments compared with calculations

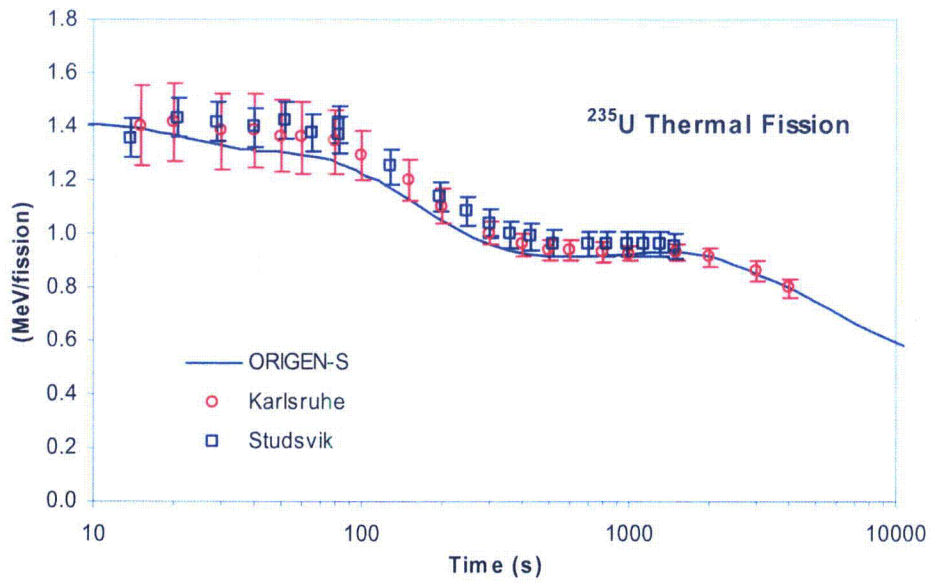


Figure 2.2 Measurements of ^{235}U fission decay heat for an equivalent fission pulse from Karlsruhe and Studsvik experiments compared with calculations

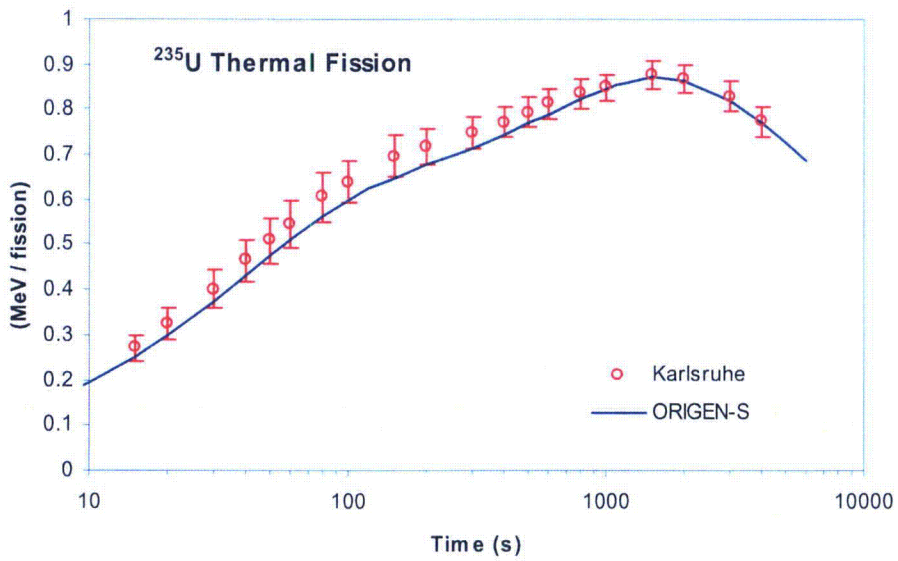


Figure 2.3 Decay heat for ^{235}U fission from Karlsruhe measurements compared with calculations for the experimental 200-s irradiation conditions

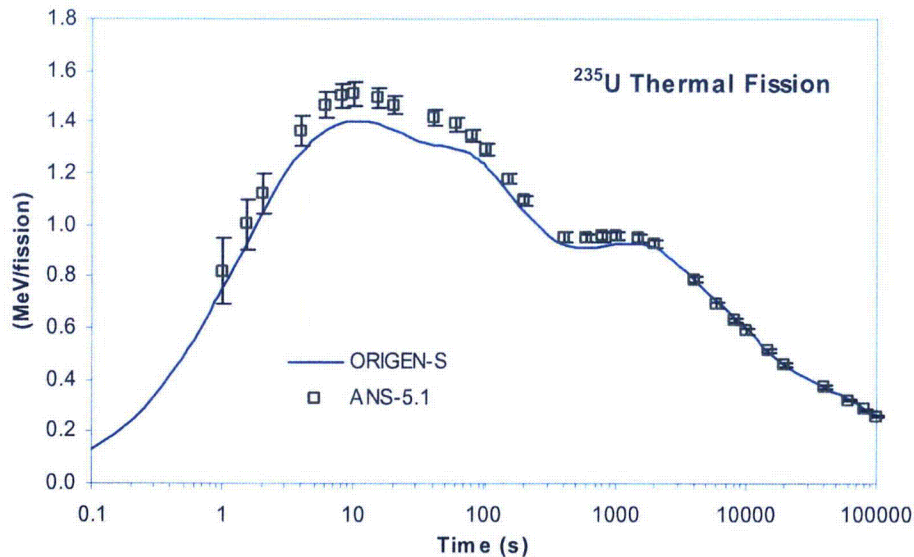


Figure 2.4 Comparison of ^{235}U fission decay heat for a fission pulse as predicted by the ANS-5.1-2005 standard with recommended uncertainties to the ORIGIN-S code result

2.3.2 ^{239}Pu Fission

Decay heat from thermal fission of ^{239}Pu has been measured at ORNL, the University of Tokyo at the YAYOI reactor, and at the University of Massachusetts Lowell. All measurements were performed using spectroscopic techniques. As discussed previously, the YAYOI reactor measurements made by Akiyama et al. were performed for fast neutron irradiation. All other measurements and the ORIGIN-S simulations involved thermal ^{239}Pu fission. The calculated and measured decay heat for ^{239}Pu fission are compared in Figure 2.5. The figure also shows the ratio of the calculated to ORNL-measured values. The calculations are within the range of uncertainty of the measurements except in the cooling time range from about 300 s to 6000 s after fission.

The differences between the decay heat generated for thermal neutron and fast neutron fission is expected to be small, < 1% (Ref. 7), and the fast experimental data (YAYOI) are combined with the thermal measurement data for the purpose of comparison with the calculations.

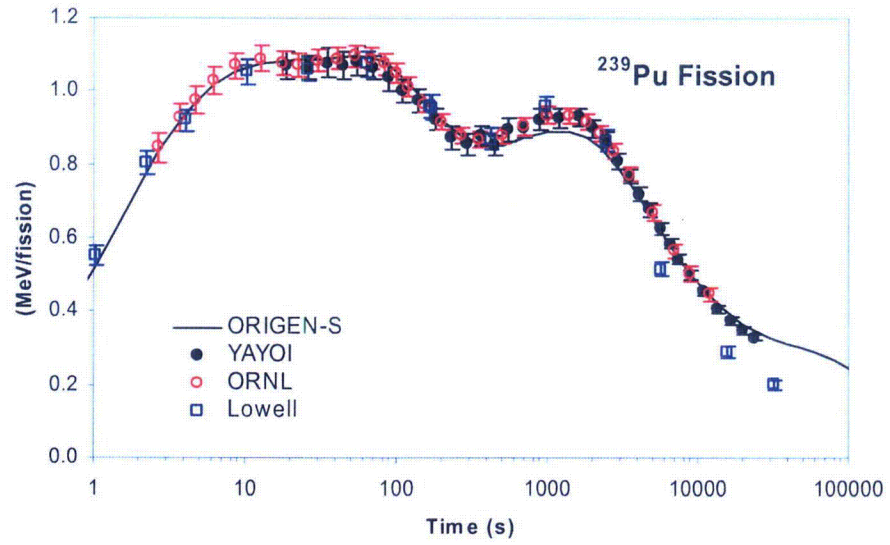


Figure 2.5 Measurements of ^{239}Pu fission decay heat for a fission pulse ORNL, Lowell, and YAYOI experiments compared with calculations

2.3.3 ^{241}Pu Fission

The predicted decay heat following a ^{241}Pu thermal fission is compared with the ORNL measurements in Figure 2.6. No other measurements for ^{241}Pu were found in the literature. The results show agreement within the assigned uncertainty of the measurements for all decay times considered.

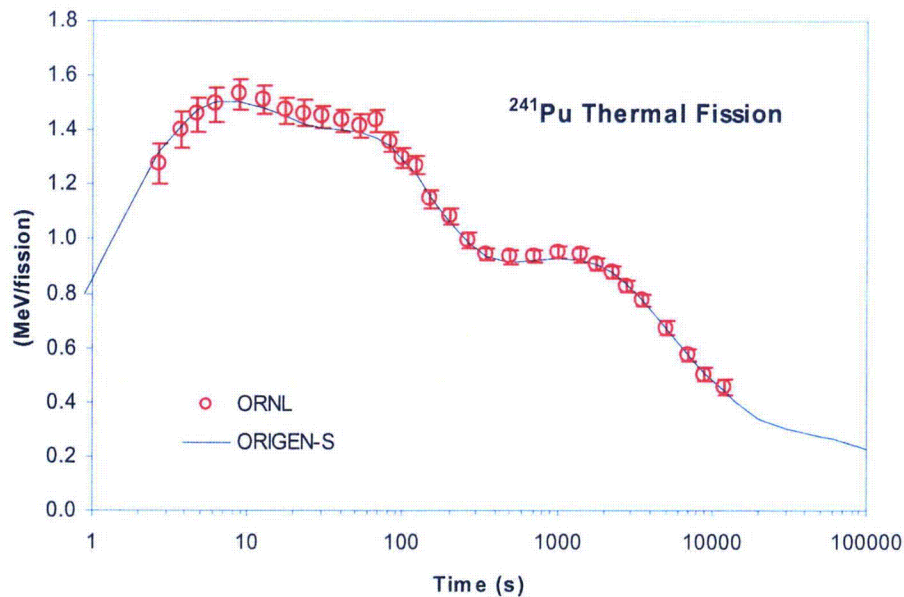


Figure 2.6 Comparison of ^{241}Pu thermal fission decay heat for a fission pulse measured by ORNL with calculations

2.3.4 ^{238}U Fast Fission

Decay heat from fast fission of ^{238}U was measured at the University of Massachusetts Lowell and at the YAYOI reactor facility. The predicted decay heat is compared with the measurement results in Figure 2.7. The Lowell measurements extend down to 0.4 s after fission, well below the range of the YAYOI data. Both sets of measurements are consistent with one another and are in generally good agreement with the predictions. The Lowell results are lower than the YAYOI results for decay times beyond about 5000 s. This is observed in many of the Lowell measurements for longer decay times and, as discussed previously, is attributed to the error in the calculated correction factor applied to account for noble gas loss. Thus, less weight is given to the Lowell results at longer decay times.

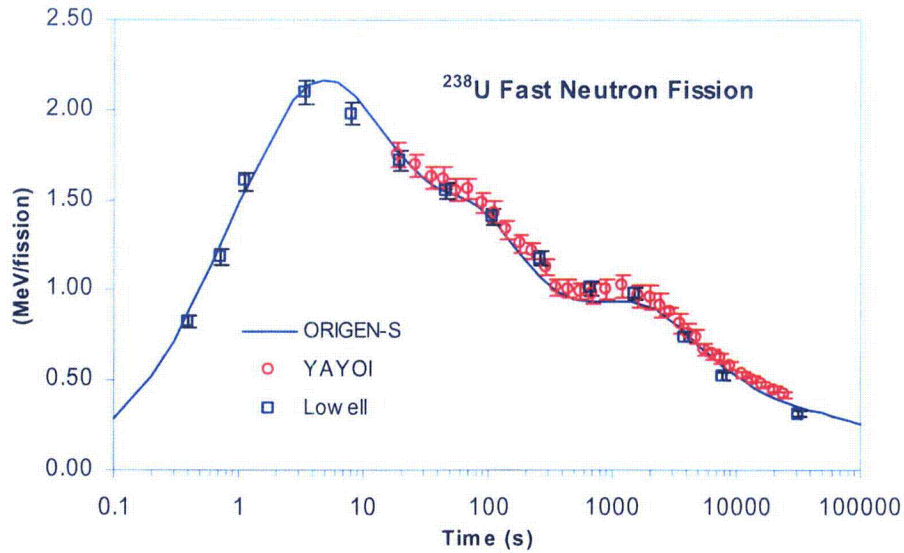


Figure 2.7 Measurements of ^{238}U decay heat for a fast fission pulse compared with calculations

2.3.5 ^{233}U and ^{232}Th Fast Fission

The calculated decay heat following a ^{233}U fast fission pulse event is compared with the YAYOI measurements in Figure 2.8. Similar results for ^{232}Th are presented in Figure 2.9. The ^{232}Th results exhibit a small underprediction in the decay heat for decay times less than about 100 s, but the calculations are within the two standard deviation uncertainty assigned to the measurements (95% confidence level). There is also an underprediction of the ^{232}Th results beyond about 6000 s. The ^{233}U results are within the assigned uncertainty of the measurements over the full range of the measurement data. There is a small trend to underpredict the measured ^{233}U results in the time range near 1000 s, as was observed for the ^{239}Pu results.

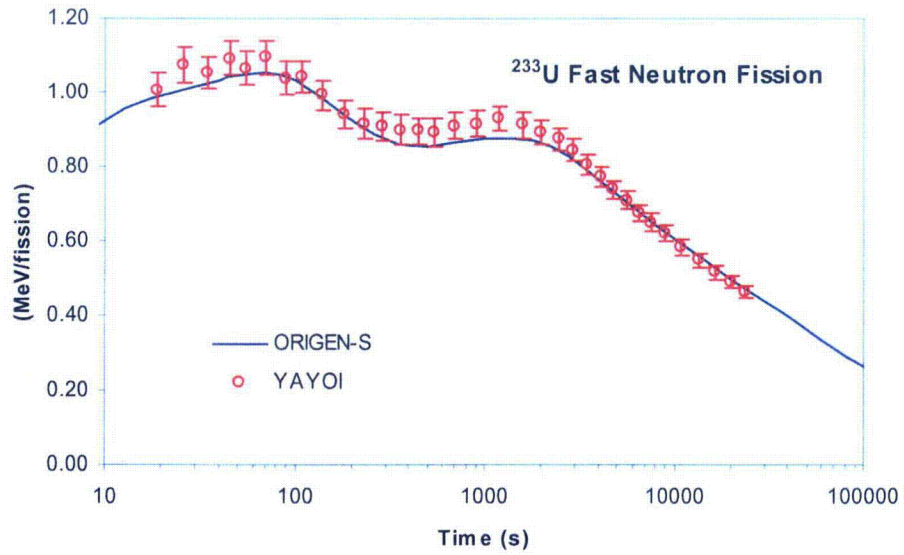


Figure 2.8 Measurements of ^{233}U decay heat (YAYOI fast reactor) for a fast fission pulse compared with calculations

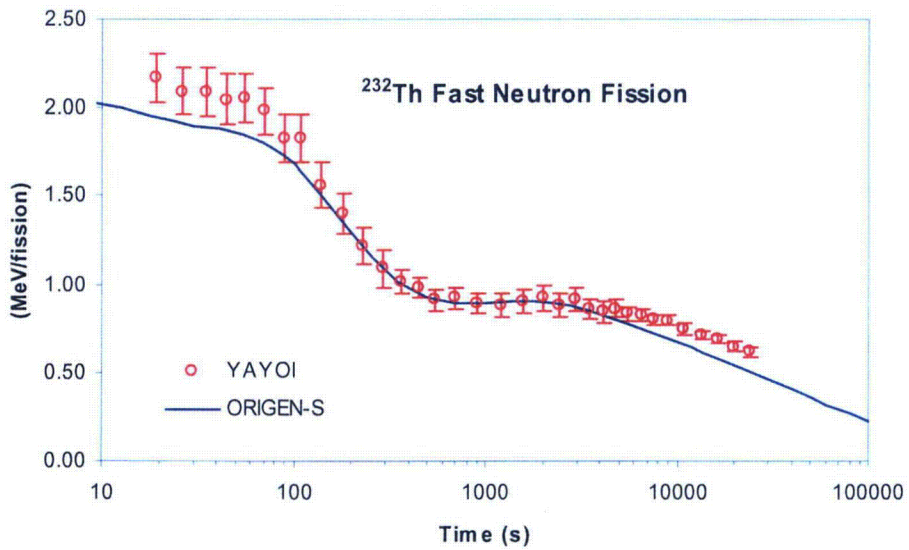


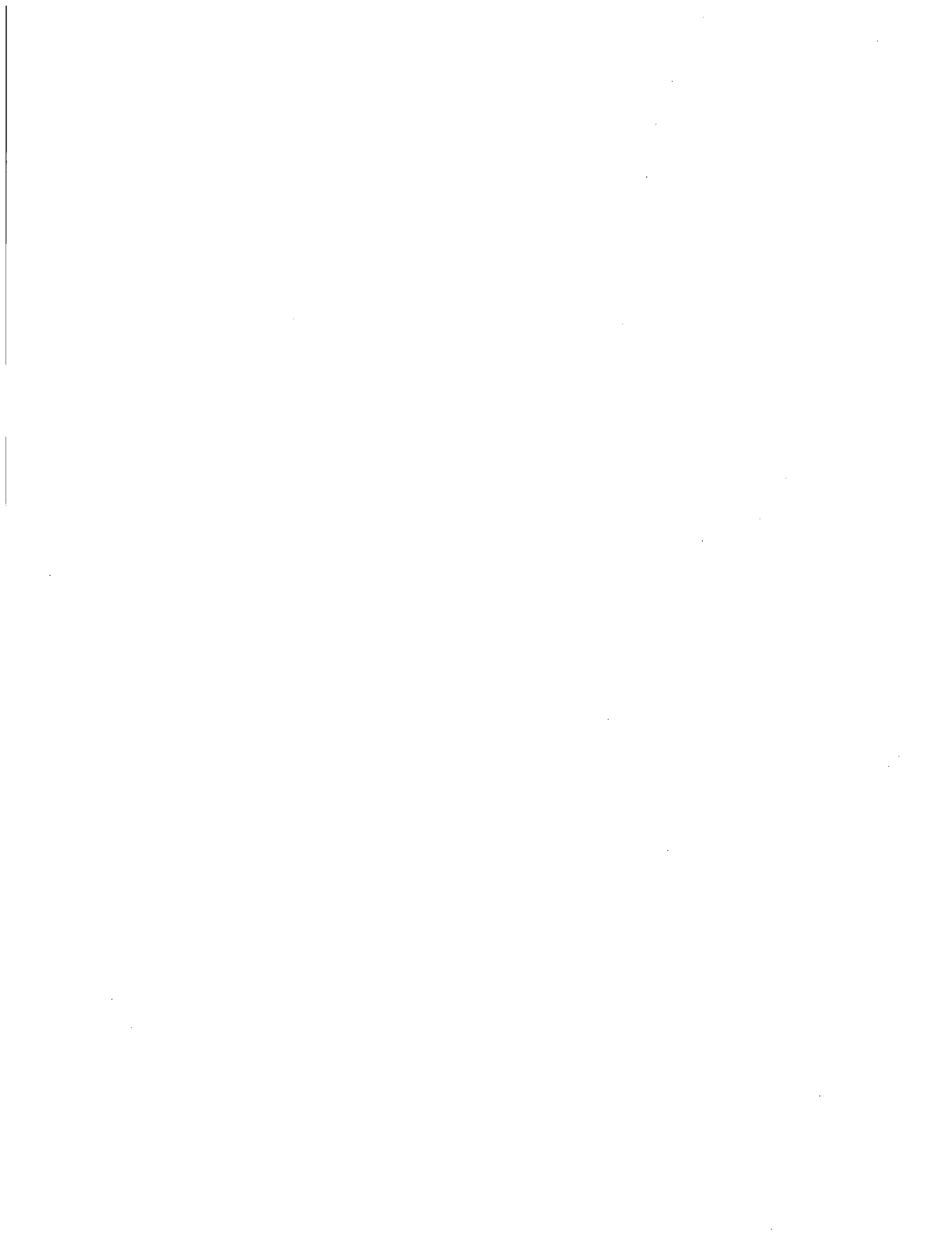
Figure 2.9 Measurements of ^{232}Th decay heat (YAYOI fast reactor) for a fast fission pulse compared with calculations

2.4 Summary of Fission Experiment Results

The predicted total energy release rate following the fission of ^{233}U , ^{235}U , ^{238}U , ^{239}Pu , ^{241}Pu , and ^{232}Th is generally seen to be within the range of experimental uncertainty over the range of the measured data. The independent measurements themselves also exhibit a remarkable consistency with one another. Nevertheless, it is noted that some earlier calorimeter measurements, not included in this study, yield systematically larger values of decay heat than the spectroscopic measurements that were considered for the present study. A separate analysis of the calorimetric and spectroscopic determinations of decay heat using least square methods by Tobias⁶ suggests that the calorimeter results are systematically larger by about 1–2% over the range of the data, but that the difference is not significant at the 95% confidence level.

The results presented here are generally consistent with other calculations using modern decay data.^{22,23} A trend to underpredict the energy release for ^{239}Pu fission after 10^3 s is observed in most simulations. Investigations comparing the separate contributions of gamma-ray energy and beta energy (available with the spectroscopic measurements) attribute the discrepancy to an error in the gamma contribution likely due to either the evaluated decay scheme or the gamma energy per decay.²³ Regarding the current level of discrepancy between measurements and predictions, it has been suggested by Dickens,²⁴ that further experiments at the present measurement uncertainty level are unlikely to resolve the small differences presently observed between predictions and measurements and that more effort is likely needed in research into decay schemes for the short-lived fission products. Work to improve the fundamental decay data used in these calculations has been initiated through the Organization for Economic Cooperation and Development, Nuclear Energy Agency (OECD/NEA) Working Party on International Nuclear Data Evaluation Cooperation (WPEC) Fission Product Decay Heat Subgroup 25.²⁵

A quantitative uncertainty analysis of the decay heat benchmark results for the fission experiments was beyond the scope of this report. Additional work in this area will be performed in the context of future development of the ANS-5.1 Standard. Nevertheless the present results demonstrate that the ORIGEN-S calculations are generally within the uncertainty range of the experimental data measured by spectroscopic techniques for most of the fissionable nuclides of importance to short-term decay heat in commercial and research reactor fuels.



3. ASSEMBLY MEASUREMENTS

Decay heat measurements of full-length spent fuel assemblies performed at two separate U.S. facilities have been reported: (1) using a pool calorimeter located at the General Electric Morris Operations (GE-Morris) spent fuel storage facility in Morris, Illinois, and (2) using a boil-off calorimeter operated at the Engine Maintenance Assembly and Disassembly (EMAD) facility located on the Nevada Test Site of Hanford Engineering Development Laboratory (HEDL). Decay heat was measured for fuel assemblies discharged from San Onofre 1, Point Beach, and Turkey Point PWRs, and from the Dresden, Cooper and Monticello BWRs. In total, measurements for 65 different assemblies at the GE-Morris and HEDL calorimeters have been reported, with multiple measurements performed on many of these assemblies.

More recent calorimeter measurements of fuel assemblies were performed at the Swedish Central Interim Storage Facility for Spent Fuel (CLAB), located in Oskarshamn, Sweden. This project, managed by SKB, has established a large database of spent fuel measurements and will continue to perform measurements in the future to ensure that changes in the decay heat are accurately simulated over time. The measurements performed to date include 39 BWR assemblies and 34 PWR assemblies from Barsebäck, Ringhals, Forsmark, and Oskarshamn nuclear power plants in Sweden. The following sections present a brief summary of the assembly measurements and describe the calorimeters operated at each of the three measurement facilities mentioned above.

3.1 Facility Descriptions

3.1.1 Hanford Engineering Development Laboratory

The Hanford Engineering Development Laboratory fuel assembly calorimeter²⁶ operated at the Engine Maintenance Assembly and Disassembly facility on the Nevada Test Site was designed by Pacific Northwest Laboratory to measure intact PWR and BWR spent fuel assemblies with decay heat rates in the range of 0.1 to 2.5 kW. The accuracy of the measurements was estimated to be $\pm 5\%$ for decay heat rates greater than about 1000 W, and $\pm 10\%$ at 100 W. The calorimeter is comprised of a double-walled stainless steel vessel approximately 5.49 m in length. The inner wall of the vessel supports a lead shield that acts to capture and account for the leakage of gamma decay energy from the calorimeter. The calorimeter system is illustrated in Figure 3.1.

The HEDL calorimeter measures decay heat by evaluating differential steam condensate collection rates, and is referred to as a boil-off type calorimeter. The calorimeter is first filled with water and brought to boiling conditions using a precision internal heater. When equilibrium steam condensate collection rate is established, the spent fuel assembly is placed within the calorimeter vessel and a boiling equilibrium condition is then reestablished with the combined heat inputs of the assembly and the vessel heater. The decay heat from the assembly is then determined directly from the differential condensate collection rate of the initial reference state and the final equilibrium state.

Decay heat measurements using the HEDL calorimeter were reported for four Westinghouse design 15×15 fuel assemblies from the Turkey Point reactor.^{27,28} Cooling times for these assemblies were approximately 2.5 years, and the discharge burnups were all between 26 and 28 GWd/MTU.

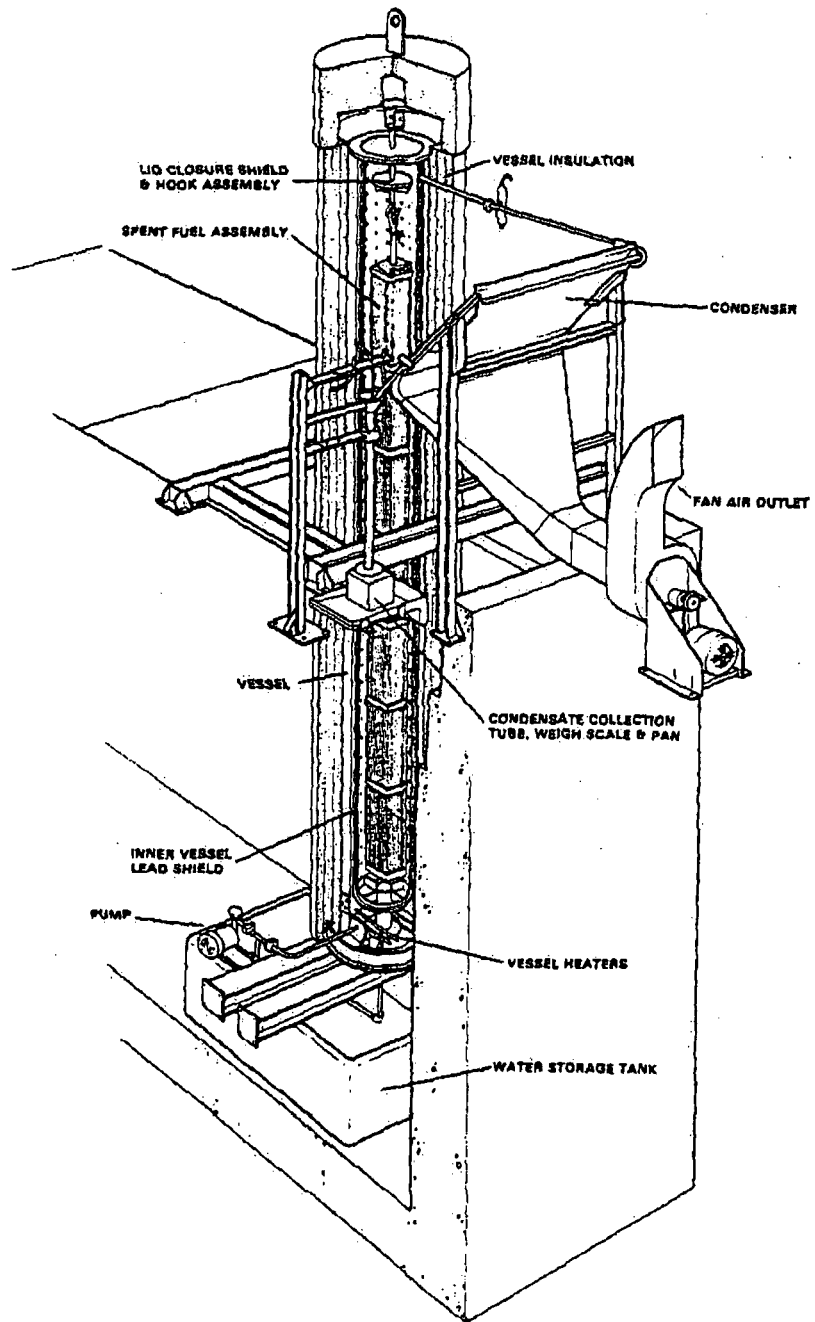


Figure 3.1 HEDL Spent Fuel Calorimeter
(Source: Schmittroth et al., Ref. 27)

3.1.2 GE-Morris Operation

The majority of spent fuel assembly decay heat measurements performed in the United States were made at a calorimeter operated at the GE-Morris Operation facility.²⁹ The calorimeter, located underwater in the spent fuel storage bay, consists of two concentric carbon steel pipes separated by urethane foam insulation to reduce heat loss to the pool. The calorimeter, shown schematically in Figures 3.2 and 3.3, is 4.6 m long (excluding the detachable head assembly). The calorimeter contains inserts for PWR and BWR fuels that maintain the assemblies in a centered position. Fuel assemblies are loaded into the calorimeter through the vessel head in a procedure similar to loading a fuel transport cask, then the head is installed, and a leak check is performed.

The principal method used to determine the thermal output of the assembly, referred to as static mode, is to measure the rate of the water temperature increase inside the vessel. The relationship between the rate of temperature rise and the thermal output is determined by calibration using an electric heater assembly. A second method, referred to as recirculation mode, involves circulating water through the vessel and determining the thermal output from the temperature change of the water flowing through the vessel and the rate of water flow. This second method was used early in the program but was not widely employed because it was found to be less reliable than the static mode of operation. The temperature rise in the vessel is measured using a series of platinum resistance temperature detectors (RTDs) mounted on the assembly insert, vessel wall, and at the inlet and outlet valves. The decay energy escaping the calorimeter as gamma radiation is measured using gamma ray detectors located at several elevations along the calorimeter's surface.

The systematic error associated with the static-mode calorimeter measurements was estimated to be about $\pm 2\%$ for a thermal output of about 700 W, increasing to $\pm 4\%$ in the 200-W range. The random error associated with the repeatability of measurements for the same assembly was determined in test runs involving 14 measurements of Cooper assembly CZ205 over an 8-month period³⁰ and yielded a random error of about $\pm 4.3\%$. The decay heat output of assembly CZ205 at the time of the test measurements was in the 300-W range.

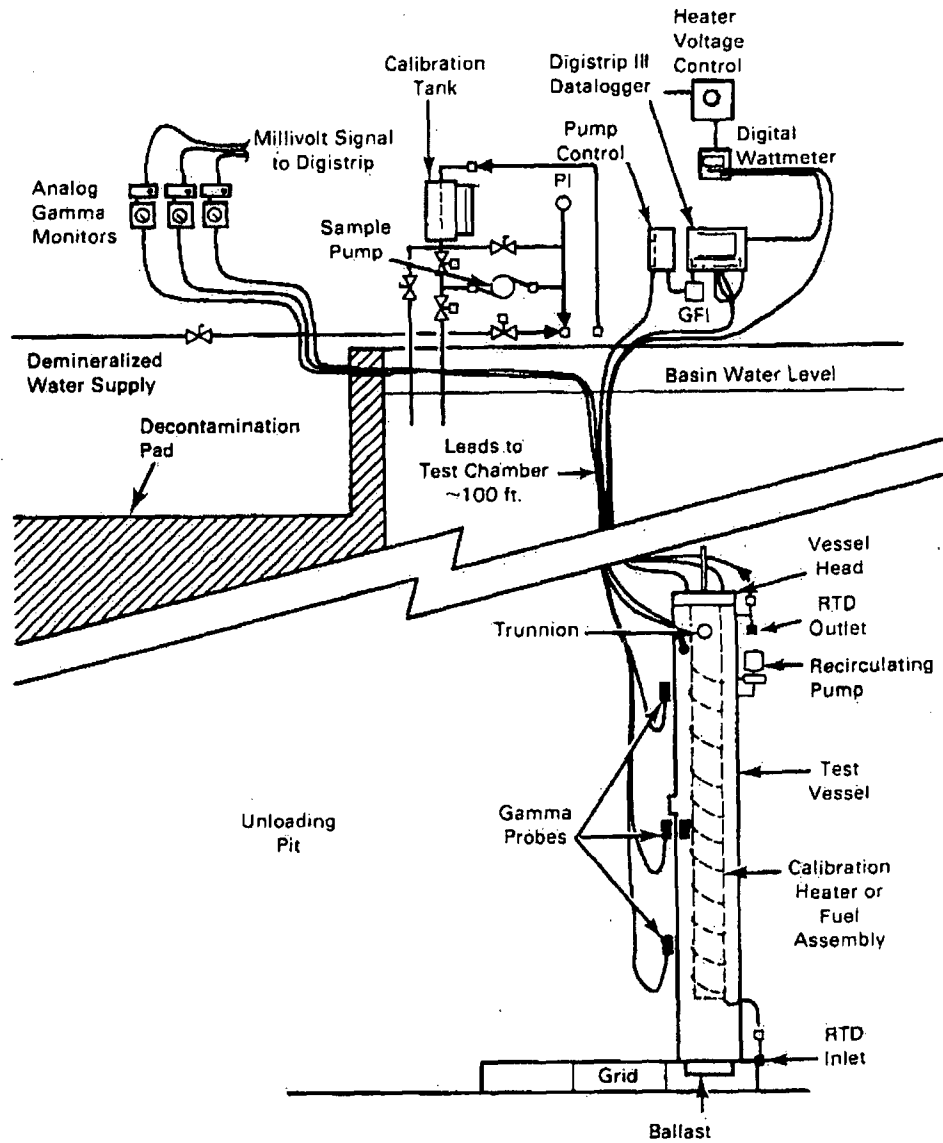


Figure 3.2 Schematic of GE-Morris calorimeter system components
 (Source: McKinnon et al., Ref. 30)

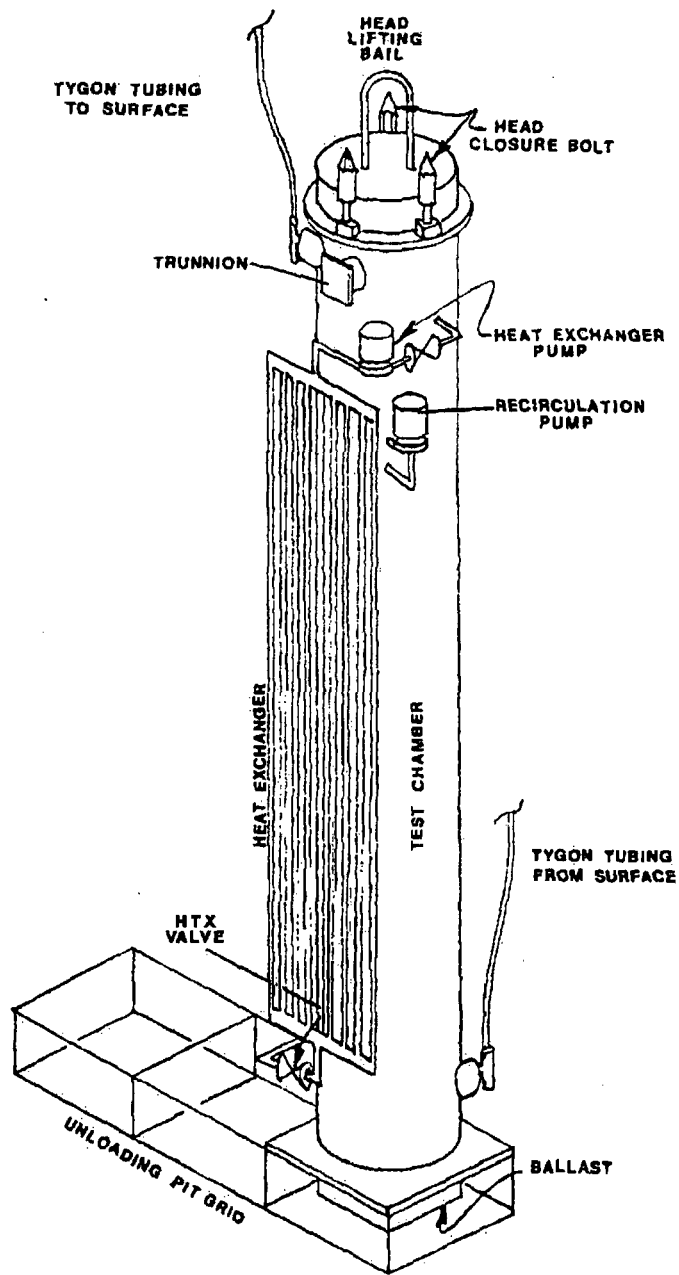


Figure 3.3 Isomeric view of GE-Morris calorimeter
 (Source: Judson et al., Ref. 29)

3.1.3 Swedish Central Interim Storage Facility for Spent Fuel

The Swedish Nuclear Fuel and Waste Management Co., SKB, operates the Central Interim Storage Facility for Spent Fuel, known as CLAB, on the east coast of Sweden near the site of the Oskarshamn nuclear power plant. To support the characterization of the spent fuel inventory at CLAB, SKB has constructed a spent fuel assembly calorimeter and performed measurements for use in validating computer code predictions of decay heat. Measurements on selected fuel assemblies are to be repeated at intervals in the future, and additional assemblies may be added as required to validate computer code predictions over the range of fuel inventory at CLAB.⁵

The design of the calorimeter at CLAB is based on the calorimeter design used at GE Morris Operation. The calorimeter is 4.9 m long and composed of two concentric pipes separated by polyurethane foam to provide insulation between the interior vessel and the pool water. There is a fixed insert for PWR fuel assemblies and a removable insert for BWR assemblies used to maintain the fuel assembly in a centered and vertical position in the calorimeter. Temperatures within the calorimeter are measured by 16 PT-100 type sensors: eight sensors in the water inside the vessel; two sensors on the inside and outside surfaces of the calorimeter; and two sensors outside the calorimeter to measure the pool water temperature. There are five gamma monitors positioned to measure the radial distribution of gamma radiation that escapes the calorimeter, and this information is used to correct the calorimeter data for gamma energy loss.

The calorimeter is generally operated in static mode using the rate of water temperature increase to establish the thermal output of the assemblies. The calorimeter can also be operated using recirculation mode (measurement of temperature difference between inlet and outlet) and in an equilibrium mode whereby the equilibrium temperature is reached without circulation. However, both of these latter methods require substantially longer measurement times than the static mode. In static mode the decay heat is evaluated by comparing the temperature increase to a calibration curve established using an electric heated assembly prior to each measurement campaign. The calibration curves are made for a series of power levels that allow the rate of temperature rise to be determined as a function of assembly decay heat. The decay heat established by the measurements is then corrected for energy loss from gamma rays escaping from the calorimeter using data from the external gamma detectors. The calorimeter, located in the spent fuel pool, is shown in Figure 3.4.

The design target accuracy for the calorimeter was about $\pm 2\%$ at the 95% confidence level. The random error associated with the measurements, based on the final design of the calorimeter, was estimated by SKB as a function of decay heat rate: for a low thermal output of about 50 W, the estimated 95% error is ± 4.5 W, or 9%. For a thermal output of about 300 W, the error is about ± 8 W or 2.7%, decreasing relatively to ± 15.5 W or 1.7% at 900 W of generated heat. The actual random error was made using eight repeat measurements of Ringhals-1 8×8 assembly 6432 over a 9-month period. The standard deviation of the data is about 0.9% for the average decay heat value of 185 W over the measurement period. This yields a 95% confidence error of less than 2% which is less than the estimated error. Evaluation of other repeat measurements for six of the BWR assemblies and four of the PWR assemblies yielded a standard deviation for this group of assemblies to be 3.94 W. For the BWR assemblies only, the value was 1.4 W, and for the PWR assemblies it was 5.8 W. These results are consistent with the random error estimated by SKB. The uncertainty analysis described includes only random sources of uncertainty and does not address potential sources of systematic bias.

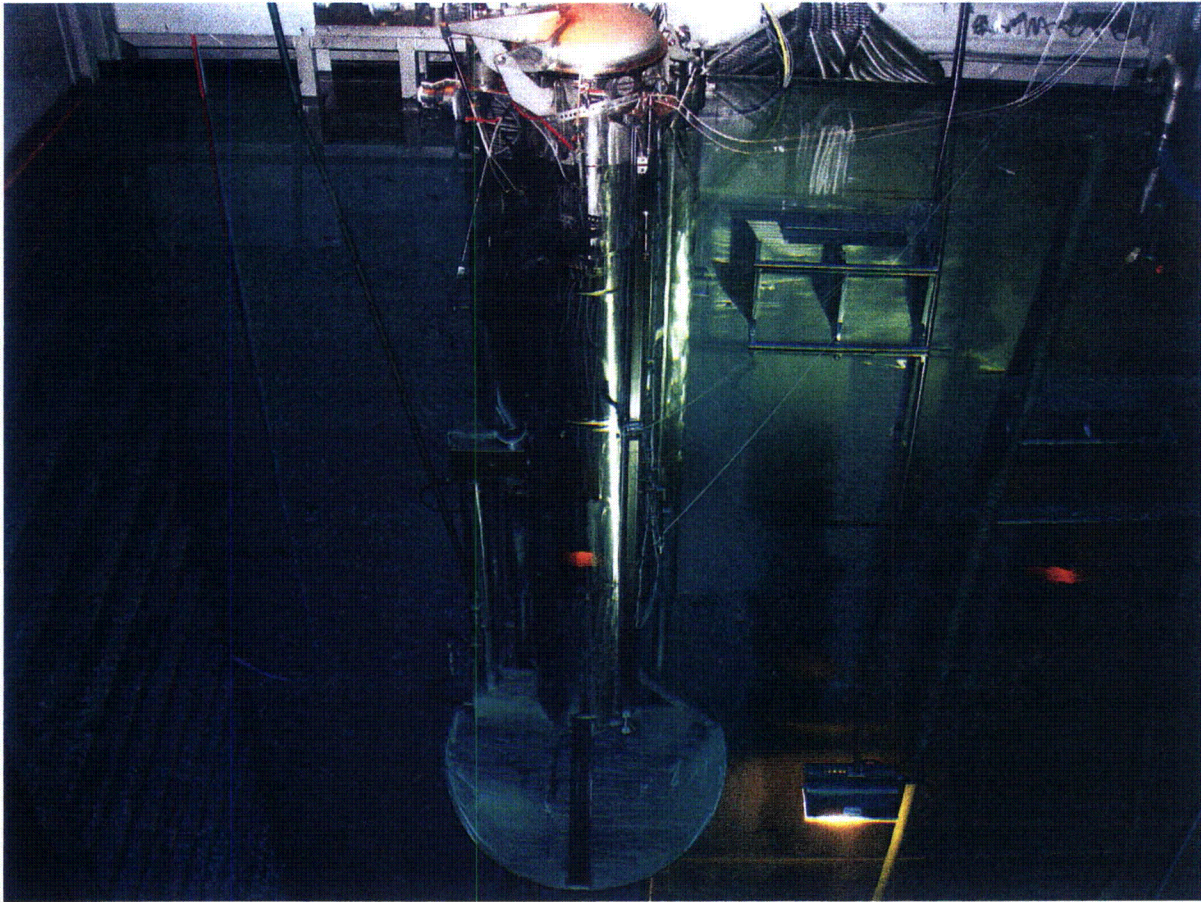


Figure 3.4 Spent fuel assembly calorimeter at the Swedish CLAB facility located at poolside and raised to show the assembly loading hatch above the water level

3.2 Summary of Measurements

A comprehensive summary of measurements performed in the U.S. has been compiled by Roddy and Mailen.³¹ These measurements, performed at the HEDL and GE-Morris Operation facilities, include spent fuel from San Onofre 1, Point Beach 2, Turkey Point 3, Dresden, Cooper and Monticello nuclear plants. The measurements of the Monticello assemblies, performed at the GE-Morris facility in 1985, represent the last measurements performed in the United States. No measurements have been reported after this date, and the calorimeters have since been decommissioned.

Table 3.1 summarizes general information on the fuel assemblies measured at each facility, including assembly design, range of fuel enrichment, and maximum assembly burnup. The number of measurements is actually greater than the number of different assemblies indicated in the table because many of the assemblies were remeasured at different decay times.

Several rebuilt fuel assemblies (reconfiguration or replacement of the fuel rods in the assembly) were measured at the CLAB facility. However, because the details of the rebuilds were not available at this time, these assemblies (not included in the data shown in Table 3.1) were excluded in the present analysis.

Table 3.1 Summary of evaluated fuel assembly decay heat measurements

Measurement facility	Reactor	Fuel design	Enrichment(s) (wt % ²³⁵ U)	Number of assemblies measured	Maximum burnup (MWd/MTU)
GE-Morris	San Onofre 1	W 14 × 14S ^a	3.865 – 4.005	8	32,363
	Point Beach 2	W 14 × 14	3.397	6	39,384
	Dresden 2	GE 7 × 7	2.128	1	5,280
	Cooper	GE 7 × 7	1.1, 2.50	54	28,048
	Monticello	GE 7 × 7	2.25	6	20,189
HEDL (EMAD)	Turkey Point	W 15 × 15	2.557	4	28,588
Swedish CLAB	Barsebäck 1	8 × 8	2.922 – 2.953	2	41,127
	Barsebäck 2	8 × 8	3.154	1	40,010
	Forsmark 1	8 × 8	2.090 – 2.970	2	34,193
	Forsmark 1	9 × 9	2.938	3	37,896
	Forsmark 2	8 × 8	2.095	1	19,944
	Forsmark 2	SVEA-64	2.850 – 2.920	3	32,837
	Forsmark 3	SVEA-100	2.770	2	31,275
	Oskarshamn 2	8 × 8	2.201 – 2.875	7	34,893
	Oskarshamn 2	SVEA-64	2.902	1	46,648
	Oskarshamn 3	8 × 8	2.577	1	35,619
	Oskarshamn 3	SVEA-100	2.711	2	40,363
	Ringhals 1	8 × 8	2.640, 2.911	9	44,861
	Ringhals 2	15 × 15	3.095 – 3.252	16	50,962
	Ringhals 3	17 × 17	2.100 – 3.404	14	47,308

^a Stainless steel cladding.

4. FUEL ASSEMBLY DATA

This section presents fuel design information and reactor operating data in sufficient detail to allow an independent evaluation of the decay heat measurements analyzed in this report. Additional and more detailed information is available from the primary references cited. The fuel design data are used to prepare physics models of the assemblies (presented in Sect. 5) with modules of the SCALE 5 code system from which assembly cross-section libraries are generated for the ORIGEN-S fuel depletion analyses. The measurement data are summarized in Appendix A, and the analysis of the measurements are presented in Sect. 6 along with the results computed using the ORIGEN-S code.

4.1 Assembly Designs—U.S. Measurements

The description of the measured assemblies from the San Onofre, Turkey Point, Point Beach, Cooper, Dresden, and Monticello reactors was obtained from a number of different sources. A common source of information for all U.S.-origin fuel was the data compiled by the Energy Information Administration (EIA) of the U.S. Department of Energy (DOE) in Nuclear Fuel Data survey Form RW-859.³² The information collected on Form RW-859 contains data on every fuel assembly irradiated in commercial nuclear reactors operating in the United States. The data are considered in the design and operation of the equipment and facilities that will be used by DOE for the future acceptance, transport, and disposal of all domestic spent fuel.

The specific fuel data from RW-859 used in this study included the assembly type, version (EIA code), initial uranium mass, enrichment, discharge cycle, and discharge burnup as reported by the utilities. Table 4.1 gives a summary of all U.S. fuel measurements evaluated in this study.

4.1.1 San Onofre 1 Assemblies

Decay heat measurements performed at the GE-Morris facility are reported for eight spent fuel assemblies from the San Onofre Unit 1 PWR reactor in report NEDG-24922-3 (Ref. 29). Fuel information and detailed operating history data are reported separately by Schmittroth in report HEDL-TME 83-32 (Ref. 28). The assemblies were all Westinghouse 14×14 design. The information in RW-859 identifies the assembly version as EIA code XSO14W. The design specifications for this assembly were obtained from a DOE report on the characteristics of potential repository waste DOE/RW-0184 (Ref. 33). The assembly design data used for the calculations are given in Table 4.2. The fuel rod configuration of the assembly, based on models used in Ref. 34, is illustrated in Figure 4.1.

The San Onofre fuel assemblies used Type 304 stainless steel cladding. Activated cobalt in the steel cladding is an important component of the decay heat during the timeframe of the measurements and must be taken into account. The mass of the stainless steel guide tubes is given as 7.2 kg per assembly in DOE/RW-0184, Vol. 3 (Ref. 33). The mass of the stainless steel cladding for the 180 fuel rods is calculated as 59.1 kg, yielding a total steel mass of 66.3 kg per assembly. This value is significantly less than the 150-kg mass used in HEDL TME-83-32 (Ref. 28). This difference may be a result of the previous calculations including components located away from the fueled sections of the assembly. However, since the flux decreases dramatically with distance from the fuel region, it is not appropriate to include these components at their actual mass. Because the fraction of activation occurring in these regions is small compared with that in the fuel region, only the amounts of steel associated with the cladding and guide tube structures were included in the present calculations. A cobalt impurity level of 800 ppm in stainless steel was assumed, a value obtained from DOE/RW-0184. The other constituents of the stainless steel are listed in Table 4.3, although cobalt is the dominant impurity in terms of the contribution to decay heat. Inconel-718, also present in the assembly as spacers and a hold-down spring,

was not included because of its relatively low importance as compared with the cladding and guide tubes. The total amount of cobalt present in the assembly cladding and guide tubes was estimated to be 53 g.

The fuel assembly irradiation data for the measured fuel assemblies designated C-01, C-16, C-19, C-20, D-01, D-46, E-18 and F-04 were obtained from Schmittroth²⁸ and are listed here in Table 4.4. The assembly irradiation data in Table 4.4 are consistent with the discharge burnup from RW-859.

Table 4.1 Summary of fuel data for U.S. assembly measurements

No.	Reactor	Assembly type	Assembly ID	Enrichment (wt % ²³⁵ U)	Uranium (kg)	Discharge burnup (MWd/MTU)	Measurement facility
1	Cooper	GE 7 × 7	CZ102	1.090	195.48	11,667	GE-Morris
2	Cooper	GE 7 × 7	CZ147	2.500	190.31	26,709	GE-Morris
3	Cooper	GE 7 × 7	CZ148	2.500	190.22	26,310	GE-Morris
4	Cooper	GE 7 × 7	CZ182	2.500	190.09	26,824	GE-Morris
5	Cooper	GE 7 × 7	CZ195	2.500	190.68	26,392	GE-Morris
6	Cooper	GE 7 × 7	CZ205	2.500	190.72	25,344	GE-Morris
7	Cooper	GE 7 × 7	CZ209	2.500	190.38	25,383	GE-Morris
8	Cooper	GE 7 × 7	CZ211	2.500	190.82	26,668	GE-Morris
9	Cooper	GE 7 × 7	CZ222	2.500	190.90	26,692	GE-Morris
10	Cooper	GE 7 × 7	CZ225	2.500	190.51	25,796	GE-Morris
11	Cooper	GE 7 × 7	CZ239	2.500	189.57	27,246	GE-Morris
12	Cooper	GE 7 × 7	CZ246	2.500	189.81	27,363	GE-Morris
13	Cooper	GE 7 × 7	CZ259	2.500	190.20	26,466	GE-Morris
14	Cooper	GE 7 × 7	CZ264	2.500	190.89	26,496	GE-Morris
15	Cooper	GE 7 × 7	CZ277	2.500	189.49	26,748	GE-Morris
16	Cooper	GE 7 × 7	CZ286	2.500	189.95	27,141	GE-Morris
17	Cooper	GE 7 × 7	CZ296	2.500	190.50	26,388	GE-Morris
18	Cooper	GE 7 × 7	CZ302	2.500	190.00	26,594	GE-Morris
19	Cooper	GE 7 × 7	CZ308	2.500	189.78	25,815	GE-Morris
20	Cooper	GE 7 × 7	CZ311	2.500	189.91	27,392	GE-Morris
21	Cooper	GE 7 × 7	CZ315	2.500	189.96	26,881	GE-Morris
22	Cooper	GE 7 × 7	CZ318	2.500	189.32	26,568	GE-Morris
23	Cooper	GE 7 × 7	CZ331	2.500	190.36	21,332	GE-Morris
24	Cooper	GE 7 × 7	CZ337	2.500	189.90	26,720	GE-Morris
25	Cooper	GE 7 × 7	CZ342	2.500	190.16	27,066	GE-Morris
26	Cooper	GE 7 × 7	CZ346	2.500	190.23	28,048	GE-Morris
27	Cooper	GE 7 × 7	CZ348	2.500	190.38	27,481	GE-Morris
28	Cooper	GE 7 × 7	CZ351	2.500	190.02	25,753	GE-Morris
29	Cooper	GE 7 × 7	CZ355	2.500	190.60	25,419	GE-Morris
30	Cooper	GE 7 × 7	CZ357	2.500	190.19	27,140	GE-Morris
31	Cooper	GE 7 × 7	CZ369	2.500	190.20	26,576	GE-Morris
32	Cooper	GE 7 × 7	CZ370	2.500	190.23	26,342	GE-Morris
33	Cooper	GE 7 × 7	CZ372	2.500	190.01	25,848	GE-Morris
34	Cooper	GE 7 × 7	CZ379	2.500	190.18	25,925	GE-Morris
35	Cooper	GE 7 × 7	CZ398	2.500	189.83	27,478	GE-Morris
36	Cooper	GE 7 × 7	CZ415	2.500	189.72	25,863	GE-Morris
37	Cooper	GE 7 × 7	CZ416	2.500	189.43	27,461	GE-Morris
38	Cooper	GE 7 × 7	CZ429	2.500	190.07	27,641	GE-Morris

Table 4.1 Summary of fuel data for U.S. assembly measurements (continued)

No.	Reactor	Assembly type	Assembly ID	Enrichment (wt % ²³⁵ U)	Uranium (kg)	Discharge burnup (MWd/MTU)	Measurement facility
39	Cooper	GE 7 × 7	CZ430	2.500	189.93	26,825	GE-Morris
40	Cooper	GE 7 × 7	CZ433	2.500	190.02	25,977	GE-Morris
41	Cooper	GE 7 × 7	CZ460	2.500	190.18	26,512	GE-Morris
42	Cooper	GE 7 × 7	CZ466	2.500	189.86	26,077	GE-Morris
43	Cooper	GE 7 × 7	CZ468	2.500	189.78	26,757	GE-Morris
44	Cooper	GE 7 × 7	CZ472	2.500	190.12	25,957	GE-Morris
45	Cooper	GE 7 × 7	CZ473	2.500	189.76	26,519	GE-Morris
46	Cooper	GE 7 × 7	CZ498	2.500	189.69	26,482	GE-Morris
47	Cooper	GE 7 × 7	CZ508	2.500	190.68	26,357	GE-Morris
48	Cooper	GE 7 × 7	CZ515	2.500	190.48	25,737	GE-Morris
49	Cooper	GE 7 × 7	CZ526	2.500	190.54	27,596	GE-Morris
50	Cooper	GE 7 × 7	CZ528	2.500	190.81	25,715	GE-Morris
51	Cooper	GE 7 × 7	CZ531	2.500	189.90	26,699	GE-Morris
52	Cooper	GE 7 × 7	CZ536	2.500	190.17	26,715	GE-Morris
53	Cooper	GE 7 × 7	CZ542	2.500	189.99	26,691	GE-Morris
54	Cooper	GE 7 × 7	CZ545	2.500	190.47	26,668	GE-Morris
55	Dresden	GE 7 × 7	DN212	2.130	194.70	5,279	GE-Morris
56	Monticello	GE 7 × 7	MT116	2.250	193.53	18,039	GE-Morris
57	Monticello	GE 7 × 7	MT123	2.250	193.53	13,027	GE-Morris
58	Monticello	GE 7 × 7	MT133	2.250	193.53	20,994	GE-Morris
59	Monticello	GE 7 × 7	MT190	2.250	193.53	15,143	GE-Morris
60	Monticello	GE 7 × 7	MT228	2.250	193.53	12,123	GE-Morris
61	Monticello	GE 7 × 7	MT264	2.250	193.53	9,160	GE-Morris
62	Point Beach 2	W 14 × 14	C-52	3.397	386.54	31,914	GE-Morris
63	Point Beach 2	W 14 × 14	C-56	3.397	386.80	38,917	GE-Morris
64	Point Beach 2	W 14 × 14	C-64	3.397	386.63	39,384	GE-Morris
65	Point Beach 2	W 14 × 14	C-66	3.397	386.54	35,433	GE-Morris
66	Point Beach 2	W 14 × 14	C-67	3.397	386.45	38,946	GE-Morris
67	Point Beach 2	W 14 × 14	C-68	3.397	386.36	37,059	GE-Morris
68	San Onofre 1	W 14 × 14 ^a	C-01	3.865	361.72	26,540	GE-Morris
69	San Onofre 1	W 14 × 14 ^a	C-16	3.865	361.72	28,462	GE-Morris
70	San Onofre 1	W 14 × 14 ^a	C-19	3.865	361.72	30,426	GE-Morris
71	San Onofre 1	W 14 × 14 ^a	C-20	3.865	361.72	32,363	GE-Morris
72	San Onofre 1	W 14 × 14 ^a	D-01	4.005	363.64	31,393	GE-Morris
73	San Onofre 1	W 14 × 14 ^a	D-46	4.005	363.64	32,318	GE-Morris
74	San Onofre 1	W 14 × 14 ^a	E-18	4.005	363.98	32,357	GE-Morris
75	San Onofre 1	W 14 × 14 ^a	F-04	3.996	372.32	30,429	GE-Morris
76	Turkey Point 3	W 15 × 15	B-43	2.559	447.79	25,595	Hanford
77	Turkey Point 3	W 15 × 15	D-15	2.557	456.12	28,430	Hanford
78	Turkey Point 3	W 15 × 15	D-22	2.557	458.00	26,485	Hanford
79	Turkey Point 3	W 15 × 15	D-34	2.557	455.24	27,863	Hanford

^a Stainless steel cladding.

Table 4.2 San Onofre Unit 1 reactor and fuel assembly design information

Parameter	Data
Assembly and reactor data	
Designer	Westinghouse Electric
Lattice geometry	14 × 14
EIA assembly code ^a	XSO14W
Active fuel rod length (cm)	304.8
Uranium mass per assembly (kg)	366 (nominal)
Rod pitch (cm)	1.4122
Number of fuel rods	180
Number of instrument tubes	1
Number of guide tubes	15
Moderator pressure (psia)	2100
Assembly pitch (cm)	19.94
Inlet temperature (K)	562.4
Outlet temperature (K)	586.9
Average moderator temperature (K)	576.5
Moderator density (g/cm ³)	0.7179
Average soluble boron level (ppm)	500
Fuel rod data	
Fuel material type	UO ₂
Fuel pellet density (% TD)	93 (10.19 g/cm ³)
Stack density (g/cm ³)	10.037
Fuel pellet diameter (cm)	0.9741
Fuel rod outside diameter (cm)	1.0719
Effective fuel temperature (K)	810
Clad material	Stainless steel – Type 304
Clad thickness (cm)	0.0419
Inner clad diameter (cm)	0.9881
Average clad temperature (K)	615
Guide tube data	
Guide tube material	Stainless steel – Type 304
Inside diameter (cm)	1.2979
Outside diameter (cm)	1.3589

^a Assigned by Department of Energy Information Administration (EIA) Form RW-859.

- 1 fuel
- 2 clad
- 3 water
- 4 gap
- 5 guide tube

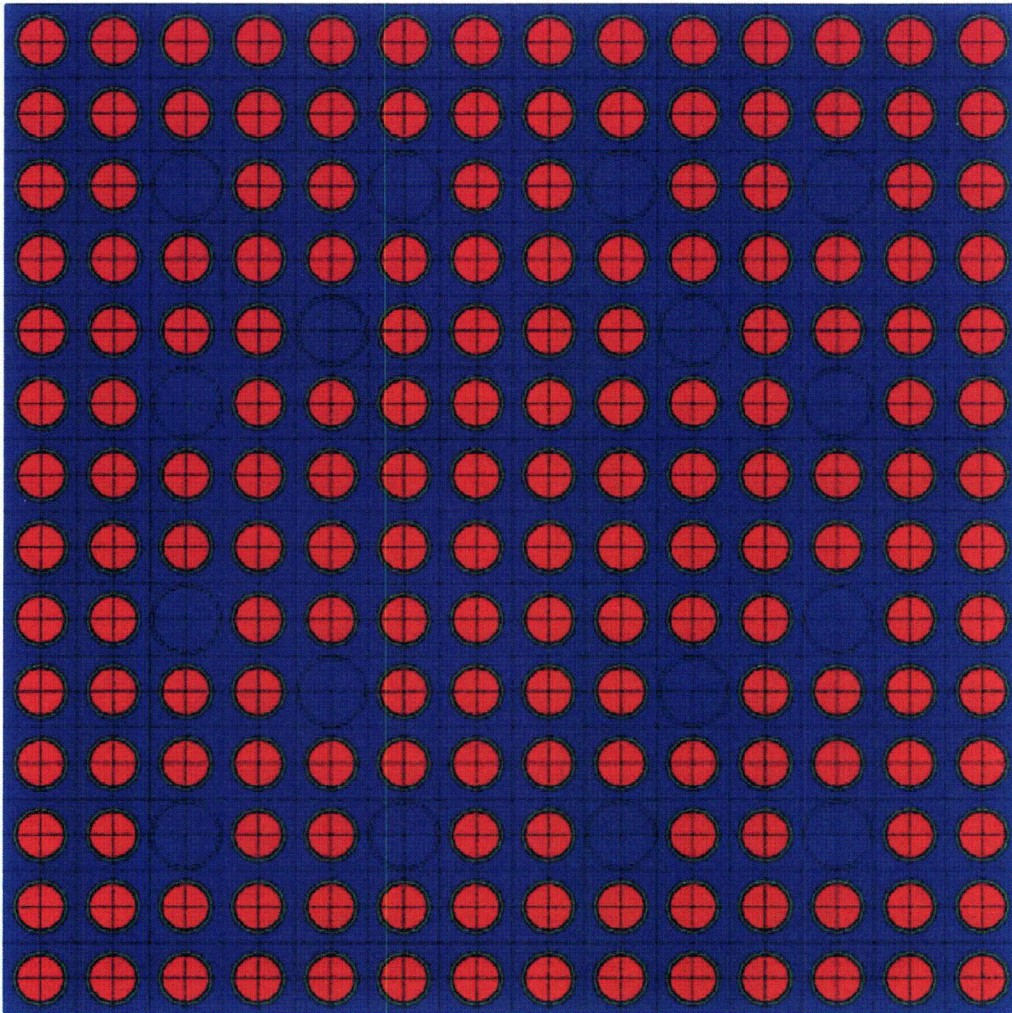


Figure 4.1 Layout of the San Onofre Westinghouse 14×14 assembly

Table 4.3 Stainless steel composition data for San Onofre fuel assemblies

Element	parts per million (ppm) ^a	grams per assembly ^b	kg per MTU ^c
Carbon	800	53	0.146
Nitrogen	1,300	86.1	0.238
Silicon	10,000	662.6	1.830
Phosphorous	450	29.8	0.082
Sulfur	300	19.9	0.055
Chromium	190,000	12,589	34.77
Manganese	20,000	1325	3.66
Iron	697,150	46,193	127.6
Cobalt	800	53.0	0.146
Nickel	89,200	5910	16.33
Niobium	100	6.6	0.018

^a From Table 2.7.3 of reference DOE/RW-0184-R1, Vol. 1 (Ref. 33).

^b Quantities based on nominal 66.3 kg stainless steel per assembly.

^c Metric Ton Uranium (10⁶ g); values assume nominal 363 kg U per assembly.

Table 4.4 San Onofre Unit 1 reactor and assembly irradiation data

Operational data	Cycle 1	Cycle 2	Cycle 3	Cycle 4	Cycle 5	Cycle 6
Startup date	1/27/68	11/20/70	2/24/72	6/30/73	4/23/75	4/04/77
Shutdown date	10/2/70	1/1/72	6/2/73	3/14/75	9/30/76	9/15/78
Operating days	979	407	464	622	526	529
EFPD days ^a	672	384	436	490	522	530
Downtime (days)	49	54	28	40	186	—
Assembly ID	Assembly burnup (MWd/MTU) ^b					
C-01	7,689	16,205	26,540			
C-16	9,077	18,452	28,462			
C-19	11,750	21,372	30,426			
C-20	14,418	23,410	32,363			
D-01		9,738	20,592	31,393		
D-46		10,029	21,055	32,318		
E-18			8,068	19,470	32,357	
F-04				6,883	19,733	30,429

^a EFPD = effective full-power days.

^b Cumulative burnup by cycle.

4.1.2 Turkey Point 3 Assemblies

Decay heat measurements were performed on five spent fuel assemblies from the Turkey Point Unit 3 PWR, operated by Florida Power and Light Company, using the boil-off calorimeter at the HEDL facility. The assemblies, B-43, D-04, D-15, D-22 and D-34, all have an EIA version code W1515WL, corresponding to a Westinghouse 15 × 15 LOPAR design, as shown in Figure 4.2. Decay heat measurements for these assemblies were previously evaluated^{27,28} against code predictions and more recently used to support the development of technical guidance³ for the NRC decay heat regulatory guidance RG 3.54 (Ref. 4).

The Turkey Point fuel and assembly design specifications are listed in Table 4.5. Each assembly contains 18.84 kg of stainless steel Type 304, 4.65 kg of Inconel-718, and 110.0 kg of Zircaloy-4. The reactor cycle information, assembly power, and discharge burnup values were taken from the values cited in the report HEDL-TME 83-32 (Ref. 28). The discharge burnup values differed by several percent (4% in the case of assembly B-43) as compared with the values reported in RW-859. The values from report HEDL-TME 83-32 are similar to those reported by Florida Power and Light Co. and used in the analyses performed in Ref. 3. The reason for the burnup discrepancy for these Turkey Point assemblies, particularly B-43, is unclear. Such discrepancies were not observed for any other assemblies used in this study. The decay times were determined in accordance with the actual date of the measurement and a Cycle 4 discharge date from RW-859 that was slightly different than that used in earlier calculations. The reactor operating history data and assembly burnup are listed in Table 4.6. Structural materials included for activation are listed in Table 4.7.

A measurement of assembly D-04 was rejected in this study. HEDL-TME 83-32 reports that the thermal equilibrium had not been established for the D-04 measurement, thus potentially biasing the measured value low. In addition, report TC-1759 (Ref. 27) indicated that four fuel rods had been removed from this assembly at the time of measurements. Thus, there is additional uncertainty in the results for this particular assembly.

- 1 fuel
- 2 clad
- 3 water
- 4 gap
- 5 guide tube

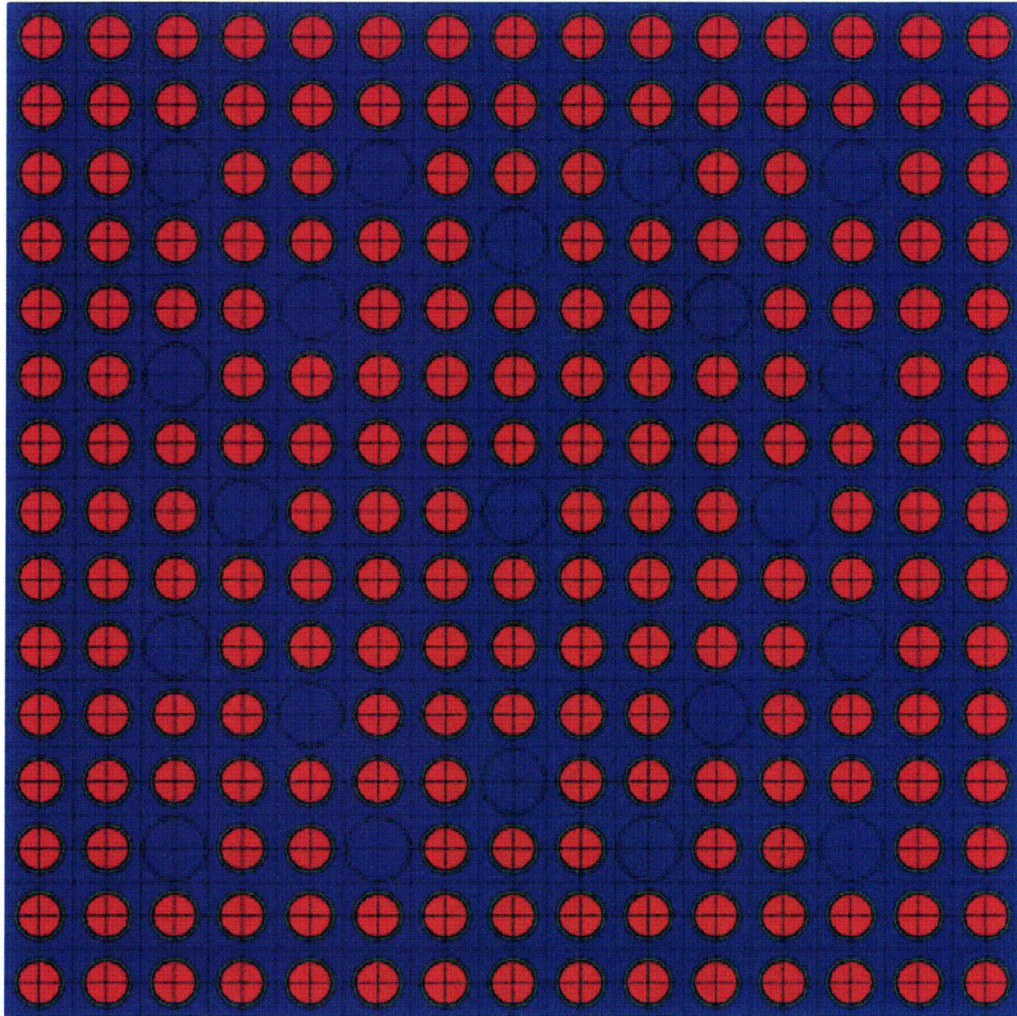


Figure 4.2 Layout of the Turkey Point Reactor Westinghouse 15×15 assembly

Table 4.5 Turkey Point 3 reactor and fuel assembly design information

Parameter	Data
Assembly and reactor data	
Designer	Westinghouse Electric
Lattice geometry	15 × 15
EIA assembly code	W1515WL
Version	LOPAR
Active fuel rod length (cm)	365.8
Uranium mass per assembly (kg)	456 (nominal)
Rod pitch (cm)	1.430
Number of fuel rods	204
Number of instrument tubes	1
Number of guide tubes	20
Moderator pressure (psia)	2100
Assembly pitch (cm)	21.50
Inlet temperature (K)	558.7
Outlet temperature (K)	611.0
Average moderator temperature (K)	570
Moderator density (g/cm ³)	0.7311
Average soluble boron level (ppm)	450
Fuel rod data	
Fuel material type	UO ₂
Fuel pellet density (% TD)	93
Stack density (g/cm ³)	10.19
Fuel pellet diameter (cm)	0.9296
Fuel rod outside diameter (cm)	1.0719
Effective fuel temperature (K)	922
Clad material	Zircaloy-4
Clad thickness (cm)	0.0618
Inner clad diameter (cm)	0.9484
Average clad temperature (K)	595
Guide tube data	
Guide tube material	Zircaloy-4
Inside diameter (cm)	1.3000
Outside diameter (cm)	1.3868

Table 4.6 Turkey Point reactor and assembly irradiation data

Operational data	Cycle 1	Cycle 2	Cycle 3	Cycle 4
Startup date	10/20/1972	12/16/1974	12/23/1975	1/16/1977
Shutdown date	10/4/1974	10/26/1975	11/15/1976	11/24/1977
Operating days	714	314	328	312
Downtime (days)	73	58	62	--
Assembly ID	Assembly Burnup (MWd/MTU)			
B-43	16,493	25,595		
D-15		9,574	19,422	28,430
D-22		10,030	19,081	26,485
D-34		9,571	18,992	27,863

Table 4.7 Activated structural components in Turkey Point and Point Beach assemblies

Element	grams per kg U ^a	kilograms per assembly	
		14 × 14 assembly ^b	15 × 15 assembly ^c
Oxygen	135	52.0	62.0
Chromium	5.9	2.3	2.7
Manganese	0.33	0.13	0.15
Iron	12.9	5.0	5.9
Cobalt	0.075	0.029	0.034
Nickel	9.9	3.8	4.5
Zirconium	221	85.0	101
Niobium	0.71	0.27	0.32
Tin	3.6	1.4	1.6

^a *Source:* NUREG/CR-5625 (Ref. 3).

^b Assumed mass of 389 kg U per assembly.

^c Assumed mass of 456 kg U per assembly.

4.1.3 Point Beach Assemblies

Decay heat measurements were performed at the GE-Morris Operation facility for six spent fuel assemblies from the Point Beach Unit 2 PWR, operated by Wisconsin Electric Power Co. (WEPCO). The results are identified in earlier studies as the WEPCO measurements.^{28,29} The Point Beach reactor assemblies were also previously evaluated in support of technical guidance for the NRC decay heat regulatory guidance RG 3.54 issued in 1999 (Ref. 4). The Point Beach reactor assemblies C-52, C-56, C-64, C-66, C-67, and C-68 have an EIA designation code W1414WL, corresponding to the Westinghouse 14×14 LOPAR design. The LOPAR design is similar to the San Onofre assembly design but has 179 fuel rods (instead of 180) and has a longer active fuel length and thus larger uranium mass.

The fuel and assembly design specifications are listed in Table 4.8. Activated structural assembly constituents are listed in Table 4.7. The fuel rod layout in the assembly is shown in Figure 4.3. The Point Beach assemblies resided in the core during Cycles 1, 2, and 3 and achieved burnup values from 31,914 to 39,384 MWd/MTU. The measurements were performed approximately 4.5 years after discharge. The enrichment of all measured assemblies was 3.397 wt % ²³⁵U. The assembly burnup and reactor operating data are listed in Table 4.9. The reactor operated at near 20% capacity for about the first 40 weeks of Cycle 1. Ascent to full power occurred near the beginning of May 1973. These two phases of operation during Cycle 1 are represented separately as two steps (Cycle 1A and 1B) to more accurately represent the low-power startup operation in the simulations. The assembly burnups for these two phases were derived from the operating times and core-average burnup values from Ref. 28.

Table 4.8 Point Beach reactor and fuel assembly design information

Parameter	Data
Assembly and reactor data	
Designer	Westinghouse
Lattice geometry	14 × 14
EIA assembly code	W1414WL
Version	LOPAR
Active fuel rod length (cm)	365.8
Uranium mass per assembly (kg)	389 (nominal)
Rod pitch (cm)	1.412
Number of fuel rods	179
Number of instrument tubes	1
Number of guide tubes	16
Moderator pressure (psia)	2000
Assembly pitch (cm)	19.82
Inlet temperature (K)	558.0
Outlet temperature (K)	589.0
Average moderator temperature (K)	579
Moderator density (g/cm ³)	0.7115
Average soluble boron level (ppm)	550
Fuel rod data	
Fuel material type	UO ₂
Fuel pellet density (% TD)	93
Stack density (g/cm ³)	9.467
Fuel pellet diameter (cm)	0.9290
Fuel rod outside diameter (cm)	1.0719
Effective fuel temperature (K)	811
Clad material	Zircaloy-4
Clad thickness (cm)	0.0618
Inner clad diameter (cm)	0.9484
Average clad temperature (K)	620
Guide tube data	
Guide tube material	Zircaloy-4
Inside diameter (cm)	1.2827
Outside diameter (cm)	1.3691

- 1 fuel
- 2 clad
- 3 water
- 4 gap
- 5 guide tube

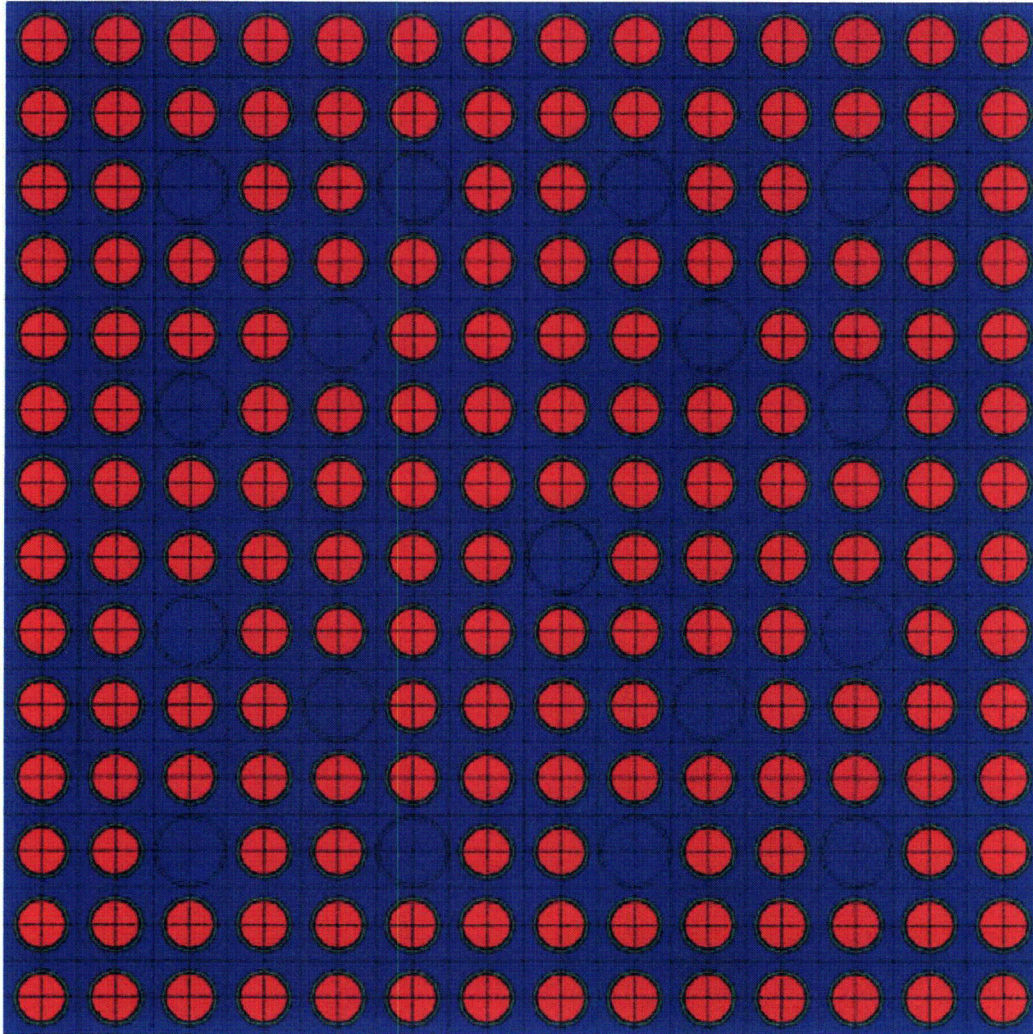


Figure 4.3 Layout of the Point Beach Reactor Westinghouse 14×14 (LOPAR) assembly

Table 4.9 Point Beach reactor operating history data

Operational data	Cycle 1A ^a	Cycle 1B	Cycle 2	Cycle 3
Startup date	8/1/1972	5/1/1973	12/20/1974	3/29/1976
Shutdown date	5/1/1973	10/16/1974	2/26/1976	3/3/1977
Operating days	273	533	433	339
Downtime (days)	0	65	32	--
Assembly ID	Assembly Burnup (MWd/MTU) ^b			
C-52	677	10,801	23,117	31,914
C-56	1,033	16,475	29,356	38,917
C-64	1,061	16,920	29,764	39,384
C-66	732	11,668	24,924	35,433
C-67	1,041	16,600	29,401	38,946
C-68	817	13,034	26,942	37,059

^a Cycle 1 is divided to present initial phase of low-power operation.

^b Cumulative burnup by cycle.

4.1.4 Cooper, Dresden, and Monticello Assemblies

The largest number of decay heat measurements performed for any single assembly design type were for General Electric (GE) 7×7 assemblies from the Cooper, Dresden, and Monticello reactors. All of the GE 7×7 measurements were performed at the GE-Morris facility. Two measurements were made for a single Dresden reactor assembly, 13 measurements for Monticello reactor assemblies, and 81 measurements for assemblies from the Cooper reactor. The RW-859 data indicate that the assemblies from Cooper included two versions of the GE 7×7 assembly; one having an EIA code G4607G2, the other having code G4607G3BD. These codes correspond to GE assembly versions GE-2 and GE-3B, respectively. The assemblies from the Dresden and Monticello reactors – EIA code G2307G2B – were both versions GE-2B.

The fuel assembly design specification for assembly versions GE-2, GE-2B, and GE-3B were obtained from DOE/RW-0184-R1 (Ref. 33) and are listed in Table 4.10. All assemblies have similar dimensions. However, the GE-3 fuel design has increased cladding thickness compared with the GE-2 design to reduce fuel failure caused by clad hydriding. The increase in cladding thickness decreased the pellet diameter and decreased the mass of uranium per assembly. The GE 7×7 assembly configuration is illustrated in Figures 4.4 and 4.5.

Fuel and moderator temperatures and moderator and channel water densities were not reported. The values listed in Table 4.10 are based on values applied in previously benchmark calculations for Cooper fuel assembly decay heat³ and isotopic validation studies,³⁵ which were derived using typical BWR plant data. The number of burnable poison rods in the GE 7×7 assemblies was also not provided. However, two of the Cooper assemblies, designated CZ346 and CZ348, were selected for destructive radiochemical analysis at the Materials Characterization Center at Pacific Northwest Laboratory, and the samples designated as Approved Testing Material 105 (ATM-105).³⁶ The report on ATM-105 gives the enrichment zoning and indicates that the assembly contained three fuel rods of 3 wt % and two fuel rods of 4 wt % gadolinium oxide (Gd_2O_3) poison, for an average of 3.4 wt %. The location of the poison rods in the CZ346 and CZ348 assemblies is illustrated in the assembly configuration shown in Figure 4.4. The same poison rod configuration and initial poison loading was assumed for all of the GE 7×7 assemblies evaluated in this study.

The Cooper assemblies had an initial assembly average enrichment of 2.50 wt % ^{235}U , with the exception of assembly CZ102, which had an enrichment of 1.09 wt % ^{235}U . The single Dresden assembly had an enrichment of 2.13 wt %. All Monticello assemblies were enriched to 2.25 wt % ^{235}U . The assembly burnup by cycle and reactor operating data are listed in Tables 4.11–4.13.

The activation of nonfuel structural components of the assembly, listed in (Table 4.13), was included in all calculations. Structural material mass was obtained from NUREG/CR-5625 (Ref. 3). These values were derived from data in Ref. 37 and weighted to reflect the relative flux levels in each component. The largest contribution of activation products to the decay heat comes from ^{60}Co , produced by the activation of cobalt as an impurity. The initial cobalt levels were estimated assuming 800 ppm cobalt in stainless steel type 304, and 10 ppm in Zircaloy-2. The activation of non-fuel structural components of the assembly, listed in (Table 4.14), was included in all calculations.

Table 4.10 Cooper, Dresden, and Monticello and fuel assembly design information

Parameter	Data		
Assembly and reactor data			
Lattice geometry	GE 7 × 7		
Designer	General Electric		
Reactor	Cooper	Dresden 2	Monticello
Versions used	GE-3B	GE-2	GE-2B
EIA assembly code	G4607G3B	G4607G2	G2307G2B
Active fuel rod length (cm)	370.8	365.8	365.8
Uranium mass per assembly (kg) ^a	190	193	193
Assembly pitch (cm)	15.24		
Rod pitch (cm)	1.875		
Number of fuel rods	49		
Inlet temperature (K)	546		
Average moderator temperature (K)	558		
Average moderator density (g/cm ³)	0.4343		
Number of Gd poison rods	5		
Channel water density (g/cm ³)	0.7627		
Channel water temperature (K)	552		
Flow tube material	Zircaloy-4		
Flow tube inside flat-to-flat (cm)	13.406		
Flow tube thickness (cm)	0.2032		
Flow tube temperature (K)	558		
Fuel rod data			
Fuel material type	UO ₂		
Fuel density (% TD)	94.0		
Fuel stack density (g/cm ³)	9.73		
Gadolinium rods, wt % poison	3.4 (average)		
Fuel pellet diameter (cm)	1.212	1.237	
Fuel rod outside diameter (cm)	1.430		
Effective fuel temperature (K)	811		
Clad material	Zircaloy-2		
Clad thickness (cm)	0.0940	0.0813	
Average clad temperature (K)	620		

^a Represents nominal values.

- 1 fuel
- 2 clad
- 3 coolant
- 5 fuel-gd (3%)
- 9 channel tube
- 10 moderator
- 11 fuel-gd (4%)

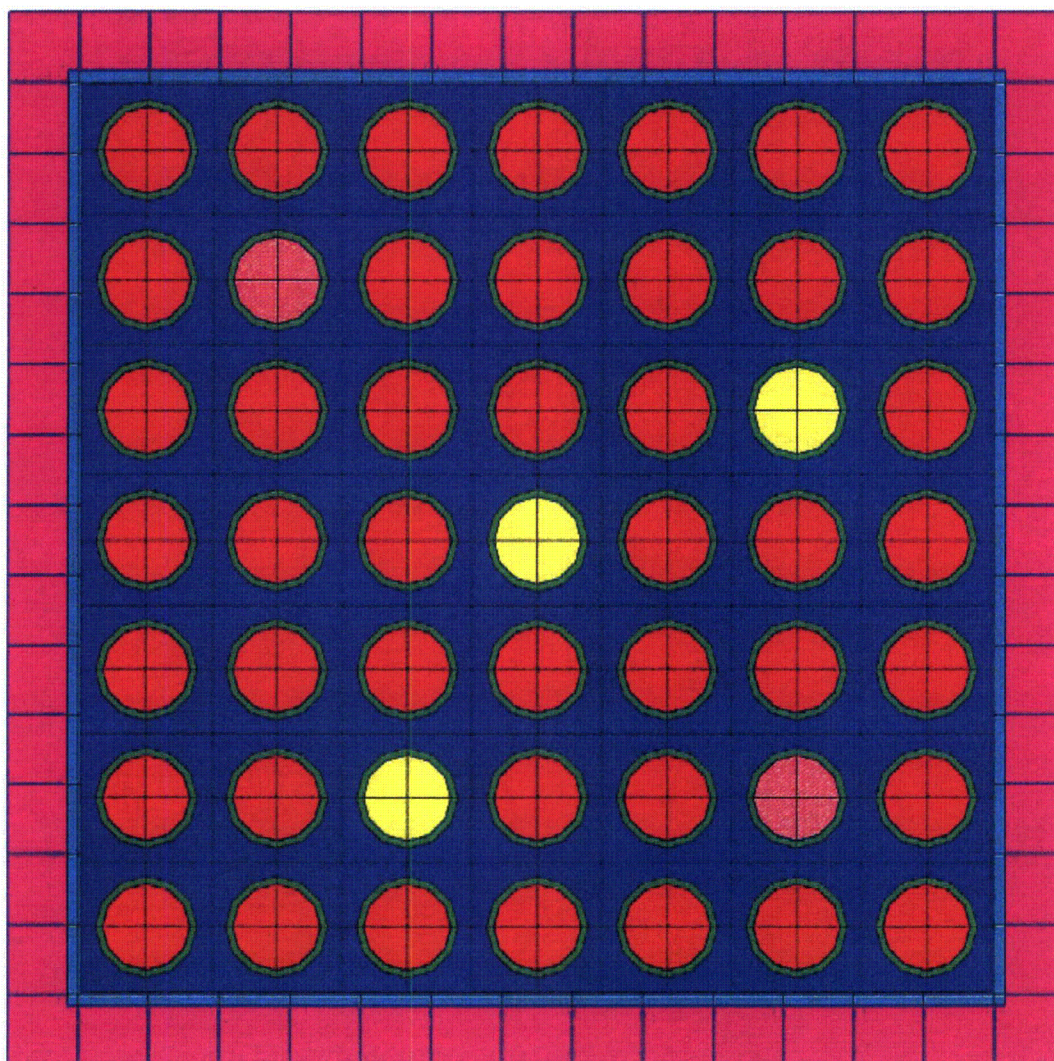


Figure 4.4 Layout for the GE 7 × 7 fuel assembly

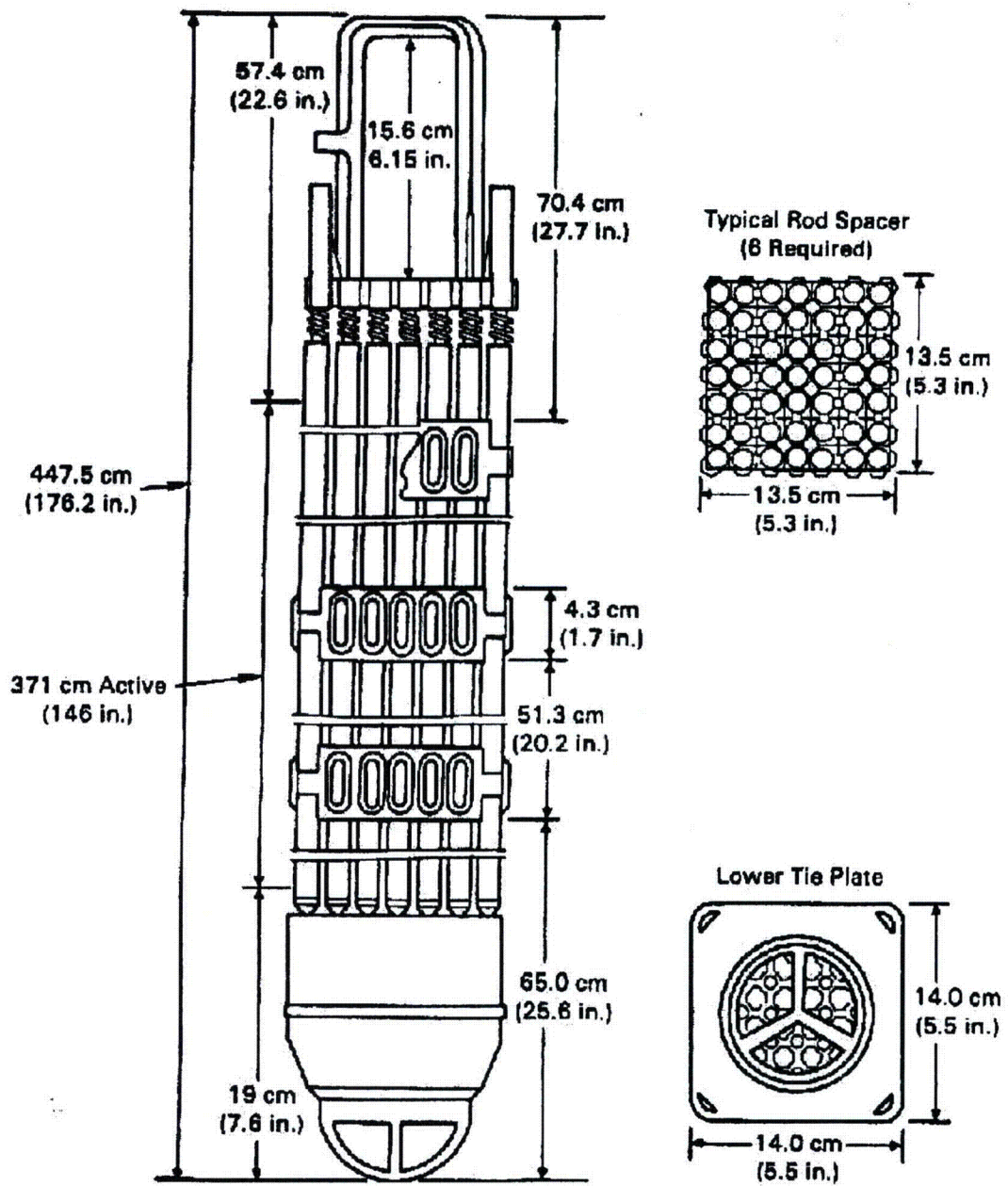


Figure 4.5 GE 7x7 fuel assembly dimensions

Table 4.11 Cooper Station reactor and assembly irradiation data

Operational data	Cycle 1	Cycle 2	Cycle 3	Cycle 4	Cycle 5	Cycle 6	Cycle 7
Startup date	7/3/1974	11/15/1976	10/18/1977	5/5/1978	5/10/1979	6/7/1980	6/7/1981
Shutdown date	9/17/1976	9/17/1977	3/31/1978	4/17/1979	3/1/1980	4/20/1981	5/21/1982
Operating days	807	306	164	347	296	317	348
Downtime (days)	59	31	35	23	98	48	--
Assembly ID	Assembly burnup (MWd/MTU)						
CZ102	9,394	11,667					
CZ147	6,773	10,381	13,490	21,231	23,421	26,709	
CZ148	5,887	10,126	13,220	20,883	23,049	26,310	
CZ182	10,710	18,421	20,412			24,464	26,824
CZ195	5,999	10,319	12,622	21,395	23,523	26,392	
CZ205	10,298	17,712	20,699			22,563	25,344
CZ209	10,651	18,320	21,430			23,726	25,383
CZ211	6,770	10,339	13,462	21,197	23,387	26,668	
CZ222	10,728	18,452	21,519			23,759	26,692
CZ225	10,672	18,355	21,455			23,489	25,796
CZ239	10,500	18,059	21,175			24,742	27,246
CZ246	10,964	18,858	22,052			24,065	27,363
CZ259	6,026	10,365	12,920	21,431	23,596	26,466	
CZ264	5,938	10,213	12,782	21,404	23,601	26,496	
CZ277	6,012	10,341	12,885	21,427	23,599	26,478	
CZ286	11,071	19,042	22,218			24,916	27,141
CZ296	5,964	10,258	13,323	20,971	22,547	26,388	
CZ302	11,637	20,016			22,174	26,594	
CZ308	11,826	20,340	21,780			23,983	25,815
CZ311	11,236	19,325	22,322			25,314	27,392
CZ315	11,415	19,634	22,565			24,526	26,881
CZ318	11,387	19,585	22,537			24,902	26,568
CZ331	12,875	18,370	21,332				
CZ337	10,861	18,681	21,594			23,806	26,720
CZ342	11,396	19,600	22,788			24,680	27,066
CZ346	11,651	20,039	21,920			25,203	28,048
CZ348	11,063	19,028	22,169			24,773	27,481
CZ351	10,741	18,475	21,287			23,859	25,753
CZ355	11,654	20,046	21,468			23,620	25,419
CZ357	11,136	19,153	22,060			25,023	27,140
CZ369	11,162	19,197	21,678			23,660	26,576
CZ370	11,511	19,799			21,946	26,342	
CZ372	11,051	19,008				21,708	25,848
CZ379	11,142	19,165	21,907			24,286	25,925
CZ398	11,221	19,300	22,212			24,499	27,478
CZ415	11,058	19,020			21,726	25,863	
CZ416	11,572	19,904	22,906			25,051	27,461
CZ429	10,878	18,711	21,610			24,842	27,641
CZ430	10,774	18,531	21,626			24,176	26,825
CZ433	11,350	19,522	19,522			21,639	25,977
CZ460	10,932	18,804	21,938			24,570	26,512
CZ466	11,012	18,940	22,148			24,290	26,077
CZ468	11,130	19,143	21,603			24,823	26,757
CZ472	10,806	18,587	21,272			23,173	25,957
CZ473	11,305	19,444	22,448			24,840	26,519
CZ498	10,853	18,666	21,362			23,584	26,482
CZ508	12,368	21,273	21,921			24,014	26,357
CZ515	11,003	18,924			21,637	25,737	
CZ526	10,938	18,814	21,548			24,788	27,596
CZ528	10,996	18,913			21,604	25,715	
CZ531	10,906	18,758	21,471			24,036	26,699
CZ536	10,996	18,913				21,604	25,715
CZ542	11,109	19,108	22,062			24,717	26,691
CZ545	11,311	19,454	22,675			24,856	26,668

Table 4.12 Dresden 2 reactor and assembly irradiation data

Operational data	Cycle 1	Cycle 1A	Cycle 2
Startup date	5/1/1970	8/5/1970	5/26/1971
Shutdown date	6/6/1970	2/27/1971	2/20/1972
Operating days	36	206	270
Downtime (days)	60	88	--
Assembly ID	Assembly burnup (MWd/MTU)		
DN212	299	2,112	5,279

Table 4.13 Monticello reactor and assembly irradiation data

Operational data	Cycle 1	Cycle 2	Cycle 3	Cycle 4
Startup date	2/19/1971	5/19/1973	5/19/1974	2/8/1975
Shutdown date	3/3/1973	3/15/1974	1/10/1975	9/12/1975
Operating days	743	300	236	216
Downtime (days)	77	65	29	--
Assembly ID	Assembly burnup (MWd/MTU)			
MT116	8,559	13,288	14,721	18,039
MT123	8,353	13,027		
MT133	8,893	13,870	17,460	20,994
MT190	4,998	7,893	11,349	15,143
MT228	3,522	5,389	8,724	12,123
MT264	3,685	5,563	7,301	9,160

**Table 4.14 Activated structural elements in Cooper, Dresden,
and Monticello assemblies**

Element	grams per kg U ^a	kilograms per assembly ^b
Oxygen	134	
Chromium	2.4	0.45
Manganese	0.15	0.029
Iron	6.6	1.2
Cobalt	0.024	0.0046
Nickel	2.4	0.45
Zirconium	516.0	98.2
Niobium	0	0
Tin	8.7	1.6

^a Values derived from NUREG/CR-5625 (Ref. 3).

^b Assumed nominal mass of 190 kg U per assembly.

4.1.4.1 Cooper Station

The Cooper Station operating history along with assembly data and burnup by cycle are given in Table 4.11. The operating data for all Cooper assemblies presented in the reports PNL-5777 (Ref. 38) and EPRI NP-4619 (Ref. 30) were normalized to yield with discharge data listed in RW-859 (Ref. 32). A review of the data confirmed that the burnup values were consistent between the different sources with the exception of assembly CZ536. PNL-5777 reports that the assembly was discharged after Cycle 7 with a burnup of 25,715 MWd/MTU, whereas RW-859 lists the discharge at Cycle 6 with a final burnup of 26,589 MWd/MTU. This discrepancy raises concerns over whether the assembly was identified correctly, and moreover, the accuracy of the decay time. Based on the calculated results for assembly CZ536 the Cycle 7 discharge date appears to be correct (e.g., a Cycle 6 discharge date would give a considerably longer decay time and produce an uncharacteristic underprediction of decay heat relative to the other measured assemblies). For this study the assembly operating history data from Table 4.1 of report PNL-5777 were applied. The initial uranium mass of each assembly was obtained from RW-859.

4.1.4.2 Dresden 2

The reactor operating information and irradiation data for Dresden 2 assembly DN212 are listed in Table 4.12. The Nuclear Fuel Data from RW-859 (Ref. 32) indicates that Dresden 2 assembly DN212 was discharged after Cycle 2. However, report EPRI NP-4619 (Ref. 30) Table 2-3 suggests the assembly was irradiated only in Cycle 1. Further analysis of the operating history for DN212 in Table A-3 of EPRI NP-4619 confirms that the assembly was likely irradiated for 2 cycles. The plant operating data in RW-859 further indicates that Cycle 1 was divided in 2 parts, identified as Cycle 1 and Cycle 1A. This is also confirmed from the detailed operating history; however, the dates of operation and shutdown are inconsistent between the two references. RW-859 indicates that Cycle 1 started on 5/29/1970 and continued for 7 d before a shut down of 67 d prior to the start of Cycle 1A. EPRI NP-4619 gives a starting date of 5/01/1970 with operation for 36 d followed by a 60-d shutdown. The data for Cycle 1A and Cycle 2 are more consistent. For this study the operating history information for assembly DN212 was modeled using Cycles 1, 1A, and 2 using the detailed reactor power data provided in Table A-3 of report EPRI NP-4619.

4.1.4.3 Monticello

The reactor operating information and irradiation data for the Monticello assemblies are listed in Table 4.13. The Monticello assembly information was obtained primarily from report PNL-5799 (Ref. 30). The experience with most of the assemblies evaluated in this study is that the total burnup obtained from the cycle burnup values reported by the utilities is consistent with the discharge burnups reported in RW-859 (note that RW-859 documents only the final burnup, not the accumulated cycle burnup). However, for the Monticello assemblies this was not the case. The difference is attributed by McKinnon et al.³⁰ to different accounting methods used by the utility. The difference between the burnup estimates obtained by the different methods was nearly 10% in some cases. On average the burnup reported in RW-859 was about 2% lower than the value based on cycle-by-cycle data, with an average relative standard deviation of $\pm 5\%$. For consistency with the other evaluations in this study, all Monticello assembly calculations were performed by normalizing the cycle burnup data to the final discharge burnup reported in RW-859.

4.2 Assembly Designs—Sweden Measurements

The decay heat measurements performed at the Swedish CLAB fuel storage facility that are evaluated in this report include 34 assemblies from 8 BWR reactor units and 30 assemblies from 2 PWR reactor units operated in Sweden. The assemblies are grouped based on the assembly design. There are four BWR designs (8×8 , 9×9 , SVEA-64 and SVEA-100) and two PWR designs (15×15 and 17×17). Each group of assemblies can be further subdivided based on the details of the assembly configuration such as fuel pellet or rod diameter, number of water rods, number of burnable absorber rods, etc. Detailed information on the assembly design, irradiation history, and axial burnup and void distributions can be found in Ref. 5.

At the time the present calculations were performed, detailed assembly enrichment zoning patterns and burnable poison rod configurations for each assembly, published in Ref. 5, were not available. Therefore, typical patterns based on past experience were applied. The assembly and fuel data for the assemblies analyzed in this study are summarized separately in Ref. 39. This report includes much of the design and operating data from Ref. 5 and also includes information on the assembly models developed for the decay heat calculations and derives other required data not provided in the SKB report. For completeness, the data relevant to the assembly models developed for this study are presented here.

4.2.1 BWR 8×8 Assemblies

The BWR 8×8 fuel assembly design data are given in Table 4.15. Assemblies that were rebuilt are not included in Table 4.15 because insufficient information was available to develop a reliable computational model. The specific density of the uranium oxide reported in the table for each assembly type is the average value over all assemblies of that type. The specific fuel density for each individual assembly can be found in Ref. 5.

There were four types of 8×8 assembly designs studied. Two of the groups (Type 1 and 2) contain assemblies with a single water rod (designated as assembly type $8 \times 8-1$). All groups except Type 4 used corner rods having dimensions slightly smaller than the rods in the rest of the assembly. Another difference between assembly types is the number of burnable absorber rods and the content of Gd_2O_3 in these rods. Several assumptions on material and dimensions had to be made when information was not available. The material for the fuel clad and the water rods was assumed to be Zircaloy-2. The outer diameter and thickness of the water rods for some of the assembly types were assumed to be the same as for the fuel rod cladding in the assemblies of the same type. Type 3 and Type 4 assemblies also contained a single zirconium spacer rod. These spacer rods have the same outside diameter as the water rods but have a solid Zircaloy interior, i.e., they do not contain water.

The BWR 8×8 assemblies were irradiated in seven different reactors: Ringhals 1, Oskarshamn 2, Oskarshamn 3, Forsmark 1, Forsmark 2, Barsebäck 1, and Barsebäck 2, and cover a burnup range from 14 to 41 GWd/MTU. The burnup and irradiation history data for each assembly and each reactor type are presented in Tables 4.16–4.22. The average coolant density, the number of burnable absorber rods, and the weight percent of Gd_2O_3 in these rods, as well as the average fuel enrichment and the initial mass of uranium, are shown in Table 4.23. The coolant density was calculated as an assembly-averaged value based on the axial void distribution for each assembly provided in Ref. 5. For assemblies from the reactor Ringhals-1, axial void information was available only for the assemblies identified as 1177 and 1186. The average of the coolant density for these two assemblies was used for the other 8×8 assemblies from the same reactor. Because specific assembly layout information data was not available at the time these calculations were performed, the location of the water rods in the 8×8 assemblies was based on typical data from other sources.⁴⁰ Assumptions were also made regarding the location of the burnable absorber

rods in the assembly; more details on these assumptions are discussed when presenting the actual computational models for each assembly type in Sect. 5. A typical 8×8 assembly layout used in the computational model is provided in Figure 4.6.

Table 4.15 Fuel assembly design data for BWR 8 × 8 assemblies

Parameter	Data			
	Type 1	Type 2	Type 3	Type 4
Assembly data				
Lattice geometry	8 × 8-1	8 × 8-1	8 × 8-1	8 × 8-2
Fuel rod active length (cm)	365.0	368.0	371.2	368.0
Assembly pitch (cm)	15.33	15.33 ^a	15.30	15.38
Moderator ^b temperature (K)	552	552	552	552
Moderator ^b density (g/cm ³)	0.75	0.75	0.75	0.75
Coolant temperature (K)	552	552	552	552
Number of normal fuel rods	51	51	51	62
Number of corner fuel rods	12	12	12	N/A
Number of water rods	1	1	0	1
Number of Zr spacer rods	0	0	1	1
Rod pitch (cm)	1.63	1.63	1.63	1.625
Rod pitch for corner rods (cm)	1.58	1.58	1.58	N/A
Rod pitch for normal-to-corner rods (cm)	1.605	1.605	1.605	N/A
Assembly channel outer dimension (cm)	13.9	13.9	13.86	13.9
Assembly channel wall thickness (cm)	0.2	0.23	0.23	0.23
Assembly channel material	Zircaloy-4	Zircaloy-4	Zircaloy-4	Zircaloy-4
Spacer material ^c	Inconel	Inconel	Inconel	Inconel
Spacer total mass (g)	810	810	810	1938
Number of absorber rods ^d	3	0/3/4	0/4/5/6	4
Gd ₂ O ₃ wt % in absorber rods ^d	2	2/3.95/5.5	2/2.55/3.2	2.5
Fuel rod data				
Fuel material type	UO ₂	UO ₂	UO ₂	UO ₂
Effective fuel density (g/cm ³)	10.168	10.316	10.621 ^e /10.429 ^f	10.171
Effective fuel temperature (K)	900	900	900	900
Fuel pellet diameter, normal rods (cm)	1.058	1.044	1.044	1.044
Fuel pellet diameter, corner rods (cm)	1.008	0.994	0.994	N/A
Fuel rod outside diameter, normal rods (cm)	1.225	1.225	1.225	1.23
Fuel rod outside diameter, corner rods (cm)	1.175	1.175	1.175	N/A
Clad material ^g	Zircaloy-2	Zircaloy-2	Zircaloy-2	Zircaloy-2
Clad thickness for normal rods (cm)	0.074	0.08	0.08	0.082
Clad thickness for corner rods (cm)	0.074	0.08	0.08	N/A
Average clad temperature (K)	573	573	573	573
Water rod data				
Water rod material ^h	Zircaloy-2 ^h	Zircaloy-2 ^h	Zircaloy-2	Zircaloy-2
Water rod outer diameter (cm)	1.225 ^h	1.225 ^h	1.225	1.5
Water rod thickness (cm)	0.074 ^h	0.074 ^h	0.074 ^h	0.08

^a Some assemblies of this type have different values; assembly pitch for assemblies with identifiers 3838, 5535 and 12078 have a pitch value of 15.38 cm, 15.40 cm, and 15.50 cm, respectively.

^b This is the moderator in the assembly channel.

^c Inconel X-750 is assumed.

^d Number varies with assembly; exact values are shown in Table 4.23.

^e For assemblies with no absorber rods.

^f For assemblies with absorber rods.

^g Zircaloy-2 is assumed.

^h Assumed.

Table 4.16 Ringhals-1 reactor and 8 × 8 assembly irradiation history data

Operational data type		Cycle 2	Cycle 3	Cycle 4	Cycle 5	Cycle 6	Cycle 7	Cycle 8	Cycle 9	Cycle 10	Cycle 11	Cycle 12	Cycle 13	Cycle 14
Startup date		10/13/1978	9/30/1979	10/8/1980	11/6/1981	9/9/1982	9/30/1983	8/28/1984	9/2/1985	10/9/1986	9/24/1987	9/11/1988	10/11/1989	8/30/1990
Shutdown date		7/12/1979	7/3/1980	7/30/1981	7/22/1982	6/18/1983	7/13/1984	8/2/1985	8/15/1986	8/21/1987	8/6/1988	9/15/1989	8/4/1990	8/9/1991
Operating days		272	277	295	258	282	287	339	347	316	317	369	297	344
Downtime days		80	97	99	49	104	46	31	55	34	36	26	26	---
Assembly ID	Design	Assembly Burnup (MWd/MTU)												
1177	8 × 8	4,486	9,369	16,334	20,430	25,484	30,320	36,242						
1186	8 × 8	4,554	9,614	15,459	19,967	24,592	28,020	30,498						
6423	8 × 8					5,401	12,064	19,440	26,198	31,635	35,109			
6432	8 × 8				5,502	10,444	16,181	23,266	30,079	34,746	36,861			
6454	8 × 8		7,120	13,000	18,936	24,831	30,918	37,236						
8327	8 × 8					3,212	9,482	15,956	21,578	28,065	34,820	36,141	37,851	
8331	8 × 8					6,974	15,132	22,493	26,648	33,319	35,903			
8332	8 × 8			5,755	11,468	16,558	23,407	29,963	32,651	34,977				
8338	8 × 8			5,660	11,130	16,282	23,202	29,963	32,634	34,830				

Table 4.17 Oskarshamn-2 reactor and 8 × 8 assembly irradiation data

Operational data type		Cycle 1	Cycle 2	Cycle 3	Cycle 4	Cycle 5	Cycle 6	Cycle 7	Cycle 8	Cycle 9	Cycle 10
Startup date		10/2/1974	7/2/1976	8/7/1977	9/3/1978	8/30/1979	8/20/1980	8/30/1981	8/23/1982	9/19/1983	8/24/1984
Shutdown date		4/16/1976	5/13/1977	6/24/1978	7/20/1979	7/12/1980	7/15/1981	7/23/1982	8/19/1983	7/1/1984	6/7/1985
Operating days		562	315	321	320	317	329	327	361	286	287
Downtime days		77	86	71	41	39	46	31	31	54	---
Assembly ID	Type	Assembly Burnup (MWd/MTU)									
1377	3	8,982	14,546								
1389	3	4,315	7,300	11,829	14,539	16,933	19,481				
1546	3	6,961					13,840	21,032	24,470		
1696	3	4,492	7,904	13,258	16,319			18,502	20,870		
1704	3	4,587	8,031	13,384	16,638			19,437			
2995	3		6,143	13,359	19,705	23,577	29,978				
6350	3						7,113	14,909	24,019		27,675

Table 4.18 Forsmark-1 reactor and 8 × 8 assembly irradiation data

Operational data type	Cycle 1A	Cycle 1B	Cycle 2	Cycle 3	Cycle 4	Cycle 5	Cycle 6	Cycle 7	Cycle 8	Cycle 9	Cycle 10
Startup date	4/23/1980	8/16/1981	8/25/1982	8/5/1983	8/6/1984	7/8/1985	7/22/1986	8/19/1987	7/10/1988	8/18/1989	9/16/1990
Shutdown date	6/25/1981	6/19/1982	7/15/1983	7/13/1984	5/31/1985	7/4/1986	7/31/1987	6/10/1988	7/14/1989	8/17/1990	5/24/1991
Operating days	428	307	324	343	298	361	374	296	369	364	250
Downtime days	52	67	21	24	38	18	19	30	35	30	---

Assembly ID	Type	Assembly Burnup (MWd/MTU)											
3838	2	6,160	13,092	15,990	19,053							21,839	25,669
KU0100	4					10,643	18,706	26,630	34,193				

Table 4.19 Forsmark-2 reactor and 8 × 8 assembly irradiation data

Operational data type	Cycle 1A	Cycle 1B	Cycle 2	Cycle 3	Cycle 4	Cycle 5	Cycle 6
Startup date	12/1/1980	8/18/1982	6/11/1983	7/13/1984	7/26/1985	8/9/1986	6/20/1987
Shutdown date	5/1/1982	5/20/1983	5/25/1984	7/5/1985	7/25/1986	5/31/1987	7/15/1988
Operating days	516	275	349	357	364	295	391
Downtime days	109	22	49	21	15	20	---

Assembly ID	Type	Assembly Burnup (MWd/MTU)						
5535	2	8,850	10,758	12,862	14,982	16,665	18,115	19,944

Table 4.20 Barsebäck-1 reactor and 8 × 8 assembly irradiation data

Operational data type	Cycle 8	Cycle 9	Cycle 10	Cycle 11	Cycle 12
Startup date	8/6/1983	7/26/1984	9/2/1985	8/18/1986	7/29/1987
Shutdown date	6/28/1984	8/7/1985	7/17/1986	7/1/1987	9/17/1988
Operating days	327	377	318	317	416
Downtime days	28	26	32	28	---

Assembly ID	Type	Assembly Burnup (MWd/MTU)				
9329	3	8,219	17,727	25,034	31,958	41,127
10288	3		9,726	17,440	25,587	35,218

Table 4.21 Barsebäck-2 reactor and 8 × 8 assembly irradiation data

Operational data type	Cycle 9	Cycle 10	Cycle 11	Cycle 12	Cycle 13	
Startup date	9/19/1987	8/7/1988	9/28/1989	8/18/1990	9/22/1991	
Shutdown date	7/6/1988	9/8/1989	7/11/1990	9/6/1991	7/2/1992	
Operating days	291	397	286	384	284	
Downtime days	32	20	38	16	--	
Assembly ID	Type	Assembly Burnup (MWd/MTU)				
14076	3	8,398	18,616	24,130	34,126	40,010

Table 4.22 Oskarshamn-3 reactor and 8 × 8 assembly irradiation history

Operational data type	Cycle 1	Cycle 2	Cycle 3	
Startup date	3/18/1985	7/26/1986	7/26/1987	
Shutdown date	7/4/1986	7/3/1987	7/8/1988	
Operating days	473	342	348	
Downtime days	22	23	37	
Assembly ID	Design	Assembly Burnup (MWd/MTU)		
12078	8 × 8	8,690	16,948	25,160

Table 4.23 Other data for BWR 8 × 8 assemblies

Assembly ID	Type	Reactor	Enrichment (wt % ²³⁵ U)	Initial U (kg)	Coolant density (g/cm ³) ^a	No. BA rods ^b	Gd ₂ O ₃ in BA (wt %)
1177	1	Ringhals 1	2.642	180.58	0.4325	3	2
1186	1	Ringhals 1	2.640	180.52	0.4596	3	2
6423	2	Ringhals 1	2.900	177.70	0.4445	4	2
6432	2	Ringhals 1	2.894	177.52	0.4445	4	2
6454	2	Ringhals 1	2.898	177.68	0.4445	4	2
8327	2	Ringhals 1	2.904	177.54	0.4445	4	2
8331	2	Ringhals 1	2.910	177.69	0.4445	4	2
8332	2	Ringhals 1	2.895	177.52	0.4445	4	2
8338	2	Ringhals 1	2.911	177.60	0.4445	4	2
1377	3	Oskarshamn 2	2.201	183.58	0.3790	0	N/A
1389	3	Oskarshamn 2	2.201	183.65	0.5053	0	N/A
1546	3	Oskarshamn 2	2.201	183.97	0.4240	0	N/A
1696	3	Oskarshamn 2	2.201	184.25	0.4894	0	N/A
1704	3	Oskarshamn 2	2.201	184.02	0.4622	0	N/A
2995	3	Oskarshamn 2	2.699	179.38	0.4135	4	2
6350	3	Oskarshamn 2	2.875	179.00	0.3967	6	3.2
12078	2	Oskarshamn 3	2.578	177.36	0.3946	3	5.5
9329	3	Barsebäck 1	2.922	178.77	0.4199	5	2.55
10288	3	Barsebäck 1	2.953	179.16	0.4029	5	2.55
14076	3	Barsebäck 2	3.15	179.57	0.3928	4	2
3838	2	Forsmark 1	2.090	177.90	0.5073	3	3.95
KU0100	4	Forsmark 1	2.970	174.92	0.4001	4	2.5
5535	2	Forsmark 2	2.095	177.69	0.5167	0	N/A

^a Axial volumetric average.

^b BA – burnable absorber rod.

- 1 fuel
- 2 clad
- 3 gap
- 4 coolant
- 9 water rod tube
- 10 water in water rod
- 11 channel box
- 12 channel moderator

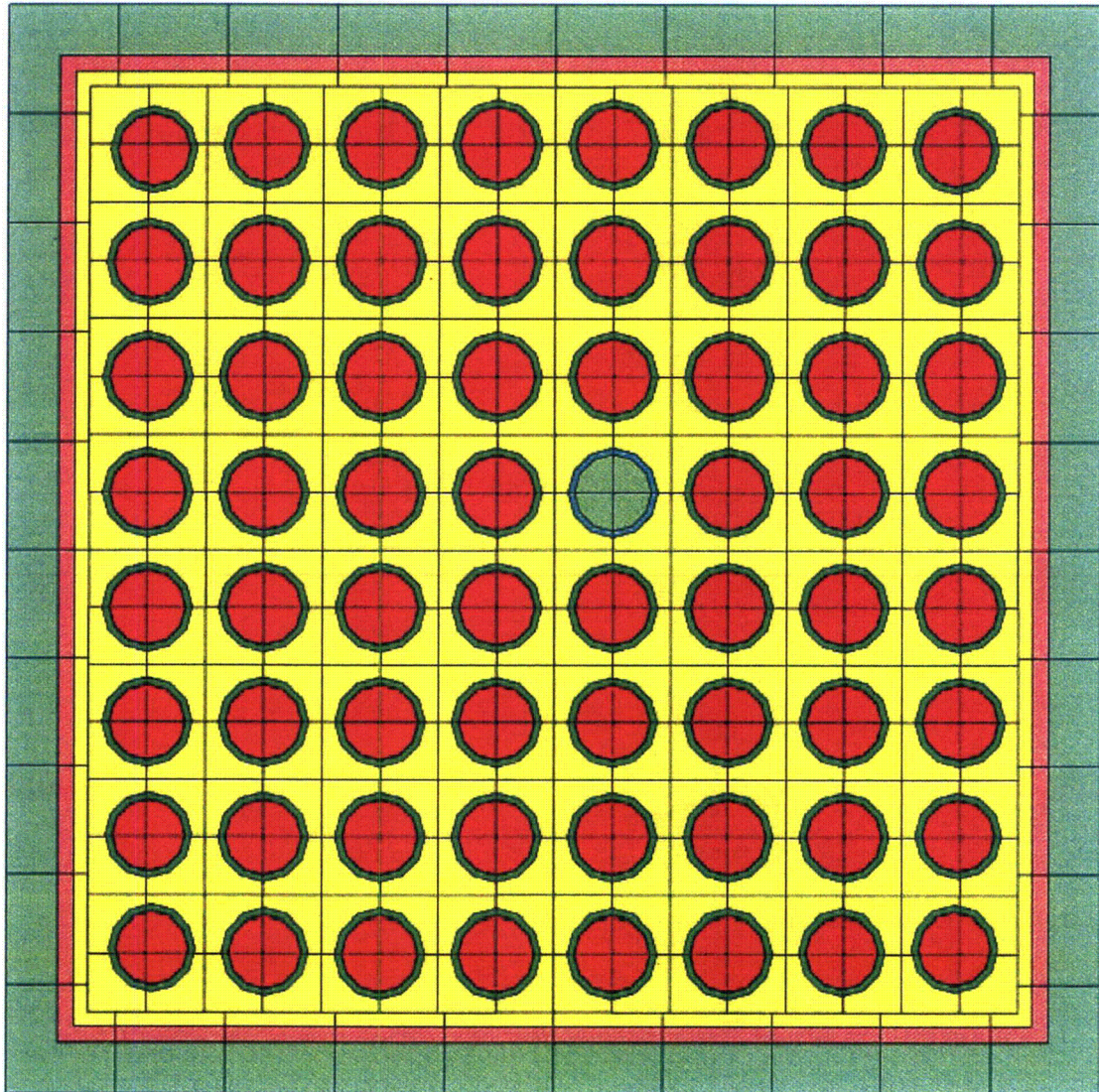


Figure 4.6 Layout of a BWR 8 × 8-1 assembly

4.2.2 BWR 9 × 9 Assemblies

Decay heat measurements were performed for three BWR 9 × 9 assemblies from the Forsmark-1 reactor. The assemblies have a total burnup in the range 35–38 GWd/MTU. The fuel assembly design data are presented in Table 4.24. Information on the Forsmark reactor operating history, assembly irradiation data, initial uranium mass, initial enrichment, and coolant density are shown in Table 4.25. Each assembly has 76 fuel rods, 4 water rods, and 1 solid Zr spacer rod. Six of the fuel rods contain a burnable absorber. The positions of the water rods and burnable absorber rods in the assembly were not available at the time, and were therefore based on design information for a similar KWU (Siemens) 9 × 9–5 assembly design used in the Barsebäck reactor. The assembly layout is shown in Figure 4.7.

Table 4.24 Fuel assembly design data for BWR 9 × 9 assemblies

Parameter	Data
Assembly and reactor data	
Lattice geometry	9 × 9
Fuel rod active length (cm)	368.0
Assembly pitch (cm)	15.38
Channel moderator temperature (K)	552
Channel moderator density (g/cm ³)	0.75
Coolant temperature (K)	552
Number of fuel rods	76
Number of water rods	4
Number of Zr spacer rods	1
Rod pitch (cm)	1.445
Assembly channel outer dimension (cm)	13.9
Assembly channel wall thickness (cm)	0.23
Assembly channel material	Zircaloy-4
Spacer material	Zircaloy-4
Spacer total mass (g)	1938
Number of absorber rods	6
Gd ₂ O ₃ wt % in absorber rods	2.5
Fuel rod data	
Fuel material type	UO ₂
Effective fuel density (g/cm ³)	10.144
Effective fuel temperature (K)	900
Fuel pellet diameter (cm)	0.95
Fuel rod outside diameter (cm)	1.1
Clad material ^a	Zircaloy-2
Clad thickness (cm)	0.0665
Average clad temperature (K)	573
Water rod data	
Water rod material ^a	Zircaloy-2
Water rod outer diameter (cm)	1.445
Water rod thickness (cm)	0.08

^a Not specified; Zircaloy-2 is assumed.

Table 4.25 Forsmark 1 reactor and 9 × 9 assembly irradiation data

Operational data				Cycle 5	Cycle 6	Cycle 7	Cycle 8	Cycle 9
Startup date				7/8/1985	7/22/1986	8/19/1987	7/10/1988	8/18/1989
Shutdown date				7/4/1986	7/31/1987	6/10/1988	7/14/1989	8/17/1990
Operating days				361	374	296	369	364
Downtime days				18	19	30	35	

Assembly data								
ID	Enrichment (wt % ²³⁵ U)	Initial U (kg)	Coolant density (g/cm ³)	Assembly Burnup (MWd/MTU)				
KU0269	2.938	177.02	0.3866	10,158	18,787	27,153	35,113	
KU0278	2.938	177.13	0.4235	10,414	17,685	24,764	29,413	35,323
KU0282	2.938	177.10	0.4247	10,122	18,800	25,844	32,112	37,896

- 1 fuel
- 2 clad
- 3 gap
- 4 coolant
- 5 fuel-gd
- 9 water rod tube
- 10 water in water rod
- 11 channel box
- 12 channel moderator

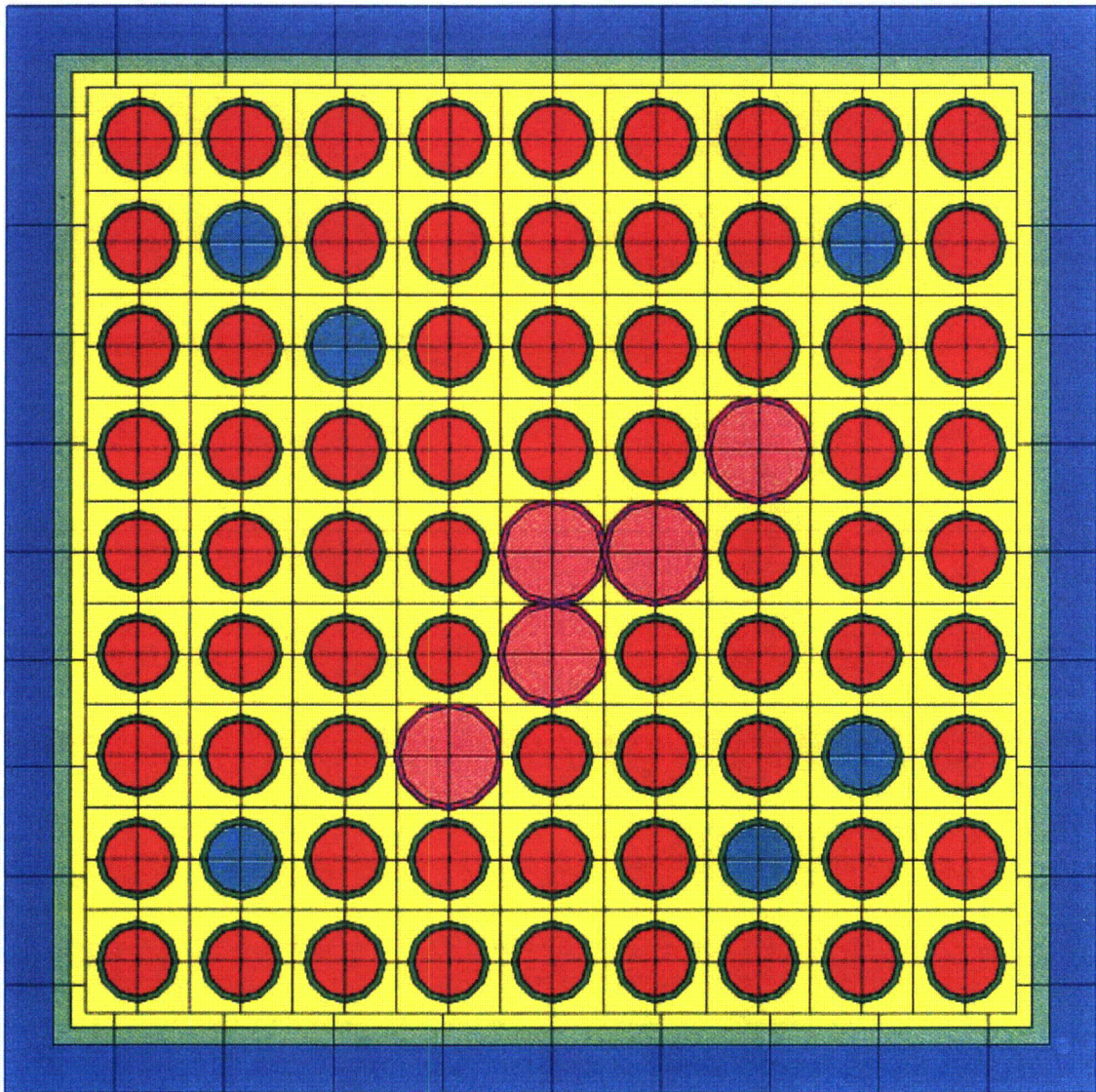


Figure 4.7 Layout of a BWR 9 × 9-5 assembly

4.2.3 BWR SVEA-64 Assemblies

Decay heat measurements were performed for four SVEA-64 assemblies: three irradiated in the Forsmark-2 reactor and one irradiated in the Oskarshamn-2 reactor. Each assembly contains four 4×4 subassemblies separated by a large water region (water cross). There are 63 fuel rods and 1 water rod in each assembly. Some of the fuel rods (4 to 6, depending on the assembly type) contain Gd_2O_3 burnable poison. Information on the assembly design is presented in Table 4.26, and data on irradiation history, coolant density, fuel enrichment and initial uranium mass is given in Tables 4.27 and 4.28. The assembly layout is shown in Figure 4.8 for an assembly with four burnable absorber rods.

Table 4.26 Fuel assembly design data for SVEA-64 assemblies

Parameter	Data
Assembly and reactor data	Type 1
Lattice geometry	8×8
Assembly pitch (cm)	15.40
Channel moderator temperature (K)	552
Channel moderator density (g/cm^3)	0.72
Coolant temperature (K)	552
Number of fuel rods	63
Number of water rods	1
Rod pitch (cm)	1.58
Assembly channel outer dimension (cm)	14.0
Assembly channel wall thickness (cm)	0.11
Assembly channel material	Zircaloy-4
Water cross material	Zircaloy-4
Water cross wall thickness (cm)	0.08
Sub-assembly inner measure ^a (cm)	6.59
Spacers material ^b	Inconel
Spacers total mass (g)	840/744 ^c
Number of absorber rods	4/5/6 ^d
Gd_2O_3 wt % in absorber rods	2.55/2.55/3.15
Fuel rod data	
Fuel material type	UO ₂
Effective fuel density (g/cm^3)	10.367
Effective fuel temperature (K)	900
Fuel pellet diameter (cm)	1.044
Fuel rod outside diameter (cm)	1.225
Clad material ^e	Zircaloy-2
Clad thickness (cm)	0.08
Average clad temperature (K)	573
Water rod data	
Water rod material	Zircaloy-2
Water rod outer diameter (cm)	1.225
Water rod thickness (cm)	0.08

^a Wall to wall distance across the subassembly box.

^b Not specified; Inconel is assumed.

^c Spacers total mass is 840 g for assemblies 11494, 11495, and 13775; 744 g for assembly 12684.

^d 4 rods for assemblies 11494 and 11495; 5 rods for assembly 13775; 6 rods for assembly 12684.

^e Zircaloy-2 is assumed.

Table 4.27 Forsmark-2 reactor and SVEA-64 assembly irradiation data

Operational data		Cycle 3	Cycle 4	Cycle 5	Cycle 6	Cycle 7	Cycle 8	Cycle 9
Startup date		7/13/1984	7/26/1985	8/9/1986	6/20/1987	8/4/1988	9/4/1989	6/12/1990
Shutdown date		7/5/1985	7/25/1986	5/31/1987	7/15/1988	8/18/1989	5/18/1990	7/12/1991
Operating days		357	364	295	391	379	256	395
Downtime days		21	15	20	20	17	25	---

Assembly data										
ID	Type	Enrichment (wt % ²³⁵ U)	Initial U (kg)	Coolant density (g/cm ³)	Assembly	Burnup	(MWd/MTU)			
11494	1	2.920	181.09	0.4348	9,098	16,676	24,136	32,431		
11495	1	2.910	181.07	0.4106	9,098	16,676	24,136	32,431		
13775	1	2.850	181.34	0.4449			8,801	18,300	23,975	27,498 32,837

Table 4.28 Oskarshamn-2 reactor and SVEA-64 assembly irradiation data

Operational data		Cycle 11	Cycle 12	Cycle 13	Cycle 14	Cycle 15	Cycle 16
Startup date		7/13/1985	9/27/1986	9/4/1987	9/10/1988	9/1/1989	10/11/1990
Shutdown date		8/16/1986	7/31/1987	8/20/1988	8/5/1989	8/10/1990	8/2/1991
Operating days		399	307	351	329	343	295
Downtime days		42	35	21	27	62	---

Assembly data										
ID	Type	Enrichment (wt % ²³⁵ U)	Initial U (kg)	Coolant density (g/cm ³)	Assembly	Burnup	(MWd/MTU)			
12684	1	2.902	182.32	0.3762	11,134	20,032	28,184	35,495	43,084	46,648

- 1 fuel
- 2 clad
- 3 coolant
- 4 gap
- 5 fuel-gd (2.55%)
- 9 channel box
- 10 moderator

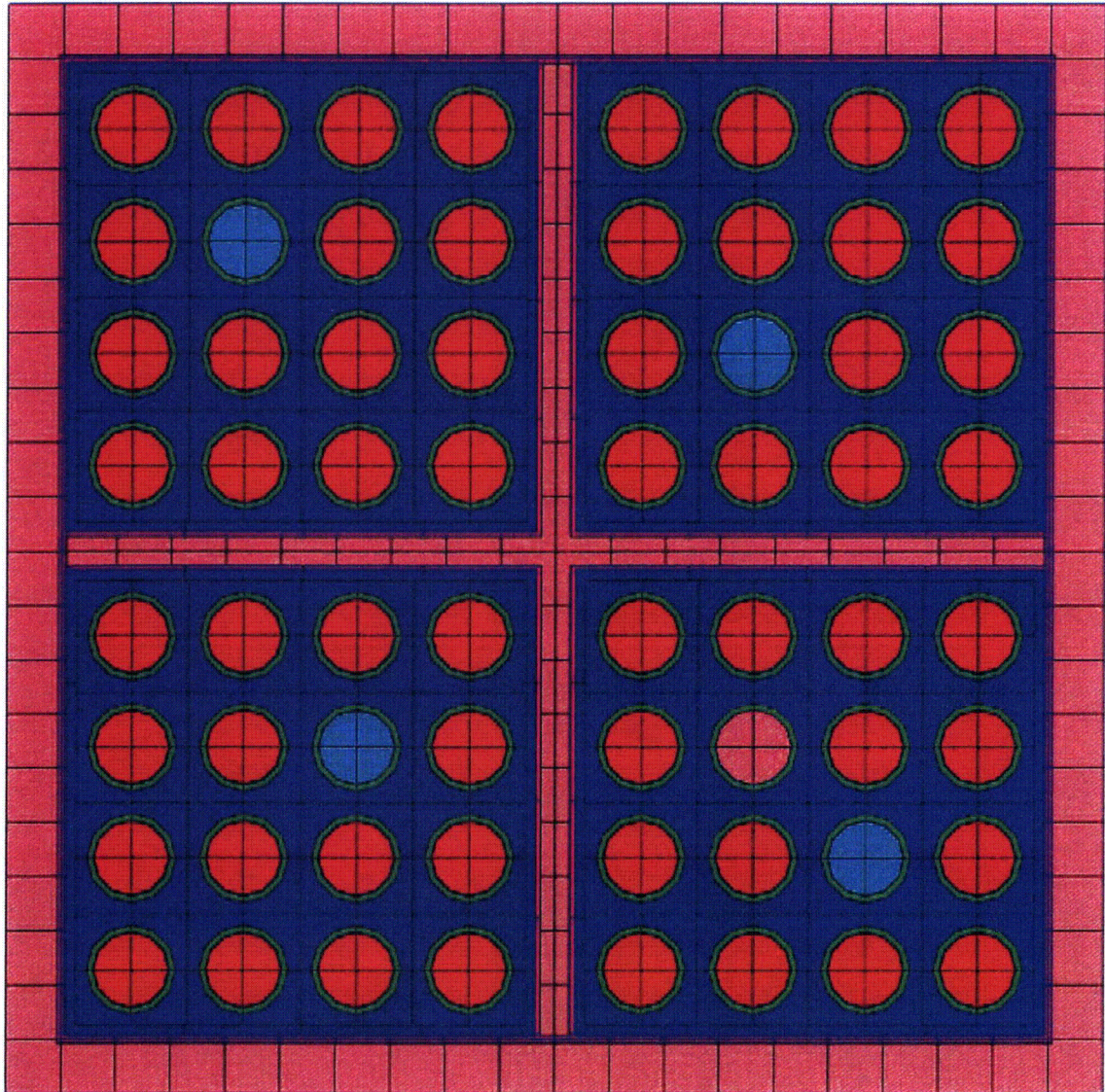


Figure 4.8 Layout of a BWR SVEA-64 assembly

4.2.4 BWR SVEA-100 Assemblies

Decay heat measurements were performed for four SVEA-100 assemblies: two of these assemblies were from the Oskarshamn-3 reactor and two from the Forsmark-3 reactor. The assemblies had a burnup range of about 31–40 GWd/MTU. Each SVEA-100 assembly contains four 5×5 sub-assemblies divided by a large water cross. There are 100 fuel rods in an assembly, some of these (5 or 8, depending of the assembly type) containing burnable poison. The assemblies contained no water rods or spacer rods. Data on the assembly design is presented in Table 4.29. Information on the reactor operating history and assembly irradiation, the average coolant density, fuel enrichment and initial uranium mass are given in Tables 4.29 and 4.30. The assembly layout is shown in Figure 4.9 for an assembly with six burnable absorber rods.

Table 4.29 Fuel assembly design data for SVEA-100 assemblies

Parameter	Data
Assembly and reactor data	Type 1
Lattice geometry	10×10
Assembly pitch (cm)	15.50
Channel moderator temperature (K)	552
Channel moderator density (g/cm^3)	0.75
Coolant temperature (K)	552
Number of fuel rods	100
Rod pitch (cm)	1.24
Assembly channel outer dimension (cm)	13.96
Assembly channel wall thickness (cm)	0.11
Assembly channel material	Zircaloy-4
Water cross material	Zircaloy-4
Water cross wall thickness (cm)	0.11
Sub-assembly inner dimension ^a (cm)	6.56
Spacer material	Inconel
Total spacer mass (g)	576/840 ^c
Number of burnable absorber rods	5/8 ^d
Gd ₂ O ₃ wt % in absorber rods	2.55/4.4
Fuel rod data	
Fuel material type	UO ₂
Effective fuel density (g/cm^3)	10.392
Effective fuel temperature (K)	900
Fuel pellet diameter (cm)	0.819
Fuel rod outside diameter (cm)	0.962
Clad material ^b	Zircaloy-2
Clad thickness (cm)	0.063
Average clad temperature (K)	573

^a Flat-to-flat distance across the subassembly box.

^b Zircaloy-2 material is assumed.

^c Total spacer mass is 576 g in assemblies 13620 and 13630; 840 g in assemblies 13847 and 13848.

^d There are 5 absorber rods in assemblies 13847 and 13848; 8 absorber rods in assemblies 13628 and 13630.

Table 4.30 Oskarshamn-3 reactor and SVEA-100 assembly irradiation data

Operational data		Cycle 2	Cycle 3	Cycle 4	Cycle 4B	Cycle 5	Cycle 6
Startup date		7/26/1986	7/26/1987	8/14/1988	12/22/1988	6/20/1989	8/1/1990
Shutdown date		7/3/1987	7/8/1988	12/10/1988	6/7/1989	6/23/1990	6/24/1991
Operating days		342	348	118	167	368	327
Downtime days		23	37	12	13	39	---

Assembly data		Assembly Burnup (MWd/t)								
ID	Type	Enrichment (wt % ²³⁵ U)	Initial U (kg)	Coolant density (g/cm ³)						
13628	1	2.711	180.77	0.3940	9,171	18,613	20,910	24,673	32,885	35,619
13630	1	2.711	180.78	0.3824	9,328	18,984	21,970	25,793	32,866	40,363

Table 4.31 Forsmark-3 reactor and SVEA-100 assembly irradiation data

Operational data		Cycle 2	Cycle 3	Cycle 4	Cycle 5
Startup date		9/2/1986	8/9/1987	9/5/1988	7/13/1989
Shutdown date		7/10/1987	8/12/1988	6/9/1989	7/13/1990
Operating days		311	369	277	365
Downtime days		30	24	34	---

Assembly data		Assembly Burnup (MWd/t)								
ID	Type	Enrichment (wt % ²³⁵ U)	Initial U (kg)	Coolant density (g/cm ³)						
13847	1	2.770	180.67	0.3816	7,857	17,217	23,779	31,275		
13848	1	2.770	180.67	0.3798	7,857	17,217	23,779	31,275		

- 1 fuel
- 2 clad
- 3 coolant
- 4 gap
- 5 fuel-gd (3.5%)
- 9 channel box
- 10 moderator

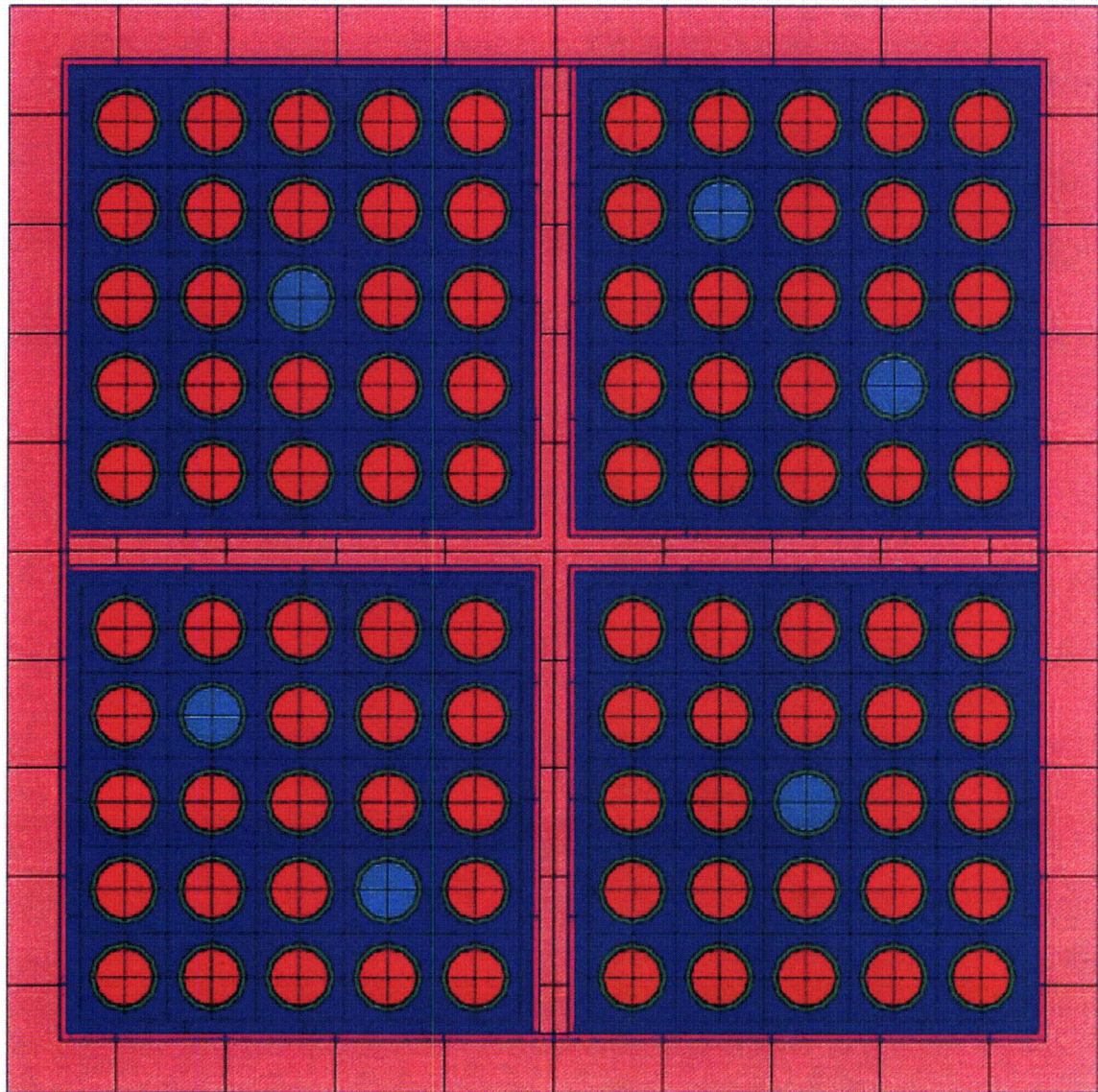


Figure 4.9 Layout of a BWR SVEA-100 assembly

4.2.5 PWR 15 × 15 Assemblies

Decay heat measurements were performed for sixteen 15 × 15 PWR assemblies that have been irradiated in the Ringhals 2 reactor. Each assembly has 204 fuel rods, 20 guide tubes and 1 instrument tube. No burnable absorber rods were present in the assembly. The assemblies are grouped into two types based on the dimensions of the fuel pellet, clad thickness, guide tube diameter, spacer material and total spacer mass. The assembly design data are presented in Table 4.32. The fuel density for each assembly type is an average value over all assemblies of that type. The irradiation history information for each assembly is presented in Table 4.33, and the fuel enrichment and initial uranium load are given in Table 4.34. The total burnup of the Ringhals 15 × 15 assemblies is in the range 28–51 GWd/MTU. The configuration of the assembly is shown in Figure 4.10.

Table 4.32 Fuel assembly design data for PWR 15 × 15 assemblies

Parameter	Data	
Assembly and reactor data	Type 1	Type 2
Lattice geometry	15 × 15	15 × 15
Fuel rod active length (cm)	365.8	365.8
Assembly pitch (cm)	21.50	21.50
Coolant density (g/cm ³)	0.72	0.72
Coolant temperature (K)	552	552
Average soluble boron level (ppm)	650	650
Number of fuel rods	204	204
Number of guide tubes	20	20
Number of instrument tubes	1	1
Rod pitch (cm)	1.43	1.43
Spacers material	Inconel	Inconel/Zircaloy-4
Spacers total mass (g)	788	720/160
Fuel rod data		
Fuel material type	UO ₂	UO ₂
Effective fuel density (g/cm ³)	10.227	10.137
Effective fuel temperature (K)	900	900
Fuel pellet diameter (cm)	0.929	0.911
Fuel rod outside diameter (cm)	1.072	1.075
Clad material	Zircaloy-4	Zircaloy-4
Clad thickness (cm)	0.0618	0.0725
Average clad temperature (K)	573	573

Table 4.33 Ringhals-2 reactor and PWR 15 × 15 assembly irradiation data

Operational data												
	Cycle 1	Cycle 2	Cycle 3	Cycle 4	Cycle 5	Cycle 6	Cycle 7	Cycle 8	Cycle 9	Cycle 10	Cycle 11	Cycle 12
Startup date	6/19/1974	7/7/1977	5/26/1978	6/25/1979	6/18/1980	6/23/1981	7/29/1982	7/28/1983	7/12/1984	6/14/1985	7/2/1986	6/18/1987
Shutdown date	4/13/1977	3/31/1978	4/3/1979	4/1/1980	4/4/1981	5/6/1982	4/28/1983	4/13/1984	4/4/1985	4/30/1986	4/25/1987	5/12/1988
Operating days	1029	267	312	281	290	317	273	260	266	320	297	329
Downtime days	85	56	83	78	80	84	91	90	71	63	54	—

Assembly data												
ID	Type	Assembly			Burnup	(MWd/MTU)						
C01	1	11,247	20,650	28,219	36,688							
C12	1	11,247	20,565	27,955	36,385							
C20	1	11,247	20,624	28,078					35,720			
D27	2			9,510	22,399	31,666		39,676				
D38	2		6,367	15,698	23,056	31,757	39,403					
E38	2			7,568	16,026	25,905	33,973					
E40	2			7,705	14,954	25,609	34,339					
F14	2				5,069	15,824	25,722	34,009				
F21	2				4,767	11,084	21,130	29,385	36,273			
F25	2				8,307	19,056	27,372	35,352				
F32	2					10,553	21,162	29,553		37,314	43,943	50,962
G11	2					6,890	17,312	25,180	32,123	35,463		
G23	2						10,268	20,303	27,921	35,633		
I09	2								6,727	15,677	24,742	32,310
I24	2								8,245	17,212	26,356	34,294
I25	2								5,207	10,198	20,001	28,999
											36,859	

**Table 4.34 Fuel enrichment and initial uranium load for
PWR 15 × 15 assemblies**

Assembly ID	Type	Enrichment (wt % ²³⁵ U)	Initial U (kg)
C01	1	3.095	455.79
C12	1	3.095	453.74
C20	1	3.095	454.76
D27	2	3.252	432.59
D38	2	3.252	434.21
E38	2	3.199	433.59
E40	2	3.199	434.24
F14	2	3.197	436.38
F21	2	3.197	435.94
F25	2	3.197	437.29
F32	2	3.197	436.99
G11	2	3.188	436.18
G23	2	3.206	436.13
I09	2	3.203	437.35
I24	2	3.203	429.60
I25	2	3.203	433.06

- 1 fuel
- 2 clad
- 3 water
- 4 gap
- 5 guide tube

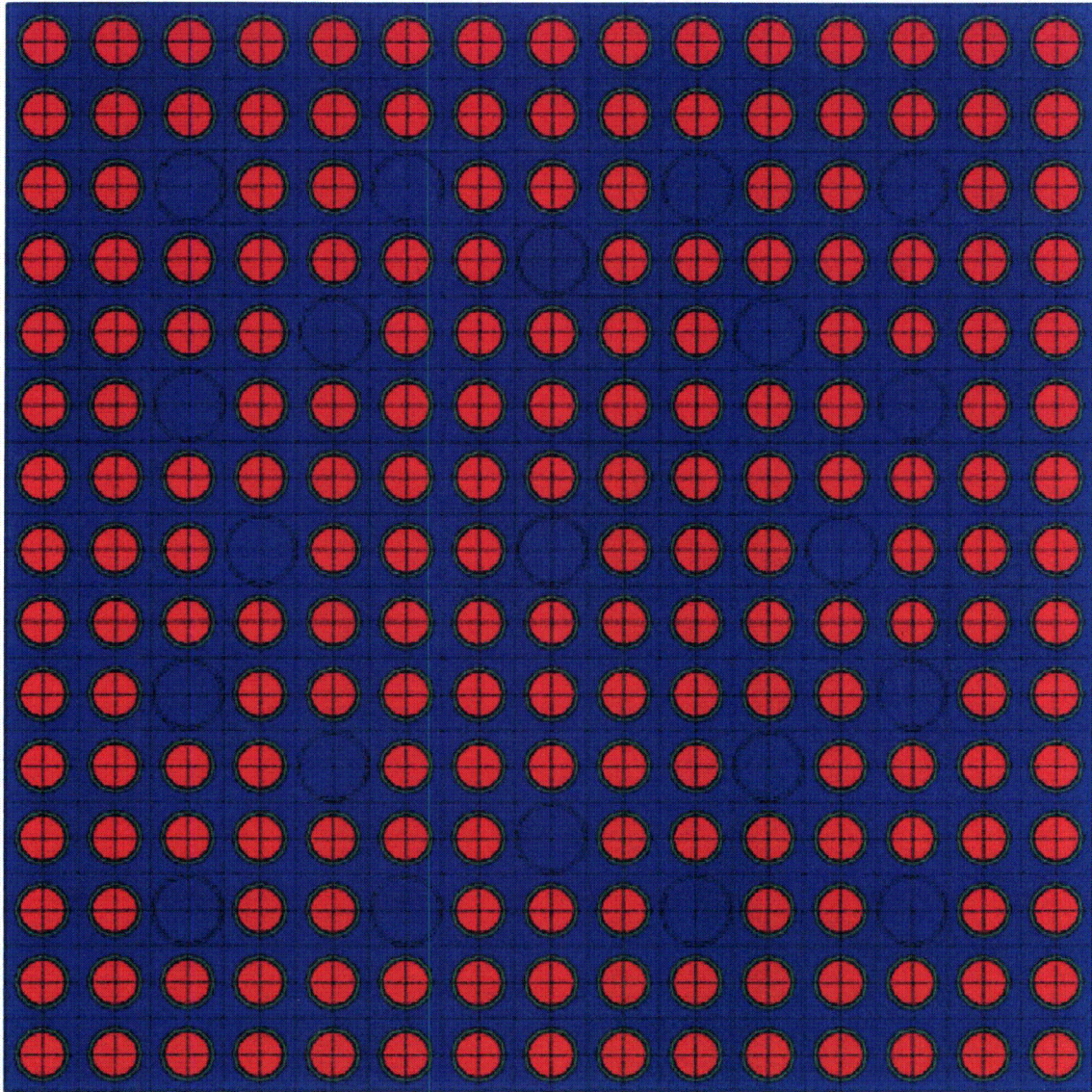


Figure 4.10 Layout of Ringhals PWR 15 × 15 assembly

4.2.6 PWR 17 × 17 Assemblies

Decay heat measurements data are available for fourteen 17 × 17 PWR assemblies that have been irradiated in the Ringhals 3 reactor. Each assembly contains 264 fuel rods, 24 guide tubes, and 1 instrument tube. Four of these assemblies (with identifiers 0C9, 1C5, 3C5 and 4C7) were exposed to burnable absorber rods located inside 12 of the 24 guide tubes. The absorber rods employ borosilicate glass as the absorber material in an annular rod configuration with inner void. The configuration of the 12 absorber rods was obtained from NUREG/CR-6761 (Ref. 41). The total burnup of the assemblies is in the range 20–42 GWd/MTU. Assembly design data are shown in Table 4.35. The fuel density shown in Table 4.35 is an average value over all assemblies. Information on irradiation history data, fuel enrichment and initial uranium load is shown in Table 4.36. A layout for an assembly containing burnable absorber rods is shown in Figure 4.11.

Table 4.35 Fuel assembly design data for PWR 17 × 17 assemblies

Parameter	Data
Assembly and reactor data	
Lattice geometry	17 × 17
Fuel rod active length (cm)	365.8
Assembly pitch (cm)	21.50
Coolant density (g/cm ³)	0.72
Coolant temperature (K)	552
Average soluble boron level (ppm)	650
Number of fuel rods	264
Number of guide tubes	24
Number of instrument tubes	1
Rod pitch (cm)	1.26
Spacers material	Inconel 718
Total spacer mass (g)	788
Fuel rod data	
Fuel material type	UO ₂
Effective fuel density (g/cm ³)	10.27
Effective fuel temperature (K)	900
Fuel pellet diameter (cm)	0.8191
Fuel rod outside diameter (cm)	0.95
Clad material ^b	Zircaloy-4
Clad thickness (cm)	0.0571
Average clad temperature (K)	573
Guide (instrument) tube data	
Tube material	Zircaloy-4
Outer diameter (cm)	1.224
Thickness (cm)	0.0406
Burnable absorber rod data	
Number of rods inserted	12
Absorber material	B ₂ O ₃ -SiO ₂
Material density (g/cm ³)	2.299
Burnable poison content (wt % B ₂ O ₃)	12.5
Outer diameter of absorber region (cm)	0.85344
Inner diameter of absorber region (cm)	0.4826
Outer diameter of outer clad (cm)	0.96774
Inner diameter of outer clad (cm)	0.87376
Outer diameter of inner clad (cm)	0.46101
Inner diameter of inner clad (cm)	0.42799

Table 4.36 Ringhals-3 reactor and PWR 17 × 17 assembly irradiation data

Operational data		Cycle 1A	Cycle 1B	Cycle 2	Cycle 3	Cycle 4	Cycle 5
Startup date		7/29/1980	9/14/1983	7/24/1984	7/11/1985	7/18/1986	8/4/1987
Shutdown date		6/2/1983	5/11/1984	5/25/1985	5/30/1986	6/18/1987	7/7/1988
Operating days		1038	240	305	323	335	338
Downtime days		104	74	47	49	47	---

Assembly data									
ID	BA rod exposure	Enrichment (wt % ²³⁵ U)	Initial U (kg)	Assembly burnup (MWd/MTU)					
2A5	No	2.100	462.03	12,228	20,107				
5A3	No	2.100	461.48	11,696	19,699				
0C9	Yes	3.101	457.64	9,884	18,076	28,426	38,442		
1C2	No	3.101	459.05	6,249	11,268	22,777	33,318		
1C5	Yes	3.101	457.99	9,884	17,986	28,397	38,484		
2C2	No	3.101	459.49	7,783	16,128	26,060	36,577		
3C1	No	3.101	458.43	7,783	16,124	26,055	36,572		
3C5	Yes	3.101	458.87	9,884	17,997	28,340	38,373		
3C9	No	3.101	459.14	7,783	16,160	26,036	36,560		
4C4	No	3.101	459.05	6,249	11,240	22,270	33,333		
4C7	Yes	3.101	458.26	9,884	17,985	28,332	38,370		
0E2	No	3.103	463.60			7,496	20,530	31,838	41,628
0E6	No	3.103	461.77				12,490	25,521	35,993
1E5	No	3.103	463.90				10,556	23,690	34,638

- 1 fuel
- 2 clad
- 3 water
- 4 gap
- 5 guide tube
- 6 ba
- 7 ba clad

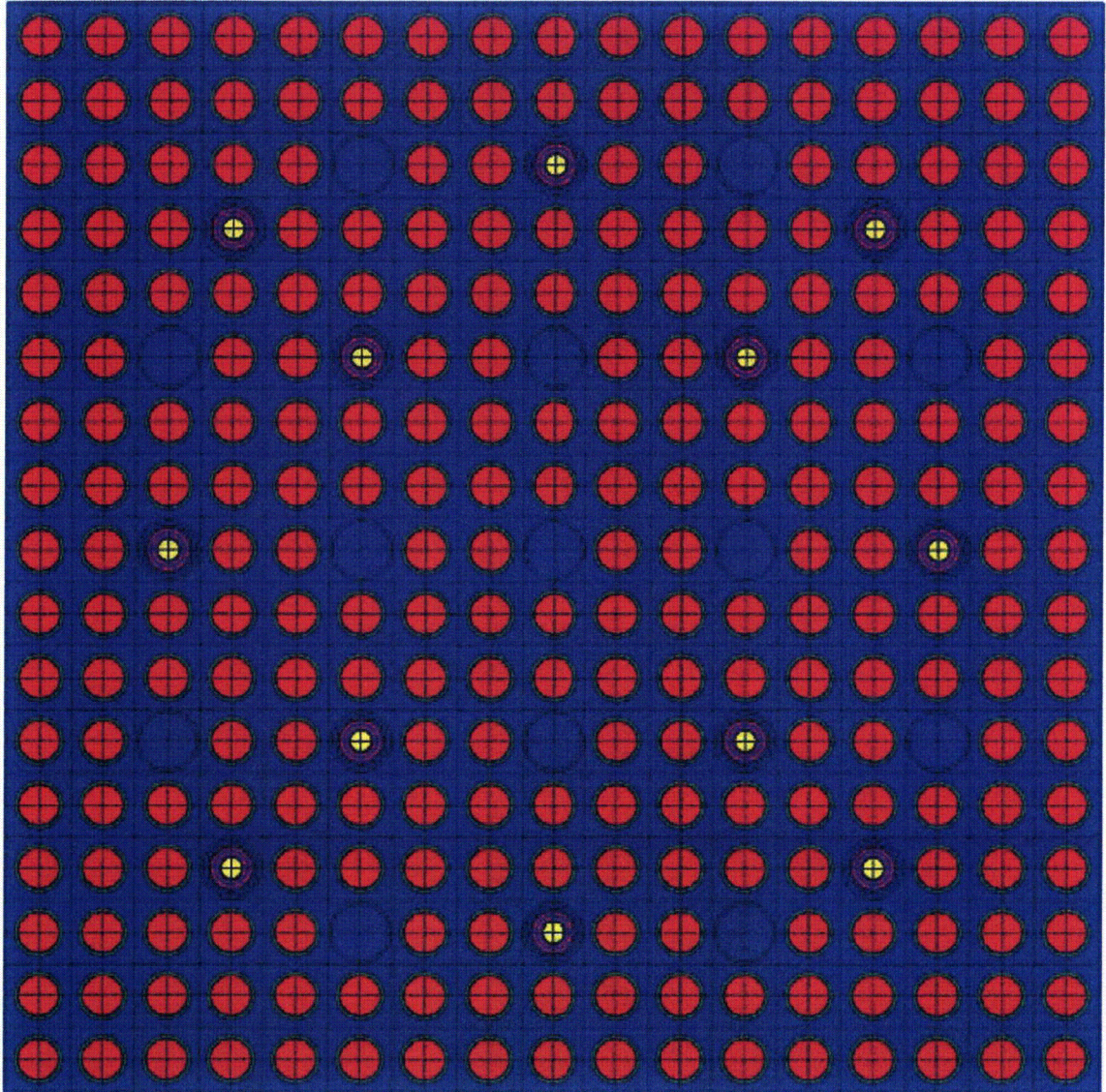


Figure 4.11 Layout of Ringhals 3 PWR 17 × 17 assembly (with burnable absorbers)

5. COMPUTATIONAL METHODS AND MODELS

The computational methodology used to analyze the decay heat measurements is described in this section. All decay heat calculations presented in this report were performed using the ORIGEN-S code. The methodology involved two steps: the first step was the generation of cross-section libraries for each of the different fuel assembly designs; the second step was the application of these libraries for the ORIGEN-S depletion and decay analyses to predict assembly decay heat. Cross-section libraries for the different fuel assembly design configurations were created using two-dimensional neutron transport methods available in the SCALE 5 code system. Calculations using one-dimension depletion methods were also performed for selected assemblies for comparison. A general description of the codes and the computational steps in this procedure are presented. Specific details on the models developed for each assembly type discussed in this study, and input examples, are also provided.

5.1 SCALE Depletion Methods and Data

SCALE is a computational system of codes and data libraries suitable for analysis of nuclear criticality safety, radiation shielding, reactor lattice physics, and spent nuclear fuel characterization. SCALE is used internationally for nuclear fuel facility, and transportation, storage facility design, and safety analyses. The configuration of SCALE used in this study is the version distributed as SCALE 5.1.

5.1.1 ORIGEN-S Code

ORIGEN-S is the depletion module in SCALE used to calculate the isotopic composition of spent fuel, the neutron and gamma radiation source intensity and energy spectra, and the decay heat released from the decay of actinides, fission products, and activated structural components. ORIGEN-S tracks the time-dependent concentrations and decay properties for 1946 individual nuclides. The decay properties of spent fuel are determined from the summation of the contributions from all nuclides in the problem. The numerical methods used in ORIGEN-S to solve the large system of coupled differential equations that describe the isotopic transmutation and decay processes are largely unchanged from other versions of the ORIGEN code.^{42,43} The matrix exponential method is employed to solve the nuclide transmutation equations as defined by a generalized matrix of transition constants. To mitigate numerical roundoff error the short-lived radioisotopes, as defined relative to the time step size, are removed from the transition matrix and are solved analytically using a generalized form of the Bateman equations that are solved by the Gauss-Seidel iterative method.

The physical geometry and layout of the assembly (e.g., fuel diameter, rod pitch, water rods configuration) has an important effect on the flux spectrum in the fuel, and thus the average value of the cross sections used in depletion simulations. Reactor operating conditions (e.g., fuel temperatures, moderator temperatures, moderator density, soluble boron level, and control absorbers) also have a strong influence on the cross sections. As the fuel is irradiated the concentrations of the fissile actinides and fission product absorbers change, resulting also in a time dependence of the flux spectrum and effective cross sections.

One of the major advantages of using SCALE for spent fuel analysis is that burnup simulations can be performed within control modules that automatically couple ORIGEN-S with neutronic transport codes to dynamically generate time-dependent cross sections for the burnup analysis. The control modules for the depletion analysis sequences contain automated procedures to generate time- and problem-dependent cross-section libraries. This allows a dramatic improvement in flexibility compared with other versions of the ORIGEN code, which provided the user with a limited set of precalculated libraries. For calculations involving fuel types or configurations not covered by available libraries, the user generally

had no access to appropriate cross-section data. The SCALE system allows the user to set up physics models of the fuel lattice and apply problem-dependent reactor conditions and operating history information to the depletion analysis.

5.1.2 Depletion Analysis Methodology

The SCALE depletion sequences perform automated problem-dependent burnup and decay analyses by automatically coupling reactor physics lattice codes to the fuel depletion code ORIGEN-S. Two depletion analysis sequences are available in SCALE 5.1: a 1-D depletion sequence SAS2H⁴⁴ that uses the XSDRNPM discrete ordinates transport code,⁴⁵ and TRITON depletion sequence⁴⁶ that uses the NEWT 2-D discrete ordinates lattice code,⁴⁷ with an option to perform 3-D depletion calculations using the KENO-V.a or KENO-VI Monte Carlo transport codes. This section provides an overview of the 1- and 2-D depletion analysis methods used in this study.

Both sequences use the SCALE Material Information Processor to calculate the material number densities and prepare geometry data for resonance self-shielding and to create the input files for each of the cross-section processing codes. The problem-specific (resonance and temperature corrected) cross sections to be used with the transport codes are prepared by the BONAMI and NITAWL cross-section processing codes. BONAMI applies the Bondarenko method of resonance self-shielding for nuclides that have Bondarenko data included in the library. The SCALE libraries typically use Bondarenko data to process group cross sections in the unresolved resonance range. NITAWL uses the Nordheim integral method to perform analytical resonance self-shielding corrections for nuclides with resolved resonance parameters in the library. An alternate self-shielding cross section module is available in SCALE 5 that uses the CENTRM code (Continuous Energy Transport Module) to calculate group-average cross sections. CENTRM computes the continuous-energy neutron flux spectrum for a 1-D system using a combination of pointwise and multigroup transport cross sections. The problem-specific neutron flux is computed on a fine energy mesh (> 10,000 points) and can be used to generate self-shielded group cross sections from continuous-energy cross sections using the PMC (Produce Multigroup Cross Sections) module.

All depletion analysis calculations performed in the present study using the NITAWL self-shielding module was used for resonance processing. Approximately 250 room-temperature critical benchmarks were used to validate the CENTRM/PMC methodology. However, there is only limited experience with using CENTRM/PMC for reactor operating condition and fuel depletion. The NITAWL module was used based on its demonstrated past performance for LWR fuel configurations. A limitation of NITAWL is that fuel rod subdivision is not permitted and fuel rods must be treated as a single region.

The main difference between the depletion sequences is the neutron transport module. TRITON uses the 2-D arbitrary polygonal mesh discrete ordinates transport code NEWT to solve for the neutron flux distribution in the assembly. NEWT represents geometrical bodies as arbitrary polygons and uses the Extended Step Characteristic method to solve for the spatial discretization. NEWT uses an automated grid generation feature that makes it easy for the user to define complex configuration. The version of NEWT released in SCALE 5.1 uses a combinatorial geometry package, similar to KENO-VI geometry, that allows the user to easily migrate between 2-D deterministic and 3-D Monte Carlo models. The SAS2H depletion analysis sequence uses the 1-D discrete ordinates code XSDRNPM, which combines features of earlier ANISN, GAM-II, and THERMOS computer programs. To enable more accurate modeling of heterogeneous systems, XSDRNPM is implemented in SAS2H using a two-pass approach that first uses cell homogenization and then applies the homogenized cross sections in a second model that may include nonfuel water regions, absorber rods, or burnable poison rods in an assembly. The SAS2H methodology and modeling procedures are described in more detail in Sect. 5.2. The NEWT geometry provides greater flexibility and accuracy in modeling heterogeneous lattices, and it allows

simulation of multiple fuel types (e.g., different enrichment zones, burnable absorbers, etc.) that can be independently depleted.

After the transport calculation is complete, the neutron flux solution is used to weight the SCALE multigroup cross sections and prepare effective one-group cross sections for use with ORIGEN-S for all nuclides available in the library. The COUPLE code performs the function of updating the ORIGEN-S cross-section library with the weighted problem-dependent cross sections derived from the transport calculations. At defined burnup intervals during the simulation, the updated nuclide concentrations from ORIGEN-S are applied to the transport analysis of the assembly lattice, and the neutron flux spectrum is recalculated. The cross sections are again updated and used by ORIGEN-S for the following computational step.

The typical calculational flow used in SCALE depletion sequences is shown in Figure 5.1 for a single burnup step. After this sequence of calculations is complete, the isotopic concentrations from the ORIGEN-S calculation are used to update each of the codes in the sequence to reflect the change in compositions and other reactor operating conditions with time. The sequence of calculations is repeated until the final discharge burnup is achieved.

The decay heat calculations based on the TRITON depletion sequences can be performed in two ways. One approach is to perform the depletion and decay analysis for each individual assembly directly using TRITON. However, there is a significant computational time associated with using the depletion sequence, particularly for the resonance self-shielding and NEWT transport calculations. A second and more efficient approach consists of (1) performing TRITON depletion simulations for each assembly type to generate a burnup-dependent cross-section library for the assembly, and then (2) using the generated library to perform standalone ORIGEN-S irradiation and decay simulations for each assembly having the same, or similar design and operating characteristics.

Time-dependent cross-section libraries are applied to standalone ORIGEN-S calculations using the ORIGEN-ARP sequence in SCALE. This sequence uses the Automatic Rapid Processing (ARP) module in SCALE to interpolate cross sections in an ORIGEN-S library parameterized as a function of fuel burnup, initial enrichment, and moderator density (in the case of BWR assemblies). Therefore, the user can employ the depletion sequences to generate burnup-dependent libraries that cover a range of discrete fuel parameters (e.g., enrichment and coolant density) and then use ARP to interpolate problem and time-dependent cross sections for any fuel type within that range. In effect, the calculation is performed using the same cross sections as those used in the depletion sequence analysis, and the method produces results with the same accuracy. However, the calculations are performed in a small fraction of the time required by coupled depletion simulation because all resonance processing and transport calculations have been performed in advance and the cross sections saved for subsequent use. This methodology was employed as the reference method for all TRITON calculations presented in this report. A more detailed description of the procedures is given in Sect. 5.1.5. Calculations were also performed for selected assemblies using SAS2H. However, these calculations were performed directly using the SAS2H sequence (without cross-section interpolation) because the sequence runs relatively quickly.

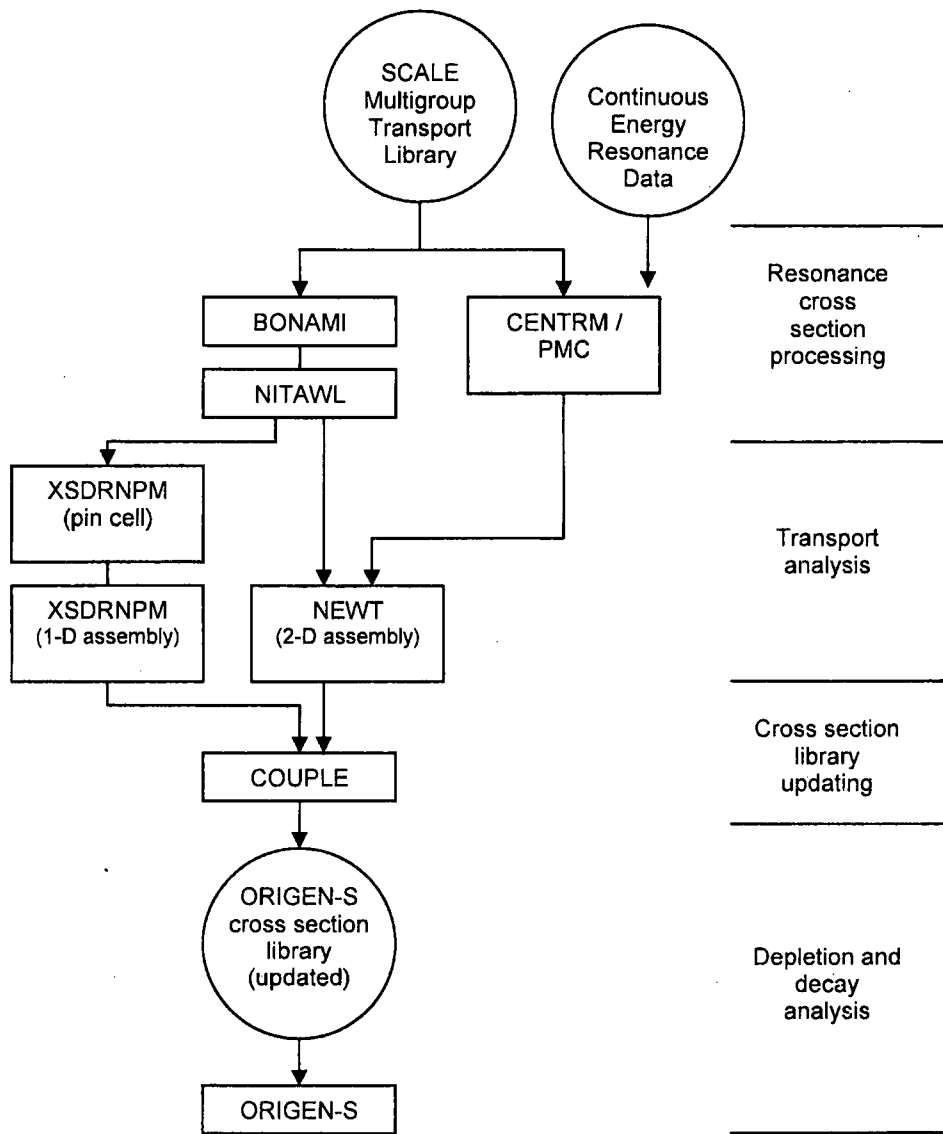


Figure 5.1 Calculational flow of SCALE depletion analysis (1-D and 2-D) for one time step

5.1.3 SCALE Cross-Section Libraries

The transport calculations (with XSDRNPM or NEWT) can be performed using any of the SCALE multigroup neutron cross-section libraries. The libraries recommended for use with the depletion analysis sequences are the SCALE 44-group and 238-group libraries, both based on ENDF/B-V. These libraries contain evaluated cross section data for more than 220 nuclides that can be collapsed and applied in the ORIGEN-S burnup simulations. The 44-group library is a broad-group version of the 238-group library, collapsed using a fuel cell spectrum based on a typical 17×17 fuel assembly. All transport calculations in this study were performed using the SCALE 44-group ENDF/B-V cross-section library. Resonance cross section selfshielding was performed using the BONAMI and NITAWL modules.

5.1.4 ORIGEN-S Data Libraries

All nuclear decay and cross-section data in the ORIGEN-S libraries have been updated with modern data. Decay data are derived from the Evaluated Nuclear Data Files (ENDF/B-VI) and the Evaluated Nuclear Structure Data File (ENSDF). Cross-section data have also been entirely updated with modern evaluations to include a wide range of reaction types. The neutron intensity and energy spectra calculations performed by ORIGEN-S are based on methods developed in the SOURCES code,⁴⁸ providing substantial improvements as compared with other codes, particularly for the neutron source associated with (α, n) reactions in the fuel matrix. In addition, all gamma ray intensity and spectra calculations are performed using an updated library of line-energy photon yields that can generate spectra in any energy group structure.

Multigroup cross sections for nuclides in the SCALE cross-section libraries can be weighted with the flux spectrum from the transport calculation and then used to prepare the effective one-group cross sections for use in the ORIGEN-S calculation. The maximum number of nuclides that can be updated with this procedure is about 220; the number of isotopic evaluations within the ENDF/B-V libraries. However, the ORIGEN-S library presently has reaction data for 854 nuclides. ORIGEN-S cross sections for those nuclides not updated with data from either the 44- or 238-group SCALE library are obtained using a different procedure. In these cases cross sections from a standard broad-group cross-section library available with ORIGEN-S are employed. The broad-group (3-group) cross sections, derived from continuous-energy cross section evaluations weighted using a typical midlife fuel spectrum for a PWR, are collapsed using time-dependent flux weighting factors derived from the problem-dependent flux solution from the transport calculation. Cross sections are available for the following reaction types: fission, radiative capture (n, γ), ($n, 2n$), ($n, 3n$), (n, p) and (n, α).

The ORIGEN-S libraries also contain direct fission product yields for 30 fissionable actinides: ^{227,228,232}Th, ²³¹Pa, ²³²⁻²³⁸U, ²³⁸⁻²⁴²Pu, ^{241,242m,243}Am, ^{237,238}Np, ^{242-246,248}Cm, ^{249,252}Cf, and ²⁵⁴Es. The yields are derived from ENDF/B-VI.

A detailed description of the sources of decay data and cross-section data implemented in the ORIGEN-S libraries can be found in Ref. 49.

5.1.5 ORIGEN-S Cross-Section Library Generation

The SCALE depletion analysis sequences perform full problem-dependent burnup simulations using design-specific information provided by the user. The depletion sequences function by iteratively performing transport calculations to update the cross sections and burnup simulations to update the nuclide concentrations. At defined intervals throughout an irradiation simulation, the transport code recalculates the cross sections to reflect the changes with burnup (time) in nuclide concentrations and

other reactor operating conditions. These coupled code systems are complex. They require detailed fuel design and operational information and require significant computer resources. The need for repeated transport calculations to recalculate the time-dependent cross sections also makes them relatively slow to execute.

As described previously, the cross-section libraries generated by these sequences may be saved and used later in standalone ORIGEN-S simulations. The libraries can be used for depletion calculations involving fuels having the same or similar configurations without the need to recalculate the cross sections each time. When cross-section libraries are generated over a range of discrete fuel parameter values, the cross sections can be interpolated to provide accurate depletion capability for a wide range of potential fuel conditions.

In ORIGEN-ARP, this interpolation function is performed using the ARP utility module. ARP reads the prepared libraries and interpolates a problem-dependent library for ORIGEN-S using the specified input. Cross sections can be interpolated as a function of burnup, enrichment, and coolant density value for situations where the conditions of the application are different than the conditions used to generate the libraries. The cross-section interpolation scheme of ARP uses a maximum of four cross-section data points with a third-order Lagrangian polynomial fit. The interpolation function will automatically search the array of independent variables to determine the appropriate points to use for the fit. The function will automatically adapt to perform a lower-order polynomial fit if fewer than four points are available. For two enrichment points, linear interpolation is performed. The interpolation is performed on all cross section data in a library, not just the cross sections for the most important actinides. Interpolation is performed for (1) the full transition matrix, (2) the neutron absorption cross section array, (3) the fission cross section array, and (4) the fission cross section multiplied by the neutrons per fission.

The interpolation procedure eliminates the need to perform reactor physics transport calculations during the burnup simulation because the parameterized cross sections are developed in advance. Because the time to perform resonance self-shielding and the neutron transport calculation typically represents the majority of time in a depletion analysis calculation, the procedure runs in a small fraction of the time required by other methods, while maintaining the full accuracy of a coupled reactor physics calculation.

5.1.5.1 Library Generation Procedures

Cross-section libraries were generated for each of the assembly designs used in this study using the 2-D transport methods of the TRITON depletion sequence. Cross sections were generated as a function of burnup and fuel enrichment for PWR assemblies; a third parameter, coolant density, was added when generating BWR cross-section libraries. Examples of the input files for each type of assembly design are listed in Appendix B. The basic steps followed in creating the cross-section libraries are described below.

1. TRITON/NEWT Lattice physics models for each assembly design were first created (see Appendix B). The models include a 2-D description of the assemblies, including geometry, material compositions, and temperatures.
2. Extra nuclides were added at trace initial concentrations (10^{-20} atoms/barn-cm) in the fuel composition description. This procedure ensures that the nuclides are included in the transport calculation as the concentrations increase during irradiation and that weighted cross sections for these nuclides are applied in the ORIGEN-S depletion simulation. This is done automatically in TRITON using the keyword `addnux=3` as a parameter entry in the input file.
3. Depletion calculations were performed using burnup steps of 3,000 MWd/MTU each, extending up to 72,000 MWd/MTU. Each depletion calculation produced a library containing 24 sets of burnup-dependent cross sections. An additional step is added at the beginning of irradiation with a short time (10^{-15} d) to generate cross sections for effectively unirradiated fuel. Each set of cross sections is referenced and accessed by its position in the library.
4. The library was subsequently thinned to remove cross-section sets in the burnup range where the cross sections show only small variations with changes in burnup (e.g., generally in the regime of higher burnup). The library thinning was performed using the ARPLIB utility of SCALE. The thinning significantly decreased library memory requirements. The positions and corresponding burnup for each cross section set in the initial and final (thinned) library are listed in Table 5.1. An example of the input for ARPLIB is listed in Appendix B.
5. The burnup calculations described above were repeated for discrete ^{235}U initial enrichment values to cover the range of enrichments corresponding to the assemblies considered in this study. The enrichment steps used in this study were 1 wt % ^{235}U (e.g., 2.0 and 3.0 wt % ^{235}U).
6. Water moderator density for BWR assemblies can change from typically about 0.7 g/cm^3 at the core inlet (bottom of assembly) to 0.2 g/cm^3 or lower at the top of the assembly due to voiding of the coolant within the flow channel caused by boiling. The voiding has the effect of hardening the neutron spectrum in the fuel (shifting the spectrum to higher energy) and therefore influences the value of the effective cross sections. To account for this effect in the current study, libraries for the BWR assemblies were generated as a function of the effective moderator density using discrete values of 0.1, 0.3, 0.5, 0.7, and 0.9 g/cm^3 . Libraries for PWR assemblies were created using a single average value for the water moderator density because the density does not change significantly with axial height.

The procedure described above was used to generate cross-section libraries for each assembly design.

Table 5.1 Cross-section positions and burnup values created in the SCALE libraries

Initial positions	Final positions	Burnup (MWd/MTU)
1	1	0^a
2	2	1500
3	3	4500
4	4	7500
5	5	10500
6	6	13500
7	7	16500
8		19500
9		22500
10		25500
11		28500
12	8	31500
13		34500
14		37500
15		40500
16		43500
17	9	46500
18		49500
19		52500
20		55500
21	10	58500
22		61500
23		64500
24		67500
25	11	70500

^a These bolded values represent the burnup of the 11 cross-section sets retained in the final cross-section library.

5.2 SAS2H Assembly Models

The reference method for calculating decay heat in this study was to use the 2-D depletion sequence TRITON because it allows a greater accuracy and flexibility in modeling the fuel assembly configurations, particularly for the more complex and heterogeneous BWR assembly designs. However, the SAS2H 1-D depletion sequence in SCALE is well established and has been widely used and demonstrated to be appropriate for a wide range of fuel assembly designs through an extensive benchmarking and validation program.^{3,35,50-52} The 1-D method also has a much better computational efficiency.

To provide a comparison between 1-D and the more recently developed 2-D depletion methods in SCALE, calculations were performed for selected assemblies measured at the Swedish CLAB facility using the SAS2H depletion analysis sequence to demonstrate the applicability of the 1-D models. A general description of the assembly models developed for SAS2H is given in Section 5.2.1.

SAS2H uses the 1-D discrete ordinates transport code XSDRNPM to simulate the lattice physics for the fuel rods and the assembly. This is accomplished by first performing a pin cell calculation to generate homogenized cell-weighted cross sections for the fuel, clad, and coolant. The homogenized pin cell mixture and cross sections are subsequently applied in a second transport calculation that can model heterogeneity in the assembly. This procedure is shown in Figure 5.2 for an illustrative example of eight fuel rods surrounding a central non-fuelled cell (×), e.g., water-filled guide tube, instrument tube, burnable absorber, or poison rod. The first XSDRNPM calculation (A) is performed for a single fuel rod and surrounding moderator associated with the simple pin cell to generate a cell-weighted mixture. The homogenized cross sections are then applied to a second XSDRNPM transport model of the assembly (B), illustrated in Figure 5.2 with the nonfuel cell centrally located in the assembly. The assembly model is represented in XSDRNPM using cylindrical geometry with equivalent region volumes. This procedure allows the user to accurately represent one level of heterogeneity in the model that would otherwise not be possible with a single 1-D transport calculation.

5.2.1 Modeling Techniques

For assemblies with multiple absorber rods or nonfuel lattice cells, the general procedure used in SAS2H is to model a single nonfuel cell in the center of the assembly and surround that cell with the volume of the homogenized fuel mixture that preserves the ratio of the nonfuel and fuel material in the assembly model. For example, an assembly with 25 nonfuelled water cells (1 instrument tube and 24 guide tubes) would be modeled as a central water cell surrounded by 1/25 of the total number of actual fuel rods in the assembly. Therefore, these models physically represent only a fraction of the entire assembly. The XSDRNPM transport model applies a reflective outer boundary condition to closely preserve the neutronic environment of the actual assembly.

For more complex assembly designs the limitations of a 1-D model may require approximations in the way the assembly model is constructed, particularly for assemblies having several levels of heterogeneity, e.g., an assembly containing both guide tubes and absorber rods. For some configurations these approximations can lead to several possible models that could be equally justifiable. In addition, the SAS2H sequence allows only one fuel mixture type. Therefore, assemblies containing fuel rods of different enrichment can not be simulated; the assembly-average enrichment is typically employed in this case.

The approach, described above, has been shown to be highly reliable for PWR assembly configurations with only one heterogeneous cell type (e.g., guide tubes or burnable absorber rods). Nonfuel regions are

generally uniformly distributed in the assembly, rather than clustered, and are symmetrical, which allows for the accurate subdivision of the assembly in the model, i.e., a subassembly model.

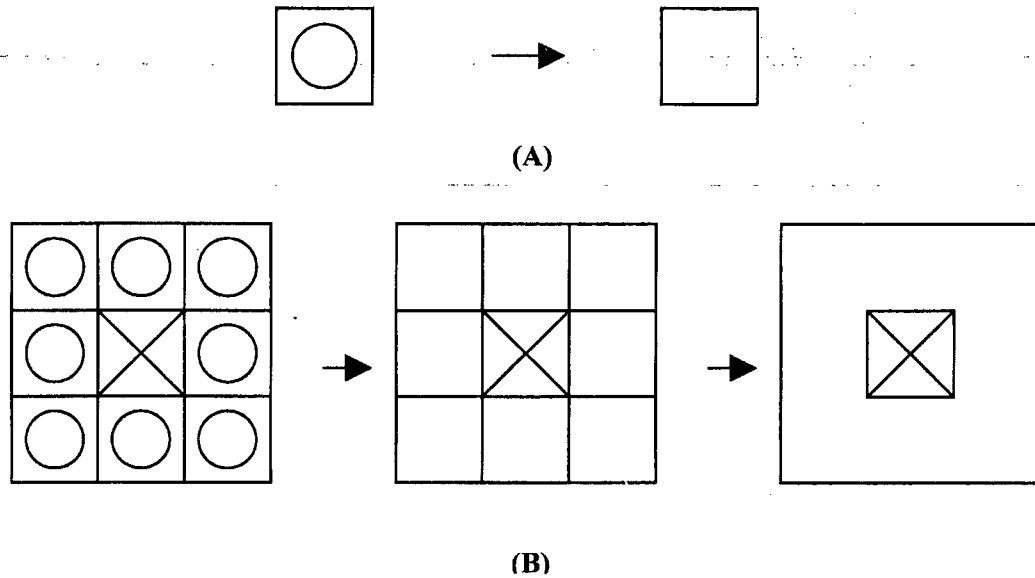


Figure 5.2 Pin-cell homogenization procedure used in SAS2H 1-D assembly models

Designs for modern BWR assemblies are generally more complex and heterogeneous than PWR assemblies. They often involve enrichment zoning, employ integral burnable poisons, have either small or large water rods (channels), and include regions of boiling water and non-boiling water in the channels and outside of the assembly flow tube. The multiple levels of heterogeneity require approximations in a 1-D model, and different approaches can yield different models for the same assembly.

Murphy⁵³ previously investigated the effect of different 1-D modeling approximations on the predicted decay heat for modern BWR assembly designs. A potential consequence of using a standard subassembly model for BWR assemblies is that the higher density (nonboiling) water in the channel region outside the assembly flow tube is placed outside of the subassembly model in order to preserve the volume fractions in the model. This, in effect, introduces higher density water from the outer channel moderator inside the assembly, increasing the level of moderation in the assembly as compared with the real situation where the channel water is located only outside of the boiling water region in the assembly. Alternate models studied by Murphy included a full-assembly model (no subdivision) that allowed a more accurate representation of the moderator regions but could not explicitly model burnable poison rods (these rods were smeared with the fuel rods in the assembly). The physical rationale for this model was that the influence of the moderator may be more important than that of the poison rods because the poisons are generally depleted early in the cycle, whereas the moderator influence is present throughout the irradiation of the assembly. The study concluded that different modeling approximations yielded only small differences in the decay heat predictions; these differences resulting primarily from the actinide compositions that are more dependent on spectral changes in the assembly than most of the fission products. The differences in the models were more apparent at long decay times where actinide contribution to decay heat becomes increasingly important. No single model prescription was found to be applicable to all designs. For example, BWR assembly designs such as the General Electric and

Framatome ANP ATRIUM (see Figure 5.3) assembly designs, characterized by large central water regions, should not be subdivided (by the number of absorber rods) in a way that does not preserve the moderating effects of the internal channel(s). For these designs, preserving the moderating effects of the channel is important, and full-assembly models (without subdivision) typically yield more accurate results. For other designs utilizing both small water tubes and burnable poison rods, the subassembly model (for example, see Ref. 40) has been shown to yield accurate isotopic results.

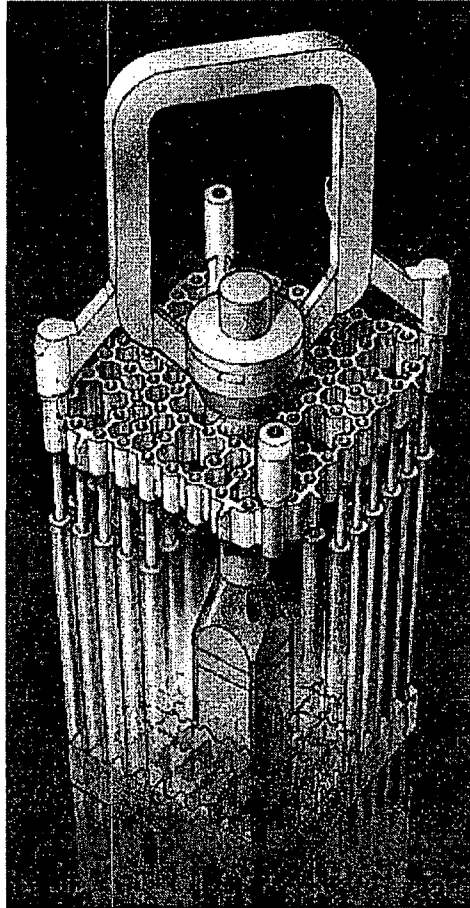


Figure 5.3 Cutaway illustration of the ATRIUM-10 assembly layout with large internal square water channel
(*Source:* AREVA Web site)

5.2.2 BWR Swedish Assemblies

5.2.2.1 8×8 Assemblies

Most of the Swedish BWR 8×8 assemblies measured at CLAB used a small number of fuel rods containing Gd_2O_3 burnable absorber (BA). The conventional approach for modeling these assemblies⁴⁰ has been to include a gadolinium-bearing rod in the center of the model and place the proportional volume of fuel around the rod. For the case of an 8×8 assembly that has five BA rods, for instance, the model represents one fifth of the assembly by putting one gadolinium-bearing rod at the center with

one-fifth of the fuel rods (e.g., one-fifth of the remaining 59 rods) surrounding this as the fuel area. The additional water in the lattice associated with any non-fuelled cells and water surrounding the assembly (inside and outside the assembly flow tube) is typically placed outside the subassembly fuel zone.

A small modification was required because many of the Swedish 8×8 assemblies contained corner rods (three rods at each corner) having a smaller diameter than non-corner fuel rods. In these assemblies, the non-corner rods were used to define the pin cell dimensions. With the larger fuel rod diameter, the effective number of fuel rods in the assembly is adjusted such that the correct fuel mass (or, alternatively, fuel area) is preserved. This effective number of fuel rods is then used in determining the size of the fuel-zone material in the approach described above. For the case of 64 fuel rods, twelve of which are corner rods, this equivalent number of normal-sized rods is roughly 62.

The 8×8 assembly model includes a square Zircaloy box defining the outside of the assembly with channel moderator as the outermost region. In all cases, these materials were apportioned to preserve the correct fraction of the assembly being modeled. Furthermore, one must account for the small amount of moderator immediately to the inside of the Zircaloy box; the full compliment of 64 cells does not fill the entire area inside the box and the extra moderator must be taken into account. Again, the fraction that corresponds to the model of the assembly is included.

The majority of the 8×8 assemblies contained one water rod, however, a small number contained none, and one assembly had two water rods. The few assemblies that had no BA rods and one water rod were each modeled as a full assembly surrounding the central water hole. The assembly with two water rods had uniform sized fuel rods (no corner rods) and four BA rods; it was modeled as one quarter subassembly model surrounding one BA rod.

5.2.2.2 9×9 Assemblies

Three Swedish 9×9 BWR assembly designs were measured at CLAB. All three contained five water rods and six BA rods per assembly; all fuel rods had a uniform diameter (i.e., no corner rods). The assemblies were modeled as one sixth of an assembly with the BA rod at the center, in a similar manner to that described for the 8×8 assemblies.

5.2.2.3 SVEA Assemblies

Two types of SVEA assemblies were studied: SVEA-64 and the SVEA-100. These are 8×8 and 10×10 fuel lattices, respectively. As previously described, a unique design feature of the SVEA assemblies is a large water cross that subdivides the assembly into quadrants, or subassemblies (see Figures 4.8 and 4.9). The arrangement is composed of four 4×4 and four 5×5 sub-assemblies, respectively. All SVEA assemblies were modeled as one quarter of the full assembly, allowing the moderator in the water cross region to be accurately modeled around each quadrant, thereby preserving the moderating influence of the water cross region.

Some assemblies contain one gadolinium-bearing (BA) rod per quadrant, which can be simulated explicitly in the SAS2H quadrant model. However, in assemblies having more than one BA rod per quadrant, the nominal amount of Gd_2O_3 in the central BA rod was adjusted by the factor $N/4$, where N is the total number of BA rods in the assembly. This approximation preserved the specified total amount of burnable poison in the assembly model and preserved the neutronic effects of the water cross region. The subassembly (quadrant) model then includes the central BA rod; the clad and water for the BA rod unit cell; the homogenized fuel zone having an area corresponding to the remaining number of fuel pins per quadrant; a water zone accounting for the water inside the Zircaloy box that encloses the quarter

assembly; the flow box for the quadrant; and finally the water associated with the water cross region. Note that all water contained in the box has a density that accounts for the void fraction. The zone outside the quarter assembly flow box accounts for water in the water cross between subassemblies and in the channel between assemblies (i.e., two sides of the quarter assembly are the water cross and two sides are the water between adjacent assemblies). The volume of the outer water zone is determined from the assembly geometry data. Any control-blade insertion for the assembly would be modeled by adding the absorber to the outermost water region, as described in previous studies.⁴⁰

5.3 TRITON Assembly Models

The assembly design information in Sect. 3 was used to prepare detailed geometry models for each assembly design. The models were used in TRITON to prepare cross-section libraries for each type of assembly. These libraries were subsequently used for the ORIGEN-S decay heat calculations. Typical configurations, obtained from literature, were used to model assemblies for which configuration details were not available. Because many assemblies for a given design type (i.e., 8×8) are unique, it was important to establish which design characteristics were required to prepare cross-section libraries that are applicable to a broad range of configurations. For example, the 8×8 design included assemblies with zero to six burnable poison rods. Because the fuel cross sections are influenced by the number of rods and the poison content, it was necessary to determine the minimum number of unique libraries that were needed to represent the different configurations and determine which configurations could be grouped together for the purposes of predicting the decay heat.

This section describes the procedure for generating burnup-dependent cross-section libraries for use with ORIGEN-S. It also discusses the additional assumptions made when developing the TRITON models for the assemblies considered in the present study.

5.3.1 ORIGEN-S Cross-Section Libraries for U.S. Assemblies

5.3.1.1 BWR GE 7×7 Library

The assembly specifications were taken from Table 4.10 for the GE-3 Cooper fuel design data. The channel water density of 0.7627 g/cm^3 was applied, a value used in isotopic benchmark analyses documented in Ref. 40. It was noted that this value was slightly different than the value of 0.669 g/cm^3 used in a previous benchmark analysis of the decay heat for the Cooper assemblies, reported in Ref. 3; this lower density value was derived to account for the displacement of water by the control cruciform by reducing the water volume of bottom axial node of the assembly by 10%.

The GE 7×7 assemblies in this study used integral burnable gadolinium (Gd) poison rods with Gd_2O_3 as burnable absorber. The previous model used for Cooper station assembly decay heat analyses³ assumed four Gd rods per assembly; a value based on typical BWR design information.⁵⁴ The Gd rods arrangement used for generating the 7×7 cross-section libraries in the current study are based on the actual Gd rod configuration of Cooper assembly CZ346 that is documented in Ref. 36. This assembly is one of the assemblies measured in the decay heat program at Morris Operations. CZ346 had five Gd rods with an average Gd_2O_3 poison concentration of 3.4 wt % (three rods with 3.0 wt %, and two rods with 4.0 wt %). The assembly model illustrating the Gd rod configuration is shown in Figure 4.4. The cross-section library generated for this assembly configuration was used for the analysis of all 7×7 assemblies, including the Dresden and Monticello assemblies.

5.3.1.2 PWR 14 × 14 Library

PWR 14 × 14 libraries were generated to calculate decay heat for 14 × 14 assemblies from San Onofre Unit 1 reactor and Point Beach Unit 2 reactor. The design differences between the two types of assemblies are significant, as can be seen from the assembly data presented in Tables 4.2 and 4.8. Therefore, two different cross-section libraries were generated, one for each type of reactor. One fuel enrichment value, of 3.397 wt % ^{235}U , was considered for the purpose of generating burnup-dependent cross sections for Point Beach assemblies, as all of the measured assemblies had the same enrichment; for San Onofre assemblies two fuel enrichment values were used, 3.5 and 4.0 wt % ^{235}U , to span the range of enrichments for all analyzed assemblies from this reactor. The TRITON assembly models are presented in Figures 4.1 and 4.3.

In terms of the predicted decay heat, a significant design difference between the San Onofre and Point Beach reactor assemblies is the use of stainless steel cladding for the San Onofre assemblies. The activation of trace levels of cobalt in steel represents a significant source of decay heat for these assemblies. To accurately simulate the activation of ^{59}Co in the clad, cell-weighted cross sections are needed in the ORIGEN-S library that reflect the differences in the neutron flux level and energy spectrum between the fuel and the clad. This was done in the TRITON depletion calculations by defining separate depletion materials in the problem for the fuel and the clad regions. A combined cell-weighted cross-section library is automatically generated by TRITON. The weighing procedure adjusts the cross sections in the combined library to reflect the flux level and spectral differences between the different regions in which each nuclide resides in such a way as to preserve the reaction rates in an homogenized, or point model.

5.3.1.3 PWR 15 × 15 Library

The library for the 15 × 15 assembly was generated using the design data presented in Table 4.5 for the Turkey Point 3 reactor. All measured assemblies have the same fuel enrichment, 2.557 wt % ^{235}U ; therefore, the burnup-dependent cross sections were generated only at this particular enrichment value. The configuration of the TRITON model is shown in Figure 4.2.

5.3.2 ORIGEN-S Cross-Section Libraries for Swedish Assemblies

Significantly more detailed fuel design and reactor operating information was available for the Swedish fuel assemblies measured at CLAB than was available for the U.S. measured assemblies. The design data for the Swedish fuel included the number of burnable poison rods and the concentration of the burnable poison in each assembly. Axial void profiles were provided for most BWR assemblies, as well as axial burnup profiles provided by the utilities. More detailed information can be found in Ref. 39.

5.3.2.1 BWR 8 × 8 Libraries

TRITON models used to generate the ORIGEN-S cross-section libraries are developed based on the assembly fuel design data provided in Table 4.15. Four types of assembly design are considered, which show slight variations in dimensions, number of burnable absorber (BA) rods and concentration of the absorber material in the absorber rods. Only one TRITON model was created for Types 1 and 5 because these assemblies had similar characteristics. For Type 2 and Type 4 however, multiple TRITON models were used because of differences in the number of BA rods and/or the concentration of the burnable absorber. The configuration of the assemblies with no BA rods is shown in Figure 4.6.

For Type 2 assemblies, the number of BA rods can be zero, three, or four. For the cases where three BA rods are present, the concentration of the absorber material (Gd_2O_3) in the BA rods can be

3.95 or 5.5 wt %. A separate cross-section library was generated for each of these 4 groups of Type 2 assemblies. Because information was not available on the BA rod locations in the assembly, assumptions were necessary. The placement of the BA rods in the assembly is illustrated in Figure 5.4 for assemblies with 3 and 4 BA rods, respectively.

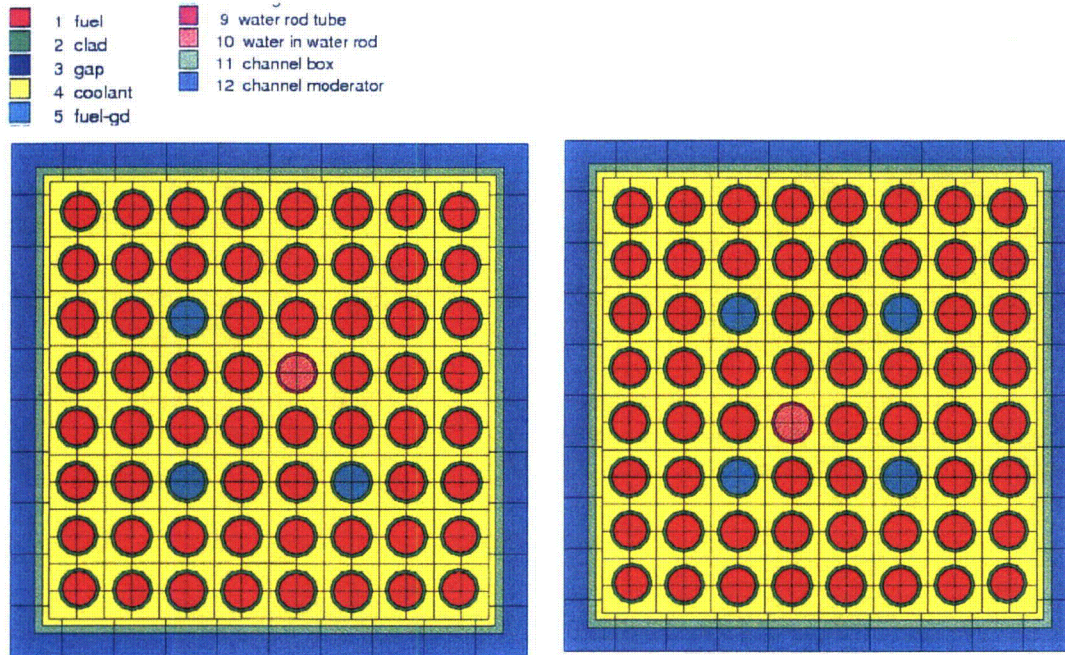


Figure 5.4 Layout for Type 2 assemblies with three and four BA rods

In the Type 4 assembly design there are assemblies with no BA rods and with three, four, or five BA rods having a Gd_2O_3 wt % of 2, 2.55, and 3.2, respectively. The same TRITON model was used to generate cross-section libraries for the all 8×8 assemblies with BA rods. An assembly with configurations of 3 and 4 BA rods is shown in Figure 5.4. The arrangement of the BA rods for Type 5 assemblies is similar to that shown in Figure 5.4; however, no corner rods are present.

Most of the 8×8 assemblies have the initial ^{235}U enrichment in the range 2–3 wt %, except the Type 4 assemblies with five BA rods. The cross-section libraries were generated for enrichment values of 2 wt % and 3 wt % ^{235}U for all assemblies categories but Type 4 with five BA rods, for which an additional 4 wt % value was considered. The same set of water moderator density values (0.1, 0.3, 0.5, 0.7, and 0.9 g/cm^3) for which the cross section are obtained was used in all cases.

5.3.2.2 BWR 9×9 Libraries

The TRITON model for the 9×9 assemblies, based on the design data shown in Table 4.24 is illustrated in Figure 4.7. Because all the assemblies in this group have the same initial fuel enrichment of 2.938 wt % ^{235}U , burnup-dependent cross sections are generated only for this enrichment value and at five coolant density points as specified previously for the 8×8 assemblies.

5.3.2.3 BWR SVEA Libraries

The burnup-dependent cross-section libraries for the SVEA-64 and SVEA-100 assemblies were generated at five fuel enrichment values (1.5, 2.0, 3.0, 4.0, 5.0, and 6.0 wt % ^{235}U) and the same set of coolant density points as for all other BWR assemblies studied. The assembly design data applied in the TRITON models are given in Tables 4.25 and 4.28, and the assembly configurations are illustrated in Figures 4.8 and 4.9. Even though there are slight differences in the actual number of BA rods and/or the Gd_2O_3 content, only one representative TRITON model was used for each SVEA design: four BA rods at 2.55 wt % Gd_2O_3 were used for the SVEA-64 model and six BA rods at 3.5 wt % Gd_2O_3 for the SVEA-100 model.

5.3.2.4 PWR 15 × 15 Libraries

The assembly design data used in the TRITON models is presented in Table 4.32. BA rods were not used in any of the 15 × 15 assemblies measured at CLAB. Two types of assemblies are shown in the table, differing by the dimension of the pellet diameter, rod diameter, and clad thickness. A separate TRITON model was used to generate a library for each type. The assembly layout is illustrated in Figure 4.10. The burnup-dependent cross sections were generated for only one fuel enrichment value, of 3.095 wt % ^{235}U , for assemblies of Type 1, as all the assemblies of this type had the same enrichment; for assemblies of Type 2, two enrichment values were used, 3.0 and 3.5 wt % ^{235}U , to cover the range corresponding to all assemblies of this type.

5.3.2.5 PWR 17 × 17 Libraries

Two models were created for the 17 × 17 assemblies: one with no BA rods and one with 12 BA rods. The detailed design information was presented in Table 4.35, and data on the number of BA rods for each assembly studied in Table 4.36. The configuration of the assembly containing 12 BA rods, based on information in Ref. 41, is illustrated in Figure 4.11. For both TRITON models, libraries were generated at four fuel enrichment values (2.0, 2.5, 3.0, and 3.5 wt % ^{235}U). The coolant density for all PWR assemblies (including 15 × 15) was 0.72 g/cm³, a value appropriate to the actual pressure and coolant average temperature values cited in Ref. 55 for each reactor. For example, the coolant data for 17 × 17 assemblies are 15.25 MPa pressure and a temperature of 576 K; the corresponding density can be determined from standard pressure-temperature tables.

6. COMPARISON OF PREDICTIONS AND MEASUREMENTS

This section compares predicted and measured decay heat rates for the assemblies measured at GE-Morris, HEDL, and the Swedish CLAB facilities. The calculations were performed using reactor operating data and fuel assembly specifications described in Sect. 4 and the SCALE computational methods and software tools presented in Sect. 5. All decay heat calculations were performed with the ORIGEN-S code using cross sections interpolated to the corresponding initial fuel enrichment, irradiation history, and operating conditions using the ARP module. Cross-section libraries for the ORIGEN-S depletion analysis were generated with the 2-D TRITON depletion sequence. Other results presented in this section include calculations that account for the axial variation of the burnup profile and void profile (in the case of BWRs only) for the Swedish assemblies that had detailed axial data available. Comparisons using the 1-D SAS2H depletion sequence are also described for selected Swedish assemblies. Finally, an estimate of the experimental error and the bias and uncertainty associated with the calculations is presented based on the comparisons of the calculations with experimental data.

6.1 Assembly Decay Heat Results

Comparisons of the measured decay heat rates for all evaluated assemblies with the corresponding values predicted by ORIGEN-S are listed in the tables of Appendix A. The results are plotted on a log-log scale (to clearly display large number of data points for low values of decay heat) in Figure 6.1. The results for the 198 assemblies are organized in the tables by measurement facility, reactor, and assembly design. Repeat measurements are indicated in the tables.

The GE-Morris measurements presented in this report are those obtained from operating the calorimeter in static mode. The recirculation mode measurements reported for some assemblies exhibited larger variability than the static mode results and were therefore not used in this study.

The Monticello assembly measurements, performed at GE-Morris Operations, were complicated due to difficulties in calorimeter calibration. Two separate calibrations, one performed in 1984 and the other in 1985, resulted in significantly different decay heat results for the same assemblies. The 1985 calibration yielded a reproducibility of about ± 2 W, whereas the 1984 calibration was no better than ± 15 W based on repeat measurements of selected assemblies.³⁰ However, an analysis of the measurements by McKinnon et al. indicated that the results using the 1985 calibration method yielded a 20-W average bias between measurements and predictions, whereas the 1984 calibration method resulted in less than a 4-W average bias. The cause of the differences, either in the method of calibration or operation, was never fully resolved. In this study the measurements reported using the 1984 calibration were used for the reason that the 20-W average bias observed with the 1985 data has not been observed in any of the other experiments.

The error in the residuals (the absolute difference between the calculations and measurements) is a useful measure of calculational and measurement error. The residuals, in units of Watts, are plotted against the measured decay heat in Figure 6.2. The relative error is the residual error divided by the measured decay heat. Plotting the relative percent error vs decay heat for all assembly measurements produces the distribution shown in Figure 6.3.

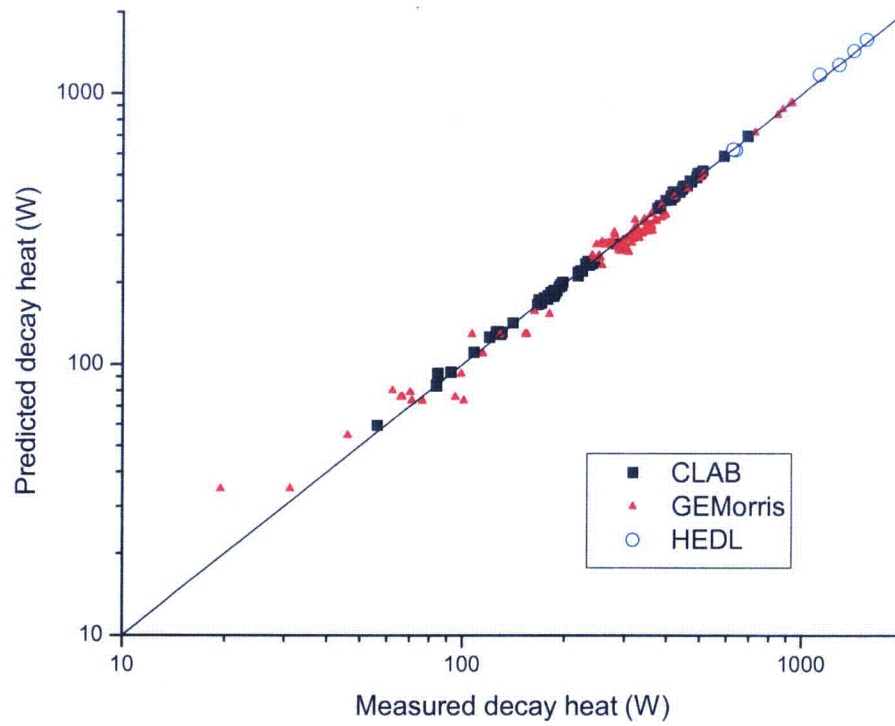


Figure 6.1 Measured vs predicted decay heat for all assemblies. The solid line represents the line of agreement between predictions and measurements (i.e., slope = 1).

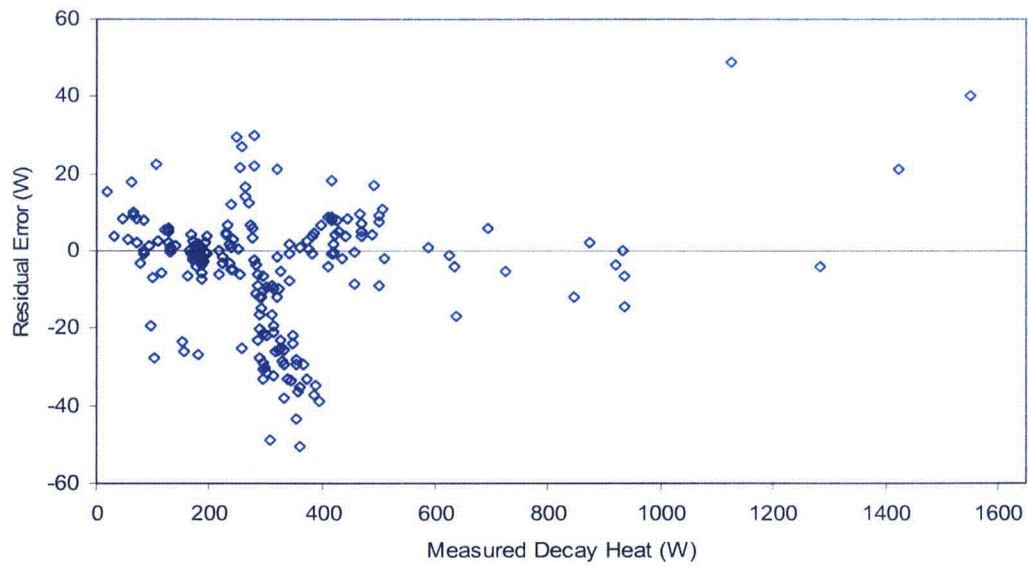


Figure 6.2 Absolute error between calculated and measured decay heat

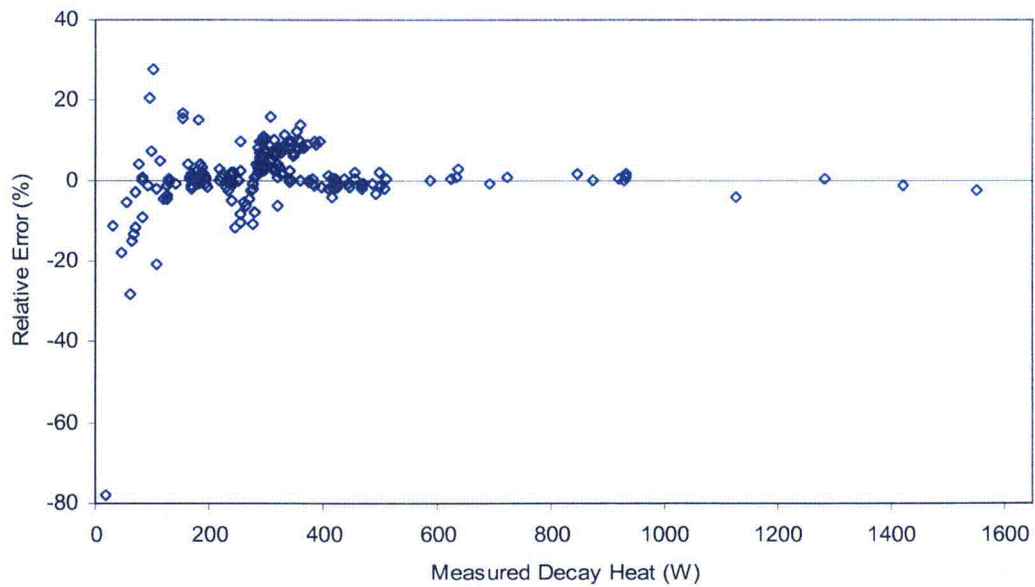


Figure 6.3 Relative error between calculated and measured decay heat

6.2 Error and Uncertainty Analysis

The results of the ORIGEN-S calculations are compared with the measured decay heat for the spent fuel assemblies to assess the accuracy of the calculations and the uncertainty in the calorimeter measurements. The objective of the analysis is to estimate the uncertainty that should be assigned to spent fuel assembly decay heat predictions made using the ORIGEN-S code.

Error is introduced into the calculations through a variety of sources including (1) the numerical method and its implementation, (2) the nuclear cross sections and decay data, (3) errors in the input data (e.g., operational data, burnup accuracy, etc.), and (4) simplifying assumptions in the modeling (e.g., operating history, assembly design, axial variations). Errors are also associated with the calorimeter measurements due to experimental uncertainties (accounting for escaped radiation, heat capacities of the assembly, etc.) as well as the measurements of quantities such as temperature and time.

6.2.1 Statistics for Uncertainty Analysis

In evaluating the calorimetric data and the calculations, it is useful to make a variety of comparisons, as will be done in succeeding sections. However, in obtaining a quantitative uncertainty measure, it is important to select the statistical variables carefully. In general, we seek to compare a calculated quantity x to a quantity that can be measured or derived based on a measurement y . The error in both measurement and calculation is represented with an additive error term ϵ ,

$$y = x + \epsilon. \quad (1)$$

If we have N pairs of experimental and calculational results (x_i, y_i) , $i = 1, 2, \dots, N$, then evaluating the resulting error terms can give us a good understanding of the combined uncertainty between the calculation and the measurements. If the errors are all independent samples from a normal distribution with mean μ and variance σ^2 , then these two quantities can be approximated by the respective sample statistics:

$$\bar{\epsilon} = \sum_i \epsilon_i / N \quad (\text{sample mean})$$

$$s^2 = \sum_i (\epsilon_i - \bar{\epsilon})^2 / (N - 1) \quad (\text{sample variance}).$$

If the mean $\mu = 0$, then the distribution is unbiased, a highly desirable result. In general, the actual mean and variance are not known, and so the sample mean and variance are the only statistics we have available. Hence, it is important to ensure that we have valid estimates for these sample statistics, which may place some constraints on exactly which quantities x and y we should actually consider. Therefore, we describe the assumptions that will enable such analysis:

1. The errors must be independent. We assume that all calorimetric measurements are independent.
2. The errors all have the same normal distribution. That is, the variance σ^2 is constant, and the collection ϵ_i , $i = 1, 2, \dots, N$ represent random samples of a normal distribution.

In evaluating the data, three possible approaches to the uncertainty analysis were considered:

Decay heat error residuals. The error residuals are simply the difference between the calculated and measured decay heats, so that x and y in Eq. (1) are the calculated and measured decay heats, and ϵ has units of Watts. As will be shown, this is a reasonable choice for the present set of data, since the error of

the residuals has a variance that is nearly constant (see Figure 6.2) and is almost normally distributed with a sample mean near zero. These observations will be further discussed in a later section, and the uncertainty analysis developed using this statistical approach.

Decay Heat Relative Error. In the case, $y = (C/E - 1)\%$, where C/E is the ratio of calculated-to-experiment decay heat, the error is dimensionless. An evaluation of the relative error for all results indicates this is not a good measurement of error, because Figure 6.3 shows that the relative error decreases as decay heat increases, i.e., σ^2 is not constant. Additional analyses for the data also indicate the distribution is not normal. The relative error can be a useful quantity for qualitative error analysis, but is not appropriate for uncertainty analysis of the data in this study.

Specific Decay Heat Error Residuals. For both calculation and measurements, the specific decay heat was evaluated using the decay heat for the assembly divided by the initial uranium loading. The error residuals are then the difference between calculated and measured specific decay heats with units of W/MTU. This quantity was evaluated in comparing results from assemblies of different sizes (e.g., BWRs and PWRs) that have significant difference in the initial uranium loadings. However, dividing by the initial loading (effectively weighting by the inverse of the loading) produced error residuals using the present data that are not normally distributed. The specific decay heat is used in this analysis for illustrative purposes only, but not to calculate uncertainties.

6.2.2 Calorimeter Measurement Error

In assigning error to the calorimeter data, the measurements were evaluated independently of the calculations by making use of multiple measurements that were available for several assemblies. While some assemblies have only a single measurement, there are a number that have more than one measurement; some just a few days apart, others spanning months or even years. We evaluated these multiple measurements as representative of all assemblies. This approach is viable since most of the measurement error is characteristic of the calorimeter design, calibration, operation, and analysis, and is not directly related to the characteristics of individual assemblies. We assumed that all calorimeter measurements, even those on the same assembly, are independent data points. This is justifiable, since in each case, the assembly is loaded, sealed, and evaluated independently of any other measurements that have been done.

If two or more measurements on the same assembly (having decayed for at least several years) are made only days apart, the results should be virtually identical, since very little decay occurs during this time. In this case, measurement uncertainty can be approximated by the sample standard deviation s , which is the square root of the sample variance:

$$s^2 = \sum_i (x_i - \bar{x})^2 / (n - 1), \quad (2)$$

where $\bar{x} = \sum_i x_i / n$ is the sample mean, n is the number of multiple measurements on that assembly, and x_i are the decay heat measurement results. If several assemblies have such closely-spaced multiple measurements, then the overall sample variance is obtained by combining the variances for individual assemblies:

$$s_{\text{tot}}^2 = \sum_k [(n_k - 1) s_k^2] / \sum_k (n_k - 1), \quad (3)$$

where the index k has been used to denote the individual assemblies, and n_k are the number of measurements for assembly k .

If multiple measurements span many weeks or months, then consideration must be made for the decrease in decay heat over that time period. Such a change may be approximated by a straight line, in which case the correlation between measurements is defined by a regression curve. Recognizing that decrease may not be linear, but rather exponential, it is also possible to fit an exponential function to the data. In either case, uncertainty is estimated with the sample standard deviation. However, a linear or exponential fit of the variance is determined not from the deviation of replicate points from each other, but by the deviation of each point from the best-fit curve. In the case of linear regression, the sample variance takes the form:⁵⁶

$$s^2 = \sum_i (a t_i + b - x_i)^2 / (n - 2), \quad (4)$$

where again x_i are the measured decay heat values and t_i are the times at which they are measured. The constants a and b are the slope and intercept, respectively, of the regression line. The sample variance is determined by dividing the sum of squares by $n - 2$, since two statistics (a and b) are to be determined from the n independent measurements. For this reason, at least three data points are necessary to make an estimate of variance for such a correlated series of measurements.

Assemblies with multiple measurements appropriate for calorimeter uncertainty analysis are indicated in Table 6.1 and the uncertainty results for each facility is summarized. Regression analysis (measurements over an extended time interval) was performed for three assemblies: CZ205 and CZ259 (measured at GE-Morris), and D-15 (measured at HEDL). For the first two assemblies, a straight line approximation was equivalent to an exponential fit, and so this was used for simplicity. In these cases, measurement error was much greater than data variations, and so the form of the fitting function was of minor importance. For the HEDL assembly measurements, an exponential function was used to fit the data. The data for these three assemblies are shown in Figure 6.4, together with the regression curves. Note that there is considerable scatter in both sets of data measured at GE-Morris.

All other replicate measurements were close enough in time to justify analysis based on the sample mean of the measurements. In this case, the greatest time spans were for Monticello assembly MT133 (14 days) and CLAB assembly 6432 (18 days). The predicted decay heat decreases over this time by about 0.2 W; the variations in calorimeter measurements far exceed this change. Thus, the uncertainty approach based on the sample mean [Eq. (2) assuming constant decay heat] is reasonable in these cases. Shown in Figure 6.5 are four assemblies with replicate measurements from the GE-Morris facility. In each case, discernable scatter from the mean exists. On the other hand, the CLAB data exhibit much less scatter so that replicate points are usually very close to each other, as observed in Figure 6.6.

Table 6.1 Measurement uncertainty estimates for each calorimeter facility

Measurement facility	Assembly	Number of repeat measurements <i>n</i>	Time range of repeat measurements (days)	Analysis method ^a	Absolute standard deviation (W)
GE-Morris	DN212	2	15	m	5.9
GE-Morris	CZ205	14	246	r	14.1
GE-Morris	CZ246	2	3	m	10.4
GE-Morris	CZ259	3	197	r	30.9
GE-Morris	MT123	3	6	m	16.7
GE-Morris	MT133	4	14	m	22.6
GE-Morris	MT228	3	12	m	15.9
Total uncertainty					16.7
HEDL	D-15	3	1115	r	95.1
CLAB	6432	2	2	m	2.00
CLAB	6432	5	18	m	1.55
CLAB	3838	2	1	m	0.45
CLAB	9329	2	2	m	0.80
CLAB	6350	2	1	m	1.77
CLAB	13847	2	0	m	0.35
CLAB	C20	4	9	m	8.24
CLAB	E38	2	1	m	0.99
CLAB	5A3	3	2	m	3.64
CLAB	5A3	2	13	m	0.34
Total uncertainty					3.94

^a Method of calculating standard deviation, s: r = regression, m = mean.

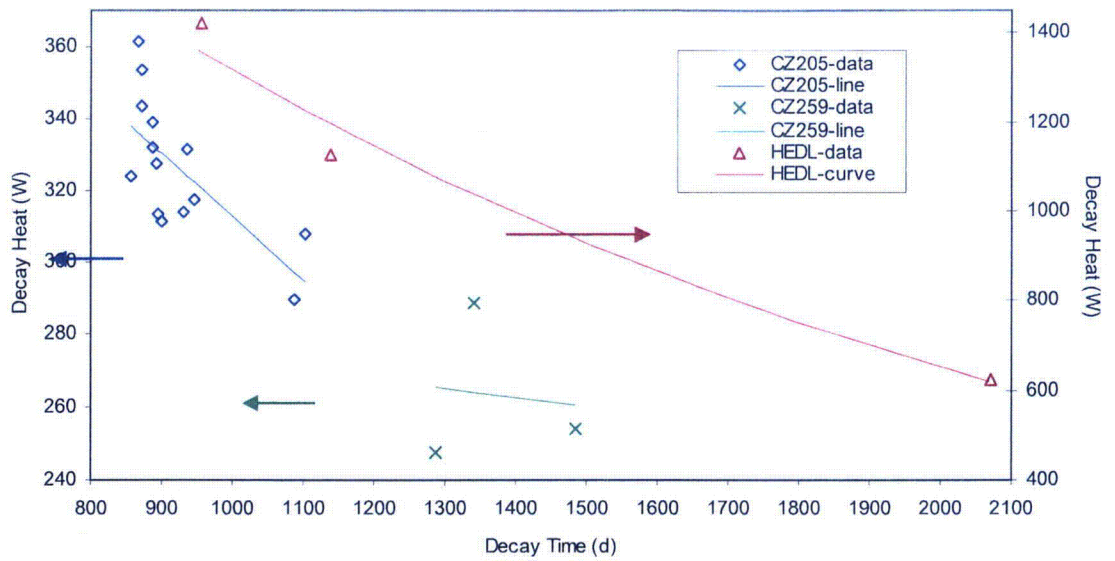


Figure 6.4 Regression analysis of repeat measurements

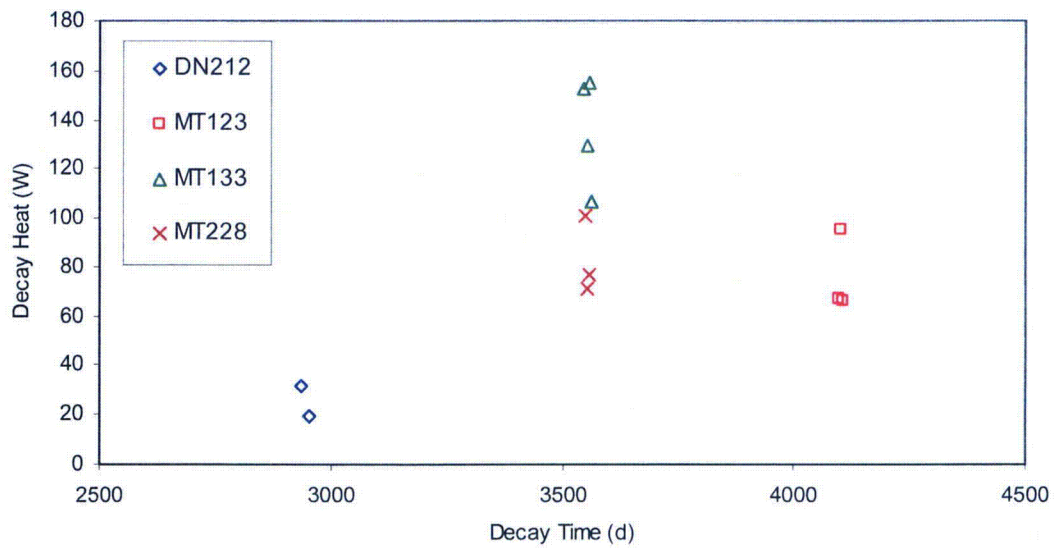


Figure 6.5 Repeat measurement results at the GE-Morris facility

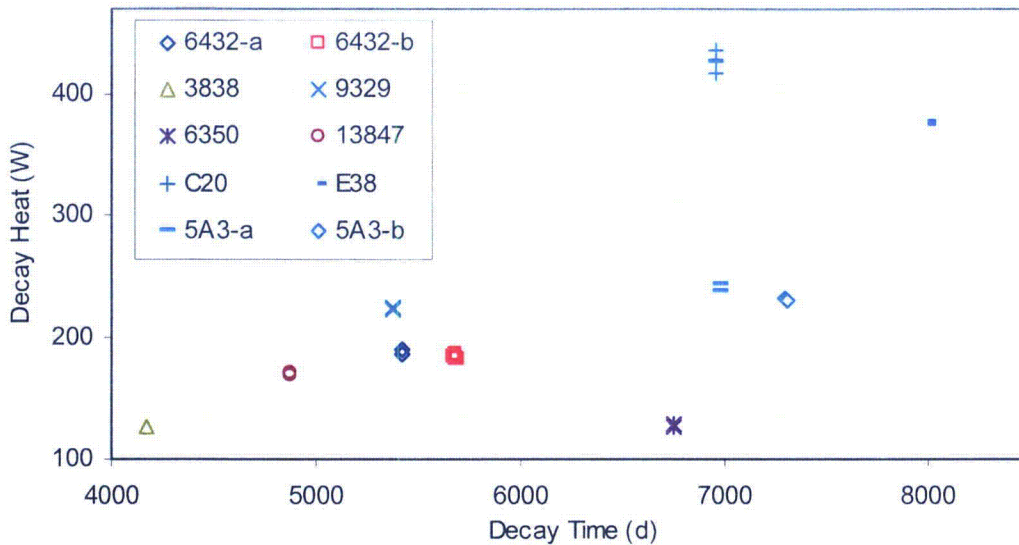


Figure 6.6 Repeat measurements made at the Swedish CLAB facility

CLAB assembly 6432 involved measurements more than 8 months apart; however, they occur in two clusters of cooling time with no measurements in between. Each cluster is therefore evaluated separately, and calculation of uncertainty is based on the sample mean for each cluster. If all points were treated using regression, the slope and intercept of the regression line would largely reflect the time difference of these two clusters (like fitting a line to 2 points), and would contribute little additional information to the uncertainty analysis. A similar situation exists for CLAB assembly 5A3, which has two clusters of measurements almost 1 year apart.

For the GE-Morris calorimeter, the uncertainty based on repeat measurements for individual assemblies range from 5.9 to 30.9 W, and the overall value of 16.7 W, obtained from Eq. (2), is of similar magnitude to the values for the individual assemblies. For the HEDL calorimeter, only one assembly had multiple measurements. The uncertainty of 95.1 W is considerably larger than the uncertainties for GE-Morris or CLAB. However, the HEDL measurements involved assemblies with much higher decay heat, so one might expect larger absolute uncertainties. The results for the CLAB measurements indicate a lower uncertainty of 3.9 W.

6.2.3 Differences Between Calculations and Experimental Data

Having evaluated the uncertainties inherent in the measured decay heat data, the data were compared with the prediction. Initial analysis was performed using the error residuals

$$\epsilon_i = y_i - x_i, \quad (5)$$

where y_i are the calculated decay heat values, and x_i are the measured values. From the plot of the residuals in Figure 6.2 it can be seen that the calculation errors are for the most part scattered within 20 W of the measurements.

Noteworthy is a group of negative residuals exceeding 20 W in the measured decay heat range of 300–400 W. Except for this group, the residuals appear equally distributed above and below the line of zero error, indicating that the calculations are as likely to overpredict as underpredict relative to measurement. The mean of the residual errors $\bar{\epsilon} = -5.03$ W for all measured assemblies combined. This error is similar to the standard deviation associated with the CLAB measurements (3.9 W) and well within those of GE-Morris (16.7 W) and HEDL (95 W). The standard deviation of the residual error about this mean is $s_{\epsilon} = 16.14$ W, similar to the GE-Morris facility measurement uncertainty, substantially lower than that of the HEDL facility, and somewhat larger than the CLAB facility uncertainty.

Except for the cluster of negative residuals noted above, the residual error has a distribution that is near normal, as illustrated by the approximate probability density function (PDF) in Figure 6.7. This PDF was derived from a smoothed histogram of the residual error. The principal peak is very near zero, and the right tail of the distribution is consistent with a normal distribution. However, for the left-hand tail, there is a second (smaller) peak that derives entirely from the aforementioned cluster of negative residuals. Further examination of this second peak shows that the data are for BWR assemblies measured at GE-Morris. The presence of bias in these measurements will be discussed at greater length later.

In spite of the bimodal form of the PDF, the entire distribution of residuals is still approximately distributed normally. A comparison of the two cumulative distribution functions is shown in Figure 6.8 (the residual distribution has been standardized as shown in the table). Using the Kolmogorov-Smirnov method⁵⁷ to make a quantitative comparison, the Kolmogorov-Smirnov statistic is $D = 0.1256$ (the maximum vertical difference between the two cumulative distributions). With a sample size of 199 points, the resulting P -value is 0.08, which suggests that the hypothesis of normality cannot be rejected with 95% confidence, but it can with 90% confidence; hence, the distribution might be normal, but is by no means assured.

This preceding analysis treats all error the same, regardless of the source. Further evaluation of the data was performed to investigate the presence of other correlations and biases. Shown in Figure 6.9 is the error from the three different measurement facilities, which indicates several biases. The GE-Morris errors exhibit a negative bias, whereas the CLAB and HEDL errors are biased slightly positive (e.g., calculations are somewhat larger than measurements). This effect is quantified by the mean values of residual error due to the different measurement facilities: $\bar{\epsilon}_{GE} = -11.5$ W, $\bar{\epsilon}_{HEDL} = 14.6$ W, $\bar{\epsilon}_{CLAB} = 2.1$ W. The causes of these discrepancies are not obvious, but are likely related to differences in either experimental procedures or input data used in the calculations (or both). An important finding is that the mean values for each facility are within the data uncertainties identified in Sect. 3.

From Figure 6.9 there also appears to be a slight trend in residual error for the HEDL measurements, although the correlation is not strong due to the large scatter in the data. Such a trend is noticeably absent for the GE-Morris and CLAB data, although both show significant data clustering, which bears further scrutiny.

The two data clusters in the CLAB data shown in Figure 6.9 can be generally grouped by reactor type, as illustrated in Figure 6.10. The BWR data have smaller error residuals and are centered approximately about zero; they also indicate a small decrease in absolute error with increasing decay heat, although it is difficult to quantify because of the random scatter of the data. By contrast, the PWR data indicate a clear positive bias. It is quite likely that there is either systematic error in the calorimeter measurements for the PWR assemblies or in the calculations (nuclear data or input data), which causes this bias. However, the effect is small, and for this reason it may be difficult to identify.

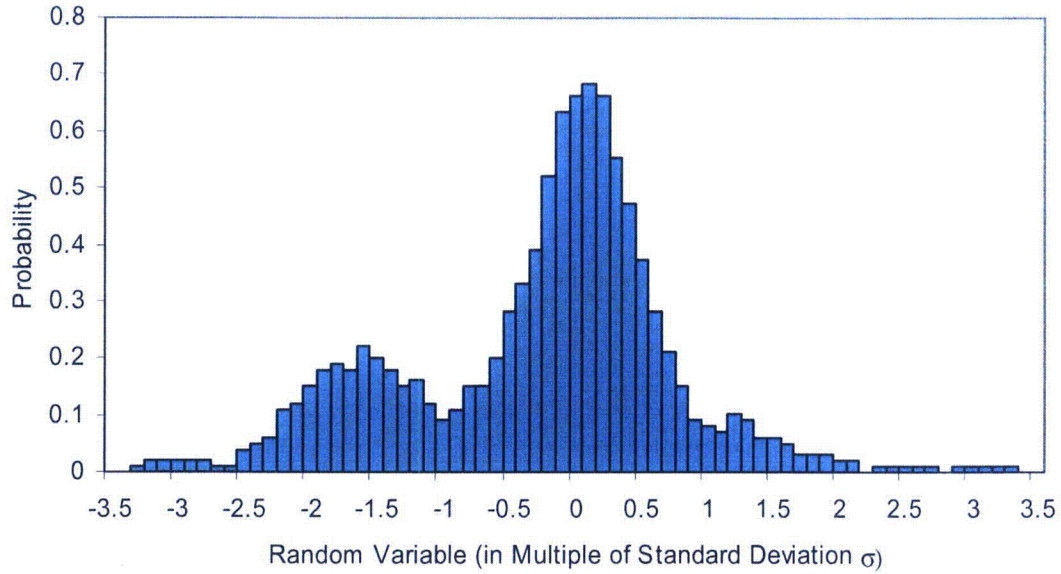


Figure 6.7 Approximate probability density function for error residuals (Ordinate axis represents units of sample standard deviation, i.e., $0s_e, \pm 1s_e, \pm 2s_e, \pm 3s_e$)

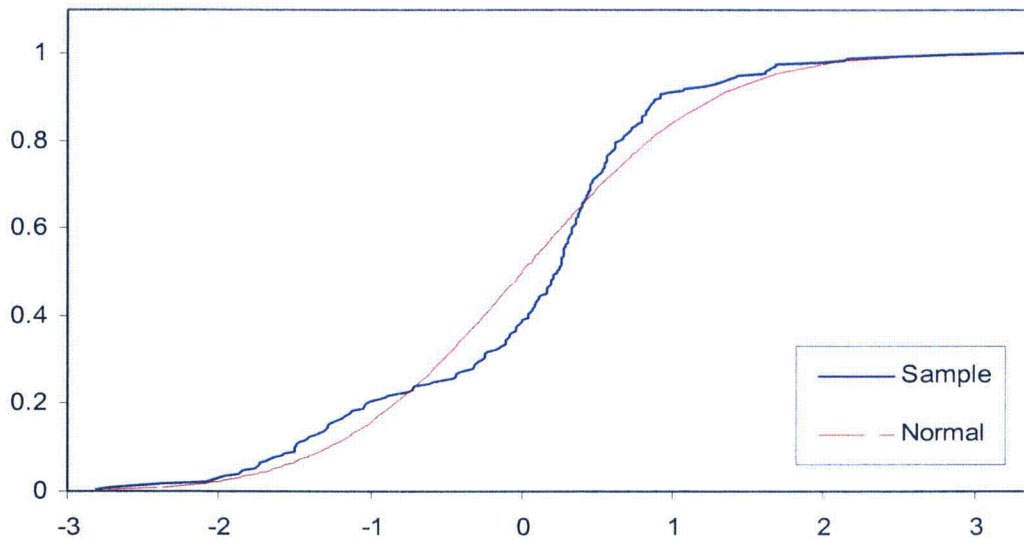


Figure 6.8 Comparison of standardized sample and normal cumulative distributions (Ordinate axis represents units of sample standard deviation, i.e., $0s_e, \pm 1s_e, \pm 2s_e, \pm 3s_e$)

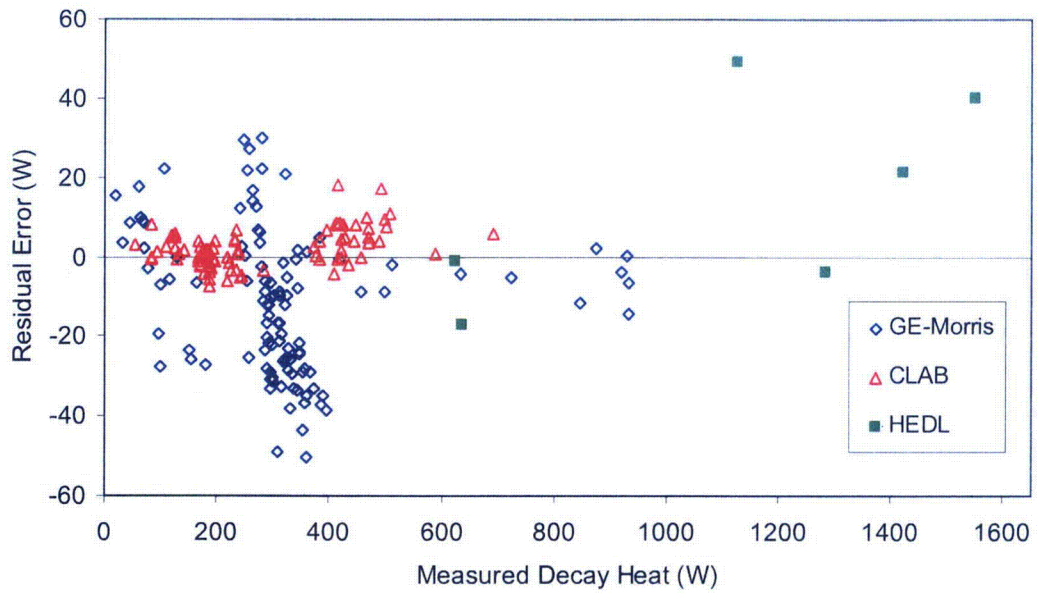


Figure 6.9 Residual error for each measurement facility

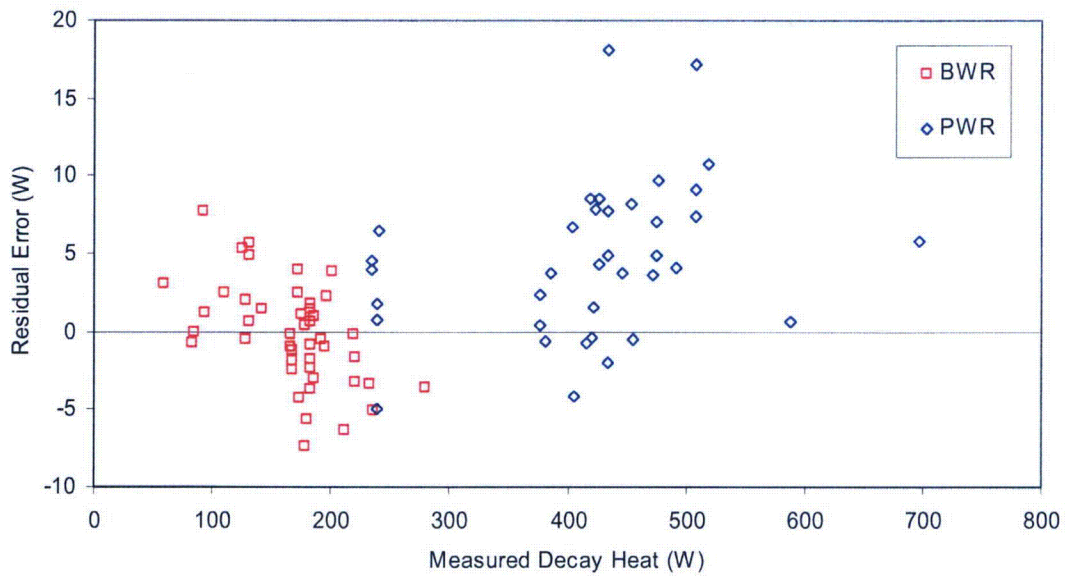


Figure 6.10 Residual error for CLAB measurements by reactor type

The clustering of residuals by reactor type as seen in the CLAB data plotted in Figure 6.10 is associated with the difference in uranium mass between the two assembly types. Because BWR assemblies typically contain about one-half the uranium mass of PWR assemblies, they have lower decay heat values for similar burnups. A more consistent basis for comparing the different assemblies is the specific decay heat, which is decay heat divided by the initial uranium mass. This basis results in a modified distribution of residuals, which are compared for the GE-Morris and CLAB facilities in Figures 6.11 and 6.12. As observed in the earlier comparisons (see Figures 6.9 and 6.10), the PWR data from GE-Morris have relatively low error, while the BWR data have much larger error and exhibit a small negative bias. However, there are no significant correlations (i.e., trends) between the error and specific decay heat.

Results for the CLAB assemblies are shown in Figure 6.13. The BWR residuals show little bias, being centered near zero. The PWR data exhibit a small positive bias relative to the BWR data, although this difference is minor. The bias could be due to the measurements or their subsequent analysis (e.g., calorimeter calibration, specific heat effect of shroud used for BWR assemblies, etc.). It could also be due to systematic calculational error, e.g., differences in the models or input data used to generate the PWR and BWR libraries for the ORIGEN-S calculations. However, the latter situation does not appear credible since the bias has been observed using a wide range of models, methods, and nuclear data, and such a bias was not observed in the GE-Morris PWR measurements involving similar assembly designs.

The GE-Morris residual errors shown in Figure 6.11 do not show a correlation with reactor type. Both reactor types exhibit a negative bias; however the PWR data are much closer to zero. The BWR data indicate a much greater scatter and stronger negative bias, opposite to the behavior observed in the CLAB results. Again it is possible that such effects are due to systematic errors in either the measurements or calculation input (or both).

Finally, the residual errors are examined as a function of assembly burnup, decay time, and enrichment in Figures 6.14–6.16. From these plots it is apparent that the errors are virtually uncorrelated with these variables (there are no obvious trends). This is true regardless of the measurement facility involved. Any slight trends or nonrandom effects are better explained by other factors (previously discussed) than by correlations with these quantities.

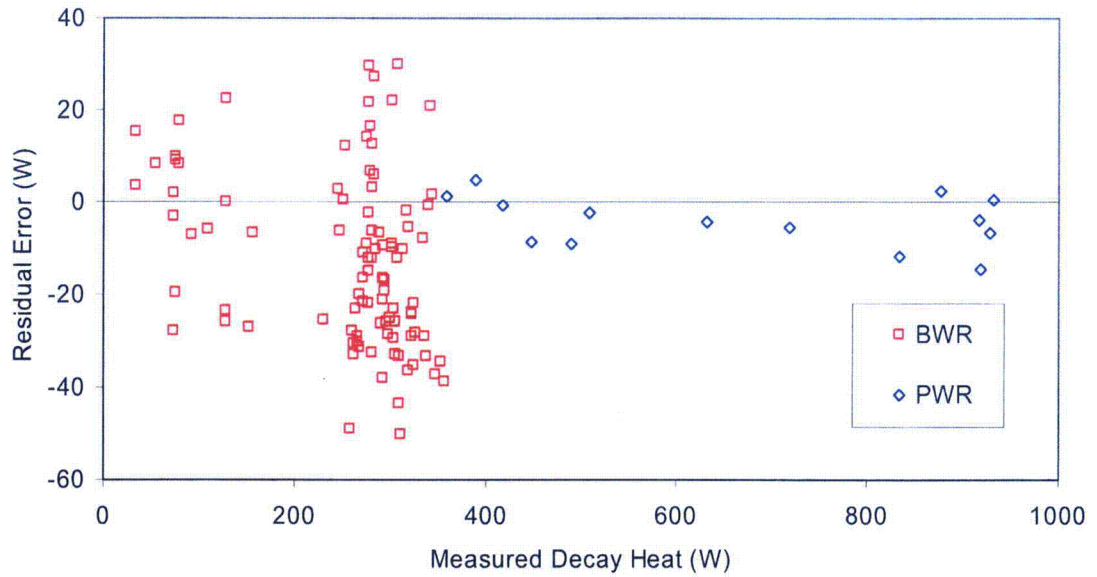


Figure 6.11 Error for GE-Morris measurements by reactor type

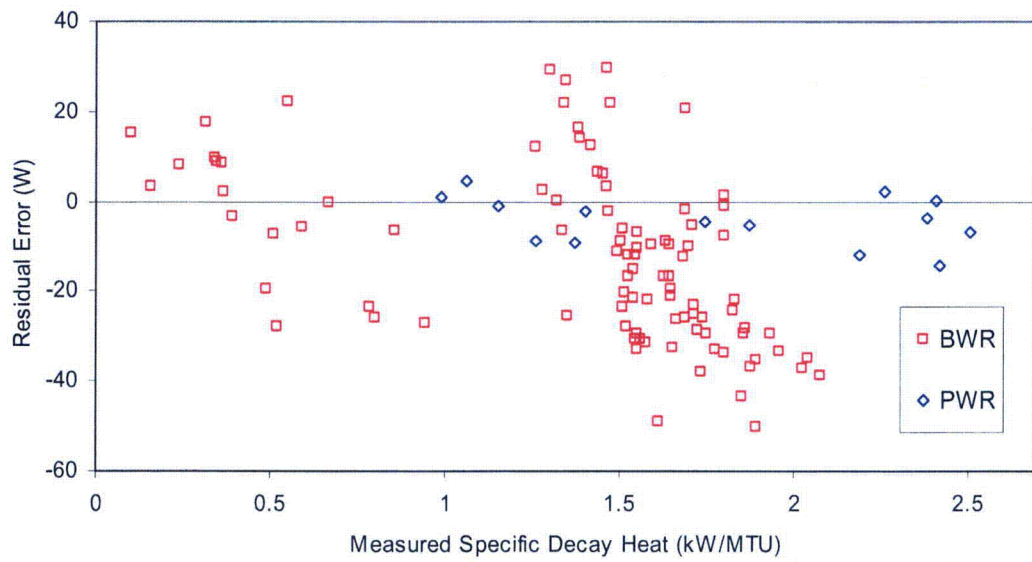


Figure 6.12 Residual error in specific decay heat for GE-Morris measurements

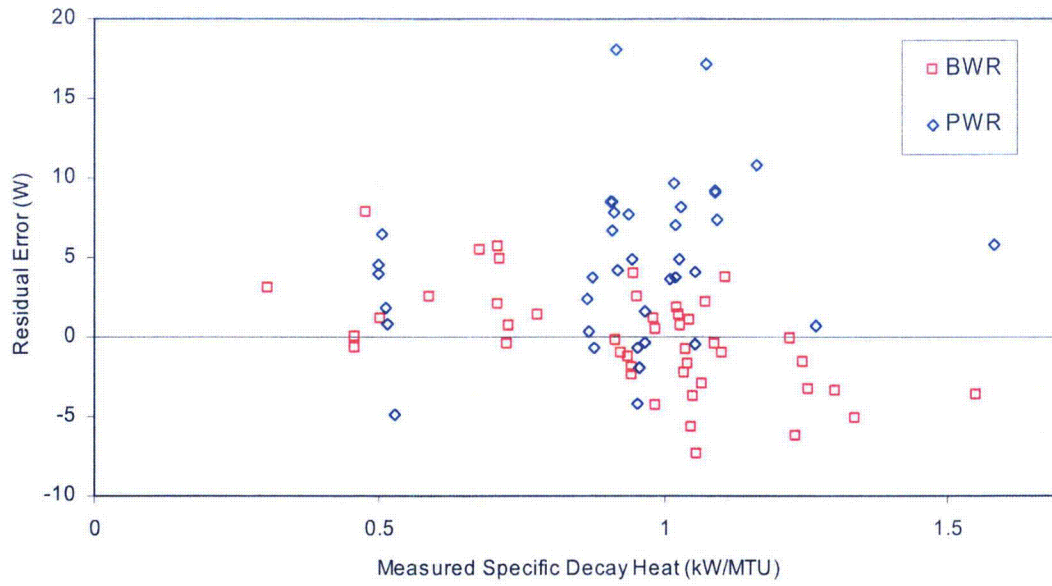


Figure 6.13 Residual error in specific decay heat for CLAB measurements

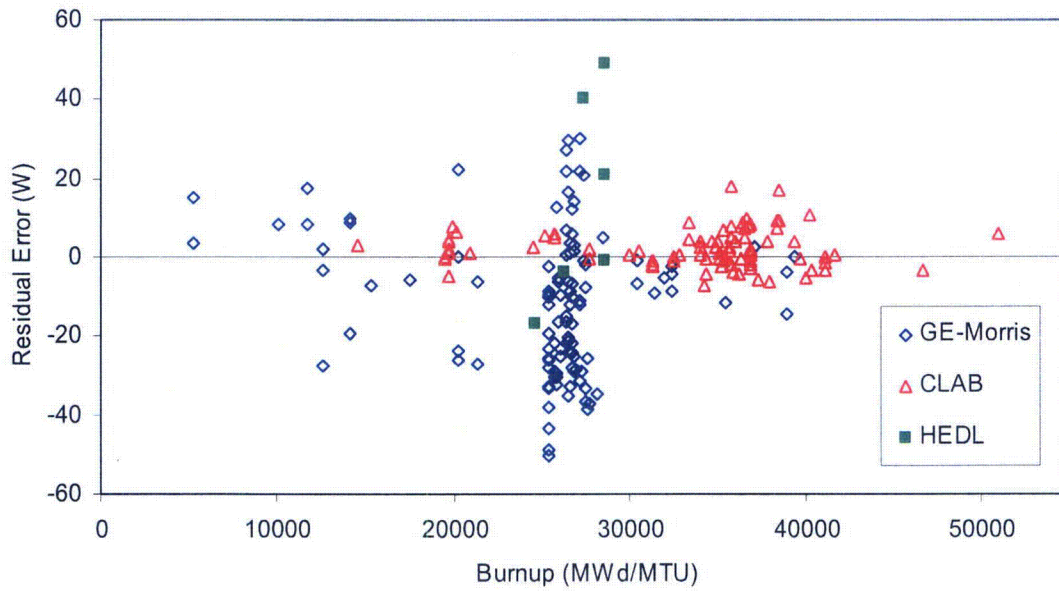


Figure 6.14 Residual error correlation with assembly burnup

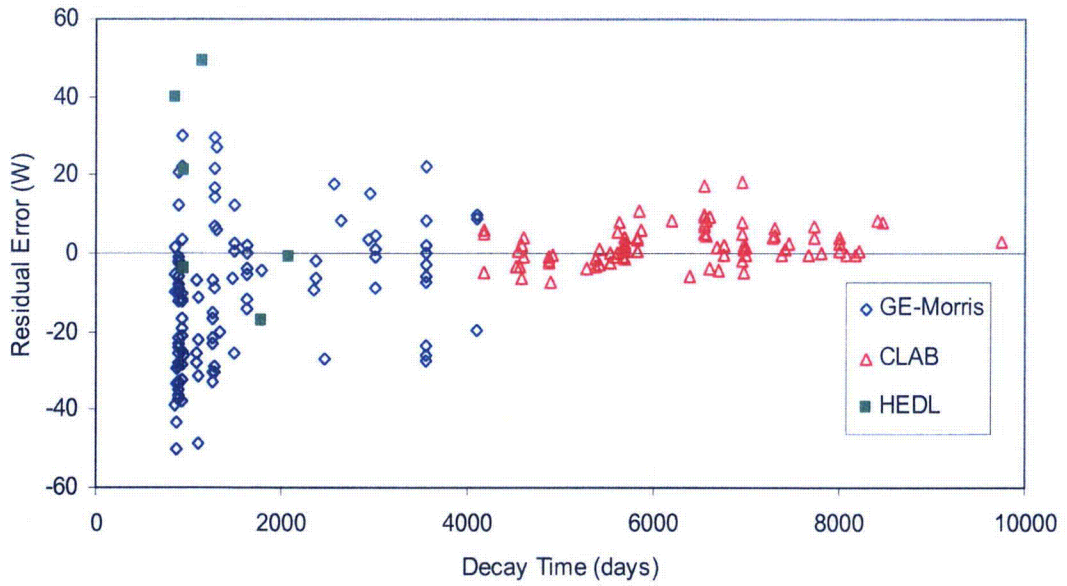


Figure 6.15 Residual error correlation with assembly cooling time

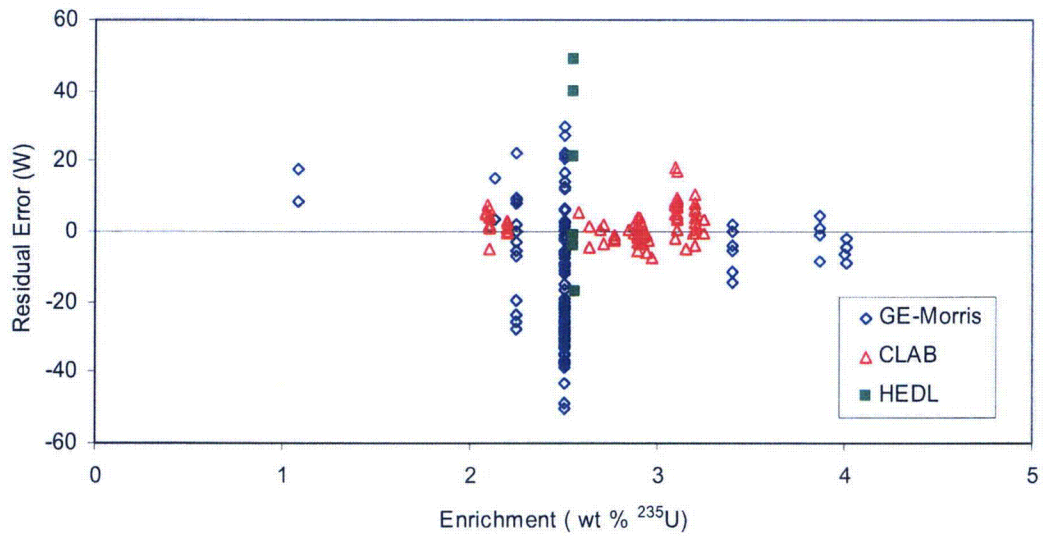


Figure 6.16 Residual error correlation with assembly enrichment

6.2.4 Sensitivities and Uncertainties in Calculations

Errors in code calculations may be introduced by modeling approximations and errors, numerical discretization, and errors in input data. Regarding modeling and numerical error, attempts have been made to minimize this and otherwise account for it with well-established numerical algorithms and thorough code QA and testing. SCALE is maintained and developed under a formal code QA plan that covers testing of the methods and data.^{58,59} The numerical method of the ORIGEN code (matrix exponential with Bateman solutions) has also been benchmarked against other independent numerical and analytical solutions for fuel irradiation and decay problems in an international code comparison⁶⁰ involving the use of common nuclear reaction and decay data. A complete discussion of numerical error is beyond the scope of this discussion. However, errors due to the numerical methods are judged to be very small with respect to other sources. We therefore focus on the error in ORIGEN calculations due to uncertain or erroneous input data.

A thorough evaluation of calculational error was undertaken for an earlier version of the code,⁶¹ and much of that study is applicable now as well. The earlier study identified a number of input parameters to which the decay heat was most sensitive. Foremost among them were power, irradiation time, and cooling time, as one would expect. Other quantities include

1. cooling time since discharge;
2. total irradiation time;
3. assembly power and power history (variations over irradiation time);
4. initial uranium mass in the assembly;
5. initial enrichment in ^{235}U ;
6. structural materials and other activated components; and
7. nuclear data (cross sections, fission yields, decay constants, energy per decay Q values, energy per fission Q values).

The amount of cobalt (^{59}Co) as an impurity in assembly structural components varies widely and may contribute to decay heat (and gamma radiation sources) due to formation of ^{60}Co by activation. However, uncertainty from this contribution is still generally small compared with other sources of error.

The most significant quantity influencing decay heat is the assembly power, and therefore it is important for the code input to be as accurate as possible. In this study the cycle power was derived from the cycle burnup. The operating times of the reactor are very well known. Therefore, the error in the power is similar to the error in the cycle burnup. The final assembly burnup for U.S. fuel assemblies was obtained from DOE Form RW-859, which reports burnup calculated by the utilities. A limited review of the uncertainties in utility-declared burnup has been reported. The accuracy of reactor records was studied in 1997 by the Electric Power Research Institute (EPRI) in its report *Determination of the Accuracy of Utility Spent-Fuel Burnup Records*.⁶² The EPRI report concluded that the uncertainty associated with the calculated core-follow burnup values is less than 2% for Westinghouse PWR assemblies. Further evaluations⁶³ using a larger sample of reactor records from nine PWR plants found uncertainties in the range of 2 to 5% at a 95%-confidence level. For more complex BWR assembly designs and reactor operations one might expect somewhat larger uncertainties for these assemblies. The relative sensitivity coefficients for the reactor power, or burnup (impact of changes in power on the predicted decay heat), are estimated in Ref. 3 to be > 1 for cooling times from 3 years to 100 years. Therefore, an error of 2% in the burnup value will yield an error of more than 2% in decay heat.

The total reactor power is, of course, not constant, but varies throughout its cycle history. The pattern of variation can be approximated by histograms representing periods of constant power. The detail necessary to accurately model the total power history of a given assembly has also been studied previously. Comparisons using early versions of the ORIGEN code indicated that using a detailed power history was slightly better than using individual cycle averages^{29,30} and that using individual cycle averages was much better than using a lifetime average. However, obtaining a correct detailed history may be problematic, and various sources for such information may yield different values, as seen in this work with the Dresden DN212 assembly history (see Sect. 3). The accuracy of calculations using cycle-average power estimates (used in this work) is estimated to be accurate to better than 2% as compared to calculations with very detailed power simulations.

Other important quantities include the nuclear data. Earlier sensitivity studies involving ORIGEN indicated only a minor importance of cross-section errors on decay heat for times less than about 100 years. Cross sections become more importance with cooling time as the higher actinides (Pu, Am, and Cm) contribute in large proportions to the decay heat. The buildup of actinides is very sensitive to cross sections. However, the earlier studies did not address high-burnup fuels (which have higher actinide content) or the complex BWR assembly designs now in use. The new designs generally make extensive use of burnable poisons, and with axial voiding, produce higher actinide inventories than in previous designs. Therefore it is reasonable to assume that the effect of cross-section errors may be somewhat larger for modern fuels than previously estimated.

6.3 SAS2H Analysis Results

Decay heat calculations evaluated in Appendix A were made using ORIGEN-S and assembly cross-section libraries created using 2-D TRITON models. Calculations for the Swedish assemblies were also performed using the 1-D SAS2H depletion analysis sequence of SCALE using the modeling procedures described in Sect. 5. SAS2H couples the 1-D XSDRNPM transport analysis code with the ORIGEN-S code to performed automated cross-section generation and fuel burnup analysis. Although the 1-D methods require more assembly model approximations than 2-D methods, particularly for heterogeneous modern BWR assembly designs, the 1-D sequence has been extensively validated and applied for a wide range of commercial spent fuel studies. The results reported here were obtained directly from SAS2H calculations; that is, a separate SAS2H calculation was performed for each assembly, rather than using the sequence to generate cross-section libraries that were later used in standalone ORIGEN-S calculations. The SAS2H results, limited in this study to the Swedish assemblies, are compared with the results of TRITON in Appendix C.

The SAS2H results are similar to those obtained using the cross-section libraries generated by TRITON for all assemblies studied. The average difference between the SAS2H and TRITON decay heat predictions are less than 1% for all Swedish assemblies. The differences are also seen to be similar for the BWR and PWR assemblies, indicating that any modeling approximations in the 1-D SAS2H models for the 8×8 , 9×9 , SVEA assemblies do not have a large impact on the results (e.g., the results for the complex BWR assembly designs are similar to the less complex PWR designs). In fact, the BWR results are on average in closer agreement than the PWR results. However, as burnup and cooling time increase the differences between the results are expected to become larger as the actinides become a more important component of decay heat. The actinide concentrations are more sensitive to the cross section variations (and hence modeling approximations) than most fission products. A comparison of the SAS2H and TRITON results suggest some degree of correlation between the deviation and the burnup. The largest differences are observed for the highest burnup assemblies.

6.4 Effect of Using Assembly Average Burnup and Coolant Density

All of the results presented so far in this report were performed with simulation models that used assembly average data and did not account for any axial variation of burnup or coolant density. Assembly burnup and water moderator densities applied in the calculations were based on a volumetric average over the axial length of the assembly. However, decay heat is not strictly a linear function of burnup; this is particularly true for the decay heat component from actinides. Coolant density also influences the cross sections and the buildup of actinides in a nonlinear manner. To study this effect and determine the accuracy of models based on assembly average data, selected assemblies measured at the Swedish CLAB facility that had detailed axial information were simulated using an explicit multizone model. In this model, separate simulations of each axial zone, characterized by the zone burnup (and coolant density in the BWR case) were performed and the assembly decay heat then determined as the sum of the decay heat values obtained for each axial zone. These results were then compared to those obtained using assembly average parameters.

For the PWR case only the axial variation in burnup was considered, the change in moderator density over the length of the assembly being relatively small. The multizone model for the PWR assemblies considered 24 axial regions of equal volume for which burnup information was available. In the BWR case both axial burnup and coolant density variations were available for 25 regions. PWR and BWR assemblies were selected to include representative assembly configurations and burnup values. The axial burnup and coolant density values, obtained from Ref. 39, are based on utility records. The specific assemblies and their main characteristics are listed in Table 6.2.

Table 6.2 Assemblies considered for axial decay heat studies

Reactor type	Reactor name	Assembly design	Assembly ID	Enrichment (wt% ²³⁵ U)	Burnup (GWd/MTU)
BWR	Oskarshamn 2	8 × 8	1389	2.2	19.481
	Barsebäck 1	8 × 8	9329	2.9	41.094
	Oskarshamn 2	SVEA-64	12684	2.9	46.648
	Oskarshamn 3	SVEA-100	13628	2.7	35.619
PWR	Ringhals 2	15 × 15	G23	3.2	35.633
	Ringhals 2	15 × 15	F32	3.2	50.962
	Ringhals 3	17 × 17	5A3	2.1	19.699
	Ringhals 3	17 × 17	1C5	3.1	38.484

The ratio of the decay heat value obtained for the one-zone model to the decay heat for the multizone model was calculated for cooling times from discharge to 150 years. This ratio, R_z , is illustrated in Figure 6.17 for the PWR and the BWR assemblies. R_z is observed to be less than 1 for the PWR assemblies selected in this study for cooling times up to about 40 to 60 years, depending on the burnup and other characteristics of the assembly. For longer times R_z is greater than 1 (i.e., the one-zone model overpredicts relative to the explicit multizone model). However, the effect is seen to be relatively small; less than 1% over all times studied. The magnitude of the effect depends on the cooling time and burnup and is most pronounced for shorter cooling times and increases with burnup.

The effect of the axial simulations for the BWR assemblies is similar to that for the PWR assemblies, however, the magnitude is larger. At longer cooling times of interest to interim storage the use of average assembly burnup and coolant density leads to an overestimation of the decay heat by up to 2.5%.

Although detailed axial calculations may not be practical for routine decay heat analysis, and this effect is relatively small (the magnitude in many cases being smaller than the experimental uncertainties), the user needs to be aware of the bias introduced in assembly models that use average data instead of detailed axial data. Importantly, it can be seen from Figure 6.17 that there is no single average value for the assembly burnup (or coolant density) that will yield results that are equivalent to a detailed axial calculation.

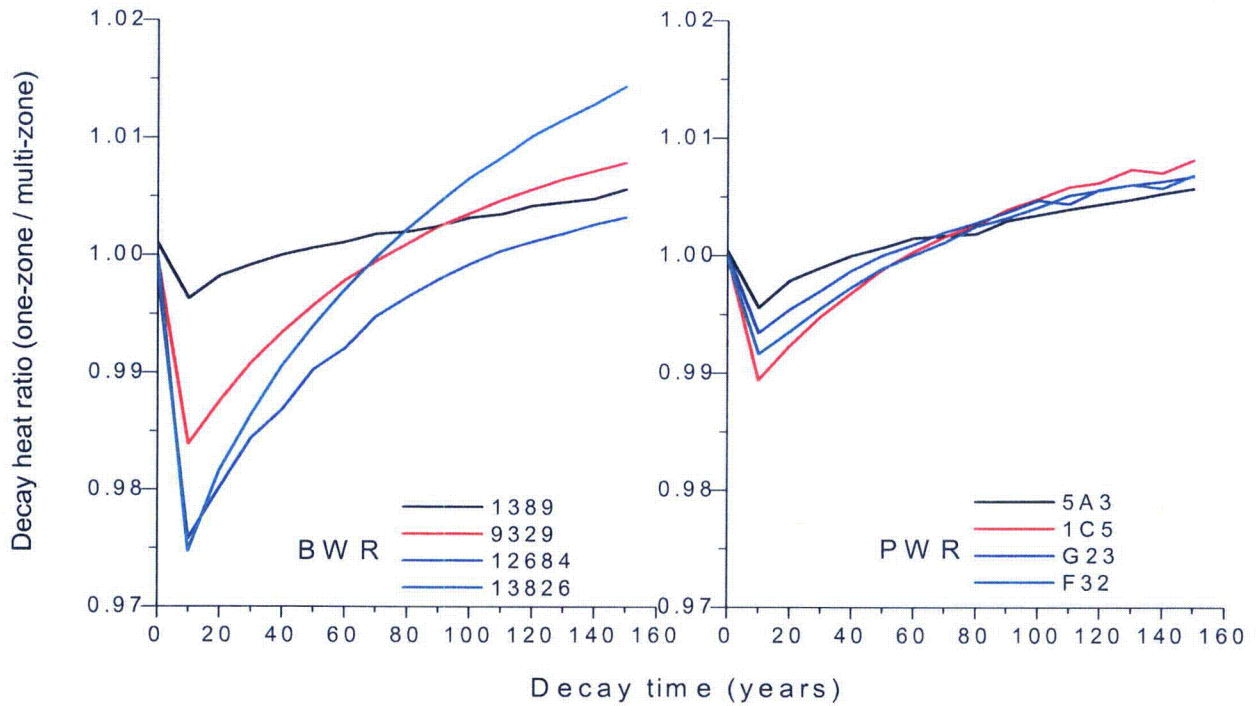


Figure 6.17 Ratio of decay heat calculated using assembly average parameters to that obtained using explicit axial calculations for selected Swedish BWR and PWR assemblies

7. SUMMARY AND CONCLUSIONS

The fuel burnup and decay code ORIGEN-S of the SCALE 5 system has been validated for decay heat predictions involving full-length spent fuel assemblies using calorimeter measurements performed at GE-Morris operation, the HEDL facility, and Swedish CLAB interim spent fuel storage facility. In all, more than 190 assembly measurements have been evaluated. The most recent CLAB measurements greatly extended the range of data available for code validation beyond that previously available in the United States. A statistical analysis of the results has been carried out based on the evaluation of all measurements, not just the most recent measurements. The decision to include all available experimental data resulted in a larger code uncertainty estimate than would have been obtained by using only the CLAB data, which have significantly lower experimental errors than the earlier GE-Morris and HEDL measurements. The use of all measurement results establishes the widest validated range of application for the code.

In addition to the full-length assembly measurements, the ORIGEN-S code was benchmarked against measurements of decay heat following the fission of the actinides ^{233}U , ^{235}U , ^{238}U , ^{239}Pu , ^{241}Pu , and ^{232}Th at short cooling times of importance to accident analyses. The results indicate that the calculations are generally within the range of experimental uncertainty for the measurements evaluated. However, several earlier calorimetric measurements not used in this study yield systematically higher decay heat values as compared with the spectroscopic measurements considered here. Further quantitative analysis of these measurements was beyond the scope of this work.

The remainder of this section summarizes the main conclusions that have been drawn from the study of the spent fuel assembly experiments.

- The validation covers a wide range of assembly designs, initial enrichments extending up to 4.0 wt % ^{235}U , burnup values up to 50,962 MWd/MTU, and cooling times extending to 27 years after discharge.
- The results show that the decay heat predicted by ORIGEN-S is generally within the range of uncertainty of the measurements. An evaluation of the calorimeter uncertainty based on repeatability of measurements gives measurement uncertainty values that are very facility dependent: ± 17 W for GE-Morris, ± 95 W for HEDL, and ± 4 W for CLAB. The approximate relative errors are: $\pm 5\%$, 10% , and 2% , respectively.
- The deviations between calculations and measurements (residuals) are observed to be normally distributed with a mean error (bias) of 0.7 W, a value close to zero. The variance of the residuals is seen to be approximately independent of the decay heat rate. The standard deviation assigned to the calculation based on all residuals is ± 17.6 W, a value very similar to the accuracy of GE-Morris measurement data, but higher than that of the CLAB data. A statistical analysis indicates that the relative errors obtained using the measured data from all facilities combined are not normally distributed. Therefore caution is needed when representing the calculation uncertainty in relative units.
- The ability to validate the accuracy of the code predictions is limited by the accuracy of the measurements; calculational uncertainty can not be demonstrated to be lower than the uncertainty inherent in the data itself. However, based on the calorimeter uncertainties estimated from repeat measurements, it is likely that the errors in the measurements themselves represent a significant component of the differences between calculations and measurements.

- The present level of uncertainty assigned to the calculations is not likely to be further reduced significantly by performing additional measurements if the results of the GE-Morris and HEDL measurements are retained because of the relatively large deviations associated with some of these data.
- The uncertainty of ± 17.6 W is relatively small for decay heat rates of 200 W or more (e.g., $< 10\%$). However, at lower decay heat rates the error becomes more significant and may become unacceptably large at longer cooling times. Again, it is not possible with the current data to determine absolutely whether this error is associated with the accuracy of the measurements or with the calculations.
- Based on an analysis of the data, there is no compelling rationale to evaluate the bias and uncertainty of the PWR assembly results separately from the BWR results. Any correlation between the two types of assemblies would be difficult to establish with any confidence given the variability of the measurement data.
- Simulation of assembly decay heat as a point model (one zone with axial and radial parameters averaged) leads to a small underprediction in the decay heat of typically $< 2\%$, caused primarily by the averaging of the axial burnup profile and void profile (for BWRs) of the assembly.
- Very similar calculated results were obtained using cross-section libraries generated by 1-D (SAS2H) and 2-D (TRITON) physics models of the fuel assembly lattice. In general, the difference due to this change in the physics models was found to be less than 2%.

Based on these findings the following recommendations are made:

- The ability to further reduce the current level of calculation uncertainty is limited by the availability of measurement data with lower errors. The use of the GE-Morris and HEDL data in the present study clearly leads to much larger uncertainties because of the large scatter in many of the measurements. At such time as the CLAB measurement range can be extended to cover the full range of the previous U.S. measurements, a reanalysis of uncertainties should be conducted using only the more precise CLAB data. Based on the results for the existing CLAB measurements, replacing the GE-Morris and HEDL data could potentially reduce the present level of code uncertainty from ± 17.6 W to approximately ± 10 W or possibly lower.
- Acquisition of additional measurement data for CLAB assemblies that cover low decay heat values of the earlier GE-Morris data, and higher decay heat range represented by the HEDL data, are desirable to improve and reduce the uncertainty in decay heat predictions.

8. REFERENCES

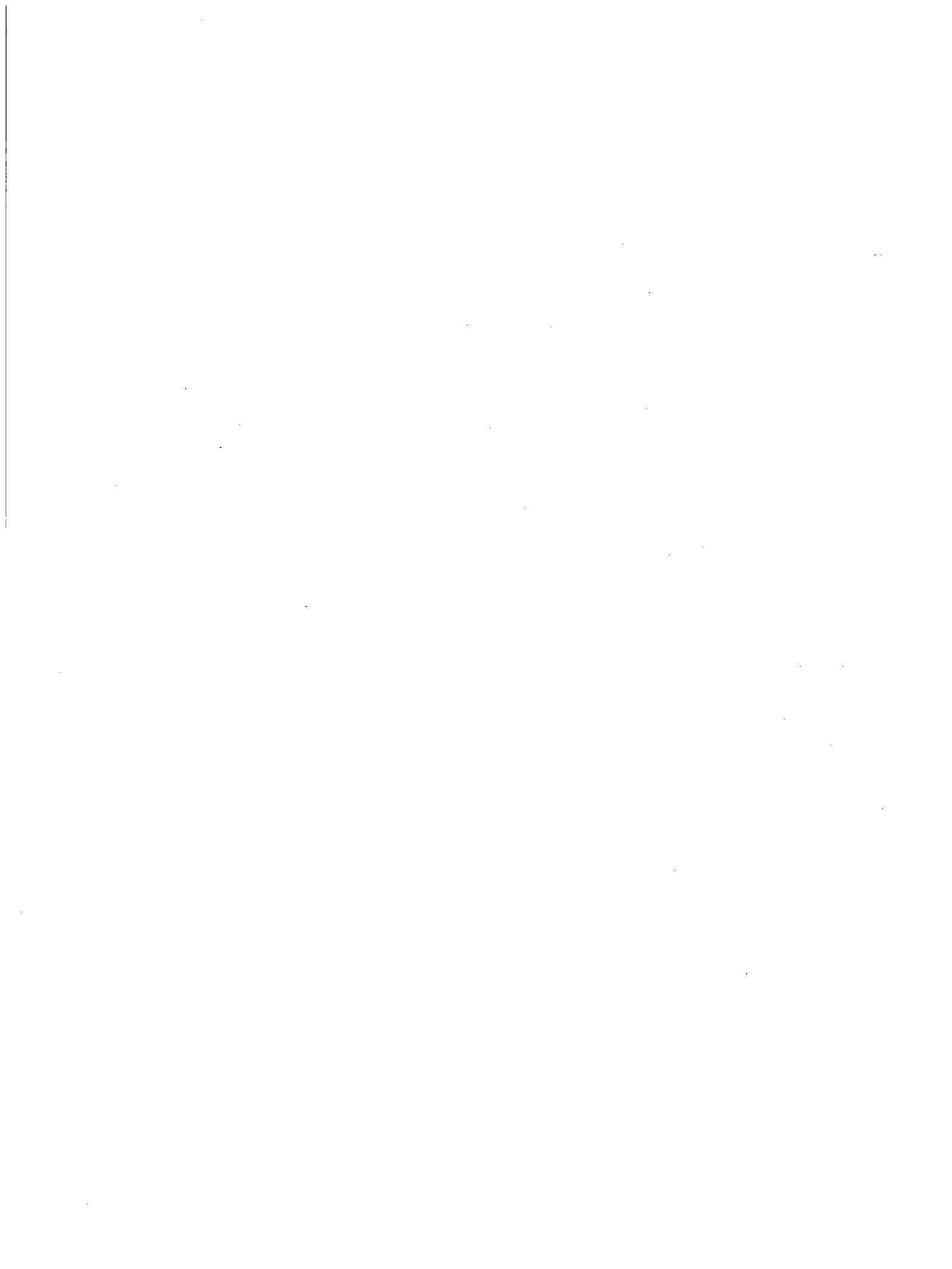
1. I. C. Gauld, O. W. Herman, and R. M. Westfall, "ORIGEN-S: SCALE System Module to Calculate Fuel Depletion, Actinide Transmutation, Fission Product Buildup and Decay, and Associated Radiation Source Terms," Vol. II, Book 1, Sect. F7 in *SCALE: A Modular Code System for Performing Standardized Computer Analyses for Licensing Evaluation*, ORNL/TM-2005/39, Version 5, Vols. I-III, April 2005. Available from Radiation Safety Information Computational Center at Oak Ridge National Laboratory as CCC-725.
2. *SCALE: A Modular Code System for Performing Standardized Computer Analyses for Licensing Evaluations*, ORNL/TM-2005/39, Version 5, Vols. I-III, April 2005. Available from Radiation Safety Information Computational Center at Oak Ridge National Laboratory as CCC-725.
3. O. W. Hermann, C. V. Parks, and J. P. Renier, *Technical Support for a Proposed Decay Heat Guide Using SAS2H/ORIGEN-S Data*, NUREG/CR-5625 (ORNL-6698), prepared for the U.S. Nuclear Regulatory Commission by Oak Ridge National Laboratory, Oak Ridge, Tenn., September 1994.
4. *Regulatory Guide 3.54 – Spent Fuel Heat Generation in an Independent Spent Fuel Storage Installation*, Rev. 1, U.S. Nuclear Regulatory Commission, January 1999.
5. F. Sturek, L. Agrenius, and O. Osifo, *Measurements of Decay Heat in Spent Nuclear Fuel at the Swedish Interim Storage Facility, Clab*, Svensk Kärnbränslehantering AB, R-05-62, December 2006.
6. A. Tobias, "Derivation of Decay Heat Benchmarks for U235 and Pu239 by a Least Squares Fit to Measured Data," Central Electricity Generating Board, CEGB – RD/B/6210/R89, May 1989.
7. J. K. Dickens, T. R. England, and R. E. Schenter, "Current Status and Proposed Improvements to the ANSI/ANS-5.1 American National Standard for Decay Heat in Light Water Reactors," *Nuclear Safety*, **32**(2) (April–June 1991).
8. A. Tobias, "Decay Heat," *Prog. Nuc. Energy* **5**(1), 1–93 (1980).
9. V. E. Schrock, "Revised ANS Standard for Decay Heat From Fission-Products," *Nucl. Technol.* **46**(2), 323–331 (1979).
10. V. E. Schrock, "Evaluation of Decay Heating in Shutdown Reactions," *Prog. Nucl. Energy* **3**(2), 125–156 (1979).
11. ANSI/ANS-5.1-2005, "Decay Heat Power in Light Water Reactors," American Nuclear Society, 2005.
12. J. K. Dickens, T. A. Love, J. W. McConnell, and R. W. Peelle, "Fission-Product Energy Release for Times Following Thermal-Neutron Fission of ^{235}U Between 2 and 14 000 s," *Nucl. Sci. Eng.* **74**, 106–129 (1980).
13. J. K. Dickens, T. A. Love, J. W. McConnell, and R. W. Peelle, "Fission-Product Energy Release for Times Following Thermal-Neutron Fission of Plutonium-239 and Plutonium-241 Between 2 and 14,000 s," *Nucl. Sci. Eng.* **78**, 126–146 (1981).

14. K. Baumung, *Measurement of ^{235}U Fission Product Decay Heat Between 15 s and 4000 s*, Kernforschungszentrum Karlsruhe, KFK-3262, 1981.
15. M. Akiyama, K. Furuta, T. Ida, K. Sakata, and S. An, "Measurements of Gamma-Ray Decay Heat of Fission Products for Fast Neutron Fission of ^{235}U , ^{239}Pu , and ^{233}U ," *J. Atomic Ener. Soc. Japan* **24**(9), 709 (1982) (in Japanese).
16. M. Akiyama, K. Furuta, T. Ida, K. Sakata, and S. An, "Measurements of Beta-Ray Decay Heat of Fission Products for Fast Neutron Fission of ^{235}U , ^{239}Pu , and ^{233}U ," *J. Atomic Ener. Soc. Japan* **24**(10), 803 (1982) (in Japanese).
17. J. Katakura, Nuclear Data Center, Japan Atomic Energy Research Institute, personal communications to I. C. Gauld, Oak Ridge National Laboratory, June 10, 2005.
18. P.-I. Johansson, "Integral Determination of the Beta and Gamma Heat in Thermal-Neutron-Induced Fission of ^{235}U and ^{239}Pu , and of the Gamma Heat in Fast Fission of ^{238}U ," pp. 857–860 in *Proceedings of the Specialists Meeting on Nuclear Data for Science and Technology, Mito, Japan, 1988*, and P.-I. Johansson, pp. 211–223 in *Proceedings of the Specialists Meeting on Data for Decay Heat Predictions, Studsvik, Sweden, 1987*.
19. W. A. Schier and G. P. Couchell, *Beta and Gamma Decay Heat Measurements Between 0.1 s—50,000 s for Neutron Fission of ^{235}U , ^{238}U , and ^{239}Pu : Final Report*, University of Massachusetts Lowell, Department of Energy report DOE/ER/40723-4, 1997, and S. Li, University of Massachusetts Lowell, Ph.D. Thesis, 1997.
20. W. A. Schier and G. P. Couchell, University of Massachusetts, Lowell, personal communications to I. C. Gauld, Oak Ridge National Laboratory, April 20, 2005.
21. R. B. Firestone, (V. S. Shirley, ed.), *Table of Isotopes*, 8th Ed., Vols. I and II, John Wiley and Sons, Inc., New York, 1999.
22. J. Katakura, "FP Decay Heat Calculation Using JENDL FP Decay Data File," in *Proceedings of the ANS Winter Meeting 2001*, November 10–12, Reno, NV, 2001.
23. T. Yoshida, T. Tachibana, F. Storrer, K. Oyamatsu, and J. Katakura, "Possible Origin of the Gamma-Ray Discrepancy in the Summation Calculations of Fission Product Decay Heat," *Nucl. Sci. Technol.* **36**(2), 135–142 (1999).
24. J. K. Dickens, "Review of New Integral Determinations of Decay Heat," pp. 199–210 in *Proceedings of the Specialists Meeting on Data for Decay Heat Predictions*, Studsvik, Sweden, September 1987.
25. Nuclear Energy Agency, *Assessment of Fission Product Decay Data for Decay Heat Calculations*, Report by the Working Party on International Evaluation Co-operation of the NEA Nuclear Science Committee, Volume 25, NEA/WPEC-25, Organization for Economic Co-operation and Development, 2007 (<http://www.nea.fr/html/science/wpec/volume25/volume25.pdf>)
26. J. M. Creer and J. W. Shupe Jr., *Development of a Water Boil-Off Spent Fuel Calorimeter System*, Pacific Northwest Laboratory, PNL-3434 (UC-70), May 1981.

27. F. Schmittroth, G. J. Neely, and J. C. Krogness, *A Comparison of Measured and Calculated Decay Heat for Spent Fuel Near 2.5 Years Cooling Time*, Hanford Engineering Development Laboratory, TC-1759, August 1980.
28. F. Schmittroth, *ORIGEN2 Calculations of PWR Spent Fuel Decay Heat Compared with Calorimeter Data*, Hanford Engineering Development Laboratory, HEDL-TME-83-32 (UC-85), January 1984.
29. B. F. Judson et al., *In-Plant Test Measurements for Spent Fuel Storage at Morris Operation – Volume 3: Fuel Bundle Heat Generation Rates*, General Electric, NEDG-24922-3, February 1982.
30. M. A. McKinnon, C. M. Heeb, and J. M. Creer, *Decay Heat Measurements and Predictions of BWR Spent Fuel*, Electric Power Research Institute, EPRI NP-4619, June 1986.
31. J. W. Roddy and J. C. Mailen, *Radiological Characteristics of Light-Water Reactor Spent Fuel: A Literature Survey of Experimental Data*, ORNL/TM-10105, Martin Marietta Energy Systems, Oak Ridge National Laboratory (December 1987).
32. *Nuclear Fuel Data*, Form RW-859, United States Department of Energy, Energy Information Administration, Washington, D.C., October 2004.
33. *Characteristics of Potential Repository Wastes*, United States Department of Energy, DOE/RW-0184-R1, Vols. 1 and 3, July 1992.
34. O. W. Hermann, *San Onofre PWR Data for Code Validation of MOX Fuel Depletion Analyses – Revision 1*, ORNL/TM-1999/108/R1, Lockheed Martin Energy Research Corp., Oak Ridge National Laboratory, March 2000.
35. O. W. Hermann and M. D. DeHart, *Validation of SCALE (SAS2H) Isotopic Predictions for BWR Spent Fuel*, ORNL/TM-13315, Lockheed Martin Energy Research Corp., Oak Ridge National Laboratory, September 1998.
36. R. J. Guenther, D. E. Blahnik, T. K. Campbell, U. P. Jenquin, J. E. Mendel, L. E. Thomas, and C. K. Thornhill, *Characterization of Spent Fuel Approved Testing Material—ATM-105*, PNL, 5109-105 (UC-802), Pacific Northwest Laboratory, 1991.
37. A. G. Croff, M. A. Bjerke, G. W. Morrison, and L. M. Petrie, *Revised Uranium-Plutonium Cycle PWR and BWR Models for the ORIGEN Computer Code*, ORNL/TM-6051, Union Carbide Corporation (Nuclear Division), Oak Ridge National Laboratory, 1978.
38. L. E. Wiles, N. J. Lombardo, C. M. Heeb, U. P. Jenquin, T. E. Michener, C. L. Wheeler, J. M. Creer, and R. A. McCann, *BWR Spent Fuel Storage Cask Performance Test: Volume II – Pre- and Post-Test Decay Heat, Heat Transfer, and Shielding Analyses*, Pacific Northwest Laboratory, PNL-5777, Vol. II (UC-85), June 1986.
39. B. D. Murphy and I. C. Gauld, *Spent Fuel Decay Heat Measurements Performed at the Swedish Central Interim Storage Facility CLAB*, NUREG/CR- (ORNL/TM-2004/113), prepared for the U.S. Nuclear Regulatory Commission by Oak Ridge National Laboratory, Oak Ridge, Tenn. (report in preparation).

40. G. M. O'Donnell, H. H. Scott, and R. O. Meyer, *A New Comparative Analysis of LWR Fuel Designs*, NUREG-1754, U.S. Nuclear Regulatory Commission, December 2001.
41. J. C. Wagner and C. V. Parks, *Parametric Study of the Effect of Burnable Poison Rods for PWR Burnup Credit*, NUREG/CR-6761 (ORNL/TM-2000/373), prepared for the U.S. Nuclear Regulatory Commission by Oak Ridge National Laboratory, Oak Ridge, Tenn., March 2002.
42. M. J. Bell, *ORIGEN – The ORNL Isotope Generation and Depletion Code*, Union Carbide Corporation (Nuclear Division), Oak Ridge National Laboratory, ORNL-4628, May 1973.
43. A. G. Croff, *A User's Manual for the ORIGEN2 Computer Code*, ORNL/TM-7175, Union Carbide Corporation (Nuclear Division), Oak Ridge National Laboratory, July 1980.
44. I. C. Gauld and O. W. Hermann, "SAS2H – A Coupled One-Dimensional Depletion and Shielding Analysis Module," Vol. I, Book 3, Sect. S2 in *SCALE: A Modular Code System for Performing Standardized Computer Analyses for Licensing Evaluation*, ORNL/TM-2005/39, Version 5, Vols. I–III, April 2005. Available from Radiation Safety Information Computational Center at Oak Ridge National Laboratory as CCC-725.
45. N. M. Greene and L. M. Petrie, "XSDRNPM: A One-Dimensional Discrete-Ordinates Code for Transport Analysis," Vol. II, Book 1, Sect. F3, in *SCALE: A Modular Code System for Performing Standardized Computer Analyses for Licensing Evaluation*, ORNL/TM-2005/39, Version 5, Vols. I–III, April 2005. Available from Radiation Safety Information Computational Center at Oak Ridge National Laboratory as CCC-725.
46. M. D. DeHart, "TRITON: A Two-Dimensional Depletion Sequence for Characterization of Spent Nuclear Fuel," Vol. I, Book 3, Sect. T1 in *SCALE: A Modular Code System for Performing Standardized Computer Analyses for Licensing Evaluation*, ORNL/TM-2005/39, Version 5, Vols. I–III, April 2005. Available from Radiation Safety Information Computational Center at Oak Ridge National Laboratory as CCC-725.
47. M. D. DeHart, "NEWT: A New Transport Algorithm for Two-Dimensional Discrete Ordinates Analysis in Non-Orthogonal Geometries," Vol. II, Book 4, Sect. F21 in *SCALE: A Modular Code System for Performing Standardized Computer Analyses for Licensing Evaluation*, ORNL/TM-2005/39, Version 5, Vols. I–III, April 2005. Available from Radiation Safety Information Computational Center at Oak Ridge National Laboratory as CCC-725.
48. W. B. Wilson, R. T. Perry, W. S. Charlton, T. A. Parish, G. P. Estes, T. H. Brown, E. D. Arthur, M. Bozoian, T. R. England, D. G. Madland, and J. E. Stewart, *SOURCES 4A: A Code for Calculating (α, n) , Spontaneous Fission, and Delayed Neutron Sources and Spectra*, LA-13638-MS, Los Alamos National Laboratory (1999).
49. I. C. Gauld and B. D. Murphy, *Updates to the ORIGEN-S Data Libraries Using ENDF/B-VI, FENDL-2.0, and EAF-99 Data*, ORNL/TM-2003/118, UT-Battelle, LLC, Oak Ridge National Laboratory, May 2004.
50. O. W. Hermann, S. M. Bowman, M. C. Brady, and C. V. Parks, *Validation of the SCALE System PWR Spent Fuel Isotopic Composition Analyses*, ORNL/TM-12667, Lockheed Martin Energy Research Corporation, Oak Ridge National Laboratory, March 1995.

51. M. D. DeHart and O. W. Hermann, *An Extension of the Validation of SCALE (SAS2H) Isotopic Prediction for PWR Spent Fuel*, ORNL/TM-13317, Lockheed Martin Energy Research Corporation, Oak Ridge National Laboratory, September 1996.
52. C. E. Sanders and I. C. Gauld, *Isotopic Analysis of High-Burnup PWR Spent Fuel Samples from the Takahama-3 Reactor*, NUREG/CR-6798 (ORNL/TM-2001/259), prepared for the U.S. Nuclear Regulatory Commission by Oak Ridge National Laboratory, Oak Ridge, Tenn., January 2003.
53. B. D. Murphy and I. C. Gauld, "Spent-Fuel Decay Heat Investigations for BWR Assemblies Using Both One- and Two-Dimensional Model Simulations," in *Transactions of the American Nuclear Society*, 2004 Winter Meeting, November 14–18, 2004, Washington, D.C., *Trans. Am. Nucl. Soc.* **91**, 670–672 (2004).
54. O. W. Hermann, C. V. Parks, J. P. Renier, J. W. Roddy, R. C. Ashline, W. B. Wilson, and R. J. LaBauve, *Multicode Comparison of Selected Source-Term Computer Codes*, ORNL/CSD/TM-251, Oak Ridge National Laboratory, Oak Ridge, Tenn., April 1989.
55. *World Nuclear Industry Handbook – 2002*, Nuclear Engineering International, 2002.
56. N. R. Draper, and H. Smith, *Applied Regression Analysis*, 2nd Ed., pp. 22–32, John Wiley & Sons, New York (1981).
57. J. D. Gibbons, *Nonparametric Methods for Quantitative Analysis*, 2nd Ed., American Sciences Press, Inc., Columbus, OH (1985). See also the Internet site:
http://www.physics.csbsju.edu/stats/KS-test.n.plot_form.html
58. S. M. Bowman, *Configuration Management Plan for the SCALE Code System*, SCALE-CMP-001, Rev. 6, September 2002.
59. S. M. Bowman, *Quality Assurance Plan for the SCALE Computational System*, SCALE-QMP-005, Rev. 1, September 2002.
60. B. Duchemin and C. Nordborg, "Decay Heat Calculation – An International Nuclear Code Comparison," OECD Nuclear Energy Agency, NEA/NEACRP/L(1989)319 (also NEANDC-275-U), 1989 (<http://www.nea.fr/html/science/docs/1989/neacrp-l-1989-319.pdf>)
61. F. Schmittroth, G. J. Neely, and D. W. Wootan, *Uncertainties in Decay Heat Calculations for Spent Fuel*, TC-1636, Hanford Engineering Development Laboratory (February 1980).
62. *Determination of the Accuracy of Utility Spent-Fuel Burnup Records*, EPRI TR-112054, Electric Power Research Institute, Palo Alto, CA, 1999.
63. H. L. Massie, Jr., *Reactor Record Uncertainty Determination*, U.S. Department of Energy, Office of Civilian Radioactive Waste Management, Areva 32-5041666-02 (DOC.20040623.0002), Las Vegas NV, 2004.



APPENDIX A

SPENT FUEL ASSEMBLY BENCHMARK DATA
SUMMARY OF EXPERIMENTAL AND CALCULATED RESULTS



Table A.1 Summary of measured and predicted PWR fuel assembly decay heat (U.S. measurements only)

Reactor	Assembly type	Assembly ID	Enrichment (wt % ²³⁵ U)	Uranium (kg)	Final burnup (MWD/t)	Discharge date	Measurement date	Cooling time (days)	Measured (W)	Calculated (W)	Residual error (W)	Relative error (C/E-1)%
Point Beach	14×14	C-52	3.397	386.54	31,914	3/3/1977	8/23/1981	1635	724.0	718.6	-5.4	-0.75%
Point Beach	14×14	C-56	3.397	386.80	38,917	3/3/1977	8/24/1981	1634	921.0	917.2	-3.8	-0.41%
Point Beach	14×14	C-64	3.397	386.63	39,384	3/3/1977	8/23/1981	1633	931.0	931.2	0.2	0.02%
Point Beach	14×14	C-66	3.397	386.54	35,433	3/3/1977	8/20/1981	1630	846.0	834.2	-11.8	-1.39%
Point Beach	14×14	C-67	3.397	386.45	38,946	3/3/1977	8/19/1981	1629	934.0	919.5	-14.5	-1.55%
Point Beach	14×14	C-68	3.397	386.36	37,059	3/3/1977	8/20/1981	1630	874.0	876.2	2.2	0.25%
San Onofre	14×14s***	C-01	3.865	361.72	26,540	6/2/1973	8/30/1981	3011	359.0	360.0	1.0	0.28%
San Onofre	14×14s	C-16**	3.865	361.72	28,462	6/2/1973	8/31/1981	3012	384.0	388.6	4.6	1.20%
San Onofre	14×14s	C-19	3.865	361.72	30,426	6/2/1973	8/30/1981	3011	418.0	417.2	-0.8	-0.19%
San Onofre	14×14s	C-20	3.865	361.72	32,363	6/2/1973	8/29/1981	3011	456.0	447.2	-8.8	-1.93%
San Onofre	14×14s	D-01	4.005	363.64	31,393	3/14/1975	8/27/1981	2358	499.0	489.9	-9.1	-1.82%
San Onofre	14×14s	D-46	4.005	363.64	32,318	3/14/1975	8/29/1981	2360	510.0	507.8	-2.2	-0.43%
San Onofre	14×14s	E-18	4.005	363.98	32,357	9/30/1976	8/28/1981	1794	635.0	630.7	-4.3	-0.68%
San Onofre	14×14s	F-04	3.996	372.32	30,429	9/15/1978	8/28/1981	1078	934.0	927.3	-6.7	-0.72%
Turkey Point	15×15	B-43	2.559	447.79	25,595	10/26/1975	9/11/1980	1782	637.0	619.9	-17.1	-2.68%
Turkey Point	15×15	D-15	2.557	456.12	28,430	11/24/1977	7/8/1980	957	1423.0	1444.0	21.0	1.48%
Turkey Point	15×15	D-15*	2.557	456.12	28,430	11/24/1977	1/6/1981	1139	1126.0	1175.0	49.0	4.35%
Turkey Point	15×15	D-15*	2.557	456.12	28,430	11/24/1977	7/28/1983	2072	625.0	623.8	-1.2	-0.19%
Turkey Point	15×15	D-22	2.557	458.00	26,485	11/24/1977	7/9/1980	958	1284.0	1280.0	-4.0	-0.31%
Turkey Point	15×15	D-34	2.557	455.24	27,863	11/24/1977	4/1/1980	859	1550.0	1590.0	40.0	2.58%

* Indicates repeat measurements on the same assembly.

** Measured value from static mode operation (recirculation mode value rejected).

*** "s" indicates stainless steel clad fuel.

Table A.2 Summary of measured and predicted BWR fuel assembly decay heat (U.S. measurements only)

Reactor	Assembly type	Assembly ID	Enrichment (wt % ²³⁵ U)	Uranium (kg)	Final burnup (MWd/t)	Discharge date	Measurement date	Cooling time (days)	Measured (W)	Calculated (W)	Residual error (W)	Relative error (C/E-1)%
Cooper	GE 7x7	CZ102	1.090	195.48	11,667	9/17/1977	9/25/1984	2565	62.3	80.0	17.7	28.35%
Cooper	GE 7x7	CZ102*	1.090	195.48	11,667	9/17/1977	12/14/1984	2645	70.4	78.7	8.3	11.83%
Cooper	GE 7x7	CZ147	2.500	190.31	26,709	4/20/1981	11/4/1984	1294	276.7	282.7	6.0	2.17%
Cooper	GE 7x7	CZ148	2.500	190.22	26,310	4/20/1981	10/23/1984	1282	273.5	280.2	6.7	2.45%
Cooper	GE 7x7	CZ182	2.500	190.09	26,823	5/21/1982	9/27/1984	860	342.6	344.1	1.5	0.44%
Cooper	GE 7x7	CZ195	2.500	190.68	26,391	4/20/1981	10/29/1984	1288	255.5	277.2	21.7	8.49%
Cooper	GE 7x7	CZ205	2.500	190.72	25,344	5/21/1982	9/24/1984	857	324.0	314.0	-10.0	-3.09%
Cooper	GE 7x7	CZ205*	2.500	190.72	25,344	5/21/1982	10/4/1984	867	361.5	311.2	-50.3	-13.91%
Cooper	GE 7x7	CZ205*	2.500	190.72	25,344	5/21/1982	10/8/1984	871	343.5	310.0	-33.5	-9.75%
Cooper	GE 7x7	CZ205*	2.500	190.72	25,344	5/21/1982	10/9/1984	872	353.2	309.8	-43.4	-12.29%
Cooper	GE 7x7	CZ205*	2.500	190.72	25,344	5/21/1982	10/23/1984	886	331.8	306.0	-25.8	-7.78%
Cooper	GE 7x7	CZ205*	2.500	190.72	25,344	5/21/1982	10/24/1984	887	338.7	305.7	-33.0	-9.74%
Cooper	GE 7x7	CZ205*	2.500	190.72	25,344	5/21/1982	10/29/1984	892	327.5	304.4	-23.1	-7.05%
Cooper	GE 7x7	CZ205*	2.500	190.72	25,344	5/21/1982	11/2/1984	896	313.1	303.3	-9.8	-3.13%
Cooper	GE 7x7	CZ205*	2.500	190.72	25,344	5/21/1982	11/5/1984	899	311.4	302.5	-8.9	-2.86%
Cooper	GE 7x7	CZ205*	2.500	190.72	25,344	5/21/1982	12/6/1984	930	314.0	294.7	-19.3	-6.15%
Cooper	GE 7x7	CZ205*	2.500	190.72	25,344	5/21/1982	12/12/1984	936	331.2	293.2	-38.0	-11.47%
Cooper	GE 7x7	CZ205*	2.500	190.72	25,344	5/21/1982	12/22/1984	946	317.1	290.9	-26.2	-8.26%
Cooper	GE 7x7	CZ205*	2.500	190.72	25,344	5/21/1982	5/13/1985	1088	289.7	261.8	-27.9	-9.63%
Cooper	GE 7x7	CZ205*	2.500	190.72	25,344	5/21/1982	5/28/1985	1103	308.0	259.1	-48.9	-15.88%
Cooper	GE 7x7	CZ209	2.500	190.38	25,383	5/21/1982	10/28/1984	891	279.5	277.2	-2.3	-0.82%
Cooper	GE 7x7	CZ211	2.500	190.82	26,679	4/20/1981	10/1/1984	1260	296.0	289.3	-6.7	-2.26%
Cooper	GE 7x7	CZ211*	2.500	190.82	26,679	4/20/1981	5/20/1985	1491	240.3	252.5	12.2	5.08%
Cooper	GE 7x7	CZ222	2.500	190.90	26,692	5/21/1982	11/4/1984	898	355.7	327.5	-28.2	-7.93%
Cooper	GE 7x7	CZ225	2.500	190.51	25,796	5/21/1982	10/2/1984	865	333.5	304.2	-29.3	-8.79%
Cooper	GE 7x7	CZ239	2.500	189.57	27,246	5/21/1982	10/30/1984	893	366.5	337.3	-29.2	-7.97%

* Indicates repeat measurements on the same assembly.

Table A.2 Summary of measured and predicted BWR fuel assembly decay heat (U.S. measurements only) (continued)

Reactor	Assembly type	Assembly ID	Enrichment (wt % ²³⁵ U)	Uranium (kg)	Final burnup (MWd/t)	Discharge date	Measurement date	Cooling time (days)	Measured (W)	Calculated (W)	Residual error (W)	Relative error (C/E-1)%
Cooper	GE 7×7	CZ246	2.500	189.81	27,362	5/21/1982	11/2/1984	896	320.9	341.8	20.9	6.51%
Cooper	GE 7×7	CZ246*	2.500	189.81	27,362	5/21/1982	11/5/1984	899	341.7	340.9	-0.8	-0.23%
Cooper	GE 7×7	CZ259	2.500	190.20	26,466	4/20/1981	10/29/1984	1288	247.6	277.1	29.5	11.91%
Cooper	GE 7×7	CZ259*	2.500	190.20	26,466	4/20/1981	12/20/1984	1340	288.5	268.4	-20.1	-6.97%
Cooper	GE 7×7	CZ259*	2.500	190.20	26,466	4/20/1981	5/14/1985	1485	254.1	247.8	-6.3	-2.48%
Cooper	GE 7×7	CZ264	2.500	190.89	26,496	4/20/1981	10/23/1984	1282	263.8	280.3	16.5	6.25%
Cooper	GE 7×7	CZ277	2.500	189.49	26,747	4/20/1981	10/27/1984	1286	262.7	276.8	14.1	5.37%
Cooper	GE 7×7	CZ277*	2.500	189.49	26,747	4/20/1981	5/26/1985	1497	243.0	245.7	2.7	1.11%
Cooper	GE 7×7	CZ286	2.500	189.95	27,141	5/21/1982	12/6/1984	930	278.4	308.3	29.9	10.74%
Cooper	GE 7×7	CZ286*	2.500	189.95	27,141	5/21/1982	5/28/1985	1103	284.2	273.1	-11.1	-3.91%
Cooper	GE 7×7	CZ296	2.500	190.50	26,388	4/20/1981	11/3/1984	1293	256.7	283.8	27.1	10.56%
Cooper	GE 7×7	CZ296*	2.500	190.50	26,388	4/20/1981	5/21/1985	1492	251.9	252.2	0.3	0.12%
Cooper	GE 7×7	CZ302	2.500	190.00	26,594	4/20/1981	10/24/1984	1283	285.6	276.7	-8.9	-3.12%
Cooper	GE 7×7	CZ308	2.500	189.78	25,815	5/21/1982	11/1/1984	895	269.7	282.2	12.5	4.63%
Cooper	GE 7×7	CZ311	2.500	189.91	27,392	5/21/1982	10/27/1984	890	356.9	320.3	-36.6	-10.25%
Cooper	GE 7×7	CZ315	2.500	189.96	26,881	5/21/1982	12/8/1984	932	328.0	299.3	-28.7	-8.75%
Cooper	GE 7×7	CZ318	2.500	189.32	26,568	5/21/1982	12/7/1984	931	277.6	280.8	3.2	1.15%
Cooper	GE 7×7	CZ331	2.500	190.36	21,332	3/31/1978	9/24/1984	2369	162.8	156.3	-6.5	-3.99%
Cooper	GE 7×7	CZ331*	2.500	190.36	21,332	3/31/1978	12/21/1984	2457	180.1	153.0	-27.1	-15.05%
Cooper	GE 7×7	CZ337	2.500	189.90	26,720	5/21/1982	11/1/1984	895	347.7	325.9	-21.8	-6.27%
Cooper	GE 7×7	CZ337*	2.500	189.90	26,720	5/21/1982	5/24/1985	1099	300.4	278.4	-22.0	-7.32%
Cooper	GE 7×7	CZ342	2.500	190.16	27,066	5/21/1982	12/7/1984	931	280.1	302.1	22.0	7.85%
Cooper	GE 7×7	CZ342*	2.500	190.16	27,066	5/21/1982	5/26/1985	1101	300.0	268.6	-31.4	-10.47%
Cooper	GE 7×7	CZ346	2.500	190.23	28,048	5/21/1982	10/27/1984	890	388.7	354.0	-34.7	-8.93%
Cooper	GE 7×7	CZ348	2.500	190.38	27,480	5/21/1982	10/31/1984	894	342.8	335.0	-7.8	-2.28%
Cooper	GE 7×7	CZ351	2.500	190.02	25,753	5/21/1982	12/10/1984	934	313.8	281.4	-32.4	-10.33%

* Indicates repeat measurements on the same assembly.

Table A.2 Summary of measured and predicted BWR fuel assembly decay heat (U.S. measurements only) (continued)

Reactor	Assembly type	Assembly ID	Enrichment (wt % ²³⁵ U)	Uranium (kg)	Final burnup (MWd/t)	Discharge date	Measurement date	Cooling time (days)	Measured (W)	Calculated (W)	Residual error (W)	Relative error (C/E-1)%
Cooper	GE 7×7	CZ355	2.500	190.60	25,419	5/21/1982	10/28/1984	891	290.5	278.4	-12.1	-4.17%
Cooper	GE 7×7	CZ357	2.500	190.19	27,140	5/21/1982	12/8/1984	932	320.3	308.1	-12.2	-3.81%
Cooper	GE 7×7	CZ369	2.500	190.20	26,575	5/21/1982	10/25/1984	888	347.6	323.4	-24.2	-6.96%
Cooper	GE 7×7	CZ370	2.500	190.23	26,342	4/20/1981	9/28/1984	1257	293.6	278.6	-15.0	-5.11%
Cooper	GE 7×7	CZ372	2.500	190.01	25,848	4/20/1981	9/27/1984	1256	294.3	263.7	-30.6	-10.40%
Cooper	GE 7×7	CZ379	2.500	190.18	25,925	5/21/1982	11/4/1984	898	287.4	281.3	-6.1	-2.12%
Cooper	GE 7×7	CZ398	2.500	189.83	27,478	5/21/1982	10/27/1984	890	372.0	338.8	-33.2	-8.92%
Cooper	GE 7×7	CZ415	2.500	189.72	25,863	4/20/1981	9/26/1984	1255	289.3	272.8	-16.5	-5.70%
Cooper	GE 7×7	CZ416	2.500	189.43	27,460	5/21/1982	10/31/1984	894	319.8	318.0	-1.8	-0.56%
Cooper	GE 7×7	CZ429	2.500	190.07	27,641	5/21/1982	10/26/1984	889	385.6	348.3	-37.3	-9.67%
Cooper	GE 7×7	CZ430	2.500	189.93	26,824	5/21/1982	10/31/1984	894	353.3	324.1	-29.2	-8.26%
Cooper	GE 7×7	CZ433	2.500	190.02	25,977	4/20/1981	9/26/1984	1255	287.4	264.1	-23.3	-8.11%
Cooper	GE 7×7	CZ433*	2.500	190.02	25,977	4/20/1981	5/21/1985	1492	256.7	231.3	-25.4	-9.89%
Cooper	GE 7×7	CZ460	2.500	190.18	26,511	5/21/1982	12/9/1984	933	313.5	292.4	-21.1	-6.73%
Cooper	GE 7×7	CZ466	2.500	189.86	26,077	5/21/1982	9/28/1984	861	302.1	292.5	-9.6	-3.18%
Cooper	GE 7×7	CZ468	2.500	189.78	26,757	5/21/1982	12/11/1984	935	325.3	300.2	-25.1	-7.72%
Cooper	GE 7×7	CZ472	2.500	190.12	25,957	5/21/1982	9/26/1984	859	325.0	319.7	-5.3	-1.63%
Cooper	GE 7×7	CZ473	2.500	189.76	26,517	5/21/1982	12/10/1984	934	293.2	281.2	-12.0	-4.09%
Cooper	GE 7×7	CZ498	2.500	189.69	26,482	5/21/1982	10/25/1984	888	359.4	324.3	-35.1	-9.77%
Cooper	GE 7×7	CZ508	2.500	190.68	26,357	5/21/1982	12/9/1984	933	310.0	293.4	-16.6	-5.35%
Cooper	GE 7×7	CZ515	2.500	190.48	25,737	4/20/1981	9/25/1984	1254	294.0	272.4	-21.6	-7.35%
Cooper	GE 7×7	CZ515*	2.500	190.48	25,737	4/20/1981	10/26/1984	1285	296.0	266.9	-29.1	-9.83%
Cooper	GE 7×7	CZ526	2.500	190.54	27,596	5/21/1982	10/1/1984	864	395.4	356.7	-38.7	-9.79%
Cooper	GE 7×7	CZ526*	2.500	190.54	27,596	5/21/1982	5/22/1985	1097	321.8	296.0	-25.8	-8.02%
Cooper	GE 7×7	CZ528	2.500	190.81	25,714	4/20/1981	10/25/1984	1284	297.6	267.3	-30.3	-10.18%
Cooper	GE 7×7	CZ531	2.500	189.90	26,699	5/21/1982	10/30/1984	893	347.2	323.2	-24.0	-6.91%

* Indicates repeat measurements on the same assembly.

Table A.2 Summary of measured and predicted BWR fuel assembly decay heat (U.S. measurements only) (continued)

Reactor	Assembly type	Assembly ID	Enrichment (wt % ²³⁵ U)	Uranium (kg)	Final burnup (MWd/t)	Discharge date	Measurement date	Cooling time (days)	Measured (W)	Calculated (W)	Residual error (W)	Relative error (C/E-1)%
Cooper	GE 7×7	CZ536	2.500	190.17	26,589	4/20/1981	9/27/1984	1256	295.2	262.2	-33.0	-11.18%
Cooper	GE 7×7	CZ542	2.500	189.99	26,691	5/21/1982	12/8/1984	932	311.9	295.2	-16.7	-5.35%
Cooper	GE 7×7	CZ545	2.500	190.47	26,668	5/21/1982	12/11/1984	935	295.2	285.0	-10.2	-3.46%
Dresden	GE 7×7	DN212	2.130	194.70	5,280	9/17/1976	10/3/1984	2938	31.2	34.8	3.6	11.44%
Dresden	GE 7×7	DN212*	2.130	194.70	5,280	9/17/1976	10/18/1984	2953	19.5	34.7	15.2	77.90%
Monticello	GE 7×7	MT116	2.250	193.53	18,039	9/12/1975	6/10/1985	3559	114.9	109.2	-5.7	-4.96%
Monticello	GE 7×7	MT123	2.250	193.53	13,027	3/15/1974	6/5/1985	4100	66.8	75.7	8.9	13.37%
Monticello	GE 7×7	MT123*	2.250	193.53	13,027	3/15/1974	6/8/1985	4103	95.3	75.7	-19.6	-20.56%
Monticello	GE 7×7	MT123*	2.250	193.53	13,027	3/15/1974	6/11/1985	4106	65.9	75.7	9.8	14.86%
Monticello	GE 7×7	MT133	2.250	193.53	20,994	9/12/1975	5/29/1985	3547	152.6	129.1	-23.5	-15.40%
Monticello	GE 7×7	MT133*	2.250	193.53	20,994	9/12/1975	6/6/1985	3555	129.0	129.0	0.0	0.00%
Monticello	GE 7×7	MT133*	2.250	193.53	20,994	9/12/1975	6/9/1985	3558	154.8	128.9	-25.9	-16.73%
Monticello	GE 7×7	MT133*	2.250	193.53	20,994	9/12/1975	6/12/1985	3561	106.7	128.9	22.2	20.81%
Monticello	GE 7×7	MT190	2.250	193.53	15,143	9/12/1975	6/8/1985	3557	99.2	92.0	-7.2	-7.30%
Monticello	GE 7×7	MT228	2.250	193.53	12,123	9/12/1975	5/30/1985	3548	101.0	73.3	-27.7	-27.39%
Monticello	GE 7×7	MT228*	2.250	193.53	12,123	9/12/1975	6/7/1985	3556	71.2	73.3	2.1	2.92%
Monticello	GE 7×7	MT228*	2.250	193.53	12,123	9/12/1975	6/11/1985	3560	76.4	73.3	-3.2	-4.12%
Monticello	GE 7×7	MT264	2.250	193.53	9,160	9/12/1975	6/5/1985	3554	46.1	54.4	8.3	17.96%

* Indicates repeat measurements on the same assembly.

Table A.3 Summary of measured and predicted PWR fuel assembly decay heat (SKB measurements only)

Reactor	Assembly type	Assembly ID	Enrichment (wt % ²³⁵ U)	Uranium (kg)	Final burnup (MWd/t)	Discharge date	Measurement date	Cooling time (days)	Measured (W)	Calculated (W)	Residual error (W)	Relative error (C/E-1)%
Ringhals 2	15×15	C01	3.095	455.79	36,688	4/4/1981	6/10/2004	8468	415.8	423.6	7.8	1.89%
Ringhals 2	15×15	C12	3.095	453.74	36,385	4/4/1981	4/6/2004	8403	410.3	418.9	8.6	2.09%
Ringhals 2	15×15	C20	3.095	454.76	35,720	4/4/1985	4/14/2004	6950	415.8	433.9	18.1	4.35%
Ringhals 2	15×15	C20*	3.095	454.76	35,720	4/4/1985	4/15/2004	6951	426.0	433.8	7.8	1.82%
Ringhals 2	15×15	C20*	3.095	454.76	35,720	4/4/1985	4/16/2004	6952	428.9	433.8	4.9	1.15%
Ringhals 2	15×15	C20*	3.095	454.76	35,720	4/4/1985	4/23/2004	6959	435.7	433.7	-2.0	-0.45%
Ringhals 2	15×15	D27	3.252	432.59	39,676	4/28/1983	4/26/2004	7669	456.1	455.6	-0.5	-0.10%
Ringhals 2	15×15	D38	3.252	434.21	39,403	5/6/1982	4/5/2004	8005	442.3	446.1	3.8	0.85%
Ringhals 2	15×15	E38	3.199	433.59	33,973	5/6/1982	3/30/2004	7999	376.3	376.7	0.4	0.10%
Ringhals 2	15×15	E38*	3.199	433.59	33,973	5/6/1982	3/31/2004	8000	374.3	376.7	2.4	0.63%
Ringhals 2	15×15	E40	3.199	434.24	34,339	5/6/1982	6/14/2004	8075	381.3	380.6	-0.7	-0.17%
Ringhals 2	15×15	F14	3.197	436.38	34,009	4/28/1983	6/18/2004	7722	381.8	385.6	3.8	0.99%
Ringhals 2	15×15	F21	3.197	435.94	36,273	4/13/1984	6/23/2004	7376	420.9	420.5	-0.4	-0.09%
Ringhals 2	15×15	F25	3.197	437.29	35,352	4/28/1983	6/21/2004	7725	396.7	403.5	6.8	1.70%
Ringhals 2	15×15	F32	3.197	436.99	50,962	5/12/1988	5/28/2004	5860	692.0	697.8	5.8	0.84%
Ringhals 2	15×15	G11	3.188	436.18	35,463	4/4/1985	5/24/2004	6990	416.4	415.7	-0.7	-0.16%
Ringhals 2	15×15	G23	3.206	436.13	35,633	4/4/1985	5/18/2004	6984	420.6	422.2	1.6	0.37%
Ringhals 2	15×15	I09	3.203	437.35	40,188	5/12/1988	5/17/2004	5849	507.9	518.7	10.8	2.12%
Ringhals 2	15×15	I24	3.203	429.60	34,294	4/30/1986	5/26/2004	6601	410.1	405.9	-4.2	-1.02%
Ringhals 2	15×15	I25	3.203	433.06	36,859	4/25/1987	4/13/2004	6198	445.8	454.0	8.2	1.84%

* Indicates repeat measurements on the same assembly

Table A.3 Summary of measured and predicted PWR fuel assembly decay heat (SKB measurements only) (continued)

Reactor	Assembly type	Assembly ID	Enrichment (wt % ²³⁵ U)	Uranium (kg)	Final burnup (MWd/t)	Discharge date	Measurement date	Cooling time (days)	Measured (W)	Calculated (W)	Residual error (W)	Relative error (C/E-1)%
Ringhals 3	17×17	0C9	3.101	457.64	38,442	5/30/1986	5/6/2004	6551	491.2	508.3	17.1	3.49%
Ringhals 3	17×17	0E2	3.103	463.60	41,628	7/7/1988	6/16/2004	5823	587.9	588.6	0.7	0.12%
Ringhals 3	17×17	0E6	3.103	461.77	35,993	7/7/1988	6/22/2004	5829	487.8	491.8	4.0	0.83%
Ringhals 3	17×17	1C2	3.101	459.05	33,318	5/30/1986	5/14/2004	6559	417.7	426.2	8.5	2.04%
Ringhals 3	17×17	1C5	3.101	457.99	38,484	5/30/1986	6/17/2004	6593	499.2	508.3	9.1	1.83%
Ringhals 3	17×17	1E5	3.103	463.90	34,638	7/7/1988	6/11/2004	5818	468.8	472.4	3.6	0.77%
Ringhals 3	17×17	2A5	2.100	462.03	20,107	5/11/1984	5/3/2004	7297	233.8	240.2	6.4	2.76%
Ringhals 3	17×17	2C2	3.101	459.49	36,577	5/30/1986	5/5/2004	6550	466.5	476.2	9.7	2.07%
Ringhals 3	17×17	3C1	3.101	458.43	36,572	5/30/1986	4/30/2004	6545	470.2	475.1	4.9	1.04%
Ringhals 3	17×17	3C5	3.101	458.87	38,373	5/30/1986	4/28/2004	6543	501.4	508.8	7.4	1.47%
Ringhals 3	17×17	3C9	3.101	459.14	36,560	5/30/1986	5/7/2004	6552	468.4	475.5	7.1	1.51%
Ringhals 3	17×17	4C4	3.101	459.05	33,333	5/30/1986	5/27/2004	6572	422.0	426.3	4.3	1.01%
Ringhals 3	17×17	4C7	3.101	458.26	38,370	5/30/1986	5/4/2004	6549	498.7	507.9	9.2	1.83%
Ringhals 3	17×17	5A3	2.100	461.48	19,699	5/11/1984	6/13/2003	6972	237.7	238.5	0.8	0.33%
Ringhals 3	17×17	5A3*	2.100	461.48	19,699	5/11/1984	6/16/2003	6975	236.7	238.5	1.8	0.77%
Ringhals 3	17×17	5A3*	2.100	461.48	19,699	5/11/1984	6/18/2003	6977	243.4	238.5	-4.9	-2.03%
Ringhals 3	17×17	5A3*	2.100	461.48	19,699	5/11/1984	4/27/2004	7291	230.9	234.9	4.0	1.71%
Ringhals 3	17×17	5A3*	2.100	461.48	19,699	5/11/1984	5/10/2004	7304	230.3	234.8	4.5	1.98%

* Indicates repeat measurements on the same assembly

Table A.4 Summary of measured and predicted BWR fuel assembly decay heat (SKB measurements only)

Reactor	Assembly type	Assembly ID	Enrichment (wt % ²³⁵ U)	Uranium (kg)	Final burnup (MWd/t)	Discharge date	Measurement date	Cooling time (days)	Measured (W)	Calculated (W)	Residual error (W)	Relative error (C/E-1)%
Barsebäck 1	8×8-1	9329	2.920	178.77	41,127	9/17/1988	6/2/2003	5371	222.8	221.2	-1.6	-0.72%
Barsebäck 1	8×8-1	9329*	2.920	178.77	41,127	9/17/1988	6/4/2003	5373	224.4	221.1	-3.3	-1.47%
Barsebäck 1	8×8-1	9329*	2.920	178.77	41,127	9/17/1988	11/20/2003	5542	218.7	218.6	-0.1	-0.05%
Barsebäck 1	8×8-1	10288	2.950	179.16	35,218	9/17/1988	11/12/2003	5534	185.8	183.5	-2.3	-1.24%
Barsebäck 2	8×8-1	14076	3.150	179.57	40,010	7/2/1992	12/9/2003	4177	240.3	235.2	-5.1	-2.12%
Forsmark 1	8×8-1	3838	2.086	177.90	25,669	7/10/1992	12/10/2003	4170	126.8	131.7	4.9	3.86%
Forsmark 1	8×8-1	3838*	2.086	177.90	25,669	7/10/1992	12/11/2003	4171	125.9	131.6	5.7	4.53%
Forsmark 1	8×8-2	KU0100	2.976	174.92	34,193	8/17/1990	1/9/2004	4893	185.3	177.9	-7.4	-3.99%
Forsmark 1	9×9-5	KU0269	2.938	177.02	35,113	8/17/1990	1/19/2004	4903	192.7	192.2	-0.5	-0.26%
Forsmark 1	9×9-5	KU0278	2.939	177.13	35,323	5/24/1991	12/22/2003	4595	195.4	194.4	-1.0	-0.51%
Forsmark 1	9×9-5	KU0282	2.939	177.10	37,896	5/24/1991	12/1/2003	4574	218.5	212.2	-6.3	-2.88%
Forsmark 2	8×8-1	5535	2.095	177.69	19,944	7/15/1988	12/18/2003	5634	84.6	92.4	7.8	9.22%
Forsmark 2	SVEA 64	11494	2.920	181.09	32,431	7/15/1988	12/2/2003	5618	166.0	165.8	-0.2	-0.12%
Forsmark 2	SVEA 64	11495	2.910	181.07	32,431	7/15/1988	11/7/2003	5593	167.6	166.6	-1.0	-0.60%
Forsmark 2	SVEA 64	13775	2.850	181.34	32,837	7/12/1991	12/19/2003	4543	178.4	178.8	0.4	0.22%
Forsmark 3	SVEA 100	13847	2.769	180.67	31,275	7/13/1990	11/13/2003	4871	170.3	168.4	-1.9	-1.12%
Forsmark 3	SVEA 100	13847*	2.769	180.67	31,275	7/13/1990	11/13/2003	4871	169.6	168.4	-1.2	-0.71%
Forsmark 3	SVEA 100	13848	2.769	180.67	31,275	7/13/1990	11/24/2003	4882	170.7	168.3	-2.4	-1.41%
Ringhals 1	8×8-1	1177	2.642	180.59	36,242	8/2/1985	11/26/2003	6690	177.9	173.6	-4.3	-2.42%
Ringhals 1	8×8-1	1186	2.640	180.52	30,498	8/2/1985	11/10/2003	6674	140.8	142.2	1.4	0.99%
Ringhals 1	8×8-1	6423	2.900	177.70	35,109	8/5/1988	2/12/2004	5669	174.2	175.3	1.1	0.63%
Ringhals 1	8×8-1	6432	2.894	177.52	36,861	8/5/1988	6/10/2003	5422	185.5	186.5	1.0	0.54%
Ringhals 1	8×8-1	6432*	2.894	177.52	36,861	8/5/1988	6/12/2003	5424	189.5	186.5	-3.0	-1.58%

* Indicates repeat measurements on the same assembly.

Table A.4 Summary of measured and predicted BWR fuel assembly decay heat (SKB measurements only) (continued)

Reactor	Assembly type	Assembly ID	Enrichment (wt % ²³⁵ U)	Uranium (kg)	Final burnup (MWd/t)	Discharge date	Measurement date	Cooling time (days)	Measured (W)	Calculated (W)	Residual error (W)	Relative error (C/E-1)%
Ringhals 1	8×8-1	6432*	2.894	177.52	36,861	8/5/1988	2/13/2004	5670	184.4	183.6	-0.8	-0.43%
Ringhals 1	8×8-1	6432*	2.894	177.52	36,861	8/5/1988	2/23/2004	5680	182.8	183.5	0.7	0.38%
Ringhals 1	8×8-1	6432*	2.894	177.52	36,861	8/5/1988	2/24/2004	5681	185.2	183.5	-1.7	-0.92%
Ringhals 1	8×8-1	6432*	2.894	177.52	36,861	8/5/1988	3/1/2004	5687	181.6	183.4	1.8	0.99%
Ringhals 1	8×8-1	6432*	2.894	177.52	36,861	8/5/1988	3/2/2004	5688	182.0	183.4	1.4	0.77%
Ringhals 1	8×8-1	6454	2.898	177.68	37,236	8/15/1986	2/17/2004	6395	186.3	180.6	-5.7	-3.06%
Ringhals 1	8×8-1	8327	2.904	177.54	37,851	8/6/1991	3/10/2004	4600	196.9	200.7	3.8	1.93%
Ringhals 1	8×8-1	8331	2.910	177.69	35,903	9/15/1989	3/11/2004	5291	187.0	183.3	-3.7	-1.98%
Ringhals 1	8×8-1	8332	2.895	177.52	34,977	8/5/1988	3/4/2004	5690	168.1	172.1	4.0	2.38%
Ringhals 1	8×8-1	8338	2.911	177.60	34,830	8/5/1988	3/9/2004	5695	169.5	172.0	2.5	1.47%
Oskarshamn 2	8×8-1	1377	2.201	183.58	14,546	5/13/1977	1/22/2004	9750	56.2	59.2	3.0	5.37%
Oskarshamn 2	8×8-1	1389	2.201	183.65	19,481	7/15/1981	11/28/2003	8171	83.9	83.2	-0.7	-0.86%
Oskarshamn 2	8×8-1	1546	2.201	183.97	24,470	8/19/1983	1/16/2004	7455	108.1	110.6	2.5	2.31%
Oskarshamn 2	8×8-1	1696	2.201	184.25	20,870	8/19/1983	12/3/2003	7411	92.4	93.6	1.2	1.27%
Oskarshamn 2	8×8-1	1704	2.201	184.02	19,437	7/23/1982	12/8/2003	7808	84.0	84.0	0.0	-0.06%
Oskarshamn 2	8×8-1	2995	2.699	179.38	29,978	7/15/1981	1/7/2004	8211	130.5	131.2	0.7	0.54%
Oskarshamn 2	8×8-1	6350	2.875	179.00	27,675	6/7/1985	12/4/2003	6754	126.9	128.9	2.0	1.58%
Oskarshamn 2	8×8-1	6350*	2.875	179.00	27,675	6/7/1985	12/5/2003	6755	129.4	128.9	-0.5	-0.39%
Oskarshamn 2	SVEA 64	12684	2.902	182.32	46,648	8/2/1991	12/16/2003	4519	282.7	279.1	-3.6	-1.27%
Oskarshamn 3	8×8-1	12078	2.577	177.36	25,160	7/8/1988	11/18/2003	5611	120.2	125.6	5.4	4.49%
Oskarshamn 3	SVEA 100	13628	2.711	180.77	35,619	6/24/1991	1/8/2004	4581	194.0	196.2	2.2	1.13%
Oskarshamn 3	SVEA 100	13630	2.711	180.78	40,363	6/24/1991	12/12/2003	4554	235.7	232.3	-3.4	-1.44%

* Indicates repeat measurements on the same assembly.

APPENDIX B

**ARPLIB INPUT FILE EXAMPLE
TRITON INPUT FILES FOR SELECTED ASSEMBLIES**

ARPLIB input file for San Onofre PWR 14 × 14 library

In this example two libraries (named `w14_e35.lib` and `w14_e40.lib`), representing two discrete enrichments (3.5 and 4.0 w t%), are thinned from 25 burnup-dependent cross section sets down to 11 final cross section sets and saved with a library name suffix `arplib`. The `#shell` commands are used to copy the libraries between the home area (`$RTNDIR`) and the SCALE working directory (`$TMPDIR`) on a Unix or Linux operating system. On a Windows OS the `cp` command is replace with `copy`, and the home directory environment variable `$RTNDIR` becomes `%RTNDIR%`.

```
#shell
cp $RTNDIR/w14*.lib ./
end
=arplib
-1
25
1 1 1 1 1 1 1 0 0 0 0 1 0 0 0 0 1 0 0 0 1 0 0 0 1
2
w14_e35.lib
w14_e35.arplib
w14_e40.lib
w14_e40.arplib
end
#shell
cp w14*.arplib $RTNDIR
end
```

TRITON input file for PWR 14 × 14 San Onofre assembly

```

=t-depl parm=nitawl
PWR 14x14 for San Onofre assembly, 4.0 wt% U-235
44groupndf5
'=====
read comp
'fuel
uo2      1 0.93 810 92234 0.03473
          92235 4.00
          92236 0.01840
          92238 95.9469 end
' important nuclides from Table 1 of ORNL/TM-12294/V1
zr-94    1 0 1.00e-20 810 end
tc-99    1 0 1.00e-20 810 end
ru-106   1 0 1.00e-20 810 end
rh-103   1 0 1.00e-20 810 end
rh-105   1 0 1.00e-20 810 end
xe-131   1 0 1.00e-20 810 end
cs-133   1 0 1.00e-20 810 end
cs-134   1 0 1.00e-20 810 end
ce-144   1 0 1.00e-20 810 end
pr-143   1 0 1.00e-20 810 end
nd-143   1 0 1.00e-20 810 end
nd-145   1 0 1.00e-20 810 end
nd-147   1 0 1.00e-20 810 end
pm-147   1 0 1.00e-20 810 end
sm-149   1 0 1.00e-20 810 end
sm-151   1 0 1.00e-20 810 end
sm-152   1 0 1.00e-20 810 end
eu-153   1 0 1.00e-20 810 end
eu-154   1 0 1.00e-20 810 end
eu-155   1 0 1.00e-20 810 end
cm-245   1 0 1.00e-20 810 end
cm-246   1 0 1.00e-20 810 end
cm-247   1 0 1.00e-20 810 end
cm-248   1 0 1.00e-20 810 end
bk-249   1 0 1.00e-20 810 end
cf-249   1 0 1.00e-20 810 end
cf-250   1 0 1.00e-20 810 end
cf-251   1 0 1.00e-20 810 end
cf-252   1 0 1.00e-20 810 end
u-232    1 0 1.00e-20 810 end
u-233    1 0 1.00e-20 810 end
u-237    1 0 1.00e-20 810 end
pu-236   1 0 1.00e-20 810 end
pu-237   1 0 1.00e-20 810 end
pu-238   1 0 1.00e-20 810 end
pu-239   1 0 1.00e-20 810 end
pu-240   1 0 1.00e-20 810 end
pu-241   1 0 1.00e-20 810 end
pu-242   1 0 1.00e-20 810 end
pu-243   1 0 1.00e-20 810 end
pu-244   1 0 1.00e-20 810 end
'clad
ss304 2 1 615 end
cobalt 2 0 1.00e-20 615 end
'water moderator with 500 ppm B
h2o    3 den=0.7179 1 576.5 end
arbmb 0.7179 1 1 0 0 5000 100 3 500e-06 576.5 end
'gap
n      4 den=0.00125 1 615 end
'guide tube
ss304 5 1 576.5 end
cobalt 5 0 1.00e-20 576.5 end
end comp
'=====
read celldata
  latticecell squarepitch pitch=1.4122 3
                        fueld=0.9741 1
                        gapd=0.9881 4
                        cladd=1.0719 2
                        end
end celldata
'=====
read depletion
-1 2 5
end depletion
'=====

```



```
1 1 1 1 1 1 1 2 1 1 1 1 1 1
1 1 1 1 1 1 1 1 1 1 1 1 1 1
1 1 2 1 1 1 1 1 1 1 1 2 1 1
1 1 1 1 2 1 1 1 1 2 1 1 1 1
1 1 1 1 1 1 1 1 1 1 1 1 1 1
1 1 2 1 1 2 1 1 2 1 1 2 1 1
1 1 1 1 1 1 1 1 1 1 1 1 1 1
1 1 1 1 1 1 1 1 1 1 1 1 1 1
end fill
end array
'-----
read bounds
all=refl
end bounds
'-----
end model
'=====
end
```



```

power=40.0 burn=75 down=0 end
power=40.0 burn=75 down=0 end
power=40.0 burn=75 down=0 end
power=40.0 burn=75 down=0 end
power=40.0 burn=75 down=0 end
end burndata
'====='
read model
BWR 7x7
'-----'
read parm
fillmix=10 epseigen=1e-4 epsinner=-1e-4
epsouter=1e-4 cmfd=yes xycmfd=4 echo=yes
end parm
'-----'
read materials
1 1 ! fuel ! end
2 1 ! clad ! end
3 2 ! coolant ! end
5 1 ! fuel-Gd (3%) ! end
9 1 ! channel tube ! end
10 2 ! moderator ! end
11 1 ! fuel-Gd (4%) ! end
end materials
'-----'
read geom
unit 1
com='fuel pin'
cylinder 10 .621
cylinder 20 .715
cuboid 40 4p0.9375
media 1 1 10
media 2 1 20 -10
media 3 1 40 -20
boundary 40 4 4
unit 2
com='fuel wih Gd 3%'
cylinder 10 .621
cylinder 20 .715
cuboid 40 4p0.9375
media 5 1 10
media 2 1 20 -10
media 3 1 40 -20
boundary 40 4 4
unit 3
com='fuel wih Gd 4%'
cylinder 10 .621
cylinder 20 .715
cuboid 40 4p0.9375
media 11 1 10
media 2 1 20 -10
media 3 1 40 -20
boundary 40 4 4
global unit 5
com='assembly'
cuboid 51 14.1825 1.0575 14.1825 1.0575
cuboid 52 14.3825 0.8575 14.3825 0.8575
cuboid 53 15.24 0 15.24 0
array 1 51 place 1 1 1.995 1.995
media 3 1 51
media 9 1 52 -51
media 10 1 53 -52
boundary 53 36 36
end geom
'-----'
read array
ara=1 nux=7 nuy=7
fill
1 1 1 1 1 1 1
1 1 2 1 1 3 1
1 1 1 1 1 1 1
1 1 1 2 1 1 1
1 1 1 1 1 2 1
1 3 1 1 1 1 1
1 1 1 1 1 1 1
end fill
end array
'-----'
read bounds
all=refl
end bounds

```

```
'-----  
end data  
'=====  
end
```

* Trace nuclides need to be included in fuel composition, as for the 7×7 assembly; not shown here for brevity.


```

read geom
unit 1
com='fuel rod'
cylinder 10 .40955
cylinder 20 .41790
cylinder 30 .4750
cuboid 40 4p.63
media 1 1 10
media 4 1 20 -10
media 2 1 30 -20
media 3 1 40 -30
boundary 40 4 4
unit 5
com='guide tube'
cylinder 10 .56135
cylinder 20 .602
cuboid 40 4p.63
media 3 1 10
media 5 1 20 -10
media 3 1 40 -20
boundary 40 4 4
unit 11
com='right half of fuel rod'
cylinder 10 .40955 chord +x=0
cylinder 20 .41790 chord +x=0
cylinder 30 .4750 chord +x=0
cuboid 40 .63 0.0 2p.63
media 1 1 10
media 4 1 20 -10
media 2 1 30 -20
media 3 1 40 -30
boundary 40 2 4
unit 12
com='top half of fuel rod'
cylinder 10 .40955 chord +y=0
cylinder 20 .41790 chord +y=0
cylinder 30 .4750 chord +y=0
cuboid 40 2p.63 .63 0.0
media 1 1 10
media 4 1 20 -10
media 2 1 30 -20
media 3 1 40 -30
boundary 40 4 2
unit 51
com='right half of guide tube'
cylinder 10 .56135 chord +x=0
cylinder 20 .602 chord +x=0
cuboid 40 .63 0.0 2p.63
media 3 1 10
media 5 1 20 -10
media 3 1 40 -20
boundary 40 2 4
unit 52
com='top half of guide tube'
cylinder 10 .56135 chord +y=0
cylinder 20 .602 chord +y=0
cuboid 40 2p.63 .63 0.0
media 3 1 10
media 5 1 20 -10
media 3 1 40 -20
boundary 40 4 2
unit 53
com='1/4 instrument tube'
cylinder 10 .56135 chord +x=0 chord +y=0
cylinder 20 .602 chord +x=0 chord +y=0
cuboid 40 .63 0.0 .63 0.0
media 3 1 10
media 5 1 20 -10
media 3 1 40 -20
boundary 40 2 2
global unit 10
cuboid 10 10.75 0.0 10.75 0.0
array 1 10 place 1 1 0 0
media 3 1 10
boundary 10 34 34
end geom
'-----
read array
ara=1 nux=9 nuy=9 typ=cuboidal
fill
53 12 12 52 12 12 52 12 12

```

```

11 1 1 1 1 1 1 1 1
11 1 1 1 1 1 1 1 1
51 1 1 5 1 1 5 1 1
11 1 1 1 1 1 1 1 1
11 1 1 1 1 5 1 1 1
51 1 1 5 1 1 1 1 1
11 1 1 1 1 1 1 1 1
11 1 1 1 1 1 1 1 1
end fill
end array
'-----
read bounds
all=refl
end bounds
'-----
end model
'=====
end

```

* Trace nuclides need to be included in fuel composition, as for the 7 × 7 assembly; not shown here for brevity.


```

read geom
unit 1
com='fuel pin'
cylinder 10 .4555
cylinder 20 .4650
cylinder 30 .5375
cuboid 40 4p0.715
media 1 1 10
media 4 1 20 -10
media 2 1 30 -20
media 3 1 40 -30
boundary 40 4 4
unit 5
com='guide tube'
cylinder 10 .6515
cylinder 20 .6945
cuboid 40 4p0.715
media 3 1 10
media 5 1 20 -10
media 3 1 40 -20
boundary 40 4 4
unit 11
com='right half of fuel pin'
cylinder 10 .4555 chord +x=0
cylinder 20 .4650 chord +x=0
cylinder 30 .5375 chord +x=0
cuboid 40 0.715 0.0 2p0.715
media 1 1 10
media 4 1 20 -10
media 2 1 30 -20
media 3 1 40 -30
boundary 40 2 4
unit 12
com='top half of fuel pin'
cylinder 10 .4555 chord +y=0
cylinder 20 .4650 chord +y=0
cylinder 30 .5375 chord +y=0
cuboid 40 2p0.715 0.715 0.0
media 1 1 10
media 4 1 20 -10
media 2 1 30 -20
media 3 1 40 -30
boundary 40 4 2
unit 51
com='right half of guide tube'
cylinder 10 .6515 chord +x=0
cylinder 20 .6945 chord +x=0
cuboid 40 0.715 0.0 2p0.715
media 3 1 10
media 5 1 20 -10
media 3 1 40 -20
boundary 40 2 4
unit 52
com='top half of guide tube'
cylinder 10 .6515 chord +y=0
cylinder 20 .6945 chord +y=0
cuboid 40 2p0.715 0.715 0.0
media 3 1 10
media 5 1 20 -10
media 3 1 40 -20
boundary 40 4 2
unit 53
com='1/4 instrument tube'
cylinder 10 .6515 chord +x=0 chord +y=0
cylinder 20 .6945 chord +x=0 chord +y=0
cuboid 40 0.715 0.0 0.715 0.0
media 3 1 10
media 5 1 20 -10
media 3 1 40 -20
boundary 40 2 2
global unit 10
cuboid 10 10.75 0.0 10.75 0.0
array 1 10 place 1 1 0 0
media 3 1 10
boundary 10 30 30
end geom
'-----
read array
ara=1 nux=8 nuy=8 typ=cuboidal
fill
53 12 12 12 52 12 12 12

```

```
11 1 1 1 1 1 1 1
11 1 1 1 1 5 1 1
11 1 1 5 1 1 1 1
51 1 1 1 1 1 1 1
11 1 5 1 1 5 1 1
11 1 1 1 1 1 1 1
11 1 1 1 1 1 1 1
end fill
end array
'-----
read bounds
all=refl
end bounds
'-----
end model
'=====
end
```

* Trace nuclides need to be included in fuel composition, as for the 7x7 assembly; not shown here for brevity.


```

read model
BWR 8x8
'-----
read parm
  fillmix=12 epseigen=1e-4 epsinner=-1e-4
  epsouter=1e-4 cmfd=yes xycmfd=4 echo=yes
end parm
'-----
read materials
1 1 ! fuel ! end
2 1 ! clad ! end
3 0 ! gap ! end
4 2 ! coolant ! end
5 1 ! fuel-Gd ! end
9 1 ! water rod tube ! end
10 2 ! water in water rod ! end
11 1 ! channel box ! end
12 1 ! channel moderator ! end
end materials
'-----
read geom
unit 1
com='fuel pin'
cylinder 10 0.522
cylinder 20 0.5325
cylinder 30 0.6125
cuboid 40 4p0.815
media 1 1 10
media 3 1 20 -10
media 2 1 30 -20
media 4 1 40 -30
boundary 40 4 4
unit 2
com='fuel wih Gd pin'
cylinder 10 0.522
cylinder 20 0.5325
cylinder 30 0.6125
cuboid 40 4p0.815
media 5 1 10
media 3 1 20 -10
media 2 1 30 -20
media 4 1 40 -30
boundary 40 4 4
unit 3
com='water rod'
cylinder 10 0.5325
cylinder 20 0.6125
cuboid 30 4p0.815
media 10 1 10
media 9 1 20 -10
media 4 1 30 -20
boundary 30 4 4
unit 11
com='fuel pin - NW corner'
cylinder 10 0.497 origin x=0.075 y=-0.075
cylinder 20 0.5075 origin x=0.075 y=-0.075
cylinder 30 0.5875 origin x=0.075 y=-0.075
cuboid 40 4p0.815
media 1 1 10
media 3 1 20 -10
media 2 1 30 -20
media 4 1 40 -30
boundary 40 4 4
unit 12
com='fuel pin - NNW and WNW off-corner'
cylinder 10 0.497 origin x=0.025 y=-0.025
cylinder 20 0.5075 origin x=0.025 y=-0.025
cylinder 30 0.5875 origin x=0.025 y=-0.025
cuboid 40 4p0.815
media 1 1 10
media 3 1 20 -10
media 2 1 30 -20
media 4 1 40 -30
boundary 40 4 4
unit 13
com='fuel pin - NE corner'
cylinder 10 0.497 origin x=-0.075 y=-0.075
cylinder 20 0.5075 origin x=-0.075 y=-0.075
cylinder 30 0.5875 origin x=-0.075 y=-0.075
cuboid 40 4p0.815
media 1 1 10

```

```

media 3 1 20 -10
media 2 1 30 -20
media 4 1 40 -30
boundary 40 4 4
unit 14
com='fuel pin - NNE and ENE off-corner'
cylinder 10 0.497 origin x=-0.025 y=-0.025
cylinder 20 0.5075 origin x=-0.025 y=-0.025
cylinder 30 0.5875 origin x=-0.025 y=-0.025
cuboid 40 4p0.815
media 1 1 10
media 3 1 20 -10
media 2 1 30 -20
media 4 1 40 -30
boundary 40 4 4
unit 15
com='fuel pin - SE corner'
cylinder 10 0.497 origin x=-0.075 y=0.075
cylinder 20 0.5075 origin x=-0.075 y=0.075
cylinder 30 0.5875 origin x=-0.075 y=0.075
cuboid 40 4p0.815
media 1 1 10
media 3 1 20 -10
media 2 1 30 -20
media 4 1 40 -30
boundary 40 4 4
unit 16
com='fuel pin - SSE and ESE off-corner'
cylinder 10 0.497 origin x=-0.025 y=0.025
cylinder 20 0.5075 origin x=-0.025 y=0.025
cylinder 30 0.5875 origin x=-0.025 y=0.025
cuboid 40 4p0.815
media 1 1 10
media 3 1 20 -10
media 2 1 30 -20
media 4 1 40 -30
boundary 40 4 4
unit 17
com='fuel pin - SW corner'
cylinder 10 0.497 origin x=0.075 y=0.075
cylinder 20 0.5075 origin x=0.075 y=0.075
cylinder 30 0.5875 origin x=0.075 y=0.075
cuboid 40 4p0.815
media 1 1 10
media 3 1 20 -10
media 2 1 30 -20
media 4 1 40 -30
boundary 40 4 4
unit 18
com='fuel pin - SSW and WSW off-corner'
cylinder 10 0.497 origin x=0.025 y=0.025
cylinder 20 0.5075 origin x=0.025 y=0.025
cylinder 30 0.5875 origin x=0.025 y=0.025
cuboid 40 4p0.815
media 1 1 10
media 3 1 20 -10
media 2 1 30 -20
media 4 1 40 -30
boundary 40 4 4
global unit 20
com='assembly'
cuboid 51 4p6.72
cuboid 52 4p6.95
cuboid 53 4p7.665
array 1 51 place 1 1 -5.705 -5.705
media 4 1 51
media 11 1 52 -51
media 12 1 53 -52
boundary 53 40 40
end geom
'-----
read array
ara=1 nux=8 nuy=8
fill
17 18 1 1 1 1 16 15
18 1 1 1 1 1 1 16
1 1 2 1 1 2 1 1
1 1 1 1 1 1 1 1
1 1 1 1 3 1 1 1
1 1 2 1 1 2 1 1
12 1 1 1 1 1 1 14

```

```
11 12 1 1 1 1 14 13
end fill
end array
'-----
read bounds
all=refl
end bounds
'-----
end data
'=====
end
```

* Trace nuclides need to be included in fuel composition, as for the 7x7 assembly; not shown here for brevity.


```

power=40.0 burn=75 down=0 end
power=40.0 burn=75 down=0 end
power=40.0 burn=75 down=0 end
end burndata
'=====
read model
Forsmark-1 BWR 9x9-5
'-----
read parm
fillmix=12 epseigen=1e-4 epsinner=-1e-4
epsouter=1e-4 cmfd=yes xycmfd=4 echo=yes
end parm
'-----
read materials
1 1 ! fuel ! end
2 1 ! clad ! end
3 0 ! gap ! end
4 2 ! coolant ! end
5 1 ! fuel-Gd ! end
9 1 ! water rod tube ! end
10 2 ! water in water rod ! end
11 1 ! channel box ! end
12 1 ! channel moderator ! end
end materials
'-----
read geom
unit 1
com='fuel pin'
cylinder 10 0.475
cylinder 20 0.4835
cylinder 30 0.55
cuboid 40 4p0.7225
media 1 1 10
media 3 1 20 -10
media 2 1 30 -20
media 4 1 40 -30
boundary 40 4 4
unit 2
com='fuel pin (Gd)'
cylinder 10 0.475
cylinder 20 0.4835
cylinder 30 0.55
cuboid 40 4p0.7225
media 5 1 10
media 3 1 20 -10
media 2 1 30 -20
media 4 1 40 -30
boundary 40 4 4
unit 3
com='water rod'
cylinder 10 0.67
cylinder 20 0.75
cuboid 30 4p0.7225
media 10 1 10
media 9 1 20 -10
media 4 1 30 -20
boundary 30 4 4
global unit 20
com='assembly'
cuboid 51 4p6.72
cuboid 52 4p6.95
cuboid 53 4p7.62
array 1 51 place 5 5 0. 0.
media 4 1 51
media 11 1 52 -51
media 12 1 53 -52
boundary 53 40 40
end geom
'-----
read array
ara=1 nux=9 nuy=9
fill
1 1 1 1 1 1 1 1 1
1 2 1 1 1 1 2 1 1
1 1 1 3 1 1 1 2 1
1 1 1 1 3 1 1 1 1
1 1 1 1 3 3 1 1 1
1 1 1 1 1 1 3 1 1
1 1 2 1 1 1 1 1 1
1 2 1 1 1 1 1 2 1
1 1 1 1 1 1 1 1 1

```

```
end fill
end array
'-----
read bounds
  all=refl
end bounds
'-----
end data
'=====
end
```

* Trace nuclides need to be included in fuel composition, as for the 7x7 assembly; not shown here for brevity.


```

read model
BWR SVEA-64
'-----
read parm
fillmix=10 epseigen=1e-4 epsinner=-1e-4
epsouter=1e-4 cmfd=yes xycmfd=4 echo=yes
end parm
'-----
read materials
1 1 ! fuel ! end
2 1 ! clad ! end
3 2 ! coolant ! end
4 0 ! gap ! end
5 1 ! fuel-Gd (2.55%) ! end
9 1 ! channel box ! end
10 2 ! moderator ! end
end materials
'-----
read geom
unit 1
com='fuel pin'
cylinder 10 .522
cylinder 20 .5325
cylinder 30 .6125
cuboid 40 4p0.79
media 1 1 10
media 4 1 20 -10
media 2 1 30 -20
media 3 1 40 -30
boundary 40 4 4
unit 2
com='fuel wih Gd 2.55%'
cylinder 10 .522
cylinder 20 .5325
cylinder 30 .6125
cuboid 40 4p0.79
media 5 1 10
media 4 1 20 -10
media 2 1 30 -20
media 3 1 40 -30
boundary 40 4 4
unit 3
com='spacer rod'
cylinder 20 .5325
cylinder 30 .6125
cuboid 40 4p0.79
media 10 1 20
media 2 1 30 -20
media 3 1 40 -30
boundary 40 4 4
unit 4
com='sub-assembly NE'
cuboid 41 4p3.295
cuboid 42 3.295 -3.375 3.295 -3.375
array 1 41 place 2 2 -0.79 -0.79
media 3 1 41
media 9 1 42 -41
boundary 42 16 16
unit 5
com='sub-assembly NW'
cuboid 51 4p3.295
cuboid 52 3.375 -3.295 3.295 -3.375
array 2 51 place 2 2 -0.79 -0.79
media 3 1 51
media 9 1 52 -51
boundary 52 16 16
unit 6
com='sub-assembly SW'
cuboid 61 4p3.295
cuboid 62 3.375 -3.295 3.375 -3.295
array 3 61 place 2 2 -0.79 -0.79
media 3 1 61
media 9 1 62 -61
boundary 62 16 16
unit 7
com='sub-assembly SE'
cuboid 71 4p3.295
cuboid 72 3.295 -3.375 3.375 -3.295
array 4 71 place 2 2 -0.79 -0.79
media 3 1 71
media 9 1 72 -71

```

```

boundary 72 16 16
global unit 8
com='assembly'
cuboid 81 4p6.87
cuboid 82 4p6.98
cuboid 83 4p7.7
hole 4 origin x=3.575 y=3.575
hole 5 origin x=-3.575 y=3.575
hole 6 origin x=-3.575 y=-3.575
hole 7 origin x=3.575 y=-3.575
media 10 1 81
media 9 1 82 -81
media 10 1 83 -82
boundary 83 24 24
end geom
'-----
read array
ara=1 nux=4 nuy=4
  fill
  1 1 1 1
  1 2 1 1
  1 1 1 1
  1 1 1 1
end fill
ara=2 nux=4 nuy=4
  fill
  1 1 1 1
  1 1 1 1
  1 2 1 1
  1 1 1 1
end fill
ara=3 nux=4 nuy=4
  fill
  1 1 1 1
  1 1 1 1
  1 1 2 1
  1 1 1 1
end fill
ara=4 nux=4 nuy=4
  fill
  1 1 1 1
  1 1 2 1
  1 3 1 1
  1 1 1 1
end fill
end array
'-----
read bounds
all=refl
end bounds
end data
'=====
end

```

* Trace nuclides need to be included in fuel composition, as for the 7 × 7 assembly; not shown here for brevity.


```

read model
BWR SVEA-100
'-----
read parm
  fillmix=10 epseigen=1e-4 epsinner=1e-4
  epsouter=1e-4 cmfd=yes xycmfd=4 echo=yes
end parm
'-----
read materials
  1 1 ! fuel           ! end
  2 1 ! clad           ! end
  3 2 ! coolant        ! end
  4 0 ! gap            ! end
  5 1 ! fuel-Gd (3.5%) ! end
  9 1 ! channel box    ! end
 10 2 ! moderator      ! end
end materials
'-----
read geom
unit 1
com='fuel pin'
  cylinder 10 .4095
  cylinder 20 .418
  cylinder 30 .481
  cuboid 40 4p0.62
  media 1 1 10
  media 4 1 20 -10
  media 2 1 30 -20
  media 3 1 40 -30
  boundary 40 4 4
unit 2
com='fuel wih Gd 3.5%'
  cylinder 10 .4095
  cylinder 20 .418
  cylinder 30 .481
  cuboid 40 4p0.62
  media 5 1 10
  media 4 1 20 -10
  media 2 1 30 -20
  media 3 1 40 -30
  boundary 40 4 4
unit 3
com='sub-assembly NE'
  cuboid 31 4p3.28
  cuboid 32 3.28 -3.39 3.28 -3.39
  array 1 31 place 3 3 0. 0.
  media 3 1 31
  media 9 1 32 -31
  boundary 32 20 20
unit 4
com='sub-assembly NW'
  cuboid 41 4p3.28
  cuboid 42 3.39 -3.28 3.28 -3.39
  array 2 41 place 3 3 0. 0.
  media 3 1 41
  media 9 1 42 -41
  boundary 42 20 20
unit 5
com='sub-assembly SW'
  cuboid 51 4p3.28
  cuboid 52 3.39 -3.28 3.39 -3.28
  array 3 51 place 3 3 0. 0.
  media 3 1 51
  media 9 1 52 -51
  boundary 52 20 20
unit 6
com='sub-assembly SE'
  cuboid 61 4p3.28
  cuboid 62 3.28 -3.39 3.39 -3.28
  array 4 61 place 3 3 0. 0.
  media 3 1 61
  media 9 1 62 -61
  boundary 62 20 20
global unit 7
com='assembly'
  cuboid 71 4p6.87
  cuboid 72 4p6.98
  cuboid 73 4p7.725
  hole 3 origin x=3.59 y=3.59
  hole 4 origin x=-3.59 y=3.59
  hole 5 origin x=-3.59 y=-3.59

```

```

hole 6 origin x=3.59 y=-3.59
media 10 1 71
media 9 1 72 -71
media 10 1 73 -72
boundary 73 20 20
end geom
'-----
read array
ara=1 nux=5 nuy=5 typ=cuboidal
fill
  1 1 1 1 1
  1 1 1 2 1
  1 1 1 1 1
  1 2 1 1 1
  1 1 1 1 1
end fill
ara=2 nux=5 nuy=5 typ=cuboidal
fill
  1 1 1 1 1
  1 1 1 1 1
  1 1 2 1 1
  1 1 1 1 1
  1 1 1 1 1
end fill
ara=3 nux=5 nuy=5 typ=cuboidal
fill
  1 1 1 1 1
  1 1 1 2 1
  1 1 1 1 1
  1 2 1 1 1
  1 1 1 1 1
end fill
ara=4 nux=5 nuy=5 typ=cuboidal
fill
  1 1 1 1 1
  1 1 1 1 1
  1 1 2 1 1
  1 1 1 1 1
  1 1 1 1 1
end fill
end array
'-----
read bounds
all=refl
end bounds
'-----
end data
'====='
end

```

* Trace nuclides need to be included in fuel composition, as for the 7 × 7 assembly; not shown here for brevity.

APPENDIX C

**SPENT FUEL ASSEMBLY BENCHMARK DATA
COMPARISON OF TRITON AND SAS2H RESULTS**

Table C.1 Comparison of TRITON and SAS2H decay heat results for selected Swedish PWR fuel assemblies

Reactor	Assembly ID	Assembly design	Enrichment (wt % ²³⁵ U)	Final burnup (MWd/MTU)	Cooling time (days)	Measured (W)	TRITON Calculated (W)	SAS2H Calculated (W)	Difference ^a (%)
Ringhals 2	C01	15×15	3.1	36,688	8468	415.8	439.3	430.4	-2.02%
Ringhals 2	C12	15×15	3.1	36,385	8403	410.3	434.4	425.4	-2.08%
Ringhals 2	C20	15×15	3.1	35,720	6950	415.8	451.9	440.1	-2.61%
Ringhals 2	C20	15×15	3.1	35,720	6951	426	451.9	440.1	-2.61%
Ringhals 2	C20	15×15	3.1	35,720	6952	428.9	451.8	440.0	-2.61%
Ringhals 2	C20	15×15	3.1	35,720	6959	435.7	451.7	439.9	-2.62%
Ringhals 2	D27	15×15	3.3	39,676	7669	456.1	473.6	464.0	-2.03%
Ringhals 2	D38	15×15	3.3	39,403	8005	442.3	461.7	453.5	-1.77%
Ringhals 2	E38	15×15	3.2	33,973	7999	376.3	390	383.1	-1.76%
Ringhals 2	E38	15×15	3.2	33,973	8000	374.3	390	383.1	-1.76%
Ringhals 2	E40	15×15	3.2	34,339	8075	381.3	394.2	387.2	-1.77%
Ringhals 2	F14	15×15	3.2	34,009	7722	381.8	398.9	393.2	-1.42%
Ringhals 2	F21	15×15	3.2	36,273	7376	420.9	433.7	428.0	-1.31%
Ringhals 2	F25	15×15	3.2	35,352	7725	396.7	418	411.6	-1.53%
Ringhals 2	F32	15×15	3.2	50,962	5860	692	732.7	713.1	-2.67%
Ringhals 2	G11	15×15	3.2	35,463	6990	416.4	428.5	423.5	-1.16%
Ringhals 2	G23	15×15	3.2	35,633	6984	420.6	436.6	430.8	-1.33%
Ringhals 2	I09	15×15	3.2	40,188	5849	507.9	535.4	530.5	-0.92%
Ringhals 2	I24	15×15	3.2	34,294	6601	410.1	419	414.7	-1.02%
Ringhals 2	I25	15×15	3.2	36,859	6198	445.8	467.3	463.3	-0.87%
Ringhals 3	0E2	17×17	3.1	41,628	5823	587.9	609	598.0	-1.80%
Ringhals 3	0E6	17×17	3.1	35,993	5829	487.8	505.6	507.6	0.40%
Ringhals 3	1C2	17×17	3.1	33,318	6559	417.7	438.3	436.3	-0.45%
Ringhals 3	1E5	17×17	3.1	34,638	5818	468.8	485.2	485.5	0.07%
Ringhals 3	2A5	17×17	2.1	20,107	7297	233.8	246.3	245.3	-0.40%
Ringhals 3	2C2	17×17	3.1	36,577	6550	466.5	491	487.2	-0.78%

**Table C.1 Comparison of TRITON and SAS2H decay heat results for selected Swedish PWR fuel assemblies
(continued)**

Reactor	Assembly ID	Assembly design	Enrichment (wt % ²³⁵ U)	Final burnup (MWd/MTU)	Cooling time (days)	Measured (W)	TRITON Calculated (W)	SAS2H Calculated (W)	Difference ^a (%)
Ringhals 3	3C1	17×17	3.1	36,572	6545	470.2	489.9	483.0	-1.42%
Ringhals 3	4C4	17×17	3.1	33,333	6572	422	438.9	436.4	-0.57%
Ringhals 3	5A3	17×17	2.1	19,699	6972	237.7	244.2	243.8	-0.17%
Ringhals 3	5A3	17×17	2.1	19,699	6975	236.7	244.2	243.8	-0.17%
Ringhals 3	5A3	17×17	2.1	19,699	6977	243.4	244.2	239.8	-1.79%
Ringhals 3	5A3	17×17	2.1	19,699	7291	230.9	240.7	239.6	-0.44%

^a (SAS2H / TRITON) - 1 × 100%.

Table C.2 Comparison of TRITON and SAS2H decay heat results for selected Swedish BWR fuel assemblies

Reactor	Assembly ID	Assembly design	Enrichment (wt % ²³⁵ U)	Final burnup (MWd/MTU)	Cooling time (days)	Measured (W)	TRITON Calculated (W)	SAS2H Calculated (W)	Difference ^a (%)
Ringhals 1	1177	8×8	2.64	36,242	6690	177.9	174	177.29	1.89%
Ringhals 1	1186	8×8	2.64	30,498	6674	140.8	142.5	144.12	1.14%
Ringhals 1	6423	8×8	2.9	35,109	5669	174.2	175.7	174.74	-0.55%
Ringhals 1	6432	8×8	2.89	36,861	5422	185.5	187	185.87	-0.60%
Ringhals 1	6432	8×8	2.89	36,861	5424	189.5	186.9	185.87	-0.55%
Ringhals 1	6432	8×8	2.89	36,861	5670	184.4	184.1	183.15	-0.52%
Ringhals 1	6432	8×8	2.89	36,861	5680	182.8	184	183.05	-0.52%
Ringhals 1	6432	8×8	2.89	36,861	5681	185.2	184	182.95	-0.57%
Ringhals 1	6432	8×8	2.89	36,861	5687	181.6	183.9	182.95	-0.52%
Ringhals 1	6432	8×8	2.89	36,861	5688	182	183.9	182.85	-0.57%
Ringhals 1	6454	8×8	2.9	37,236	6395	186.3	181.1	179.69	-0.78%
Ringhals 1	8327	8×8	2.9	37,851	4600	196.9	201.2	199.61	-0.79%
Ringhals 1	8331	8×8	2.91	35,903	5291	187	183.7	182.39	-0.71%
Ringhals 1	8332	8×8	2.89	34,977	5690	168.1	172.5	171.33	-0.68%
Ringhals 1	8338	8×8	2.91	34,830	5695	169.5	172.5	170.46	-1.18%
Forsmark 1	3838	8×8	2.09	25,669	4170	126.8	131.7	132.72	0.77%
Forsmark 1	3838	8×8	2.09	25,669	4171	125.9	131.7	132.71	0.77%
Forsmark 1	KU0100	8×8-2	2.98	34,193	4893	185.3	179.3	178.61	-0.38%
Forsmark 2	5535	8×8	2.1	19,944	5634	84.6	92.5	92.61	0.12%
Oskarshamn 2	1377	8×8	2.2	14,546	9750	56.2	59.4	59.26	-0.24%
Oskarshamn 2	1389	8×8	2.2	19,481	8171	83.9	83.4	84.03	0.76%
Oskarshamn 2	1546	8×8	2.2	24,470	7455	108.1	110.9	111.00	0.09%
Oskarshamn 2	1696	8×8	2.2	20,870	7411	92.4	93.8	92.56	-1.32%
Oskarshamn 2	1704	8×8	2.2	19,437	7808	84	84.1	84.43	0.39%
Oskarshamn 2	2995	8×8	2.7	29,978	8211	130.5	131.6	131.87	0.21%
Oskarshamn 2	6350	8×8	2.88	27,675	6754	126.9	129.1	129.22	0.09%

**Table C.2 Comparison of TRITON and SAS2H decay heat results for selected Swedish BWR fuel assemblies
(continued)**

Reactor	Assembly ID	Assembly design	Enrichment (wt % ²³⁵ U)	Final burnup (MWd/MTU)	Cooling time (days)	Measured (W)	TRITON Calculated (W)	SAS2H Calculated (W)	Difference ^a (%)
Oskarshamn 2	6350	8×8	2.88	27,675	6755	129.4	129.2	129.22	0.02%
Oskarshamn 3	12078	8×8	2.58	25,160	5611	120.2	125.6	126.81	0.96%
Barsebäck 1	9329	8×8	2.92	41,127	5371	222.8	221.7	222.08	0.17%
Barsebäck 1	9329	8×8	2.92	41,127	5373	224.4	221.7	221.98	0.13%
Barsebäck 1	9329	8×8	2.92	41,127	5542	218.7	219.2	219.65	0.21%
Barsebäck 1	10288	8×8	2.95	35,218	5534	185.8	183.8	183.15	-0.35%
Barsebäck 2	14076	8×8	3.15	40,010	4177	240.3	235.7	232.83	-1.22%
Forsmark 1	KU0269	9×9-5	2.94	35,113	4903	192.7	191.9	191.26	-0.33%
Forsmark 1	KU0278	9×9-5	2.94	35,323	4595	195.4	194.1	193.81	-0.15%
Forsmark 1	KU0282	9×9-5	2.94	37,896	4574	218.5	211.9	211.93	0.01%
Forsmark 2	11494	SVEA-64	2.92	32,431	5618	166	166	164.92	-0.65%
Forsmark 2	11495	SVEA-64	2.91	32,431	5593	167.6	166.9	164.89	-1.20%
Forsmark 2	13775	SVEA-64	2.85	32,837	4543	178.4	179	177.87	-0.63%
Oskarshamn 2	12684	SVEA-64	2.9	46,648	4519	282.7	280.1	276.82	-1.17%
Forsmark 3	13847	SVEA-100	2.77	31,275	4871	170.3	168.5	168.60	0.06%
Forsmark 3	13847	SVEA-100	2.77	31,275	4871	169.6	168.5	168.60	0.06%
Forsmark 3	13848	SVEA-100	2.77	31,275	4882	170.7	168.5	168.40	-0.06%
Oskarshamn 3	13628	SVEA-100	2.71	35,619	4581	194	196.5	196.02	-0.24%
Oskarshamn 3	13630	SVEA-100	2.71	40,363	4554	235.7	232.9	229.83	-1.32%

^a (SAS2H / TRITON) - 1 × 100%.

BIBLIOGRAPHIC DATA SHEET

(See instructions on the reverse)

NUREG/CR-6972
(ORNL/TM-2008/015)

2. TITLE AND SUBTITLE

Validation of SCALE 5 Decay Heat Predictions for LWR Spent Nuclear Fuel

3. DATE REPORT PUBLISHED

MONTH	YEAR
February	2010

4. FIN OR GRANT NUMBER

Y6517

5. AUTHOR(S)

I. C. Gauld, G. Ilas, B. D. Murphy, and C. F. Weber

6. TYPE OF REPORT

Technical

7. PERIOD COVERED (Inclusive Dates)

8. PERFORMING ORGANIZATION - NAME AND ADDRESS (If NRC, provide Division, Office or Region, U.S. Nuclear Regulatory Commission, and mailing address; if contractor, provide name and mailing address.)

Oak Ridge National Laboratory
Managed by UT-Battelle, LLC
Oak Ridge, TN 37831-6170

9. SPONSORING ORGANIZATION - NAME AND ADDRESS (If NRC, type "Same as above"; if contractor, provide NRC Division, Office or Region, U.S. Nuclear Regulatory Commission, and mailing address.)

Division of Systems Analysis
Office of Nuclear Regulatory Research
U.S. Nuclear Regulatory Commission
Washington, DC 20555-0001

10. SUPPLEMENTARY NOTES

M. Aissa, NRC Project Manager

11. ABSTRACT (200 words or less)

This report documents the validation of ORIGEN-S computer code predictions of decay heat using experimental benchmarks involving irradiated nuclear fuels. The experiments include the measurements of decay heat for (1) pulse fission irradiations for many fissionable materials in spent fuel for cooling times of interest to severe accident analyses (< 105 s), and for (2) full-length fuel assemblies over longer cooling times of importance to spent fuel storage and transportation. The fuel assembly measurements evaluated in this study include all previously reported measurements performed in the United States at the General Electric Morris Operations facility and at Hanford Engine Maintenance Assembly and Disassembly facility in Nevada. Recent fuel assembly decay heat measurements carried out at the Swedish Central Interim Storage Facility for Spent Fuel, CLAB, are also included. The purpose of this report is to evaluate the computational bias and uncertainty associated with decay heat predictions when using the ORIGEN-S code and cross-section libraries generated employing modules and nuclear data libraries of the SCALE 5 code system. This validation study includes a broader range of assembly designs, fuel enrichments, cooling times, and higher burnup values than has been reported previously. The results will be used to develop technical guidance and recommended margins for uncertainty in decay heat predicted with ORIGEN-S.

12. KEY WORDS/DESCRIPTORS (List words or phrases that will assist researchers in locating the report.)

SCALE, ORIGEN-S, spent nuclear fuel, decay heat

13. AVAILABILITY STATEMENT

unlimited

14. SECURITY CLASSIFICATION

(This Page)

unclassified

(This Report)

unclassified

15. NUMBER OF PAGES

16. PRICE



Federal Recycling Program





UNITED STATES
NUCLEAR REGULATORY COMMISSION
WASHINGTON, DC 20555-0001

OFFICIAL BUSINESS